



**UNIVERSITÀ DEGLI STUDI DI CAMERINO**

**School of Advanced Studies**

**DOCTORAL COURSE IN**

**Physical and Chemical Processes in Earth Systems**

**XXXIV cycle**

**INFERRING SEISMOGENIC SOURCES BY MULTI-METHOD APPROACH: CASE-STUDIES FROM NORTHERN-CENTRAL APENNINES AND ADRIATIC REGION**

**PhD Student**

**Simone Teloni**

**Supervisor**

**Prof. Chiara Invernizzi**

**Co-Supervisor**

**Prof. Gilberto Pambianchi**

**Prof. Marco Menichetti**

## **ACKNOWLEDGEMENTS**

# TABLE OF CONTENTS

Acknowledgements .....	i
Table of Contents.....	ii
List of Figures .....	v
List of Tables .....	vii
Abbreviations .....	viii
<b>1. Introduction.....</b>	<b>1</b>
1.1. Study aims.....	4
1.2. Identification and characterization of seismic sources: state of the art.....	5
1.3. Integrated, multidisciplinary adopted methods: their potential and limitations.....	9
1.4. Thesis structure .....	15
1.5. References.....	17
<b>2. The seismogenic fault system of the <math>M_w</math> 6.4, November 2019 Albania earthquake: new insights into the structural architecture and active tectonic setting of the outer Albanides .....</b>	<b>26</b>
2.1. Introduction.....	27
2.2. Regional tectonic framework.....	27
2.3. Seismotectonics of the Durrës region and the 2019-2020 earthquakes.....	32
2.4. Stress field analysis .....	36
2.5. Crustal geological section across the northern outer Albanides and the thrust front .....	40
2.6. Discussion.....	42
2.6.1. <i>Implications for thrust belt architecture and active tectonics.....</i>	<i>43</i>
2.7. Concluding remarks .....	45
2.8. References.....	46
<b>3. Plio–Quaternary structural evolution of the outer sector of the Marche Apennines south of the Conero promontory, Italy .....</b>	<b>52</b>
3.1. Introduction.....	53

<b>3.2. Geological setting.....</b>	<b>56</b>
<b>3.3. Dataset and working methods.....</b>	<b>59</b>
<b>3.4. Results by wells and seismic profiles interpretation.....</b>	<b>61</b>
3.4.1. <i>Transects.....</i>	61
3.4.2. <i>Characteristics and distribution of the Plio-Quaternary deformation .....</i>	65
<b>3.5. Discussion.....</b>	<b>68</b>
<b>3.6. Conclusions.....</b>	<b>74</b>
<b>3.7. References.....</b>	<b>75</b>
<b>4. The seismotectonic role of transversal structures in the Plio-Quaternary evolution of the Outer Marche Apennines .....</b>	<b>83</b>
<b>4.1. Introduction.....</b>	<b>84</b>
<b>4.2. Tectonic setting, main structural and evolutionary characteristics .....</b>	<b>85</b>
<b>4.3. Materials and methods.....</b>	<b>91</b>
<b>4.4. Results: seismicity close to transversal structures .....</b>	<b>93</b>
4.4.1. <i>The Cattolica Fault System.....</i>	93
4.4.2. <i>The Metauro valley offshore Fano Fault System.....</i>	94
4.4.3. <i>The Cupramontana Fault System .....</i>	95
4.4.4. <i>The South Conero Fault System.....</i>	96
<b>4.5. Discussions.....</b>	<b>98</b>
4.5.1. <i>Seismotectonic considerations .....</i>	98
4.5.2. <i>General discussion.....</i>	100
<b>4.6. Conclusions.....</b>	<b>104</b>
<b>4.7. References.....</b>	<b>105</b>
<b>5. Morphostructural evidence of active along-strike segmentation of the Umbria-Marche Apennines, Italy .....</b>	<b>116</b>
<b>5.1. Introduction.....</b>	<b>117</b>
<b>5.2. Geological and morphostructural setting.....</b>	<b>118</b>
<b>5.3. Seismicity.....</b>	<b>124</b>

<b>5.4. Materials and methods.....</b>	<b>126</b>
5.4.1. <i>Topography analysis.....</i>	<i>126</i>
5.4.2. <i>Quantitative analysis of the river network.....</i>	<i>127</i>
<b>5.5. Results.....</b>	<b>129</b>
5.5.1. <i>Features of topography.....</i>	<i>129</i>
5.5.2. <i>Swath profiles.....</i>	<i>132</i>
5.5.3. <i>Longitudinal river profiles analysis.....</i>	<i>134</i>
5.5.4. <i>Ksn index.....</i>	<i>138</i>
<b>5.6. Discussion.....</b>	<b>140</b>
5.6.1. <i>Along-strike variation of uplift.....</i>	<i>140</i>
5.6.2. <i>The role of transversal structures.....</i>	<i>142</i>
<b>5.7. Conclusions.....</b>	<b>143</b>
<b>5.8. References.....</b>	<b>144</b>
<b>6. Discussion and conclusions .....</b>	<b>155</b>
<b>6.1. Implication for seismic hazard improvement.....</b>	<b>161</b>
<b>6.2. Further works.....</b>	<b>163</b>
<b>6.3. References.....</b>	<b>164</b>

## LIST OF FIGURES

Fig. 1.1 - Seismic hazard map of the Umbria-Marche Apennines (MPS04 modified after Stucchi et al. 2004). .....	3
Fig. 1.2 - The European Seismic Hazard Map (ESHM2020 – Danciu et al. 2021) .....	8
Fig. 1.3 - The location of the ENI s.p.a., ViDEPI seismic reflection profiles and boreholes analyzed in this study. The instrumental seismicity recorded by INGV seismic stations and provided by the ISIDe on-line catalogue is also shown. ....	11
Fig. 1.4 - Elevation map of the Umbria-Marche Apennines showing the location of the investigated main trunks and swath profiles analyzed in morphotectonic analysis. ....	14
Fig. 2.1 - Map showing epicenter location and focal mechanisms for the 2019-2020 Albania seismic sequence (in red) and previous seismic events recorded by INGV since 1985 .....	29
Fig. 2.2 - Tectonic sketch map of Albania (after Roure et al. 2004). ....	31
Fig. 2.3 - WSW-ENE vertical section showing hypocentral distribution for the seismic events recorded by ISIDe ( <a href="http://terremoti.ingv.it/iside">http://terremoti.ingv.it/iside</a> ) since 1985.....	36
Fig. 2.4 - Stress field analysis from 2019-2020 Albania focal mechanism solutions. ....	39
Fig. 2.5 - Interpreted seismic section across the outer Albanides (after Roure et al. 2004).....	40
Fig. 2.6 - WSW-ENE regional geological section across the northern outer Albanides (sedimentary cover structure based on Roure et al. 2004, and Frasheri et al. 2009).....	41
Fig. 3.1 - On shore schematic geological map of the Marche region (modified after Conti et al., 2020 .....	54
Fig. 3.2 - Synthetic stratigraphic scheme of the Messinian–Pleistocene of the Central Periadriatic Basin (CPB; slightly modified from (Ghielmi et al., 2019). ....	58
Fig. 3.3 - Stratigraphic correlation between the ELISA 1 well and a segment of the ViDEPI B-441 seismic profile.....	60
Fig. 3.4 - Transect 8 .....	62
Fig. 3.5 -Transect 9.....	63
Fig. 3.6 - Transect 10.....	63
Fig. 3.7 - Transect 11.....	64

Fig. 3.8 - Transect 12.....	64
Fig. 3.9 - Schematic map of the distribution and thickness of Lower Pliocene deposits within the Marche region and the adjacent Adriatic Sea .....	66
Fig. 3.10 - Structural sketch map of the outer Marche area south of Conero Promontory.....	68
Fig. 3.11 - Sketch diagram showing the evolution of the Coastal Structure from the Early to Middle Pliocene across two representative cross-sections. ....	72
Fig. 3.12 - Kinematic sketch map of the outer Marche area south of Conero Promontory.....	73
Fig. 4.1 - Geo-Structural sketch of outer sector of Umbria-Marche Apennines (modified after Pierantoni et al., 2013; Pierantoni et al., 2019; Costa et al., 2021 and Conti et al., 2020 .....	87
Fig. 4.2 - VIDEPI interpreted seismic profile: 3(2).....	89
Fig. 4.3 - Cattolica Fault System (1916 and 2013 seismic sequences data).....	93
Fig. 4.4 - Metauro-Fano Fault System and seismic sequences data. Results of the stress inversion analysis are shown in the right square .....	95
Fig. 4.5 - The Cupramontana Fault System and the 2012 and 2013 seismic sequence. Results of the stress inversion analysis are shown in the right square .....	96
Fig. 4.6 - The South Conero Fault System and seismic sequence. Results of the stress inversion analysis are shown in the right square.. .....	98
Fig. 4.7 - Geological sketch map representing the main active and seismogenic structures belonging to the outer sector.....	102
Fig. 5.1 - Structural map of Umbria-Marche Apennines and foothill (modified from Pierantoni et al., 2019 and Costa et al. 2021).....	119
Fig. 5.2 - WSW-ENE regional geological section across the Umbria-Marche Apennine fold and thrust belt .....	121
Fig. 5.3 - Geological sketch of Umbria-Marche Apennines and foothill (modified from Conti et al., 2020) .....	122
Fig. 5.4 - Instrumental seismicity with magnitude higher than 3 for the eastern Central Italy and surrounding area from 1985 to present. ....	125
Fig. 5.5 - Elevation map of the Umbria-Marche Apennines with location of the investigated main trunks, and correlative hydrographic basin, and the swath profiles .....	130

Fig. 5.6 - Elevation maps from neighbourhood statistical analysis in ArcGIS environment applied to the 30 m NASA ASTERDEM of the study area; a) maximum elevation map, b) minimum elevation map, c) mean elevation map, and d) local relief map.....	131
Fig. 5.7 - Elevation maps from neighbourhood statistical analysis in ArcGIS environment applied to the 30 m NASA ASTERDEM of the study area; a) maximum elevation map, b) minimum elevation map, c) mean elevation map, and d) local relief map.....	134
Fig. 5.8 - Longitudinal profiles and chi plot (performed by Topotoolbox MATLAB-based software) of the 18 rivers analysed in the present work.....	136
Fig. 5.9 - Topographic map showing the knickpoints/knickzones spatial distribution along the 18 river channels analysed in the study area .....	137
Fig. 5.10 - Chi plots of the main rivers of hydrographic basins (locations and numbering in Fig. 5.5), constructed using a best fit m/n value of 0.59 .....	138
Fig. 5.11 - Ksn index map of the eastern central Apennines identifying the alluvial basins (black outlines) and the spatial distribution of ksn.....	139
Fig. 6.1 - Geological sketch map showing the major active and seismogenic fault systems identified and discussed in the present work. ....	161

## LIST OF TABLES

Tab. 1.1 - GIS input data used in the present work. ....	7
Tab. 1.2 – Crustal model and set up used by Monachesi et al. 2021 in <i>Hypoellipse software</i> for the seismic events localization.....	12
Tab. 2.1 - Seismological information for the 2019-2020 seismic sequence (from INGV - ISIDE <a href="http://terremoti.ingv.it/iside">http://terremoti.ingv.it/iside</a> ; uncertainties are provided where available in the catalogue). ....	34
Tab. 2.2 - Earthquake focal mechanisms dataset used to perform the stress analyses. Data related to the 2019-2020 seismic sequence are shown in bold.....	37
Tab. 4.1 - Earthquake focal mechanism dataset derived from available catalogue ( <a href="http://www.an.ingv.it/BB/home.html">http://www.an.ingv.it/BB/home.html</a> , last accessed 15 January 2022) and the literature (Santini et al., 2011, Mazzoli et al., 2015) and used to perform the stress field analysis. ....	92



## **ABBREVIATIONS**

**CFS:** Cattolica Fault System

**CPTI:** Catalogo Parametrico dei Terremoti Italiani

**CUFS:** Cupramontana Fault System

**DEM:** Digital elevation model

**DISS:** Database of Individual Seismogenic Sources

**DTM:** Digital terrain model

**FMS:** Focal mechanism solution

**M:** Magnitude

**MASH:** Marche Adriatic Structural High

**MFFS:** Metauro valle-Fano Fault System

**NAFT:** Northern Albanide Frontal Thrust

**OAMS:** Olevano-Antrodoco-M.ti Sibillini thrust

**SCFS:** South Conero Fault System

**UMAF:** Umbria-Marche Apennines and Foothills

**UMSTZ:** Umbria-Marche-Sabina Thrust Zone

# 1. INTRODUCTION

Italy is the country with the highest seismic risk in Europe, with the largest number of earthquakes in the last 500 years (CPTI15, Rovida, A. et al., 2022), and with one of the greatest number of victims since 1900, equivalent to about 160.000 fatalities (Italian Civil Protection Department, 2018).

The long-lasting seismic sequence that started on 24 August 2016 (Amatrice-Visso-Norcia) and struck a large area of central Apennine, partially overlapping the areas affected by the 1997 Umbria–Marche (Mw 5.8 mainshock) to the north and 2009 L’Aquila seismic sequence to the south (Mw 6.1 mainshock) (Fig. 1.1) is just one of the very last seismic sequences that affected the central Apennines with catastrophic scenarios. Nine major seismic events with Mw greater than 5 (Mw>5) occurred in few months (ISIDe Working Group, 2007) with epicenters spread over c. 50 km following an NNW–SSE strike along the central Apennines. The two strongest earthquakes Mw 6.0 (24 August 2016) and Mw 6.5 (30 October 2016), with the latter representing the largest earthquake in Italy since the Mw 6.9 1980 Irpinia event (Azzarro et al., 2016), caused 298 casualties, hundreds of injuries and almost 30.000 homeless, with several villages totally destructed (Pucci et al., 2017). Furthermore, the earthquakes severely damaged some strategic infrastructures such as roads, viaducts, bridges, strategic facilities worsening the early emergency phase. In fact, during this sequence, macroseismic (Mercalli–Cancani–Sieberg – MCS) intensities up to X or XI (ruinous or catastrophic) were observed (Galli et al., 2016), and IMCS  $\geq$  VII (very strong) interested an area of about 2.100 Km<sup>2</sup> (Galli et al., 2016, available online <https://emidius.mi.ingv.it/>).

The coseismic effects of the Amatrice-Visso-Norcia seismic sequence have been largely measured and studied with more than 4.000 direct and secondary effects associated with the earthquakes identified by the EMERGEO Working Group (Civico et al., 2018). Direct coseismic effects are the result of surface fracturing and faulting processes (Emergeo Working Group, 2018), mainly linked to the reactivation of pre-existing faults (Boncio et al., 2004; Pizzi & Galadini, 2009; Bonini et al., 2016). In turn, gravitational slope deformations such as activation/re-activation of superficial landslides and rockfalls represent secondary coseismic effects, responsible of the interruption of the main traffic circulation across the central Apennines (e.g. the Sasso Pizzuto landslide into the deeply incised Nera River valley; Romeo et al., 2017).

The above listed examples show how coseismic effects associated with large earthquakes may affect the communities and their socio-economic systems, and how a strong post-disaster management and resilience is essential to mitigate the seismic risks. In fact, the mitigation of seismic risk of an area requires a deep knowledge of the territory in terms of the environmental and architectural characteristics, fundamental to produce a reliable seismic hazard assessment. For this reason, in a seismic hazard evaluation for a given site, it is necessary identifying the seismic sources, which can generate strong earthquakes, estimating the magnitudes and frequency of the earthquake's occurrence.

Since the pioneering work of Cornell (Cornell, 1968), seismic hazard assessment depends on several factors, among which one of the most important is represented by the delineation of the seismic sources, often poorly understood because extensively covered by Quaternary deposits or located in offshore sites. In fact, their identification depends on the accuracy of the available geological, geophysical, and seismological data combined with tectonic knowledge, near-fault geomorphology, subsurface geophysical techniques, and remote sensing analysis. In the last years, these methodologies have been largely implemented within the active tectonic studies, including a better understanding of the Pleistocene regional geomorphology through the improvement of analytical modeling of large-scale landscape features.

In Italy, the active faults identification process, and the direct estimation of their seismogenic potential, is still characterized by uncertainties and debated interpretations (Bosi, 1975; Scandone et al., 1992; Michetti et al., 2000). However, during the last decades new models and methods of investigation have been developed to identify and depict the seismogenic sources associated to large historical earthquakes. Only in recent time, a homogeneous and updatable database of possible seismogenic sources for medium to large size seismic events has been compiled by the Istituto Nazionale di Geofisica e Vulcanologia (INGV). It is a georeferenced repository of tectonic, faults and paleoseismological information for the Italian territory and surrounding area (Database of Individual Seismogenic Sources - DISS Working Group, 2021, online available at <https://diss.ingv.it/>).

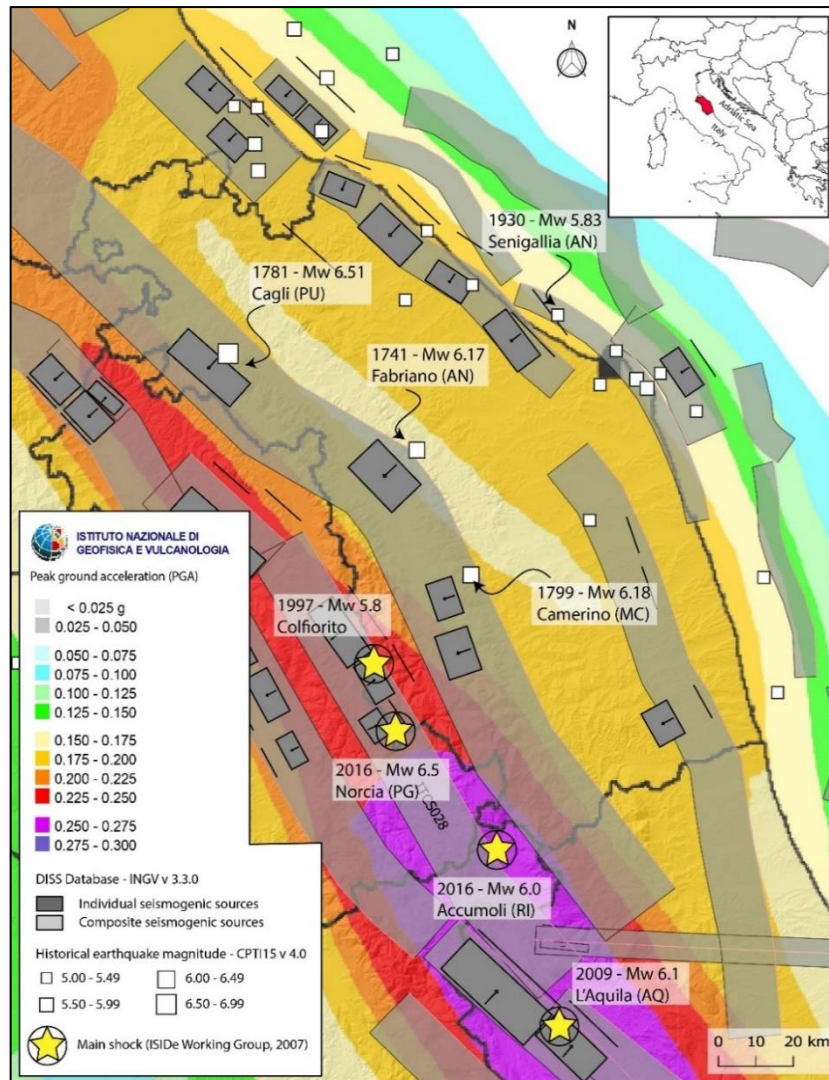


Fig. 1.1 - Seismic hazard map of the study area (MPS04 modified after Stucchi et al. 2004). The main shocks of the major seismic sequences affecting the central Apennine in the last decades are plotted using the location from the ISIDe database (ISIDe Working Group. 2007), The light grey polygons represent the composite seismicogenic sources and the dark polygons are the individual seismicogenic sources according to the Database of Individual Seismogenic Sources (Basili et al., 2008; DISS Working Group 2021). White squares represent historical earthquakes by CPTIv4.0 catalog (Rovida A., 2022).

Despite the latest important update of the published DISS database, several historical earthquakes still do not have an associated seismicogenic source with surface evidence, and at the same time, several faults interpreted as active, do not have historical earthquakes that could prove this assumption. These examples well represent the situation of the central Apennine, where several structures are debated. The absence or the ambiguity of this information make any seismic risk mitigation planning difficult.

## 1.1. Study aims

The huge amount of seismic energy released in historical time (Locati M., et al. 2022; Rovida A., 2022: both available online at <https://emidius.mi.ingv.it/CPTI15-DBMI15>) and since the advent of instrumental measures (ISIDe Working Group. 2007) in Italy, together with the important social and economic effects associated with earthquakes, encourage the scientists to make new important progresses in the seismic hazard models – MPS04 (Stucchi M. et al. 2004). The application of a multidisciplinary approach, consisting in a combination of data derived from geology, geomorphology, seismology, and modeling may represent the reading key in a post-seismic building reconstruction and in the seismic risk mitigation, allowing the identification and characterization of important seismogenic structures.

The present study was performed for the topic ‘Natural disasters risk reduction - Geoenvironmental monitoring and modeling in seismic area’, in the frame of “Dottorato Innovativo” promoted by the Regione Marche. The partnership with research institutions has seen the collaboration with REDI (REducing risks of natural DISasters ([www.redi-research.eu](http://www.redi-research.eu)), a research consortium for innovation and training. The mission is to contribute to interdisciplinary research-actions to boost community disaster preparedness, response, and recovery.

Two main aims are considered for this PhD work:

- 1) the identification of seismogenic sources through a multidisciplinary approach based on field observation, seismological, geophysical and remote sensing data through the integration of seismotectonic and morphotectonic investigations;
- 2) a substantial contribution to the knowledge of the neotectonic activity of the study areas through the identification and characterization of the seismogenic faults geometries in areas of central Apennines characterized by outcropping/ buried and/or active/silent faults.

Finally, the results of this study together with other tools funded by the Public Administrations, such as Seismic Microzonation Studies, can contribute to a better urban planning of the territory in areas already stricken by earthquakes, and assist the reconstruction phase, but especially in territories characterized by a silent seismic activity, can contribute to mitigating the risk associated with strong earthquakes and related coseismic effects at surface.

## 1.2. Identification and characterization of seismic sources: state of the art

In tectonically complex areas such as the central Apennine or the outer sector of the Marche Region, the identification of active seismogenic sources is often difficult (Brozzetti et al., 2017). This is mainly due to their polyphasic (e.g., compressive and extensional) tectonic history and to the different juxtaposed lithological sequences that may obliterate or even hide surface geological evidence of the faults presence (Lettis et al., 1997; Mirabella et al., 2022). On the other hand, seismological and geophysical data themselves may not be sufficient to identify seismogenic sources because of the irregular geometry of faults (Bally & Snelson, 1980; Wernicke & Burchfiel, 1982; Suppe, 1983; Gibbs, 1984 among many others).

In summary, the identification and characterization of seismogenic faults are often influenced by several issues, which can be described as follows:

- seismicity data accuracy: catalogue-based studies are clearly of central importance in seismotectonic studies to investigate the spatio-temporal and size distribution of seismicity in specified study areas (Renner & Slejko, 1994; Mazzoli et al., 2014; Barchi & Collettini, 2019; Miccolis et al., 2021; Tondi et al., 2021). However, uncertainties in location of seismic events (horizontal and vertical component) and magnitudes reported in seismic catalogues (Scudero et al., 2021) may significantly change the estimation of the derived parameters. In this regard, the identification of earthquake sources based on instrumental seismicity and historical earthquakes (Rovida, A. et al., 2016) is difficult due to poor accuracy in the epicenter identification and magnitude calculation, related to an insufficient seismic network. In fact, different degrees of accuracy in the seismological datasets, make the correlation between fault trace and clusters of hypocenters difficult or impossible (Jackson and White, 1989; Collettini & Sibson, 2001);
- low strain rate: the relatively low seismic activity in regions affected by low strain rates (Caporali et al., 2003; Galvani et al., 2012; Serpelloni et al., 2021) complicates the geologists' work, because the presence of active faulting at surface is unclear and their interpretation is controversial (Chiaraluce et al., 2005). Within the multiphases tectonic of Central Apennines, the currently active tectonic regime began in relatively recent times and thus the younger active faults may not have developed yet a clear geological and geomorphological evidence at surface. On the contrary, older tectonic structures would be still undoubtedly recognizable in the field, and they could easily reactivate sympathetically, thus appearing active in the geological record, if the fault is well oriented with respect to the present stress field;

- hidden or blind structures: in the study area, only limited portions of active brittle fault zones are exposed at the surface, due to the combination of limited exhumation rates and erosion (Roberts & Michetti, 2004; Wegmann & Pazzaglia, 2009). In fact, many seismically active structures are hidden or blind due to the presence of thick siliclastic deposits, like in the Periadriatic foothill, which bury active external front of the fault and thrust belt (Miccadei et al., 2021). Furthermore, the intense and diffuse human activity (Coltorti, 1997) and the high erosion rate (Buccolini et al., 2010), both quite common in tectonically active region, tend to obliterate the superficial earthquake imprints making the identification of active features possible only using an indirect approach. Inland, recent, or ongoing tectonic activity and fault reactivation in individual seismic events can be studied by analyzing geologic exposures (Galadini et al., 2001; Faure Walker et al., 2021) or by detecting river drainage anomalies (Di Bucci et al., 2003; Mayer et al., 2003; Della Seta et al., 2008; Nesci et al., 2012);

In order to solve the above-mentioned issues, a multi-methodological approach was adopted in this thesis to investigate the neotectonics activity of the central Apennines. It consists in an integration of geology surface data, deep seismic reflection profiles interpretation and seismological analysis. This approach allows identifying the major seismogenic sources and hence their geometry and kinematics within a specific study area (Massa & Zuppetta, 2009; Bello et al., 2021; Ferrarini et al., 2021; Boncio et al., 2021). However, the morphotectonic analysis is also integrated to reveal active tectonics along the Marche Periadriatic sector, representing one of the first attempt in this area.

The multi-disciplinary data analysis is based on available catalogs in GIS (Geographic Information System) environment, which integrates faults, instrumental seismicity, historical earthquakes, morphometric parameters by DTM (Digital Terrain Model), processing and interpretation of high resolution deep seismic reflection profiles from petroleum industry (ENI S.p.A.) and from open-source catalogues (Tab. 1).

The seismotectonic database for the present study is in GIS environment (software used: QGIS), and includes different available datasets like active faults, instrumental and historical earthquake catalogues, moment tensor, crustal thickness estimates and morphometric parameters derived by DTM analysis. The repository of active faults was created collecting geometries provided by the DISS (DISS Working Group 2021, <https://diss.ingv.it/>), a set of potential seismogenic sources linked to earthquakes larger than M 5.5, in Italy and surrounding areas, and active and capable faults from ITHACA (ITHACA Working Group, 2019,

<http://sgi.isprambiente.it/ithaca>). Furthermore, various geological and structural maps derived from published articles have been used to consider surface data at different scales in the present study (Mazzoli et al., 2005; Pierantoni et al., 2013; Chicco et al., 2019; Conti et al., 2020).

Among the major steps in seismic hazard assessments, a complete list of earthquakes and their characteristics is essential. This includes instrumental data derived from both online catalogues and literature (ISIDe Working Group, 2007; Cattaneo et al., 2017; Spallarossa et al., 2021). The basic reference for the historical earthquakes in Italy is represented by the CPTI15-DBMI15 v4.0 – INGV, which includes parametric earthquake information, from 1000 AD to 2020 AD. Focal mechanisms, used to perform the stress inversion analysis and stress field reconstruction are from the RCMT catalogue (Pondrelli S. et al. 2002, <http://rcmt2.bo.ingv.it/>), the Beach Balls catalogue of INGV Ancona (Monachesi G. et al. 2021, [www.an.ingv.it](http://www.an.ingv.it)), and from literature (Santini et al., 2011; Mazzoli et al., 2014). These data collection have been largely used in all the chapters for the fault’s delineation. The built database is available and attached to this thesis.

CATEGORY	LAYER NAME	GIS FEATURE TYPE	DATA SOURCE
Geology	ITHACA	Shapefile (lines)	<a href="http://sgi2.isprambiente.it">http://sgi2.isprambiente.it</a>
	DISS	Shapefile (lines+polygons)	<a href="https://diss.ingv.it">https://diss.ingv.it</a>
	Geological map	Shapefile (lines+polygons)	<a href="https://www.geological-map.it">https://www.geological-map.it</a>
Focal Mechanism Solutions	INGV_RCMT catalogue	Shapefile (points)	<a href="http://rcmt2.bo.ingv.it">http://rcmt2.bo.ingv.it</a>
	INGV_BB catalogue	Shapefile (points)	<a href="http://www.an.ingv.it">http://www.an.ingv.it</a>
	FMS_ (others by literature)	Shapefile (points)	
Seismic hazard map	ESHM2020_Europe	Raster	<a href="http://efehrcms.ethz.ch">http://efehrcms.ethz.ch</a>
	MPS04_Italy	Raster	<a href="https://data.ingv.it">https://data.ingv.it</a>
Instrumental seismicity	INGV_ISIDe	Shapefile (points)	<a href="http://iside.rm.ingv.it">http://iside.rm.ingv.it</a>
	INGV_2009-2016	Shapefile (points)	<a href="https://www.annalsofgeophysics.eu">https://www.annalsofgeophysics.eu</a>
	Spallarossa et al. 2021	Shapefile (points)	<a href="https://zenodo.org">https://zenodo.org</a>
Historical seismicity	INGV_CPTI15-DBMI15	Shapefile (points)	<a href="https://emidius.mi.ingv.it">https://emidius.mi.ingv.it</a>
Seismic reflection profiles	ENI S.p.A.	Shapefile (lines+points)	ENI data room
	ViDEPI project	Shapefile (lines+points)	<a href="https://www.videpi.com">https://www.videpi.com</a>
DEM	NASA_30m_AsterGDEM	Raster	<a href="https://asterweb.jpl.nasa.gov">https://asterweb.jpl.nasa.gov</a>

Tab. 1.1 - GIS input data used in the present work.



Data from the overseas were also investigated and used to calibrate the methodology. This is the case of the 2019-2020 Albania seismic sequence (Mw 6.4 main shock), chosen because it represents an analogue that can be combined to better support the results from the central Apennines (Fig. 1.2). In fact, the Durres region is characterized by the presence of buried faults covered by a thick Neogene siliciclastic deposits (similar to the Adriatic foothill). In this regard, the occurrence of a moderate seismic sequence provided new geological and seismological constrain for seismogenic source identification. This in turn may play a key role in the building of a reliable seismic hazard evaluation.

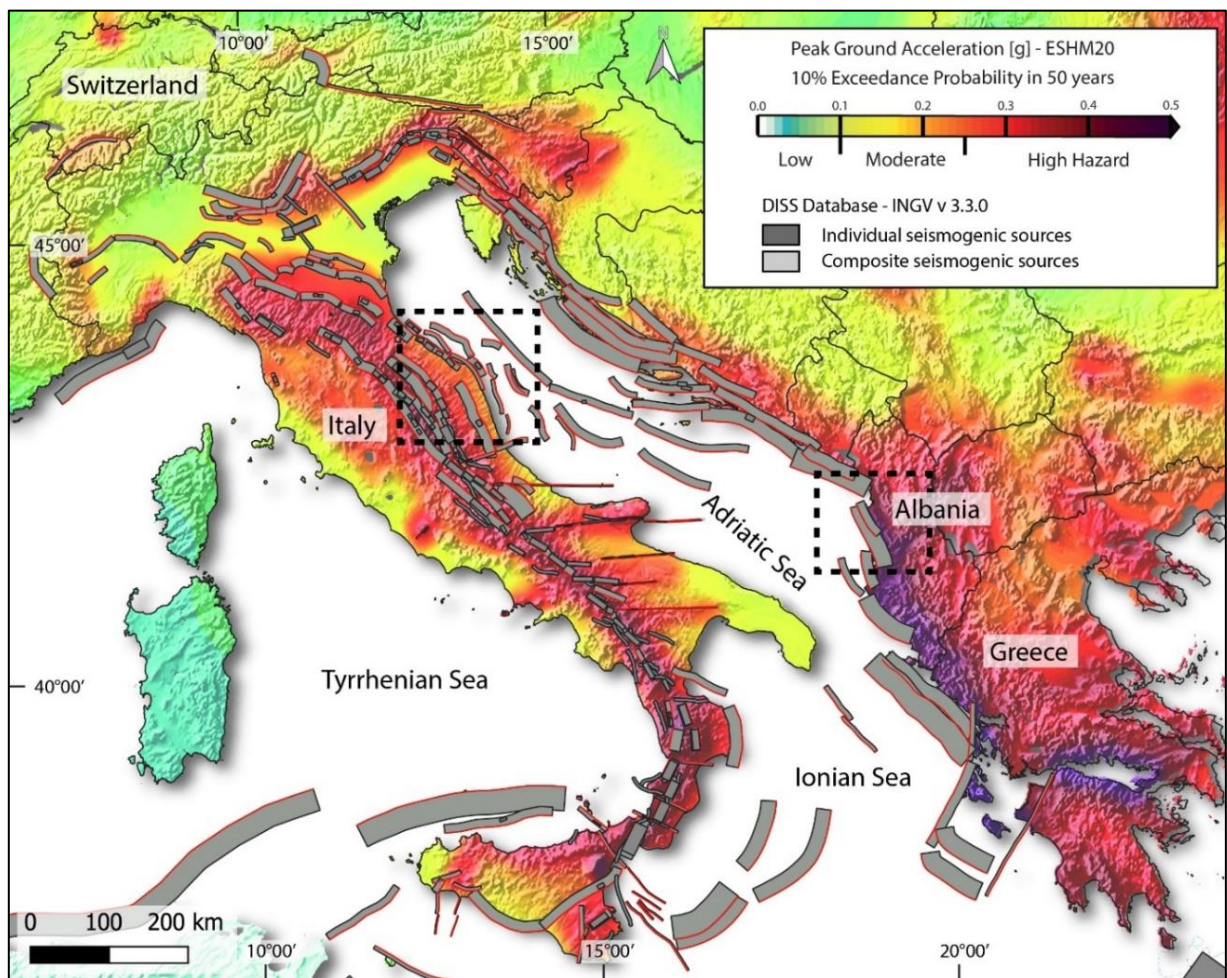


Fig. 1.2 - The European Seismic Hazard Map (ESHM2020 – Danciu et al. 2021) displays the ground shaking (i.e. Peak Horizontal Ground Acceleration) to be reached or exceeded with a 10% probability in 50 years, corresponding to the average recurrence of such ground motions every 475 years. Low hazard areas ( $PGA \leq 0.1g$ ) are colored in blue-green, moderate hazard areas in yellow-orange and high hazard areas ( $PGA > 0.25g$ ) in red. The study areas are represented in back dotted squares: i) the Albania pilot case study; ii) the Adriatic sector of central Apennines.

The 30 meters resolution NASA – AsterDEM (<https://asterweb.jpl.nasa.gov>) is the starting point for the morphotectonic analysis in chapter 5. The DTM analysis, using several ArcGIS plug-ins and MATLAB toolkits (Schwanghart & Scherler, 2014) allowed to provide new morphometric features like knickpoints, the normalized steepness index (ksn) and map of areas affected by uplift or denudation processes (Burbank and Anderson, 2001; Bull, 2008).

### **1.3. Integrated, multidisciplinary adopted methods: their potential and limitations**

**Preliminary processes and interpretation of seismic reflection profiles:** the seismic reflection survey in the Apennines is very challenging due to the mechanical properties of outcropping and subsurface lithologies (fractured Mesozoic-Paleogene carbonate succession) which greatly hinder the penetration of seismic signal, and to a remarkably complex structural setting. In addition, available seismic data are acquired and processed for deep targets, using the technology available in the early 1980s (Stucchi et al. 2006).

In the present work, SW-NE and NW-SE seismic reflection profiles kindly provided by ENI S.p.A. and available from ViDEPI project (see Fig. 1.3 for the location) are interpreted to identify and characterize the geometry of active faults in the Umbria-Marche Apennines and foothills.

The seismic profiles are calibrated using well logs, geological sections proposed by Coward et al. (1999) and Mazzoli et al. (2005) and the available geological maps (Centamore et al. 1991, Pierantoni et al. 2013, Conti et al., 2020).

The ENI seismic profiles are migrated, whereas the ViDEPI profiles are stacked and interpreted. Both ENI and ViDEPI seismic profiles are in raster format and interpreted or re-interpreted for the purposes of this work.

All the seismic profiles are adapted at the same scale (1: 100 000 horizontal scale and 2 cm s<sup>-1</sup> vertical scale) to obtain homogeneous and comparable features. Based on previously published data (Maesano et al. 2013) and other studies focused on the Outer Marche Region (Chicco et al., 2019; Pierantoni et al., 2019), a velocity of 2 km s<sup>-1</sup> is assumed for the Plio-Quaternary sequence, giving rise to an almost identical scale in two dimensions for all the profiles. For the underlying successions, the velocity gradually increases up to 6 km s<sup>-1</sup> for the Anidriti di Burano Formation and the crystalline basement (Mirabella et al. 2008; Porreca et al. 2018). The assumed velocity implies an adequately accurate fault planes inclination and the thickness of

the Plio-Quaternary sequences (over the top-Messinian), whereas below this horizon the dip angle of the fault planes should be even higher than that described in the interpretation of the seismic profile.

The Miocene–Quaternary tectonic evolution is constrained based on the recognition of the top-Messinian (locally top-pre-Pliocene) and near-top-Lower Pliocene seismo-stratigraphic markers. These latter are reconstructed directly within the transects using the well logs or based on the intersections with other seismic profiles. The base of the Quaternary sequence is also highlighted where possible and the Quaternary sequence itself is separated from the Upper Pliocene sequence. In some cases, the base of the Quaternary is only a geometric surface and not constituting synchronous horizons.

**Seismological and seismotectonic investigation:** the instrumental seismicity is generally extracted by the ISIDe catalogue (Fig. 1.3, ISIDe Working Group, 2007) providing earthquake parameters since 1985 from the Italian National Seismic Network and obtained by integrating locations performed in near-real time with data from the Italian Seismic Bulletin. The seismological database of the 2016-2017 Amatrice-Visso-Norcia seismic sequence is provided by Spallarossa et al. (2021). The dataset contains re-localized earthquakes recorded by the permanent Italian National Seismic Network (RSNC) and was enhanced during the sequence by temporary stations deployed by the INGV and the British Geological Survey. All the data are then filtered deleting the earthquake with horizontal error  $erh > 2.5$  km, vertical error  $erz > 2.5$  km, which are considered reliable to avoid uncertainties due to epicenters position and hypocenter artefacts (10 km fixed depth). For inland earthquakes, this method can provide an accurate estimation owing to the densely located seismic stations and good azimuthal coverage. However, as all the stations are inland, there is an higher location error for offshore earthquakes. In this regard, the seismic catalogue for central-eastern Italy proposed by Cattaneo et al. (2017) is used to perform high accuracy seismic analysis of offshore events.

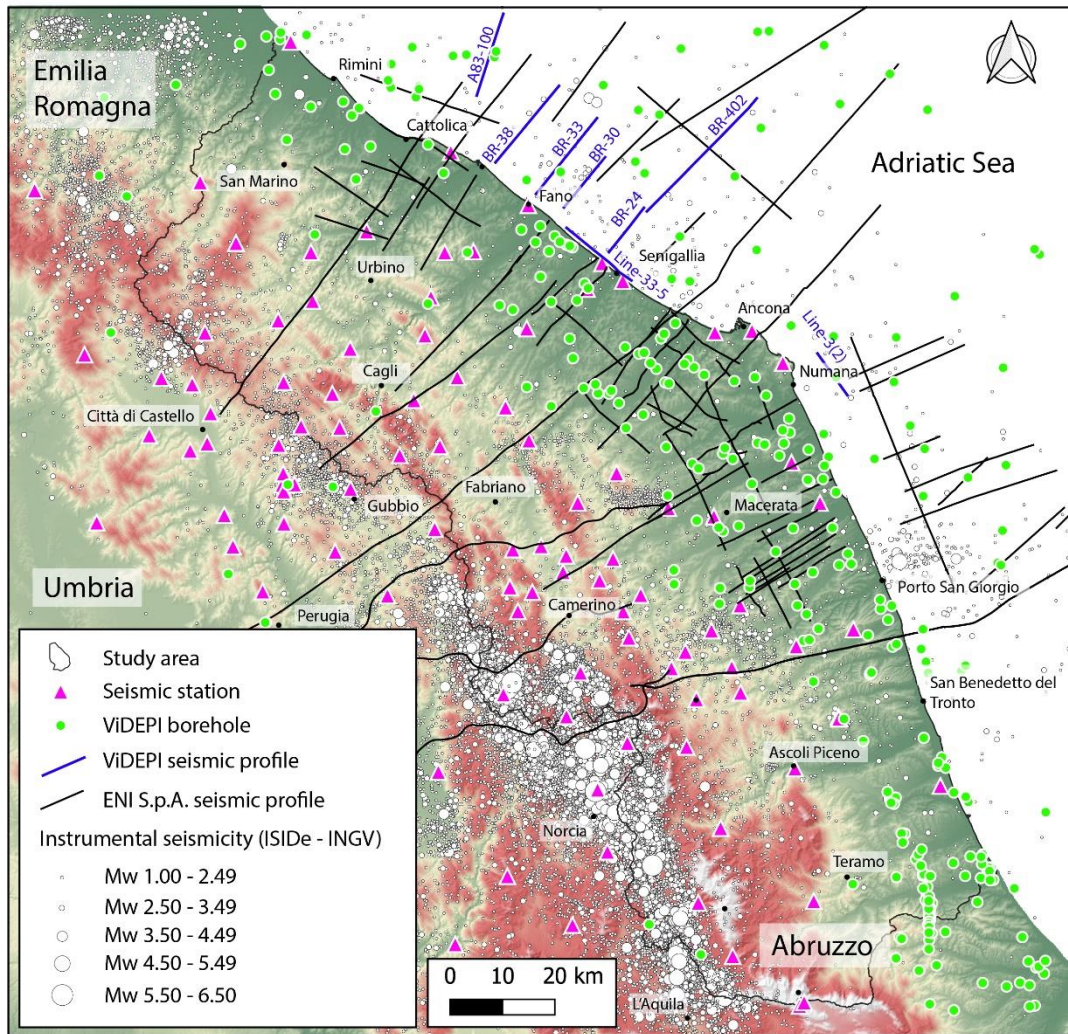


Fig. 1.3 – Elevation map (performed by 30 m NASA AsterDEM) showing the distribution of the ENI s.p.a. and ViDEPI seismic reflection profiles (respectively in black and blue lines) and boreholes (green circles) used in this study. The instrumental seismicity recorded by INGV seismic stations (magenta triangles) and provided by the ISIDe on-line catalogue (ISIDe Working Group, 2007) is also shown.

The focal mechanisms used to perform the stress field analysis are generally provided by the *European-Mediterranean Regional Centroid Moment Tensors (RCMT)* catalogue (Pondrelli et al. 2002, <http://rcmt2.bo.ingv.it/>) that collects seismic moment tensor solutions that are routinely computed since 1997 for earthquakes with moderate magnitude ( $M > 4.5$ ) in the Mediterranean region. The RCMT method represents an extension of the standard CMT algorithm using the inversion of intermediate period surface waves of seismograms recorded by MedNet (Mediterranean Network) at regional distance, and allowing to compute moment tensors also for moderate events ( $4.5 < M < 5.5$ ) with similar reliability as given by the standard CMT analysis (Ekström et al., 1998, Pondrelli et al. 2002).

In order to perform the stress field analysis also for baseline seismicity ( $M < 4$ ), the FMS are provided by the Beach Balls (BB) catalogue of INGV Ancona (Monachesi G. et al. 2021, [www.an.ingv.it](http://www.an.ingv.it)).

In this dataset, data having more than 24 polarities are extracted by the ReSIICO seismic network for seismic events (magenta triangles in figure 1.3, Cattaneo et al., 2019) and the localization are calculated by *Hypoellipse* software (set up model in Tab. 1.2). The focal mechanism solutions are calculated by FPFIT, a Fortran software for the calculation and visualization of FMS (Reasenberg, 1985). During this step, the seismic events having horizontal and vertical errors higher than 10 km are automatically deleted.

<i>Reset Test</i>		<i>Velocity model</i>		<i>Option card</i>	
1	1.87	04.50	000.00	MISSING STATIONS	1
2	0	05.00	001.00	GLOBAL OPTION	1
7	25	05.50	002.00	MAGNITUDE OPTION	3
10	3	06.20	004.00	TABULATION OPTION	4
11	15	06.30	010.00	SUMMARY OPTION	2
12	90	07.00	025.00	PRINTER OPTION	0
14	3	08.00	030.50	BLANK SOURCE	V
15	3			WEIGHT OPTION	1.33 2. 4.
18	3			TABULATION OPTION	-4
19	0.2				
21	30				

Tab. 1.2 – Crustal model and set up used by Monachesi et al. 2021 in *Hypoellipse* software for the seismic events localization.

The WinTensor software is used to calculate the active stress (Delvaux and Sperner 2003) starting from the nodal planes of the fault plane solutions provided by the previously mentioned catalogues.

The analysis is performed applying three different methods: (1) the PBT kinematic axes method (Turner 1953); (2) the improved version of the right dihedron method of Angelier and Mechler (1977); and (3) the rotational optimization method proposed by Delvaux and Sperner (2003).

The PBT kinematic axes method is largely used in structural geology. It is based on the Mohr–Coulomb fracture criterion and calculates the stresses from the orientation of single fault planes, where P is the compression axis, B is the neutral axis (contained in the fault plane) and T is the extension axis (Sippel et al. 2009). This method can be applied assuming that all the faults are formed and moved by the same stress field.

The improved right dihedron method allows to obtaine four parameters of the reduced stress tensor: the principal stress axes  $\sigma_1$  (maximum compression),  $\sigma_2$  (intermediate compression) and  $\sigma_3$  (minimum compression) and the stress ratio R (also defined as stress regime; [Angelier 1989](#)),

where

$$R = \frac{\sigma_2 - \sigma_3}{\sigma_1 - \sigma_3}$$

The stress ratio is a well-defined, useful indicator of the state of stress.  $R = 0$  or  $R = 1$  defines an axial state of stress characterized by  $\sigma_1 > \sigma_2 = \sigma_3$  or  $\sigma_2 > \sigma_3$  respectively. Otherwise, a value of  $0 < R < 1$  indicates a triaxial state of stress.

The rotational optimization method is an inversion procedure included in WinTensor that allows the misfits using both nodal planes of the focal mechanism to be decreased. In this procedure, the software considers the plane having the smaller misfit value as active. The average misfit angle and the quality of the stress tensor estimation are expressed on a scale ranging from A (best result) to E (worst result) according to the World Stress Map quality ranking scheme (Heidbach et al. 2016; [www.world-stress-map.org/](http://www.world-stress-map.org/)).

**The analysis of the digital elevation models (DEM) in the morphometrical studies of the landscape:** the geomorphic and morphometrical characteristics of the central Apennines and Marche foothills have been investigated using the 30-m resolution DEM data derived from NASA ASTER imagery, downloaded for free from the website <https://asterweb.jpl.nasa.gov/gdem.asp> (released on August 5, 2019).

The digital elevation model is created from remote sensing data and usually contain anomalies and holes associated to extreme relief, water bodies and cloud cover (Wobus et al., 2006) and before to be analysed for the morphotectonic investigation, a preliminary process in ArcGIS environment is needed.

The fill function (hydrology add-in tools) is used to fill the artefact and the flow direction, flow accumulation, watershed, and stream order algorithms are then performed to extract the river network and river long profiles from the Uso River to the north to the Vomano River to the south (blue lines in Fig. 1.4).

The river long profiles, having a longitudinal trend perpendicular to the trend of the chain, are analyzed to detect tectonic signals on the different sides of the mountain range (e.g., knickpoint/knickzones) and although river network occupies a small portion of the land surface,

a longitudinal river profile is one of the most sensitive indicators of rock uplift rate than other morphological properties (Whipple et al., 2007).

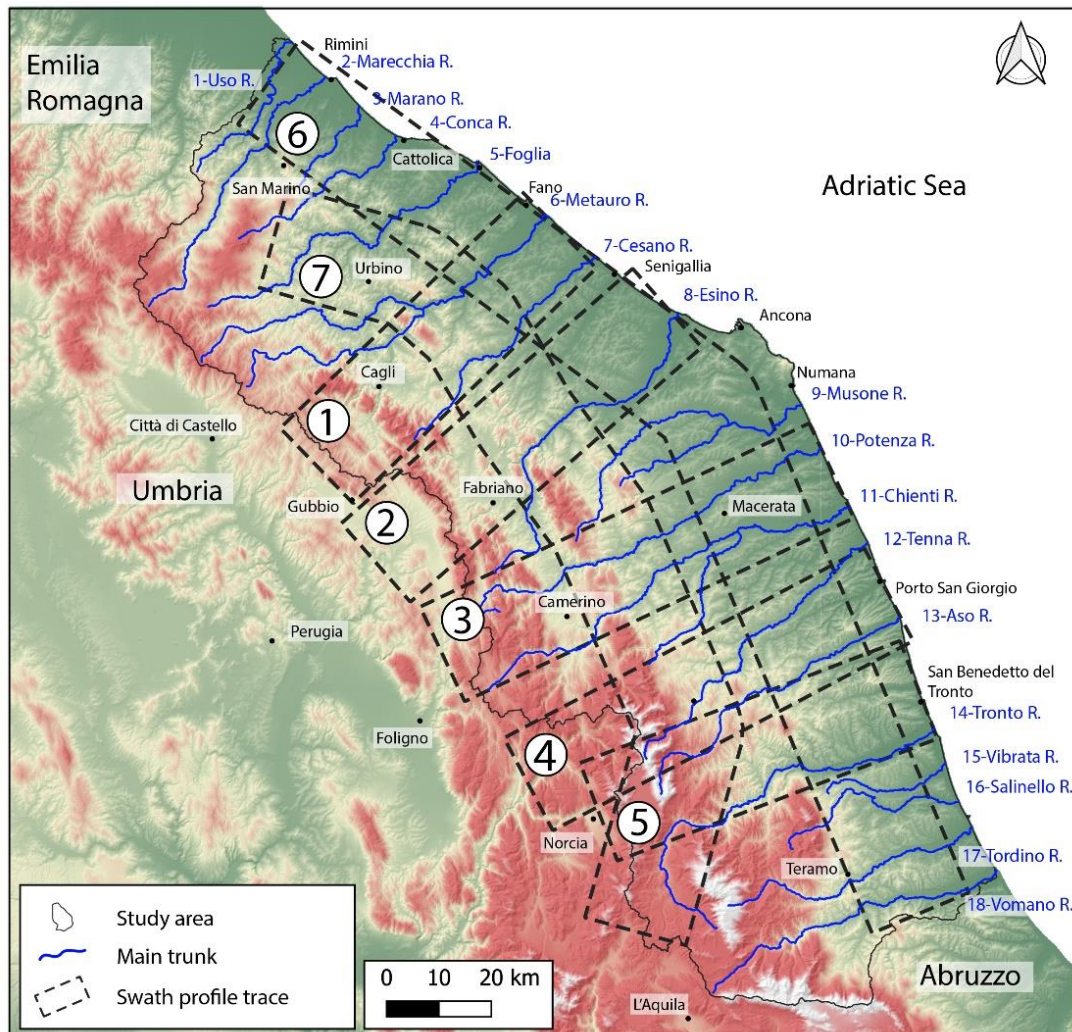


Fig. 1.4 - Elevation map (performed by 30 m NASA AsterDEM) of the Umbria-Marche Apennines showing the location of the investigated main trunks (blue lines), and 20 km wide swath profiles analyzed in Chapter 5.

The 20 km large swath profiles (dashed polygons in Fig. 1.4) are extracted by the *SwathProfiler* ArcGIS tool (Pérez-Peña et al., 2017) and analyzed to detect anomalies in elevation changes of the topographic surface. They are automatically delineated showing statistical values such as the minimum, mean, maximum and local relief (maximum-minimum elevation).

The filled DEM and the drainage pattern are then used to perform the slope/area analysis within the study area (Fig. 1.4) and to derive the spatial distribution of the normalized channel steepness index ( $K_{sn}$ ) by Topotoolbox, a MATLAB-based software (Schwanghart & Scherler, 2014).

## 1.4. Thesis structure

This thesis deals with interdisciplinary research to define the active and potentially seismogenic sources of the central Apennine. New seismotectonic and morphotectonic studies are integrated with geology survey and seismic reflection data from O&G industry (ENI S.p.A) to investigate the neo-tectonic activity in this area.

The combination of these methodologies allowed the identification of ENE-WSW inherited fault segments in the Marche Region. The baseline seismicity and the available focal mechanisms have been used to characterize their geometry and kinematics. The morphotectonic studies highlighted the active/passive role of these transversal structure, acting as seismogenic sources in the outer sector and passive barriers along the Apennine chain, confining the seismic sequence. In detail:

- **Chapter 2 – *The use of high-resolution seismological data in seismotectonic analysis for the identification of the 2019-2020 Albania seismic sequence.***

This work represents a pilot study applying a multidisciplinary approach aimed for seismic sources characterization related to the 2019 Albania seismic sequence. We address geometric and kinematic properties of the Mw 6.4 26 November 2019 Durrës earthquake, the strongest earthquake in Albania in the past 40 years. For this pilot study the instrumental baseline seismicity since 1985 provided by the INGV- ISIDE catalogue (ISIDE Working Group, 2007) have been used to improve the seismotectonic understanding of the Durres region. Furthermore, the focal mechanism from the RCMT catalogue (Pondrelli, et al 2002) are then used to perform the stress inversion analysis by Win Tensor Software (Delvaux & Sperner, 2003) confirming an ENE-trending horizontal maximum compression. Finally, the identification of the Northern Albanides Front Thrust (NAFT) has been constrained by well, geological and seismic data. (Teloni, S., Invernizzi, C., Mazzoli, S., Pierantoni, P. P., & Spina, V. (2021). Seismogenic fault system of the Mw 6.4 November 2019 Albania earthquake: new insights into the structural architecture and active tectonic setting of the outer Albanides. *Journal of the Geological Society*, 178(2). <https://doi.org/10.1144/jgs2020-193>)

- **Chapter 3 – *Defining the structural setting of the Southern Marche outer sector by seismic profiles interpretation.***

The present analysis is based on several subsurface seismic reflection profiles and well data, kindly provided by ENI S.p.A. and available on the VIDEPI project ([www.videpi.com](http://www.videpi.com)), together with surface geologic–stratigraphic knowledge of Plio–



Quaternary evolution from the literature. The seismic profiles, have been used to draw five transects allowing the identification of a series of NNW-SSE structures, interrupted by a major ENE–WSW transversal fault located south to the Conero promontory, and the reconstruction of the Plio-Quaternary evolution of the outer Marche southern sector. The activity of this structure has been constrained by the involvement of Quaternary deposits in deformation processes, instrumental seismicity, and focal mechanisms. (Costa, M., Chicco, J., Invernizzi, C., Teloni, S., & Pierantoni, P. P. (2021). Plio–Quaternary Structural Evolution of the Outer Sector of the Marche Apennines South of the Conero Promontory, Italy. *Geosciences*, 11(5)).

- **Chapter 4 – *Faults characterization and seismological analysis through instrumental seismicity in the Adriatic sector of central Apennines.***

The instrumental-baseline seismicity ( $M_w > 1.5$ ) from ISIDe catalogue (ISIDe Working Group 2007) has been used with the aim of detecting the active structures and clarifying the seismotectonic framework of this area of the outer sector of the Apennine chain. In particular, the distribution of these seismic sequences (swarm) allowed to identify four major fault systems and the stress inversion analysis performed by WinTensor software using focal mechanisms indicate the presence of active and deeply rooted NE-SW strike slip faults related to a local N-S compression. (Costa, M., Pierantoni, P. P., Teloni, S., Invernizzi, C. - Active transversal structures on the Outer Marche Apennines (Italy): structural characteristics and seismological evidence – submitted on 16 May 2022)

- **Chapter 5 – *Morphological evidence of crustal blocks vertical motion in central Apennines based on a large-scale morphotectonic approach.***

A large-scale morphotectonic approach carried out on major catchments of Marche Region and surrounding area, combined with geological and seismological data, has been used to highlight the role of active tectonics at surface and to describe differences in the Quaternary evolution of outer central Apennines and foothills, providing information for the correct assessment of earthquake hazard in a large and densely populated area of Emilia-Romagna, Marche and Abruzzo Region. (Teloni S., Valente E., Ascione, A., Mazzoli S., Pierantoni P. P., Invernizzi C. - Morphostructural evidence of active along-strike segmentation of the Umbria-Marche Apennines, Italy – Under submission).

- **Chapter 6 – *Discussions and conclusions.***

Results of the present PhD work are summarized and discussed to highlight their implications and some new perspectives and possible contribution into seismic hazard assessment.

## 1.5. References

- Angelier, J., & Mechler, P. (1977). Sur une methode graphique de recherche des contraintes principales egalement utilisables en tectonique et en seismologie: la methode des diedres droits. *Bulletin de la Société géologique de France*, 7(6), 1309-1318
- Angelier, J. (1989). From orientation to magnitudes in paleostress determinations using fault slip data. *Journal of structural geology*, 11(1-2), 37-50
- Azzaro R., D'Amico S., Mostaccio A., Scarfi L., Tuvè T., 2016. Rilievo macrosismico del terremoto ibleo dell'8 febbraio 2016 - ore 16:35 locali - Relazione. Istituto Nazionale di Geofisica e Vulcanologia (INGV), Catania, 6 pp. <https://doi.org/10.13127/QUEST/20160208>
- Bally, A. W., & Snelson, S. (1980). Realms of subsidence.
- Barchi, M. R., & Collettini, C. (2019). Seismicity of central Italy in the context of the geological history of the Umbria-Marche Apennines. *Special Paper of the Geological Society of America*, 542. <https://doi.org/10.1130/2019.2542> (09)
- Basili, R., Valensise, G., Vannoli, P., Burrato, P., Fracassi, U., Mariano, S., Tiberti, M. M., & Boschi, E. (2008). The Database of Individual Seismogenic Sources (DISS), version 3: Summarizing 20 years of research on Italy's earthquake geology. *Tectonophysics*, 453(1-4). <https://doi.org/10.1016/j.tecto.2007.04.014>
- Bello, S., de Nardis, R., Scarpa, R., Brozzetti, F., Cirillo, D., Ferrarini, F., di Lieto, B., Arrowsmith, R. J., & Lavecchia, G. (2021). Fault Pattern and Seismotectonic Style of the Campania – Lucania 1980 Earthquake (Mw 6.9, Southern Italy): New Multidisciplinary Constraints. *Frontiers in Earth Science*, 8. <https://doi.org/10.3389/feart.2020.608063>
- Boncio, P., Lavecchia, G., Milana, G., & Rozzi, B. (2021). Seismogenesis in Central Apennines, Italy: an integrated analysis of minor earthquake sequences and structural data in the Amatrice-Campotosto area. *Annals of Geophysics*, 47(6). <https://doi.org/10.4401/ag-3371>
- Boncio, P., Lavecchia, G., & Pace, B. (2004). Defining a model of 3D seismogenic sources for Seismic Hazard Assessment applications: The case of central Apennines (Italy). *Journal of Seismology*, 8(3).
- Bonini, L., Maesano, F. E., Basili, R., Burrato, P., Carafa, M. M. C., Fracassi, U., Kastelic, V., Tarabusi, G., Tiberti, M. M., Vannoli, P., & Valensise, G. (2016). Imaging the tectonic framework of the 24 August 2016, Amatrice (central Italy) earthquake sequence: New roles for old players? *Annals of Geophysics*, 59(FastTrack5). <https://doi.org/10.4401/ag-7229>

- Bosi, C. 1975. Preliminary observations on probably active faults in the central Apennines, *Bollettino della Societa Geologica Italiana*, vol.94, 4, pp.827-859.
- Bally, A. W., & Snelson, S. (1980). REALMS OF SUBSIDENCE. Memoir - Canadian Society of Petroleum Geologists.
- Brozzetti, F., Cirillo, D., de Nardis, R., Cardinali, M., Lavecchia, G., Orecchio, B., Presti, D., & Totaro, C. (2017). Newly identified active faults in the Pollino seismic gap, southern Italy, and their seismotectonic significance. *Journal of Structural Geology*, 94, 13–31. <https://doi.org/10.1016/j.jsg.2016.10.005>
- Buccolini, M., Gentili, B., Materazzi, M., & Piacentini, T. (2010). Late Quaternary geomorphological evolution and erosion rates in the clayey peri-Adriatic belt (central Italy). *Geomorphology*, 116(1–2). <https://doi.org/10.1016/j.geomorph.2009.10.015>
- Bull, W. B. (2008). Tectonic Geomorphology of Mountains: A New Approach to Paleoseismology. <https://doi.org/10.1002/9780470692318>
- Burbank and Anderson. (2001). *Tectonic Geomorphology*. John Wiley & Sons, Chichester.
- Caporali, A., Martin, S., & Massironi, M. (2003). Average strain rate in the Italian crust inferred from a permanent GPS network - II. Strain rate versus seismicity and structural geology. *Geophysical Journal International*, 155(1). <https://doi.org/10.1046/j.1365-246X.2003.02035.x>
- Cattaneo, M., Frapiccini, M., Ladina, C., Marzorati, S., & Monachesi, G. (2017). A mixed automatic-manual seismic catalog for central-eastern Italy: Analysis of homogeneity. *Annals of Geophysics*, 60(6). <https://doi.org/10.4401/AG-7333>
- Cattaneo M., Monachesi G., Frapiccini M., Calamita C., Pantaleo D., Carluccio I., Ladina C., Marzorati S. (2019). ReSIICOeqs. Database of the Central Eastern Italy Seismometric Network: locations [Data set]. Istituto Nazionale di Geofisica e Vulcanologia (INGV). <https://doi.org/10.13127/resiico/eqs>
- Centamore, E., Pambianchi, G. et al. 1991. Ambiente fisico delle Marche: geologia – geomorfologia– idrogeologia, Regione Marche, Giunta Regionale scala 1:100.000 (W 0°21’–E 1°30’/N 44°00’–N 42°40). *Studi Geologici Camerti*, 1991/2, 125–131
- Chiaraluce, L., Barchi, M., Collettini, C., Mirabella, F., & Pucci, S. (2005). Connecting seismically active normal faults with Quaternary geological structures in a complex extensional environment: The Colfiorito 1997 case history (northern Apennines, Italy). *Tectonics*, 24(1). <https://doi.org/10.1029/2004TC001627>

- Chicco, J. M., Pierantoni, P. P., Costa, M., & Invernizzi, C. (2019). Plio-Quaternary tectonics and possible implications for geothermal fluids in the Marche Region (Italy). *Tectonophysics*, 755, 21–34. <https://doi.org/10.1016/J.TECTO.2019.02.005>
- Civico, R., Pucci, S., Villani, F., Pizzimenti, L., de Martini, P. M., Nappi, R., Agosta, F., Alessio, G., Alfonsi, L., Amanti, M., Amoroso, S., Aringoli, D., Auciello, E., Azzaro, R., Baize, S., Bello, S., Benedetti, L., Bertagnini, A., Binda, G., ... Zambrano, M. (2018). Surface ruptures following the 30 October 2016 Mw 6.5 Norcia earthquake, central Italy. *Journal of Maps*, 14(2). <https://doi.org/10.1080/17445647.2018.1441756>
- Collettini, C., & Sibson, R. H. (2001). Normal faults, normal friction? *Geology*, 29(10).
- Coltorti, M. (1997). Human impact in the Holocene fluvial and coastal evolution of the Marche region, Central Italy. *Catena*, 30(4), 311–335.
- Conti, P., Cornamusini, G., & Carmignani, L. (2020). An outline of the geology of the northern Apennines (Italy), with geological map at 1:250,000 scale. *Italian Journal of Geosciences*, 139(2). <https://doi.org/10.3301/IJG.2019.25>
- Cornell, C. A. (1968). Engineering seismic risk analysis. *Bulletin of the Seismological Society of America*, 58(5). <https://doi.org/10.1785/bssa0580051583>
- Coward, M. P., De Donatis, M., Mazzoli, S., Paltrinieri, W., & Wezel, F. C. (1999). Frontal part of the northern Apennines fold and thrust belt in the Romagna-Marche area (Italy): Shallow and deep structural styles. *Tectonics*, 18(3), 559-574
- Danciu L., Nandan S., Reyes C., Basili R., Weatherill G., Beauval C., Rovida A., Vilanova S., Sesetyan K., Bard P-Y., Cotton F., Wiemer S., Giardini D. (2021) - The 2020 update of the European Seismic Hazard Model: Model Overview. EFEHR Technical Report 001, v1.0.0,
- Della Seta, M., del Monte, M., Fredi, P., Miccadei, E., Nesci, O., Pambianchi, G., Piacentini, T., & Troiani, F. (2008). Morphotectonic evolution of the Adriatic piedmont of the Apennines: An advancement in the knowledge of the Marche-Abruzzo border area. *Geomorphology*, 102(1). <https://doi.org/10.1016/j.geomorph.2007.06.018>
- Delvaux, D., & Sperner, B. (2003). New aspects of tectonic stress inversion with reference to the TENSOR program. *Geological Society Special Publication*, 212, 75–100. <https://doi.org/10.1144/GSL.SP.2003.212.01.06>
- DISS Working Group (2021). *Database of Individual Seismogenic Sources (DISS), Version 3.3.0: A compilation of potential sources for earthquakes larger than M 5.5 in Italy and surrounding*

areas. *Istituto Nazionale di Geofisica e Vulcanologia (INGV)*.  
<https://doi.org/10.13127/diss3.3.0>.

- Di Bucci, D., Mazzoli, S., Nesci, O., Savelli, D., Tramontana, M., de Donatis, M., & Borraccini, F. (2003). Active deformation in the frontal part of the Northern Apennines: Insights from the lower Metauro River basin area (northern Marche, Italy) and adjacent Adriatic off-shore. *Journal of Geodynamics*, 36(1–2), 213–238. [https://doi.org/10.1016/S0264-3707\(03\)00048-6](https://doi.org/10.1016/S0264-3707(03)00048-6)
- Ekström, G., Nettles, M., & Dziewoński, A. M. (2012). The global CMT project 2004–2010: Centroid-moment tensors for 13,017 earthquakes. *Physics of the Earth and Planetary Interiors*, 200, 1-9
- Faure Walker, J., Boncio, P., Pace, B., Roberts, G., Benedetti, L., Scotti, O., Visini, F., & Peruzza, L. (2021). Fault2SHA Central Apennines database and structuring active fault data for seismic hazard assessment. *Scientific Data*, 8(1). <https://doi.org/10.1038/s41597-021-00868-0>
- Ferrarini, F., de Nardis, R., Brozzetti, F., Cirillo, D., Arrowsmith, J. R., & Lavecchia, G. (2021). Multiple Lines of Evidence for a Potentially Seismogenic Fault Along the Central-Apennine (Italy) Active Extensional Belt—An Unexpected Outcome of the MW6.5 Norcia 2016 Earthquake. *Frontiers in Earth Science*, 9. <https://doi.org/10.3389/feart.2021.642243>
- Galadini, F., Meletti, C., & Vittori, E. (2001). Major active faults in Italy: Available surficial data. *Geologie En Mijnbouw/Netherlands Journal of Geosciences*, 80(3–4). <https://doi.org/10.1017/s001677460002388x>
- Galli, P., Peronace, E., Bramerini, F., Castenetto, S., Naso, G., Cassone, F., & Pallone, F. (2016). The MCS intensity distribution of the devastating 24 august 2016 earthquake in central Italy (Mw 6.2). *Annals of Geophysics*, 59(FastTrack5). <https://doi.org/10.4401/ag-7287>
- Galvani, A., Anzidei, M., Devoti, R., Esposito, A., Pietrantonio, G., Pisani, A. R., Riguzzi, F., & Serpelloni, E. (2012). The interseismic velocity field of the central Apennines from a dense GPS network. *Annals of Geophysics*, 55(5). <https://doi.org/10.4401/ag-5634>
- Gibbs, A. D. (1984). Structural evolution of extensional basin margins Overall basin geometry. *J. Geol. Soc. London*, 141.
- Heidbach, O., Custodio, C., Kingdon, A., Mariucci, M. T., Montone, P., Müller, B., & Ziegler, M. (2016). Stress map of the Mediterranean and Central Europe 2016.
- INGV Seismological Data Centre. (2006). Rete Sismica Nazionale (RSN). Istituto Nazionale di Geofisica e Vulcanologia (INGV), Italy. <https://doi.org/10.13127/sd/x0fxnh7qfy>

- ISIDE Working Group. (2007). Italian Seismological Instrumental and parametric Database (ISIDE). In *Istituto Nazionale di Geofisica e Vulcanologia*.
- Italian Civil Protection Department (2018) National Risk Assessment 2018. Overview of the potential major disasters in Italy. Updated December 2018
- ITHACA Working Group (2019). ITHACA (ITaly HAZard from CApable faulting), A database of active capable faults of the Italian territory. Version December 2019. ISPRA Geological Survey of Italy. Web Portal <http://sgi2.isprambiente.it/ithacaweb/Mappatura.aspx>
- Jackson, J.A. and N.J. White (1989). Normal faulting in the upper continental crust: observations from regions of active extension. *Struct. Geol.* 11, 15-36.
- Lettis, W. R., Wells, D. L., & Baldwin, J. N. (1997). Empirical observations regarding reverse earthquakes, blind thrust faults, and quaternary deformation: Are blind thrust faults truly blind? *Bulletin of the Seismological Society of America*, 87(5). <https://doi.org/10.1785/bssa0870051171>
- Lahr, J. C. (1999). HYPOELLIPSE: A computer program for determining local earthquake hypocentral parameters, magnitude, and first motion pattern (p. 119). Denver, Colorado: US Geological Survey
- Locati M., Camassi R., Rovida A., Ercolani E., Bernardini F., Castelli V., Caracciolo C.H., Tertulliani A., Rossi A., Azzaro R., D'Amico S., Antonucci A. (2022). Database Macrosismico Italiano (DBMI15), versione 4.0. Istituto Nazionale di Geofisica e Vulcanologia (INGV). <https://doi.org/10.13127/DBMI/DBMI15.4>
- Maesano, F. E., Toscani, G., Burrato, P., Mirabella, F., D'Ambrogi, C., & Basili, R. (2013). Deriving thrust fault slip rates from geological modeling: examples from the Marche coastal and offshore contraction belt, Northern Apennines, Italy. *Marine and Petroleum Geology*, 42, 122-134
- Massa, B., & Zuppetta, A. (2009). Integrated approach to investigation of active tectonics: An example from the Calore River Fault System, southern Italy. *Bollettino Della Societa Geologica Italiana*, 128(2). <https://doi.org/10.3301/IJG.2009.128.2.505>
- Mayer, L., Menichetti, M., Nesci, O., & Savelli, D. (2003). Morphotectonic approach to the drainage analysis in the North Marche region, central Italy. In *Quaternary International*.

- Mazzoli, S., Pierantoni, P. P., Borraccini, F., Paltrinieri, W., & Deiana, G. (2005). Geometry, segmentation pattern and displacement variations along a major Apennine thrust zone, central Italy. *Journal of Structural Geology*, 27(11). <https://doi.org/10.1016/j.jsg.2005.06.002>
- Mazzoli, S., Macchiavelli, C., & Ascione, A. (2014). The 2013 Marche offshore earthquakes: New insights into the active tectonic setting of the outer northern Apennines. *Journal of the Geological Society*, 171(4). <https://doi.org/10.1144/jgs2013-091>
- Miccadei, E., Carabella, C., & Paglia, G. (2021). Morphoneotectonics of the Abruzzo Periadriatic area (Central Italy): Morphometric analysis and morphological evidence of tectonics features. *Geosciences (Switzerland)*, 11(9). <https://doi.org/10.3390/geosciences11090397>
- Miccolis, S., Filippucci, M., de Lorenzo, S., Frepoli, A., Pierri, P., & Tallarico, A. (2021). Seismogenic Structure Orientation and Stress Field of the Gargano Promontory (Southern Italy) From Microseismicity Analysis. *Frontiers in Earth Science*, 9. <https://doi.org/10.3389/feart.2021.589332>
- Michetti A.M., Serva L. and Vittori E. coord. (2000): ITHACA. Italy Hazard from Capable Faulting. A database of active capable faults of the Italian onshore territory. ANPA, CD-ROM.
- Mirabella, F., Barchi, M. R., & Lupattelli, A. (2008). Seismic reflection data in the Umbria Marche Region: limits and capabilities to unravel the subsurface structure in a seismically active area. *Annals of Geophysics*.
- Mirabella, F., Braun, T., Brogi, A., & Capezzuoli, E. (2022). Pliocene-Quaternary seismogenic faults in the inner Northern Apennines (Valdelsa Basin, southern Tuscany) and their role in controlling the local seismicity. *Geological Magazine*, 159(6). <https://doi.org/10.1017/S0016756822000036>
- Monachesi G., Ladina C., Calamita C., Pantaleo D., Cattaneo M., Marzorati S., Frapiccini M., D'Alema E., Carannante S. (2021). Beach Balls in central-eastern Italy [Data set]. Istituto Nazionale di Geofisica e Vulcanologia (INGV). <https://doi.org/10.13127/bb2021>
- Nesci, O., Savelli, D., & Troiani, F. (2012). Types and development of stream terraces in the Marche Apennines (central Italy): A review and remarks on recent appraisals. In *Geomorphologie: Relief, Processus, Environnement* (Issue 2). <https://doi.org/10.4000/geomorphologie.9838>
- Pérez-Peña, J. v., Al-Awabdeh, M., Azañón, J. M., Galve, J. P., Booth-Rea, G., & Notti, D. (2017). SwathProfiler and NProfiler: Two new ArcGIS Add-ins for the automatic extraction of swath

- and normalized river profiles. *Computers and Geosciences*, 104. <https://doi.org/10.1016/j.cageo.2016.08.008>
- Pierantoni, P., Deiana, G., & Galdenzi, S. (2013). Stratigraphic and structural features of the Sibillini Mountains (Umbria- Marche Apennines, Italy). *Italian Journal of Geosciences*, 132(3). <https://doi.org/10.3301/IJG.2013.08>
- Pierantoni, P. P., Chicco, J., Costa, M., & Invernizzi, C. (2019). Plio-Quaternary transpressive tectonics: a key factor in the structural evolution of the outer Apennine–Adriatic system, Italy. *Journal of the Geological Society*, 176(6), 1273-1283
- Pizzi, A., & Galadini, F. (2009). Pre-existing cross-structures and active fault segmentation in the northern-central Apennines (Italy). *Tectonophysics*, 476(1–2). <https://doi.org/10.1016/j.tecto.2009.03.018>
- Pondrelli, S. 2002. European-Mediterranean Regional Centroid-Moment Tensors Catalog (RCMT) [Data set]. Istituto Nazionale di Geofisica e Vulcanologia (INGV). <https://doi.org/10.13127/rcmt/euromed>.
- Porreca, M., Minelli, G., Ercoli, M., Brobia, A., Mancinelli, P., Cruciani, F., ... & Barchi, M. R. (2018). Seismic reflection profiles and subsurface geology of the area interested by the 2016–2017 earthquake sequence (Central Italy). *Tectonics*, 37(4), 1116-1137
- Pucci, S., de Martini, P. M., Civico, R., Villani, F., Nappi, R., Ricci, T., Azzaro, R., Brunori, C. A., Caciagli, M., Cinti, F. R., Sapia, V., de Ritis, R., Mazzarini, F., Tarquini, S., Gaudiosi, G., Nave, R., Alessio, G., Smedile, A., Alfonsi, L., ... Pantosti, D. (2017). Coseismic ruptures of the 24 August 2016, Mw 6.0 Amatrice earthquake (central Italy). *Geophysical Research Letters*, 44(5). <https://doi.org/10.1002/2016GL071859>
- Reasenber, P. A. (1985). FPFIT, FPLOT, and FPPAGE: Fortran computer programs for calculating and displaying earthquake fault-plane solutions. US Geol. Surv. Open-File Rep., 85-739
- Renner, G., & Slejko, D. (1994). Some comments on the seismicity of the Adriatic region. *Bollettino Di Geofisica Teorica Ed Applicata*, 36(141–144).
- Roberts, G. P., & Michetti, A. M. (2004). Spatial and temporal variations in growth rates along active normal fault systems: An example from The Lazio-Abruzzo Apennines, central Italy. *Journal of Structural Geology*, 26(2). [https://doi.org/10.1016/S0191-8141\(03\)00103-2](https://doi.org/10.1016/S0191-8141(03)00103-2)



- Romeo, S., di Matteo, L., Melelli, L., Cencetti, C., Dragoni, W., & Fredduzzi, A. (2017). Seismic-induced rockfalls and landslide dam following the October 30, 2016 earthquake in Central Italy. *Landslides*, 14(4). <https://doi.org/10.1007/s10346-017-0841-8>
- Rovida A., Locati M., Camassi R., Lolli B., Gasperini P., Antonucci A. (2022). Catalogo Parametrico dei Terremoti Italiani (CPTI15), versione 4.0. Istituto Nazionale di Geofisica e Vulcanologia (INGV). <https://doi.org/10.13127/CPTI/CPTI15.4>
- Rovida, A., Locati, M., Camassi, R., Lolli, B., & Gasperini, P. (2016). CPTI15, the 2015 version of the Parametric Catalogue of Italian Earthquakes. *Istituto Nazionale Di Geofisica e Vulcanologia*.
- Santini, S., Saggese, F., Megna, A., & Mazzoli, S. (2011). A note on central-northern marche seismicity: New focal mechanisms for events recorded in years 2003-2009. *Bollettino Di Geofisica Teorica Ed Applicata*, 52(4). <https://doi.org/10.4430/bgta0025>
- Scandone, P., et al., 1992. Struttura geologica, evoluzione cinematica e schema sismotettonico della penisola italiana. CNR-GNDT 1990 Congress, Vol. I, pp. 119-135.
- Schwanghart, W., & Scherler, D. (2014). Short Communication: TopoToolbox 2 - MATLAB-based software for topographic analysis and modeling in Earth surface sciences. *Earth Surface Dynamics*, 2(1). <https://doi.org/10.5194/esurf-2-1-2014>
- Scudero, S., Marcocci, C., & D'Alessandro, A. (2021). Insights on the Italian Seismic Network from location uncertainties. *Journal of Seismology*, 25(4).
- Serpelloni, E., Anzidei, M., Baldi, P., Casula, G., & Galvani, A. (2021). GPS measurement of active strains across the Apennines. *Annals of Geophysics*, 49(1). <https://doi.org/10.4401/ag-5756>
- Sippel, J., Scheck-Wenderoth, M., Reicherter, K., & Mazur, S. (2009). Paleostress states at the south-western margin of the Central European Basin System—application of fault-slip analysis to unravel a polyphase deformation pattern. *Tectonophysics*, 470(1-2), 129-146
- Spallarossa, D., Cattaneo, M., Scafidi, D., Michele, M., Chiaraluce, L., Segou, M., & Main, I. G. (2021). An automatically generated high-resolution earthquake catalogue for the 2016-2017 Central Italy seismic sequence, including P and S phase arrival times. *Geophysical Journal International*, 225(1). <https://doi.org/10.1093/gji/ggaa604>
- Stucchi, E., Mirabella, F., & Ciaccio, M. G. (2006). Comparison between reprocessed seismic profiles: Seismologic and geologic data—A case study of the Colfiorito earthquake area Data Comparison in Colfiorito Area. *Geophysics*, 71(2), B29-B40

- Stucchi M., Meletti C., Montaldo V., Akinci A., Faccioli E., Gasperini P., Malagnini L., Valensise G. (2004). Pericolosità sismica di riferimento per il territorio nazionale MPS04 [Data set]. Istituto Nazionale di Geofisica e Vulcanologia (INGV). <https://doi.org/10.13127/sh/mps04/ag>
- Suppe, J. (1983). Geometry and kinematics of fault-bend folding. *American Journal of Science*, 283(7). <https://doi.org/10.2475/ajs.283.7.684>
- Tondi, E., Jablonská, D., Volatili, T., Michele, M., Mazzoli, S., & Pierantoni, P. P. (2021). The Campotosto Linkage Fault Zone between the 2009 and 2016 Seismic Sequences of Central Italy: Implications for Seismic Hazard Analysis. *Bulletin of the Geological Society of America*, 133. <https://doi.org/10.1130/B35788.1>
- Wegmann, K. W., & Pazzaglia, F. J. (2009). Late Quaternary fluvial terraces of the Romagna and Marche Apennines, Italy: Climatic, lithologic, and tectonic controls on terrace genesis in an active orogen. *Quaternary Science Reviews*, 28(1–2), 137–165. <https://doi.org/10.1016/j.quascirev.2008.10.006>
- Wernicke, B., & Burchfiel, B. C. (1982). Modes of extensional tectonics. *Journal of Structural Geology*, 4(2). [https://doi.org/10.1016/0191-8141\(82\)90021-9](https://doi.org/10.1016/0191-8141(82)90021-9)
- Whipple, K. X., Wobus, C. W., Crosby, B., Kirby, E., & Sheehan, D. (2007). New Tools for Quantitative Geomorphology : Extraction and Interpretation of Stream Profiles from Digital Topographic Data. GSA Short Course ([Http://Geomorphtools.Org/Tools/StPro/Tutorials/StPro\\_UserGuidees\\_Final.Pdf](http://Geomorphtools.Org/Tools/StPro/Tutorials/StPro_UserGuidees_Final.Pdf)), November
- Wobus, C. W., Crosby, B. T., & Whipple, K. X. (2006). Hanging valleys in fluvial systems: Controls on occurrence and implications for landscape evolution. *Journal of Geophysical Research: Earth Surface*, 111(2). <https://doi.org/10.1029/2005JF000406>

## 2. THE SEISMOGENIC FAULT SYSTEM OF THE $M_w$ 6.4, NOVEMBER 2019 ALBANIA EARTHQUAKE: NEW INSIGHTS INTO THE STRUCTURAL ARCHITECTURE AND ACTIVE TECTONIC SETTING OF THE OUTER ALBANIDES

S. Teloni<sup>1</sup>, C. Invernizzi<sup>1</sup>, S. Mazzoli<sup>1</sup>, P.P. Pierantoni<sup>1\*</sup>, V. Spina<sup>2</sup>

<sup>1</sup> *School of Science and Technology - Geology Division, University of Camerino, Via Gentile III da Varano, 62032 Camerino (MC), Italy*

<sup>2</sup> *Total Upstream Denmark A/S, Amerika Plads, Copenhagen*

**Abstract:** A seismic sequence that affected the Durrës region in late 2019 to early 2020 sheds new light into the structural architecture and active tectonic setting of the northern outer Albanides. Stress inversion analysis using the focal mechanisms confirms that the area is dominated by ENE trending, horizontal maximum compression. Seismogenic sources consist mainly of ENE dipping thrust faults roughly parallel to the coastline. Hypocenter distribution indicates that most of the earthquakes, including the  $M_w = 6.4$  main shock, nucleated within the basement, while only some of the shallow aftershocks tend to cluster around the deeper portion of previously identified seismogenic structures within the sedimentary cover. Our results, unravelling for the first time the fundamental role of deeply rooted, crustal ramp-dominated thrusting in seismogenesis, imply a profound reconsideration of the seismotectonic setting of the region in view of a correct assessment of seismic hazard in this densely populated area of Albania.

**Keywords:** *seismotectonics, fold and thrust belts, basement faults, Adriatic Sea, active thrusts*

## 2.1. Introduction

Starting in the autumn 2019, a seismic sequence affected the Albanian coastal area north of Durrës (Fig. 2.1a), claiming 51 victims and causing severe damage. The main shock of the sequence occurred on 26-11-2019 (at 02:54:11 UTC; Fig. 2.1b) at a hypocentral depth of  $22 \pm 1$  km according to the data made available by the Istituto Nazionale di Geofisica e Vulcanologia (INGV; a similar depth of 22 km is indicated also by the USGS catalogue available at <https://earthquake.usgs.gov/earthquakes/search/>). Preliminary evaluations assign magnitudes  $M_b = 6.3$  and  $M_w = 6.4$  (RCMT data available at <http://rcmt2.bo.ingv.it/>) to this event. The main event was preceded by a series of shocks, including a  $M_w 5.7$  earthquake at a hypocentral depth of 17 km, while the seismic sequence that followed the main event includes a  $M_w 5.5$  shock at a hypocentral depth of 20 km. The available focal mechanisms (<http://rcmt2.bo.ingv.it/>) show similar, dominantly thrust fault plane solutions with mostly NNW-SSE striking nodal planes (Fig. 2.2) and sub-horizontal to gently dipping, mainly WSW-ENE trending P axes.

The 2019-2020 earthquake sequence provides new, fundamental constraints not only on the active tectonic setting of the region, but also on the crustal architecture of the outer Albanides. The area was already well known as the locus of a moderate – yet significant – tectonic activity, as also testified by historical seismicity (Duni *et al.* 2010). However, as active slip along the outermost basement thrusts was not known to occur prior to this earthquake sequence, here we show that the recent earthquakes are pivotal in outlining the active crustal frontal structure of the thrust belt.

## 2.2. Regional tectonic framework

Albania (Fig. 2.2) includes a significant sector of the Dinarides – Albanides – Hellenides mountain belt. This is a SW verging fold and thrust belt that developed since the Late Jurassic within the general framework of Africa-Eurasia major plate convergence (Velaj 2015). As it is typical for mountain belts belonging to the Alpine orogen, the Albanides are conventionally divided into two major tectonic domains: the Internal Albanides and External Albanides (Fraseri *et al.* 2009).

The Internal (or Inner) Albanides consist of Triassic and Jurassic successions included within the Mirdita, Rubiku, Korabi and Gashi nappes. These tectonic units, accreted to the Eurasian continental margin by the end of the Mesozoic, experienced multiple shortening events (Velaj

2015). The Korabi unit includes the oldest formations exposed in Albania: unconformably overlying a greenschist facies basement of Paleozoic age, Permo-Triassic siliciclastic rocks give way upward to a Triassic-Jurassic carbonate platform succession (Tremblay *et al.* 2015). The Korabi unit is overthrust by the Rubiku unit, which consists mainly of a Triassic-Jurassic volcano-sedimentary (dominantly carbonate) succession (Muceku *et al.* 2006, Bortolotti *et al.* 1995). The tectonic pile is capped by the Mirdita unit, which consists of a Middle Jurassic ophiolitic suite also including mantle rocks (Saccani *et al.* 2018).

In the northernmost part of Albania, the Gashi unit (carbonate and metamorphic rocks of Permian and Triassic age; Prenjasi *et al.* 2011) tectonically overlies the Albanian Alps unit (Permian terrigenous rocks and Triassic-Cretaceous platform carbonates overlain by Paleocene-Lower Eocene siliciclastic deposits), which is traditionally included in the External Albanides (Muceku *et al.* 2008).

The External (or outer) Albanides derive from shortening of part of the former Adria continental margin, of African plate affinity (e.g., Robertson and Shallo 2000, and references therein). They include the Krasta-Cukali, Kruja, Ionian and Sazani tectonic units that were affected by top-to-the-WSW thrusting (Fraseri *et al.* 2009).

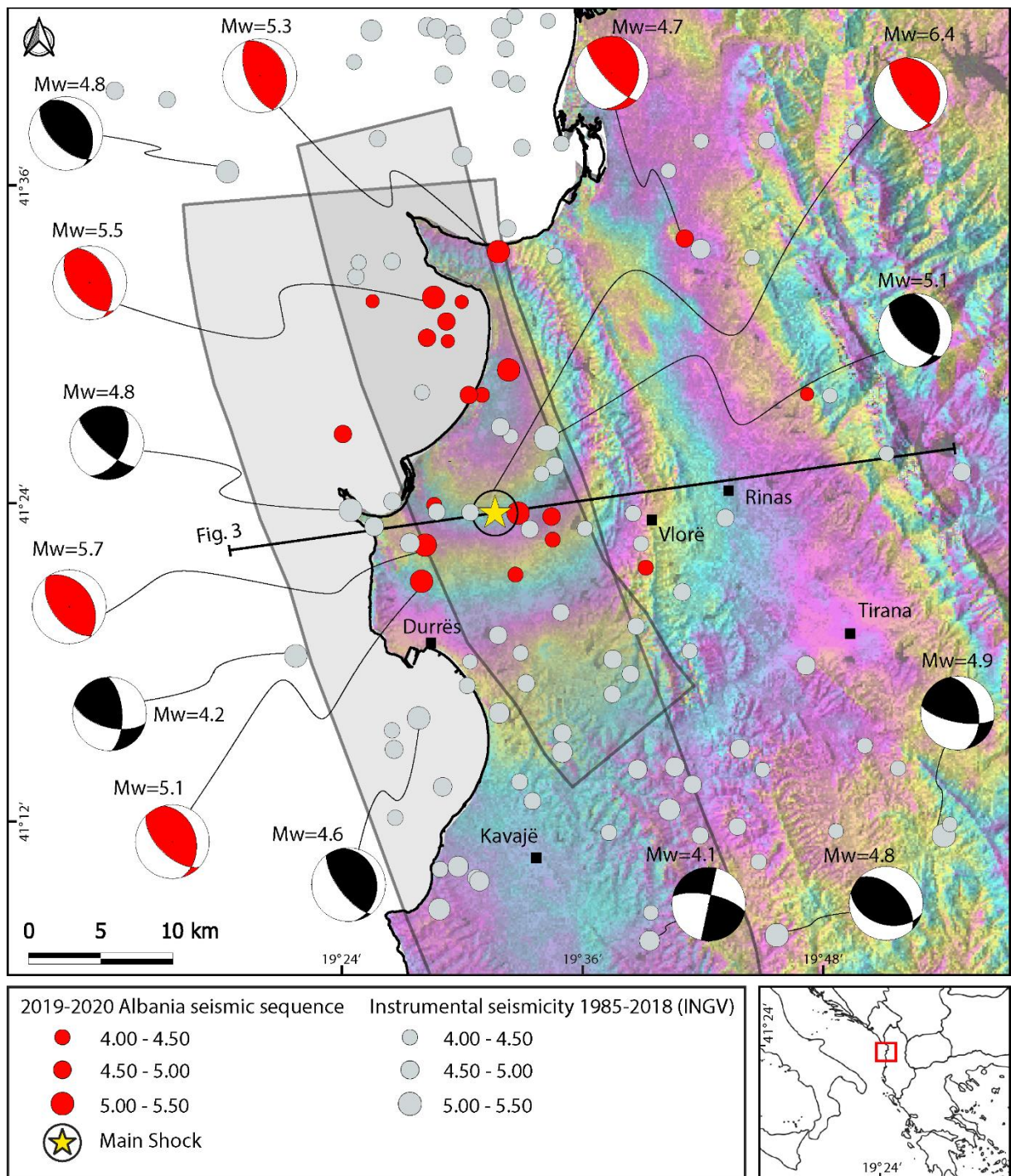


Fig. 2.1 - Map showing epicenter location and focal mechanisms for the 2019-2020 seismic sequence (in red) and previous seismic events recorded by INGV since 1985 (in grey). The epicenters are plotted using the location from the ISIDe database (<http://terremoti.ingv.it/iside>), while magnitude (MW) and focal mechanism data are from the RCMT catalogue (Pondrelli 2002; <http://rcmt2.bo.ingv.it/>). Light grey polygons represent the ‘composite seismogenic sources’ according to the Database of Individual Seismogenic Sources (Basili et al., 2008; DISS Working Group, 2018). The co-seismic interferogram from Sentinel 1 (26-11-2019, 00:00 UTC to 08-12-2019, 00:00 UTC; <http://sarviews-hazards.alaska.edu/>; last access: 18-02-2020) is shown as an overlay draped onto the digital elevation model (<https://www.eea.europa.eu/>).

The Krasta-Cukali unit consists of Triassic siliciclastic rocks and neritic limestones, Jurassic deep-sea sediments, Lower Cretaceous siliciclastic turbidites, Upper Cretaceous pelagic limestones and Maastrichtian to Eocene siliciclastic turbidites (Fraseri *et al.* 1995).

Originally interposed between the Apulia carbonate platform (to the west) and a further carbonate platform (Kruja) to the east, the Ionian Basin formed as a result of Triassic to Early Jurassic rifting preceding the opening of the Tethys Ocean (Roure *et al.* 1995; Robertson and Shallo 2000). Overlying a crystalline basement, Triassic evaporites at the base of the succession consist of intercalated gypsum, anhydrides and dolomitic limestone (Velaj 2001). The stratigraphically overlying Lower Jurassic succession includes both shallow water carbonates (formed at the crest of tilted fault blocks) and basin strata. Pelagic limestones, marls and shales characterize the entire overlying Mesozoic and Paleogene succession (Zappaterra 1990; Mecaj and Mahmutaj 1995). Oligocene turbiditic strata, consisting of fine-grained sandstones, siltstones and marls, occur at the top of the unit and mark syn-orogenic sedimentation in a subsiding foreland basin (Roure *et al.* 2004; Bega and Soto 2017). Syn-orogenic foredeep sediments not older than Oligocene in age occur also on top of the Mesozoic-Paleogene carbonate platform succession of the Kruja unit (Shehu 1995; Robertson and Shallo 2000). The Sazani unit, which is exposed in the westernmost part of Albania along the Adriatic coast, is characterized by a shallow-water carbonate succession (of late Triassic to Oligocene age) essentially continuous with that of the Apulia carbonate platform. This is overlain by a foreland basin succession mainly consisting of resedimented carbonates of Early Miocene – Pliocene age (Fraseri *et al.* 1996).

The outer Albanides fold and thrust belt is subdivided into two distinct structural provinces by the NE-trending Vlora-Elbasan ‘lineament’ (Fig. 2.2). The southern structural province is characterized by extensive outcrop of folded and faulted Mesozoic carbonates of the Ionian Basin, detached along Triassic evaporites. On the other hand, seismic interpretation (Roure *et al.*, 1995) provides no evidence of décollement at the Triassic evaporite level in the northern structural province, which is dominated by the thick Oligocene to Plio-Quaternary clastic succession of the Peri-Adriatic Depression (see below). The Vlora-Elbasan ‘lineament’ is commonly interpreted as a Cenozoic major transfer zone, controlled by an inherited deep-seated basement fault (e.g., Lacombe *et al.*, 2009, and references therein). In particular, a Triassic/Jurassic strike-slip origin is inferred for this structure (Nieuwland *et al.*, 2001).

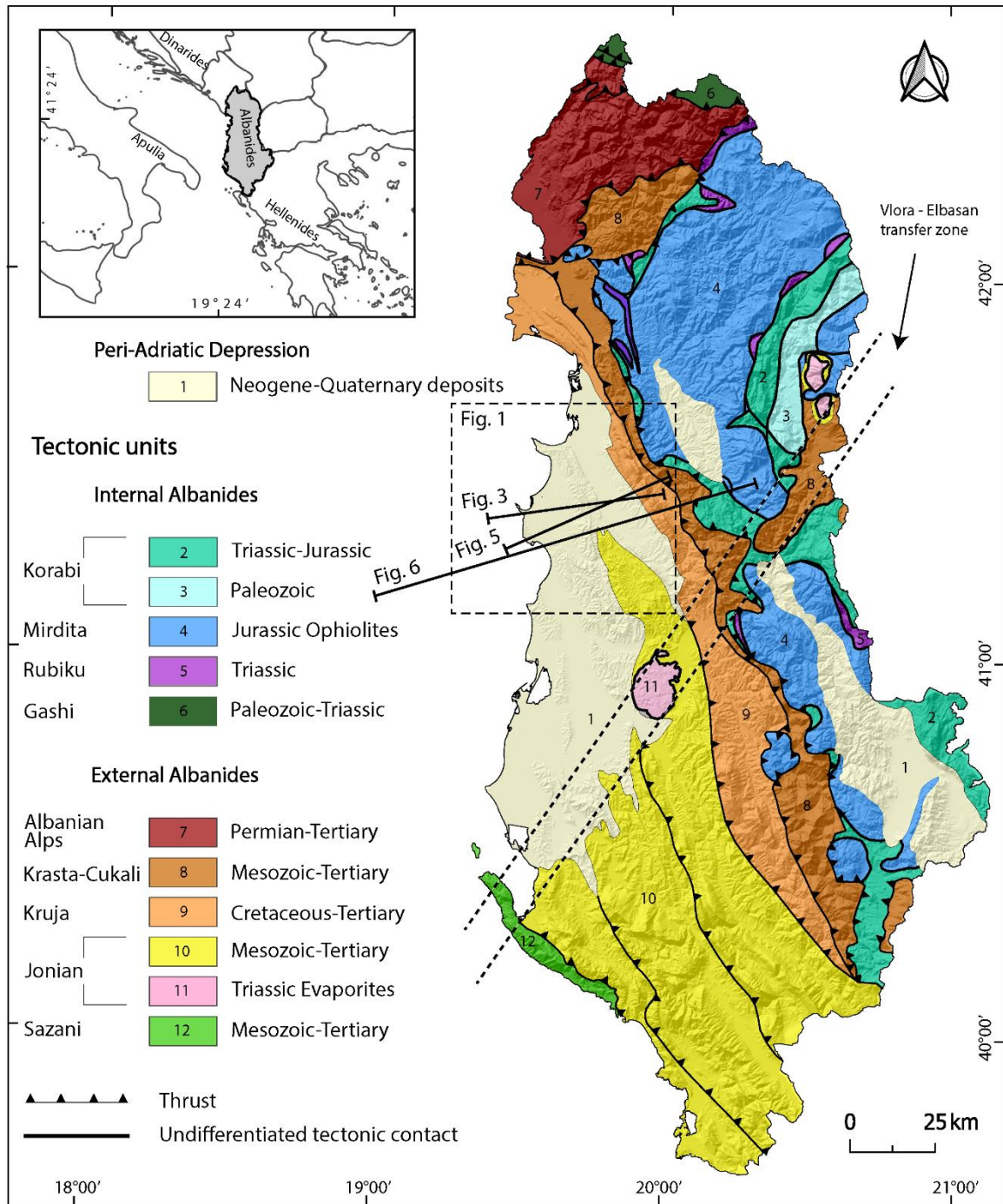


Fig. 2.2 - Tectonic sketch map of Albania (after Roure *et al.* 2004 and Muceku *et al.* 2008, modified and draped onto the digital elevation model; <https://www.eea.europa.eu/>), showing the location of the map of Fig.2.1, and of cross-sections (Figs. 2.3 and 2.6) and seismic line (Fig. 2.5).

The development of a wide flexural basin on top of the External Albanides lithosphere since late Oligocene times was associated with the tectonic load provided by the Internal Albanides (including the Mirdita ophiolite) and the far travelled Krasta-Cukali unit. Growth anticlines involving the Ionian Basin succession started to develop in late Oligocene-Aquitian times,



during an early deformation stage post-dated by the deposition of Langhian–Serravallian clastic strata (Lacombe *et al.*, 2009). A later shortening event is best documented north of the Vlora-Elbasan ‘lineament’, in the Peri-Adriatic Depression. This latter represents a foreland basin interposed between the Dinarides – Albanides – Hellenides, to the east, and the Apennines exposed in the Italian peninsula to the west (Roure *et al.* 2004; Velaj 2015). This basin hosts an up to 10 km thick syn-flexural and syn-kinematic siliciclastic succession including nearshore and littoral facies deposits in its eastern and southern portions, while deeper water and turbiditic facies sediments are dominant in the northern and western (offshore) sectors. These foredeep deposits allow effectively constraining the timing of the deformation, as Pliocene backthrusts deform and offset a Messinian unconformity observed on seismic sections (Nieuwland *et al.*, 2001; Roure *et al.* 2004).

Seismic interpretation was also used to infer the occurrence of Mesozoic steep normal faults involving the basement in deep regional geological sections (Roure *et al.* 2004). However, the attitude and possible role of these inherited structures in fold and thrust development are not constrained at all, most probably due to poor quality of the seismic signal at the relevant depths.

### **2.3. Seismotectonics of the Durrës region and the 2019-2020 earthquakes**

Instrumental seismicity of the Durrës area predating the 2019-2020 seismic sequence was recorded by the INGV seismic network ISIDe (<http://terremoti.ingv.it/iside>) since 1985. The area, dominated by an active thrust tectonic regime, was characterized by low to medium magnitude (maximum  $M_w \leq 5.1$ ), dominantly shallow events tending to cluster along the coastline. Deep earthquakes (located at depths in excess of 10 km) were scattered. Available data indicated a dominantly horizontal, ENE-WSW oriented maximum compression along the Adriatic coast and adjacent offshore of the Durrës region. The seismotectonic setting of the region before the 2019-2020 seismic sequence is outlined in the Database of Individual Seismogenic Sources (Basili *et al.* 2008; DISS Working Group 2018). According to the DISS, seismogenic sources – both individual and ‘composite’, the latter encompassing several individual seismogenic sources – consist in the study area of ENE dipping thrust faults (Fig. 2.3) roughly parallel to the coastline (Fig. 2.1). These structures are not exposed at the surface/seafloor, as they are blind/buried thrusts whose upper tip lines are contained within the Neogene deposits of the Peri-Adriatic Depression. The ‘composite seismogenic source’ labelled ALCS018 has a maximum assigned  $M_w = 5.8$ , whereas that labelled ALCS002 has a maximum assigned  $M_w = 7.2$ . This latter ‘composite seismogenic source’ is the closest one, among those

included in the DISS, to some of the 2019-2020 seismic events. Location of the latter by different institutions shows a certain degree of variability (Ganas *et al.* 2020, and references therein), which is not substantially reduced by the use of aperture radar interferometry (InSAR) and geodetic data to revise event location based on co-seismic deformation (compare, e.g., Caporali *et al.* 2020, with Ganas *et al.* 2020 and Govorčin *et al.* 2020). In this study we use earthquake locations provided by the ISIDe online catalogue (<http://terremoti.ingv.it/iside>), as this is based on a dense network of seismic stations suitably distributed around the epicentral area. There, INGV seismic stations recorded 22 earthquakes with  $3.8 \leq M_w \leq 6.4$  from 21-09-2019 to 28-01-2020 (data available at <http://terremoti.ingv.it/iside>). These events are referred to in this paper as the 2019-2020 seismic sequence. The  $M_w = 6.4$  main shock located by INGV falls approximately 6 km south of the site onto which of the concentric fringe pattern yielded by the co-seismic interferogram from Sentinel 1 is roughly centred (Fig. 2.1). In terms of magnitude, the seismic events are distributed as follows (as the database includes different magnitude types –  $M_w$ ,  $M_L$ ,  $M_b$  – magnitudes are indicated generically with  $M$  in Table 1): 1 event with  $M \geq 6$ ; 6 events with  $5 \leq M < 6$ ; 11 events with  $4 \leq M < 5$ ; 4 events with  $3 \leq M < 4$ . The main shock of the sequence occurred on 26-11-2019 (at 02:54:11 GMT). The main event was preceded by three main foreshocks from 21-09-2019 to 26-11-2019 and magnitudes  $4.4 \leq M_w < 5.7$ , and was followed by eighteen aftershocks included in the INGV online catalogue. Available locations show hypocentral depths in the range of 10 – 36 km (mostly around 20 km).

DATE	TIME [UTC]	LAT [°]	LONG [°]	DEPTH [KM]	M	TYPE
21/09/2019	14:04:27	41.38 ±0.01	19.46 ±0.01	19.5 ±2	5.4	ML
21/09/2019	14:15:55	41.36 ±0.01	19.46 ±0.01	19.7 ±2	5.2	ML
26/11/2019	01:47:56	41.36 ±0.01	19.54 ±0.02	21.8±2	4.4	ML
26/11/2019	02:54:11	41.40	19.52 ±0.01	22.1 ±1	6.2	Mw
26/11/2019	02:59:24	41.40	19.54	10	5.1	mb
26/11/2019	03:03:00	41.49	19.53	10	5.3	mb
26/11/2019	03:57:53	41.53	19.42	10.1	3.9	ML
26/11/2019	05:56:22	41.47 ±0.01	19.51 ±0.01	21.8 ±1	4.3	ML
26/11/2019	06:08:23	41.54 ±0.01	19.47 ±0.01	20.2 ±2	5.4	ML
26/11/2019	07:12:32	41.53	19.49	20	3.8	ML
26/11/2019	07:27:02	41.51 ±0.01	19.4 6 ±0.01	18 ±2	4.8	ML
26/11/2019	12:14:13	41.40	19.47	9.5	4.2	ML
26/11/2019	13:05:00	41.57	19.68	36	4.7	ML
26/11/2019	17:06:02	41.48	19.78	30.4	4	ML
26/11/2019	17:19:15	41.52	19.48 ±0.01	21.3 ±1	4.6	ML
27/11/2019	14:45:25	41.56	19.52	25	5.4	ML
28/11/2019	10:52:42	41.45 ±0.01	19.39 ±0.01	14.4 ±1	4.8	ML
28/11/2019	23:00:45	41.37 ±0.01	19.65 ±0.02	23.2 ±2	4.2	ML
30/11/2019	20:53:53	41.51 ±0.01	19.48 ±0.03	22.7 ±5	4	ML
02/12/2019	08:26:26	41.38 ±0.01	19.57 ±0.02	16.6 ±2	4.2	ML
19/12/2019	16:03:14	41.40	19.57	10	4.7	mb
28/01/2020	20:15:11	41.47	19.50	12.9	5	mb

Tab. 2.1 - Seismological information for the 2019-2020 seismic sequence (from INGV - ISIDe <http://terremoti.ingv.it/iside>; uncertainties are provided where available in the catalogue).



Fig. 2.3 - (A) WSW-ENE vertical section showing hypocentral distribution for the seismic events recorded by ISIDE (<http://terremoti.ingv.it/iside>) since 1985. The 2019-2020 seismic events (red and orange) are separated from the historical seismicity (black). Hypocenters and focal mechanisms are projected onto a plane normal to the thrust faults identified as ‘composite seismogenic structures’ by the DISS ([Basili \*et al.\* 2008; DISS Working Group 2018](#)). Some earthquake clustering at a 10 km depth represents an artefact due to the conventionally assigned depth to not well-constrained events in the seismic catalogue. The seismogenic structures are displayed using the parameters defined in the latter catalogue (ALCS002: minimum depth = 2 km, maximum depth = 15 km, fault plane dipping 32° to the ENE; ALSC018: minimum depth = 2 km, maximum depth = 10 km, fault plane dipping 37° to the ENE). Basement geometry after Roure *et al.* (2004). (B) Hypocentral distribution for the 2019-2020 seismic events for which both vertical and horizontal uncertainties are provided in the ISIDE (<http://terremoti.ingv.it/iside>) catalogue (error bars are shown in the same section of diagram A).

In a WSW-ENE oriented vertical section, perpendicular to the strike of the ENE gently dipping nodal plane of the focal mechanism of the main shock, the shallow hypocenters tend to cluster around the deeper portion of the projected fault segment of the DISS ‘composite seismogenic source’ labelled ALCS002 (Fig. 2.3A). On the other hand, even taking into account the uncertainties in the top-basement horizon resulting from depth conversion of available seismic reflection profiles (Roure *et al.* 2004) and the error bars associated with earthquake location (Fig. 2.3B), the deeper hypocenters – including the main shock – appear to be located in the basement. Their overall eastward deepening distribution is consistent with the ENE gently dipping fault to which the main shock has been referred to also based on surface deformation (Ganas *et al.* 2020), although the uncertainties in hypocenter location (Fig. 2.3B) do not allow ruling out alternative interpretations such as that proposed by Govorčín *et al.* (2020).

## 2.4. Stress field analysis

The stress field analysis was performed with WinTensor<sup>TM</sup> software (Delvaux and Sperner 2003) using the nodal planes of the fault plane solutions provided by the European-Mediterranean RCMT Catalogue solutions (Pondrelli 2002; <http://rcmt2.bo.ingv.it/>; Table 2) for: (i) eleven earthquakes with  $4.2 \leq M_w < 5.2$  recorded from July 1997 to June 2019, and (ii) the six stronger earthquakes of the 2019-2020 seismic sequence ( $4.7 \leq M_w < 6.4$ ). The focal mechanisms were used to calculate the active stress field by applying three different methods: (i) the PBT kinematic axes method (Turner 1953), (ii) the improved version of the Right Dihedron Method by Angelier and Mechler (1977), and (iii) the Rotational Optimization Method proposed by Delvaux and Sperner (2003).

DATE	TIME [UTC]	MW	STRIKE A	DIP A	RAKE A	STRIKE B	DIP B	RAKE B
<b>28/11/1999</b>	00:59:47	4.8	320	25	91	138	65	90
<b>05/09/2007</b>	05:08:15	4.8	26	49	158	131	73	43
<b>20/01/2014</b>	06:00:15	4.6	351	24	115	143	68	79
<b>08/03/2014</b>	15:06:32	4.2	41	35	104	204	56	80
<b>08/03/2014</b>	15:12:32	4.3	15	31	135	145	69	67
<b>29/12/2014</b>	20:34:13	4.8	334	32	106	135	59	80
<b>27/03/2016</b>	13:09:30	4.2	105	60	33	357	62	145
<b>04/07/2018</b>	09:01:08	5.13	356	34	125	135	63	69
<b>04/07/2018</b>	09:08:58	4.47	13	62	170	108	81	28
<b>04/07/2018</b>	11:24:20	4.53	9	53	167	107	79	38
<b>05/07/2018</b>	22:49:02	4.44	344	36	102	149	55	82
<b>21/09/2019</b>	<b>14:04:27</b>	<b>5.7</b>	<b>328</b>	<b>37</b>	<b>95</b>	<b>142</b>	<b>53</b>	<b>86</b>
<b>21/09/2019</b>	<b>14:15:54</b>	<b>5.1</b>	<b>346</b>	<b>36</b>	<b>117</b>	<b>134</b>	<b>59</b>	<b>72</b>
<b>26/11/2019</b>	<b>02:54:10</b>	<b>6.4</b>	<b>352</b>	<b>22</b>	<b>115</b>	<b>145</b>	<b>71</b>	<b>80</b>
<b>26/11/2019</b>	<b>06:08:22</b>	<b>5.5</b>	<b>339</b>	<b>43</b>	<b>105</b>	<b>139</b>	<b>49</b>	<b>77</b>
<b>26/11/2019</b>	<b>13:05:00</b>	<b>4.7</b>	<b>14</b>	<b>28</b>	<b>143</b>	<b>138</b>	<b>73</b>	<b>67</b>
<b>27/11/2019</b>	<b>14:45:25</b>	<b>5.3</b>	<b>342</b>	<b>30</b>	<b>93</b>	<b>158</b>	<b>60</b>	<b>88</b>

Tab. 2.2 - Earthquake focal mechanisms dataset (from the European-Mediterranean RCMT Catalogue solutions; <http://rcmt2.bo.ingv.it/>) used to perform the stress analyses. Data related to the 2019-2020 seismic sequence are shown in bold.

The PBT kinematic axes method is largely used in structural geology. It is based on the Mohr-Coulomb fracture criterion and calculates the stresses from the orientation of single fault planes, for which P is the compression axis, B is the neutral axis (contained in the fault plane), and T

is the extension axis (Sippel *et al.* 2009). This method can be applied assuming that all faults were formed and moved by the same stress field.

The Improved Right Dihedron Method allows one to obtain four parameters of the reduced stress tensor: the principal stress axes  $\sigma_1$  (maximum compression),  $\sigma_2$  (intermediate compression) and  $\sigma_3$  (minimum compression), and the stress ratio R (also defined as stress regime; Angelier 1989):

$$R = \frac{\sigma_2 - \sigma_3}{\sigma_1 - \sigma_3} \quad (1)$$

The stress ratio is a well-defined, useful indicator of the state of stress:  $R = 0$  or  $R = 1$  define an axial state of stress characterized by  $\sigma_1 > \sigma_2 = \sigma_3$  or  $\sigma_1 = \sigma_2 > \sigma_3$ , respectively. Otherwise, a value of  $0 < R < 1$  indicates a triaxial state of stress.

The Rotational Optimization Method is an inversion procedure included in WinTensor<sup>TM</sup> that allows one to decrease the misfits using both nodal planes of the focal mechanism. By this procedure, the software considers as active the plane having the smaller misfit value. The average misfit angle and the quality of the stress tensor estimation are expressed on a scale ranging from A (best result) to E (worst result) according to the World Stress Map quality ranking scheme (QR) (<http://www.world-stress-map.org/>).

The stress inversion using the three different methods provided very consistent, stable results (Fig. 2.4). They show a compressional stress regime ( $R = 0.5$  for the 2019-2020 seismic sequence) characterized by a maximum horizontal compression trending WSW-ENE. This is in good agreement with previous results of stress inversion from focal mechanisms of moderate earthquakes in Albania (Dushi *et al.* 2015) and with the general framework of active stress in this part of the Mediterranean area (Heidbach *et al.* 2016), thus confirming the consistency of the regional active stress field. Angle of plunge and trend of the principal stress axes obtained from the PBT kinematic axes method and the Rotational Optimization Method (this latter reaching a B stress tensor quality) applied to the 2019-2020 seismic sequence are the same:  $\sigma_1$  ( $15^\circ/241^\circ$ ),  $\sigma_2$  ( $10^\circ/148^\circ$ ) and  $\sigma_3$  ( $72^\circ/025^\circ$ ). The improved version of the Right Dihedron Method yielded only slightly different results for the 2019-2020 seismic sequence:  $\sigma_1$  ( $16^\circ/243^\circ$ ),  $\sigma_2$  ( $09^\circ/151^\circ$ ) and  $\sigma_3$  ( $72^\circ/032^\circ$ ).

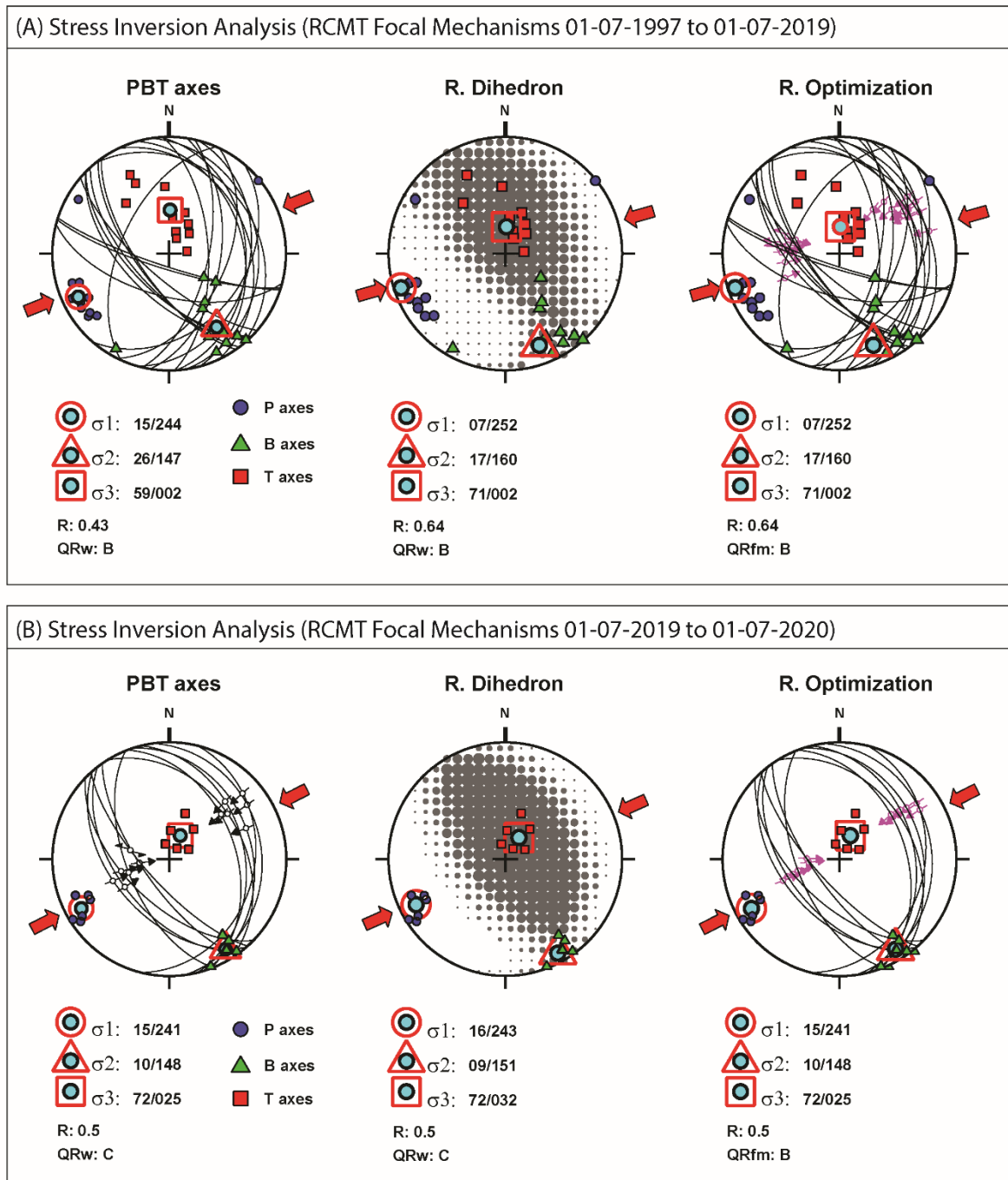


Fig. 2.4 - Stress field analysis results performed by WinTensor<sup>TM</sup> (Delvaux and Sperner 2003) using the three different methods explained in the text, applied onto the seismological dataset available from the European-Mediterranean RCMT Catalogue solutions (<http://rcmt2.bo.ingv.it/>). (a) Analysis based on 1997 to June 2019 seismicity. (b) Analysis based on the focal mechanisms of the 2019-2020 seismic sequence. [The obtained principal stress axes are shown.](#)



## 2.5. Crustal geological section across the northern outer Albanides and the thrust front

Figure 2.2 shows the trace of an ENE-WSW oriented, 115 km long regional cross section built across the outer western sector of the Albanides fold and thrust belt, in the epicentral area of the 2019-2020 earthquake sequence. The crustal cross-section incorporates published seismic data (Roure *et al.* 2004; Muceku *et al.* 2008; Frasheri *et al.* 2009) calibrated by well logs, geological and seismological data.  $M \geq 4$  earthquake hypocenters (compare with Fig. 2.3) were plotted along the cross-section to illustrate how they cluster and fit with interpreted tectonic structures. The interpreted seismic profile of Fig. 2.5 provides constraints on the central portion of the geological section of Fig. 2.6 (located in Figs. 2.2 and 2.3).

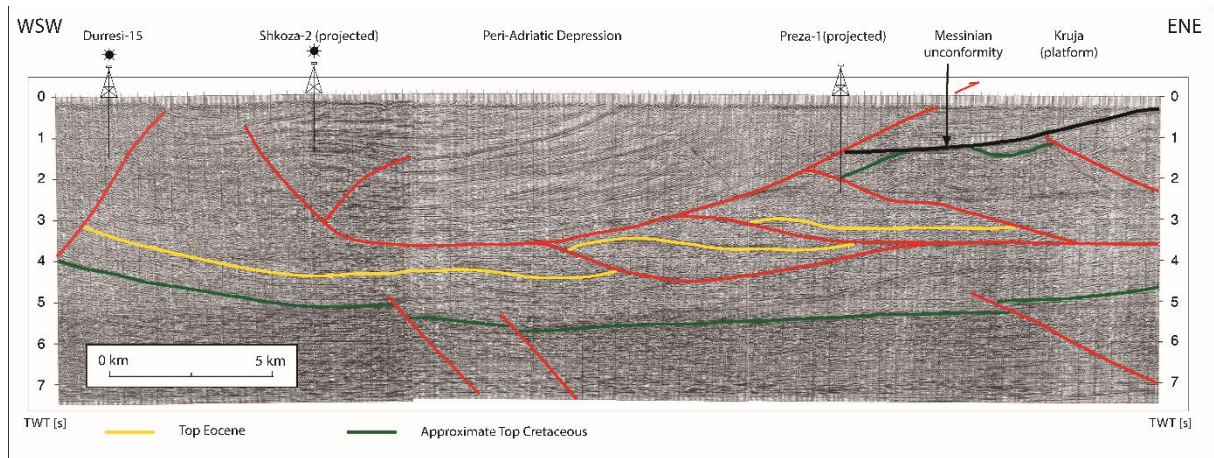


Fig. 2.5 - Interpreted seismic (time) section across the outer Albanides (after Roure *et al.* 2004, modified; located in Fig. 2).

The eastern portion of the seismic line shows the structures involving the Kruja carbonate platform and the stratigraphically overlying foredeep clastic succession. A series of east-dipping thrust faults forms a W-transported thrust stack sealed by a Messinian unconformity. As a whole this structure forms a triangle zone (of intercunaneous wedge type according to McClay 1992) affecting the Cenozoic succession in its frontal portion. The backthrust at the top of the wedge also offsets the succession overlying the Messinian unconformity (Figs. 2.5 and 2.6), thus testifying a recent (*i.e.*, Plio-Quaternary) activity of this structure. Part of the thrust slip is also shown in the interpreted seismic line of Figure 2.5 to be passed to a pop-up located farther west, involving the Neogene clastic succession (penetrated by a hydrocarbon exploration well). A low-displacement thrust occurs in the footwall of the thrust stack, offsetting the Mesozoic succession in the eastern deep portion of the seismic profile (Fig. 2.5).

According to Roure *et al.* (2004), this fault may interact with the pre-existing extensional basin architecture, as it cuts across the platform-to-basin transition (Kruja paleoslope) and is likely rooted down into the basement (Fig. 2.6).

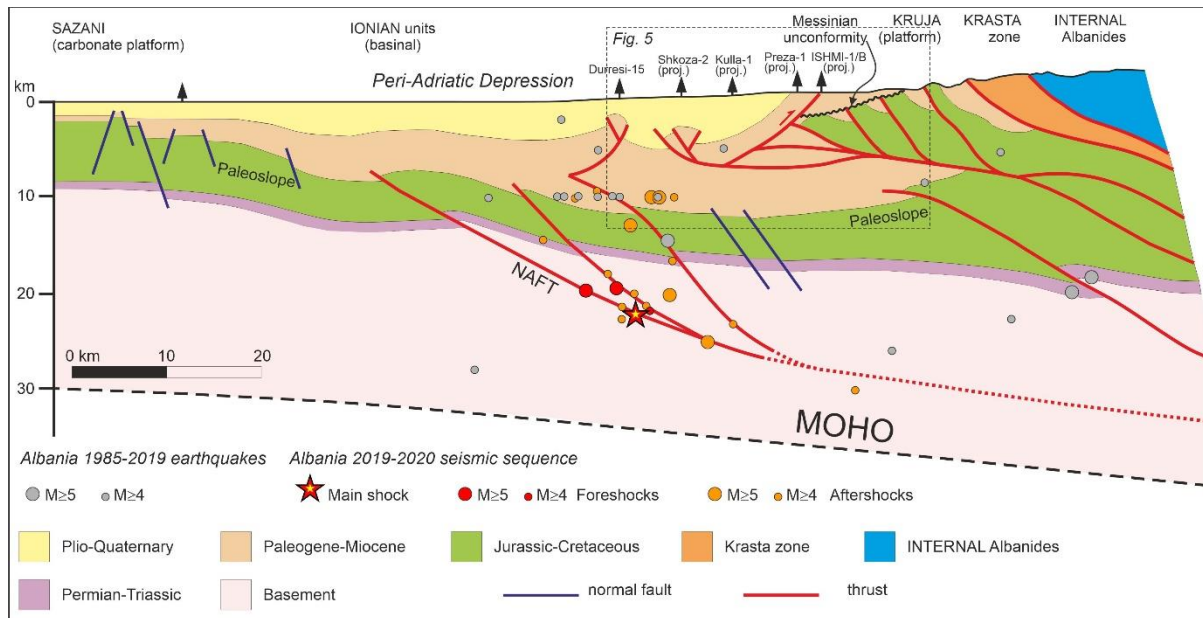


Fig. 2.6 - WSW-ENE regional geological section across the northern outer Albanides (sedimentary cover structure based on Roure *et al.* 2004, and Frasheri *et al.* 2009, modified) showing earthquake hypocenters (red dots are the events of the 2019-2020 seismic sequence; grey dots represent previous seismic events recorded since 1985 by ISIDE: <http://terremoti.ingv.it/iside>; earthquake clustering at a 10 km depth is due to an artefact, refer to Fig. 2.3) and approximate extent of the portion covered by the seismic line of Fig. 2.5. No internal stratigraphy is shown for the Internal Albanides and Krasta units, which are not relevant for this study.

The next pop-up to the west is located close to the edge of the seismic profile. There, a backthrust was interpreted by Roure *et al.* (2004) as a steep fault down to a depth of 4 s two-way-time along the western edge of the line, with no envisaged connection with any thrust detachment within the Cenozoic portion of the sedimentary cover. This pop-up is interpreted to represent a shallow structure linked with a basement fault at depth, as shown in the cross-section of Fig. 2.6. The upper portion (i.e., that included within the sedimentary cover) of the thrust bounding the pop-up to the west roughly coincides with the thrust fault segment of the DISS ‘composite seismogenic source’ labelled ALCS002 (Fig. 2.3). It is worth noting that some of the shallower aftershocks of the 2019-2020 seismic sequence appear to cluster in the vicinity of this fault segment, although the uncertainty associated with the location of these shallow events does not allow to draw any firm conclusion about its actual role in seismogenesis. Further

west, the outermost anticline of the fold and thrust belt, constrained by means of offshore geophysical datasets by Frasheri *et al.* (2009), may be confidently associated with the frontal thrust of the system. This consists of a blind thrust whose leading segment is shown in the cross-section of Fig. 2.6 as a moderately dipping basement fault, becoming gently dipping at the hypocentral depth of the  $M_w$  6.4, November 2019 earthquake. This fault and additional low-displacement basement thrusts offsetting the Ionian basin succession are interpreted in the cross-section of Fig. 2.6 to detach along a middle crustal décollement.

## 2.6. Discussion

Recent studies (Tavani *et al.*, 2018, 2020; Basilici *et al.* 2020) suggested that detachment along a middle crustal décollement may occur in those portions of fold and thrust belts that developed by shortening of the original proximal domain of the pre-existing passive continental paleomargin. As opposed to the thinning-related disruption characterizing the necking and hyperextended domains of the continental paleomargin, the ductile middle crust layer retains its integrity in the proximal domain. Therefore, it provides a significant mechanical weakness that favors its re-use as a décollement during crustal shortening, as it is envisaged to have occurred in the outer Albanides at the latitude of our cross-section (Fig. 2.6). Here the middle crust may have been further weakened during the late stages of plate convergence following the deposition of a huge thickness of clastic sediments in the Peri-Adriatic Depression, leading to heating of the crystalline basement as a result of thermal blanketing by sediment deposition and radiogenic heat production within the sediments (Copley *et al.* 2009). Such thermal weakening is believed to have controlled the latest Miocene to Pliocene onset of extensional tectonics in the mountains of eastern Albania (Meco and Aliaj 2000) and a related stage of increased exhumation at  $\sim 4\text{--}6$  Ma (Muceku *et al.* 2008), subparallel thrusting and normal faulting being in this model a result of gravitational potential energy differences between the lowlands of western Albania and the mountains in the east (Copley *et al.* 2009). This interpretation, which links the latest Miocene to Pliocene initiation of normal faulting in the belt interior with the reduced size of the topographic contrast that could be supported by the lowlands as a result of thermal weakening of the basement, provides a rough estimate of  $\sim 5$  Ma for the timing of middle crustal décollement and related activation of a creeping detachment within the basement (inferred in our cross-section of Fig. 2.6). Aseismic strain accumulation by stable sliding along the middle crustal décollement leads to the episodic seismic rupture of

otherwise locked upper crustal thrust splays branching out from it, as envisaged for other fold and thrust belts characterized by a similar tectonic setting (Basilici *et al.* 2020).

In the foreland, west of the thrust front, offshore seismic data image a series of normal faults in the Sazani (Apulia) carbonate platform and associated paleoslope (Fraseri *et al.* 2009). The development of these normal faults is probably related to the well-known extensional processes affecting the fore-bulge and the outer portions of flexural foreland basins (e.g., Vitale *et al.* 2012; Di Martire *et al.* 2015; Tavani *et al.* 2018b), which in turn could be superposed onto – and have led to the reactivation of – pre-existing Mesozoic rift-related structures.

### *2.6.1. Implications for thrust belt architecture and active tectonics*

This study provides a comprehensive picture of the structural architecture of the northern sector of the outer Albanides. In particular, a critical reassessment of published geological sections and subsurface data, integrated with the new seismological datasets made available by the 2019-2020 seismic sequence, allowed us to unravel the basement-involved thrusting style characterizing the frontal portion of the fold and thrust belt at the latitude of Durrës (i.e., around 41°20' N). The offshore thrust front in this sector of the fold and thrust belt is defined by a seismogenic, upper crustal blind fault that we term here Northern Albanide Frontal Thrust (NAFT). As was already evident from the geological sections published by Roure *et al.* (2004), the mechanical role of the Triassic evaporites occurring at the base of the Ionian basin succession appears to be negligible at this latitude, where there is little or no basement-cover decoupling of the Ionian basin units. This is in contrast with the structural style displayed by the same units more to the south, where detachment-dominated thrusting (*sensu* Butler and Mazzoli 2006) of the sedimentary cover appears to have been promoted by an efficient décollement level represented by the Triassic evaporites (which also formed large diapirs in this region; e.g., Robertson and Shallo 2000; Lacombe *et al.* 2009). It may be envisaged that the northward transition from thin-skinned deformation of the sedimentary cover to basement-involved thrusting is associated with an overall decreasing thickness of the Triassic evaporites – likely accompanied by an increasing dolomitic limestone component (Velaj 2001) – resulting in a degraded quality of detachment. Such stratigraphic variations are controlled by NE-SW striking transversal ‘lineaments’ interpreted to be related with deep-seated basement faults (e.g., Nieuwland *et al.* 2001; Lacombe *et al.* 2009). We suggest that these long-lived fault zones – the major of them being represented by the Vlora-Elbasan one (Fig. 2.2) – acted as major

transfer zones accommodating the along-strike change in tectonic style from thin-skinned deformation of the sedimentary cover to upper crustal-scale thrusting.

The cumulative low displacement of the basement thrusts characterizing our interpretation of the northern outer Albanides (Fig. 2.6) is consistent with their recent development postdating Oligocene-Miocene shortening. Line-length balancing of the top-basement horizon in the section of Fig. 2.6 yields a cumulative shortening of 6 km associated with the upper crustal thrust ramps. Assuming an initiation of basement-involved thrusting at  $\sim 5$  Ma as discussed above, a shortening rate of  $\sim 1.2$  mm/y is obtained. This value, although representing a first-order approximation due to the uncertainties in the timing of basement thrusting and cross-section construction at depths exceeding 10 km, is anyway fully consistent with recent geodetic data from permanent Global Navigational Satellite System (GNSS) stations in the ETRF2000 'European fixed' reference frame (available at [http://pnac.swisstopo.admin.ch/divers/dens\\_vel/combvel\\_se\\_all\\_cmb\\_grd\\_east.jpg](http://pnac.swisstopo.admin.ch/divers/dens_vel/combvel_se_all_cmb_grd_east.jpg)) yielding a SW-ward motion of  $1.2 \pm 0.7$  mm yr<sup>-1</sup> projected onto our section of Fig. 2.6.

Instrumental seismicity recorded since year 1985 suggests a current activity of several of these basement thrusts, thus indicating overall synchronous thrusting across the frontal part of the orogen. The 2019-2020 seismic sequence itself appears to have ruptured at least two different thrusts. The foreshocks and the main shock (Fig. 2.3) ruptured a basement fault that we identify as the NAFT in the crustal section of Fig. 2.6. Subsequent seismicity migrated in part upward, as indicated by some of the aftershocks that nucleated within the sedimentary cover (Fig. 2.3A). These latter aftershocks appear to have ruptured the shallower portion of an inner thrust (Fig. 2.6), in a sort of break-back sequence. It is worth noting that also the hypocenters of pre-2019 earthquakes appear to be mostly located within the sedimentary cover (Figs. 2.3A and 2.6). Although the artificial alignment of many of these events at 10 km depth (refer to Fig. 2.3) does not allow to obtain an accurate picture of pre-2019 seismicity, the previously elusive thrust fault motion at basement depths could have led to the definition of relatively shallow seismogenic sources confined within the sedimentary cover (Basili *et al.* 2008; DISS Working Group 2018; Fig. 2.3).

Our interpretation of the seismogenic structure responsible for the 26-11-2019 main shock is also at variance with respect to that recently provided by Govorčín *et al.* (2020). These Authors, based on differential InSAR and geodetic data, reconstructed the geometry and slip of the 2019 causative fault and they concluded that both a steep SW-dipping and a shallow NE-dipping fault could fit the data equally well. However, as the slip on the modelled SW-dipping fault

occurs at depths of 11-23 km – therefore more similar to the depths of the main shock and aftershocks of the 2019-2020 seismic sequence – they favour earthquake nucleation along this steep ( $71^\circ$ ) backthrust. Although we are fully aware that the ENE-ward deepening of seismicity cannot provide conclusive evidence for a ENE dipping active thrust due to the uncertainties associated with the hypocentral locations (Fig. 2.3B), we note that: (i) all previous studies based on coseismic surface deformation patterns favour the ENE gently dipping nodal plane of the focal mechanism (Fig. 2.1) as the causative fault for the  $M_w = 6.4$  event (Caporali *et al.* 2020; Ganas *et al.* 2020), and (ii) almost pure dip-slip reverse motion along a  $71^\circ$  dipping fault would be mechanically extremely unfavorable. In any case, the two different models may be tested by analyzing post-seismic deformation in the months and years to come. Afterslip is well known to occur during years or even decades following the main shock (e.g., Copley 2014; Copley and Reynolds 2014). In our interpretation, post-seismic afterslip is likely to characterize the upper part of the NAFT, eventually (possibly) contributing to further growth of the frontal hanging-wall anticline offshore (Fig. 2.6). On the other hand, post-seismic afterslip along the steep backthrust envisaged by Govorčín *et al.* (2020) would result in a distinct surface deformation pattern onshore (in an area close to the city of Tirana), this type of surface deformation being commonly unravelled by InSAR and GPS measurements (Copley 2014; Copley and Reynolds 2014). Taking into account the important implications of the different seismotectonic models in terms of seismic hazard, monitoring surface deformation by means of InSAR and geodetic data analysis is strongly recommended over the months and years to come. This is particularly relevant as Govorčín *et al.* (2020) further suggested that, since the fault rupture did not reach the surface, an up-dip stress propagation onto the still locked shallow portion of their steep backthrust would substantially increase the seismic hazard for Albanian cities (including the capital Tirana).

## 2.7. Concluding remarks

The seismological evidence provided by the 2019-2020 earthquakes, analyzed in this study by stress inversion performed on the focal mechanisms available from the RCMT catalogue (Pondrelli 2002; <http://rcmt2.bo.ingv.it/>), is consistent with the roughly horizontal, ENE-WSW trending active maximum compression characterizing the region. The integrated analysis of epicenter distribution, hypocenter depth and fault plane solutions suggests that coseismic slip associated with the  $M_w = 6.4$ , November 2019 Albania earthquake occurred along a NNW-SSE striking, ENE dipping thrust fault (Fig. 2.6). Hypocentral distribution shows that the 2019-

2020 seismic events are located in a depth range of 10-36 km and tend to deepen moving eastward. The shallower aftershocks could have involved rupturing along the ‘composite seismogenic sources’ included in the DISS catalogue (particularly that labelled ALCS002; Basili *et al.* 2008; DISS Working Group 2018; Fig. 2.3A). However, hypocenter distribution indicates that most of the earthquakes, including the Mw = 6.4 main shock, were nucleated within the basement, well below the envisaged lower tips of the seismogenic structures displayed in the latter catalogue (Fig. 2.3).

As earthquake nucleation appears to have occurred mainly in the crystalline upper crust, an enhanced seismotectonic model for the northern sector of the outer Albanides should take into account the fundamental role of active, deep-seated faults – particularly the NAFT – that have been clearly overlooked so far. The outcomes of this study provide new constraints on the identification of such deep seismogenic sources and to the definition of their dimensional parameters. This, in turn, bears major implications for a correct assessment of earthquake hazard in a large and densely populated area of Albania. More in general, the evidence provided in this study for a deep seismogenic thrust system in a foreland basin setting may be of interest for similar tectonic contexts worldwide.

## 2.8. References

- Angelier, J. and Mechler, P. 1977. Sur une méthode graphique de recherche des contraintes principales également utilisable en tectonique et en séismologie: la méthode des dièdres droits. *Bulletin de la Société géologique de France*, 7(19), 1309-1318.
- Angelier, J. 1989. From orientation to magnitudes in paleostress determinations using fault slip data. *Journal of structural geology*, 11(1-2), 37-50.
- Basili, R., Valensise, G., Vannoli, P., Burrato, P., Fracassi, U., Mariano, S., Tiberti, M.M. and Boschi, E. 2008. The Database of Individual Seismogenic Sources (DISS), version 3: summarizing 20 years of research on Italy’s earthquake geology. *Tectonophysics*, 453, 20-43, doi:10.1016/j.tecto.2007.04.014.
- Basilici, M., Ascione, A., Megna, A., Santini, S., Tavani, S., Valente, E., And Mazzoli, S. 2020. Active deformation and relief evolution in the western Lurestan region of the Zagros mountain belt: new insights from tectonic geomorphology analysis and finite element modeling. *Tectonics*, e2020TC006402. <https://doi.org/10.1029/2020TC006402>.

- Bega, Z. and Soto, J.I. 2017. The ionian fold-and-thrust belt in Central and Southern Albania: a petroleum province with triassic evaporites. In *Permo-Triassic Salt Provinces of Europe, North Africa and the Atlantic Margins* (pp. 517-539). Elsevier. <https://doi.org/10.1016/B978-0-12-809417-4.00025-2>.
- Bortolotti, V., Kodra, A., Marroni, M., Mustafa, F., Pandolfi, L., Principi, G. and Saccani, E. 1995. Geology and petrology of ophiolitic sequences in the Mirdita region (northern Albania): *Ofioliti*, v. 21, p. 3–20.
- Butler, R. W. and Mazzoli, S. 2006. Styles of continental contraction: A review and introduction, in *Styles of Continental Contraction*, Special papers-Geological Society of America, 414(1), edited by S. Mazzoli, and R. W. H. Butler, pp. 1-10, GSA, Boulder, Colorado.
- Caporali, A., Floris, M., Chen, X., Nurçe, B., Bertocco, M. and Zurutuza, J. 2020. The November 2019 Seismic Sequence in Albania: Geodetic Constraints and Fault Interaction. *Remote Sensing*, 12(5), 846.
- Copley, A., Boait, F., Hollingsworth, J., Jackson, J. and McKenzie, D. 2009. Subparallel thrust and normal faulting in Albania and the roles of gravitational potential energy and rheology contrasts in mountain belts. *Journal of Geophysical Research*, 114, B05407. <https://doi.org/10.1029/2008JB005931>.
- Copley, A. 2014. Postseismic afterslip 30 years after the 1978 Tabas-e-Golshan (Iran) earthquake: observations and implications for the geological evolution of thrust belts, *Geophysical Journal International*, 197, 665-679, <https://doi.org/10.1093/gji/ggu023>.
- Copley, A. and Reynolds, K. 2014. Imaging topographic growth by long-lived postseismic afterslip at Sefidabeh, east Iran, *Tectonics*, 33, <https://doi.org/10.1002/2013TC003462>.
- Delvaux, D. and Sperner, B. 2003. Stress tensor inversion from fault kinematic indicators and focal mechanism data: the TENSOR program. In: *New Insights into Structural Interpretation and Modelling* (D. Nieuwland Ed.). Geological Society, London, Special Publications, 212: 75-100.
- Di Martire, D., Ascione, A., Calcaterra, D., Pappalardo, G. and Mazzoli, S. 2015. Quaternary deformation in SE Sicily: Insights into the life and cycles of forebulge fault systems. *Lithosphere*, 7 (5), 519-534, doi: 10.1130/L453.1.
- DISS Working Group 2018. Database of Individual Seismogenic Sources (DISS), Version 3.2.1: A compilation of potential sources for earthquakes larger than M 5.5 in Italy and surrounding areas. <http://diss.rm.ingv.it/diss/>, Istituto Nazionale di Geofisica e Vulcanologia; DOI:10.6092/INGV.IT-DISS3.2.1.



- Duni, L., Bozo, L., Kuka, N. and Begu, E. 2010. An Upgrade of the Microzonation Study of the Centre of Tirana City. *International Conferences on Recent Advances in Geotechnical Earthquake Engineering and Soil Dynamics*. 3.
- Dushi E., Koci R., Begu E. and Bozo Rr. 2018. Stress Inversion from Focal Mechanism of Moderate Earthquakes in Albania. Presented at 18th International Multidisciplinary Scientific GeoConference SGEM 2018, 02-08 July, 2018, doi: 10.5593/sgem2018/1.1/S05.123.
- Frashëri, A., Nishani, P., Bushati, S. And Hyseni, A. 1995. Geophysical Study of the Albanides: *Bolletino di Geofisica Teorica ed Applicata*. 37(146), 83-108.
- Frasheri, A., Nishani, P., Bushati, S. and Hyseni, A. 1996. Relationship between tectonic zone of the Albanides, based on results of geophysical studies. In: *PeriTethys Memoir 2: Structure and Prospects of Alpine Basins and Forelands* (P. Ziegler and F. Horvath, eds). *Mémoires du Muséum national d'histoire naturelle*. Paris, 170, 485–511.
- Frasheri, A., Bushati, S. and Bare, V. 2009. Geophysical outlook on structure of the Albanides. *Journal of the Balkan Geophysical Society*, 12:9–30.
- Ganas, A., Elias, P., Briole, P., Cannavo, F.; Valkaniotis, S., Tsironi, V. and Partheniou, E.I. 2020. Ground Deformation and Seismic Fault Model of the M6.4 Durrës (Albania) Nov. 26, 2019 Earthquake, Based on GNSS/INSAR Observations. *Geosciences* 2020, 10, 210. <https://doi.org/10.3390/geosciences100602>.
- Govorčin, M., Wdowinski, S., Matoš, B., And Funning, G.J. 2020. Geodetic source modeling of the 2019, Mw 6.3 Durrës, Albania earthquake: partial rupture of a blind reverse fault. *Geophysical Research Letters*, e2020GL088990. <https://doi.org/10.1029/2020GL088990>.
- Heidbach, O., Custodio, C., Kingdon, A., Mariucci, M. T., Montone, P., Müller, B., Pierdominici, S., Rajabi, M., Reinecker, J., Reiter, K., Tingay, M., Williams, J., Ziegler, M., 2016. Stress map of the Mediterranean and Central Europe 2016. *World Stress Map*. Potsdam, Germany, GFZ Data Services. <https://doi.org/10.5880/WSM.Europe2016>.
- McClay, K.R., 1992. Glossary of thrust tectonics terms In McClay, K.R., ed., *Thrust tectonics*. London, Chapman & Hall, p. 419–433.
- Mecaj, s. And Mahmutaj, L. 1995. The main lithologo-petrographic characteristics of carbonate and terrigenous deposits in the south-western external Albanides. In Paper presented at ALBPETROL-95 symposium, Fier, Albania.

- Meco, B. And Aliaj, S. 2000. Geology of Albania. Beiträge zur regionalen Geologie der Erde, 28. Borntraeger, Berlin.
- Muceku, B., Mascle, G. and Tashko, A. 2006. First results of fission-track thermochronology in the Albanides. In: Tectonic Development of the Eastern Mediterranean Region (A.H.F. Robertson and D. Mountrakis, eds). Geological Society, London, Special Publications, 260, 539–556.
- Muceku, B., P. van der Beek, M. Bernet, P. Reiners, G. Mascle, and Tashko, A. 2008. Thermochronological evidence for Mio-Pliocene late orogenic extension in the north-eastern Albanides (Albania), Terra Nova, 20, 180–187.
- Nieuwland, D.A., Oudmayer, B.C., and Valbona, U., 2001. The tectonic development of Albania: explanation and prediction of structural styles. Mar. Pet. Geol. , 18, 161–177.
- Pondrelli, S. 2002. European-Mediterranean Regional Centroid-Moment Tensors Catalog (RCMT) [Data set]. Istituto Nazionale di Geofisica e Vulcanologia (INGV). <https://doi.org/10.13127/rcmt/euomed>.
- Prenjasi, E., Karriqi, A., Nazaj, S. and Gjoni, K. 2011. Tectonic Setting and Hydrocarbon Potential of the Albanides Fold-and-Thrust Belts. In The Geology in Digital Age: Proceedings of the 17th Meeting of the Association of European Geological Societies (p. 93). Serbian Geological Society.
- Roure, F. and Sassi, W. 1995. Kinematics of deformation and petroleum system appraisal in Neogene foreland fold-and-thrust belts. Petroleum Geoscience, 1(3), 253-269.
- Roure, F., nazaj, Sh., Mushka, K., fili, I., Cadet, J. P. and., Bonneau, M. 2004. Kinematic evolution and petroleum systems – an appraisal of the Outer Albanides. In: Thrust Tectonics and Hydrocarbon Systems (K.R. McClay, ed.). AAPG Mem., 82, 474–493.
- Roure, F., Swennen, R., Schneider, F., Faure, J.L., Ferket, H., Guilhaumou, N., Osadetz, K., Robion, P.h., Vandeginste, V., 2005. Incidence of tectonics and natural fluid migration on reservoir evolution in foreland fold-and-thrust belts. Oil Gas Sci. Technol. Rev. IFP, 60, 67–106.
- Robertson, A. H. F., and Shallo, M. 2000. Mesozoic-Tertiary tectonic evolution of Albania in its regional Eastern Mediterranean context. Tectonophysics, 316, 197–254.

- Saccani, E., Dilek, Y. and Photiades, A. 2018. Time-progressive mantle-melt evolution and magma production in a Tethyan marginal sea: A case study of the Albanide-Hellenide ophiolites. In: *Lithosphere* (2018) 10 (1): 35–53. <https://doi.org/10.1130/L602.1>.
- Shehu, H. 1995. The geological feature and oil and gas bearing perspective of Kruja tectonic zone. In Paper presented at the ALBPETROL-95 symposium, Fier, Albania.
- Sippel, J., Scheck-Wenderoth, M., Reicherter, K. and Mazur, S. 2009. Paleostress states at the South-Western margin of the Central European Basin System—application of fault-slip analysis to unravel a polyphase deformation pattern. *Tectonophysics*, 470(1–2), 129–146. doi:10.1016/j.tecto.2008.04.010.
- Tavani, S., Parente, M., Puzone, F., Corradetti, A., Gharabeigli, G., Valinejad, M., Morsalnejad, and Mazzoli, S. 2018a. The seismogenic fault system of the 2017 Mw 7.3 Iran-Iraq earthquake: constraints from surface and subsurface data, cross-section balancing and restoration. *Solid Earth*, 9, 821–831. doi:10.5194/se-9-821-2018.
- Tavani, S., Corradetti, A., Sabbatino, M., Morsalnejad, D. and Mazzoli, S. 2018b. The Mesozoic fracture pattern of the Lurestan region, Iran: The role of rifting, convergence, and differential compaction in the development of pre-orogenic oblique fractures in the Zagros Belt. *Tectonophysics*, 749, 104–119. doi:10.1016/j.tecto.2018.10.031.
- Tavani, S., Camanni, G., Nappo, M., Snidero, M., Ascione, A., Valente, E. and Mazzoli, S. (2020). The Mountain Front Flexure in the Lurestan region of the Zagros belt: Crustal architecture and role of structural inheritances. *Journal of Structural Geology*, 104022. Doi:10.1016/j.jsg.2020.104022.
- Tremblay, A., Meshi, A., Deschamps, T., Goulet, F. and Goulet, N. 2015. The Vardar zone as a suture for the Mirdita ophiolites, Albania: Constraints from the structural analysis of the Korabi-Pelagonia zone. *Tectonics*, 34, 352–375, doi:10.1002/2014TC003807.
- Turner, F.J. 1953. Nature and dynamic interpretation of deformation lamellae in calcite of three marbles. *American Journal of Science*, 251(4):276–298.
- Velaj, T. 2001. Evaporites in Albania and their impact on the thrusting processes. *Journal of the Balkan Geophysical Society*, 4(1), 9–18.
- Velaj, T. 2015. The structural style and hydrocarbon exploration of the subthrust in the Berati Anticlinal Belt, Albania. *Journal of Petroleum Exploration and Production Technology*, 5, 123–145. doi:10.1007/s13202-015-0162-1.

Vitale, S., Dati, F., Mazzoli, S., Ciarcia, S., Guerriero, V. and Iannace, A. 2012. Modes and timing of fracture network development in poly-deformed carbonate reservoir analogues, Mt. Chianello, southern Italy. *Journal of Structural Geology*, 37, 223-235, doi: 10.1016/j.jsg.2012.01.005.

Zappaterra, E. 1990. Carbonate paleogeographic sequences of the Periadriatic region. *Bollettino della Società Geologica Italiana*, 109, 5–20.

### 3. PLIO–QUATERNARY STRUCTURAL EVOLUTION OF THE OUTER SECTOR OF THE MARCHE APENNINES SOUTH OF THE CONERO PROMONTORY, ITALY

M. Costa<sup>1</sup>, J. M. Chicco<sup>2</sup>, C. Invernizzi<sup>3\*</sup>, S. Teloni<sup>3</sup> and P.P. Pierantoni<sup>3</sup>

<sup>1</sup> Via Selvelli, 6, 61032 Fano, Italy,

<sup>2</sup> Department of Earth Sciences, University of Turin, Via Valperga Caluso, 35, 10125 Torino, Italy,

<sup>3</sup> School of Science and Technology, Geology Division, University of Camerino, Via Gentile III da Varano, 62032 Camerino, (MC), Italy.

**Abstract:** Some new results and preliminary remarks about the Plio–Quaternary structural and evolutionary characteristics of the outer Marche Apennines south in the Conero promontory are presented in this study. The present analysis is based on several subsurface seismic reflection profiles and well data, kindly provided by ENI S.p.A. and available on the VIDEPI list, together with surface geologic–stratigraphic knowledge of Plio–Quaternary evolution from the literature. Examples of negative vs. positive reactivation of inherited structures in fold and thrust belts are highlighted. Here, we present an example from the external domain of the Marche Apennines, which displays interesting reactivation examples from the subsurface geology explored. The study area shows significant evolutionary differences with respect to the northern sector of the Marche region previously investigated by the same research group. The areal distribution of the main structures changes north and south of the ENE–WSW oriented discontinuity close to the Conero promontory. Based on the old tripartite classification of the Pliocene, the results of this work suggest a strong differential subsidence with extension occurring during the Early Pliocene and principal compressive deformation starting from the Middle Pliocene and decreasing or ceasing during the Quaternary. The main structure in this area is the NNW–SSE Coastal Structure, which is composed of E-vergent shallow thrusts and high-angle deep-seated normal faults underneath. An important right-lateral strike–slip component along this feature is also suggested, which is compatible with the principal NNE–SSW shortening direction. As mentioned, the area is largely characterized by tectonic inversion. Starting from Middle Pliocene, most of the Early Pliocene normal faults became E-vergent thrusts.

**Keywords:** *Plio-Quaternary evolution, outer Marche Apennines, seismic reflection profiles, tectonic inversion, Coastal Structures, extensional and contractional deformation.*

### 3.1. Introduction

In the Apennines of Italy, and especially the Adriatic foreland domain, it is possible to infer the foreland deformation process and explore the impacts of inherited faults and basins on the subsequent evolution thanks to the milder deformation in the area and the good geological and geophysical record documenting an interaction between normal, thrust, and strike–slip faults.

Foreland domains are often affected by inherited rift-related or flexure-related syn-sedimentary normal faults becoming involved in the advancing fold-and-thrust belt. This introduces an element of further complications into the evolution of the foredeep systems subsequently involved in the mountain belts, as evidenced by numerous studies in different contexts, such as the Northern Apennines, Po Plain, and South-Eastern Pyrenean foreland basins (Boccaletti, et al., 1990; Ghielmi et al., 2010; Turrini et al. 2016; Odlum et al., 2019 among others).

The tectonic and structural features of the Umbria-Marche Apennines (Figure 3.1) are widely described in the literature, and several models have been proposed. The most important model is found in Bally et al., 1986, which proposes a thin-skinned imbricate belt detached above the crystalline basement (see also Calamita et al. 1986). This model indicates strong shortening (in the order of hundreds of kilometers) and important repetitions of the sedimentary cover. Further studies on the geometries and evolution of the outer Marche sector, as well as their extent, style, and age of deformation, are thoroughly reported in many works. Among others, Centamore et al., 1991; Pierantoni et al., 2005; Amadori et al., 2019; Cantalamessa et al., 1987; Ori et al., 1991; Invernizzi, 1992; Ghielmi et al., 2013 mainly focus on stratigraphic record, geological setting and sedimentary evolution, Barchi et al. 2012 on the anatomy of the Apennine orogen, De Donatis et al., 1998; Mazzoli et al., 2005; Scisciani et al., 2001; Scisciani et al., 2002; Scisciani et al., 2005 Mancinelli et al., 2020 on the structural and deformation style, Barchi et al., 2012; Tavarnelli et al., 2019 on the role of inherited structures and tectonic inversion.

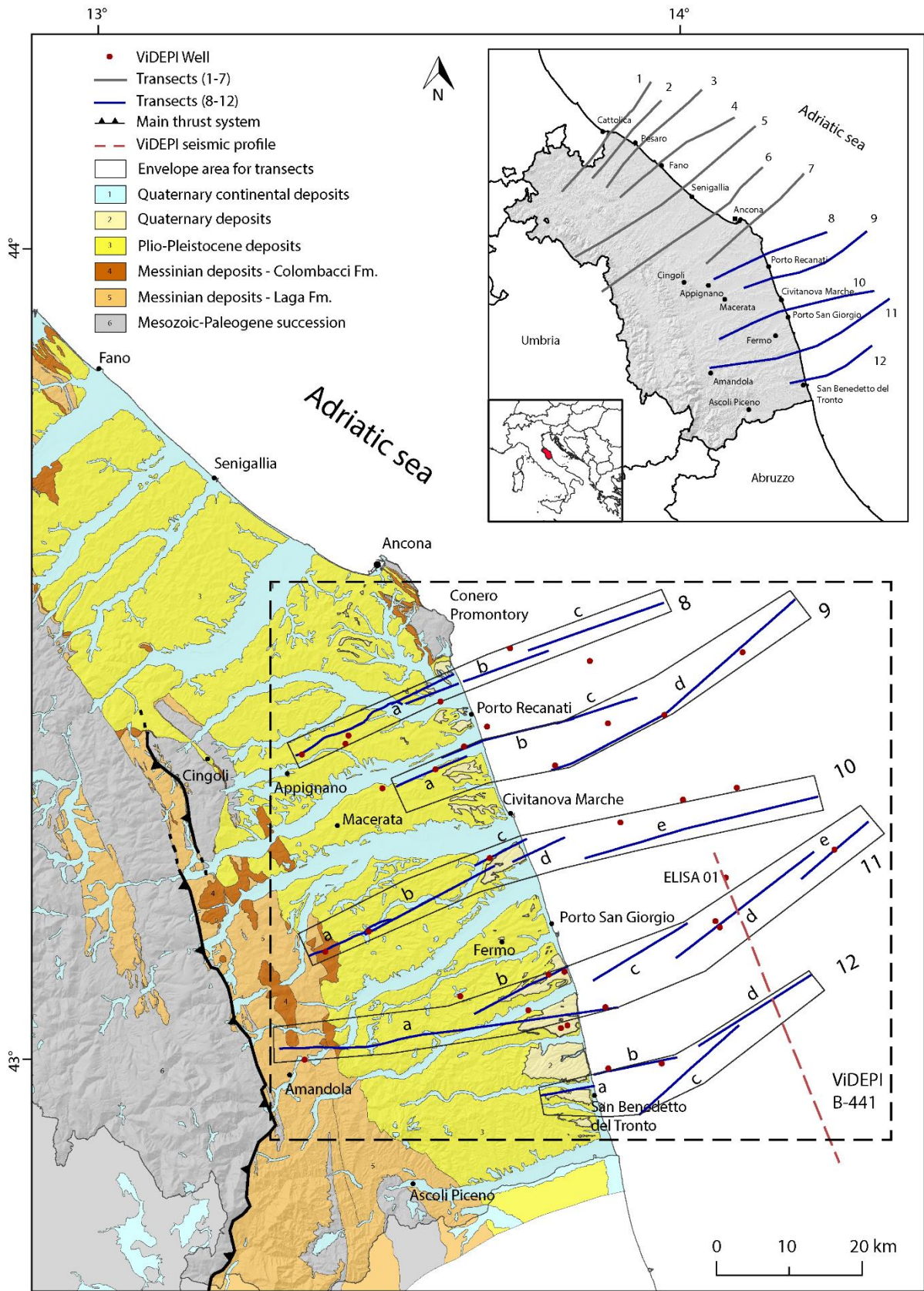


Fig. 3.1 - On shore schematic geological map of the Marche region (modified after Conti et al., 2020. The work in Pierantoni et al. 2013 was considered for the thrust location. Dashed square: study area; dashed line: ViDEPI

The acquisition of new data (such as the CROP project, well stratigraphy and seismic reflection profiles, and sedimentological and paleo-thermometric data) has shed new light on the evolution of the area and introduced models that indicate the crystalline basement's involvement (thick-skinned model) and the reactivation of inherited faults (inversion tectonic model). As a main outcome, the amount of shortening affecting this area was progressively reduced from hundreds of kilometers to tens of kilometers (Scisciani et al., 2014).

New observations about onshore and offshore outcropping and buried Neogene–Quaternary structures, as well as their possible implications for deep geothermal fluid circulation, were recently integrated into the tectonic framework of the northern outer Marche Apennines (Pierantoni et al., 2019; Chicco et al., 2019). These studies highlighted new findings mainly characterized by the presence of positive flower structures to be considered as common features along the whole outer sector of the Northern Apennine chain (Pierantoni et al., 2019). This suggests the more relevant influence of strike–slip kinematics in recent times, with implications for seismic assessment and deep fluid circulation (Chicco et al., 2019).

The southern sector of the outer Marche Apennines has been long investigated by authors who addressed specific features in this area as related to a complex foreland–foredeep geometry. In particular, several works explore the influence of thrust-system propagation on the distribution of sedimentary sequences, their 3D geometric organization, and the burial and exhumation history of these units (Bigi et al., 1999; Artoni et al., 2013; Milli et al., 2007; Bigi et al., 2009; Bigi et al., 2011). These features were identified as the link between the inner, uplifted, and Early Miocene Apennine fold-and-thrust belt and the outer and younger belt to the east (Bigi et al., 2011). The interpretations of integrated structural and stratigraphic studies indicate this to be the result of turbidite deposition in a complex foredeep, strongly affected by tectonic activity and Messinian–Pliocene climate changes (Milli et al., 2007; Ghielmi et al., 2019 and references therein).

This paper represents a continuation of the above-mentioned studies (Pierantoni et al., 2019; Chicco et al., 2019) and aims at highlighting the significant structural and depositional differences between the Northern and Southern outer Marche Apennine, as well as discussing the timing and style of deformation in the outermost sector of the belt toward the Adriatic foreland, where milder deformation and mainly buried structures are present.

To this end, a detailed study along the sector south of the Conero promontory to San Benedetto del Tronto was conducted (Figure 3.1) using seismic reflection profile interpretations and well data for hydrocarbon purposes, kindly provided by ENI S.p.A. Available online:



<https://www.videpi.com/videpi/sismica/sismica.asp> (accessed on 30 of March, 2021), and published studies further contributed to acquiring complete information and enriching the results in our previous works.

### **3.2. Geological setting**

At the continental scale, the Alps and Apennines orogens are located in the hanging wall of two opposite subduction zones. The Alps resulted from the Cretaceous to present via the European plate being subducted beneath the Adriatic plate to the east, whereas the Apennines resulted from the Eocene to the present via subduction of the Adriatic plate to the west (Carminati et al and references therein). The Adriatic plate itself is also subducted below the Dinarides to the east in its easternmost part (Carminati et al., 2012; Cuffaro et al., 2010).

The arcuate-shaped, NE-verging Umbria–Marche Apennines form the external part of the Northern Apennines foreland fold-and-thrust belt (see Deiana and Piali, 1994 and references therein). This belt resulted from the convergence between a mosaic of minor blocks of the Africa–Eurasia plates, such as the European Corsica–Sardinia plate to the West and the African–Adria plate to the east (Dewey et al., 1989; Schettino et al., 2006; Turco et al., 2012; Pierantoni et al., 2020 and references therein).

In the Umbria–Marche area, starting from the Miocene, the previously rifted and telescoped African-bearing continental margin was involved in the compressive phase. Here, different styles and degrees of the positive inversion of pre-orogenic faults controlled the location, geometry, and evolution of compressive structures in several cases (Calamita et al. 2002; Tavarnelli et al., 2004; Mazzoli et al., 2005; Centamore and Rossi, 2009; Scisciani, 2009; Scisciani et al., 2019; Artoni, 2013). In addition, the inner portion of the chain was involved in the Late Miocene to present day extension (Barchi et al., 2012; Pierantoni et al., 2013; Bonini et al., 2019; Mazzoli et al., 2002), with episodes of negative inversion (Scisciani, 2009; Calamita et al., 2000; Cello et al., 2000; Tondi et al., 2020).

The study area belongs to the outer Umbria–Marche Apennines chain. The general tectonic–sedimentary evolution of the Umbria–Marche sequence can be framed in three main stages: pre-, syn-, and post-orogenic sedimentation (Pierantoni et al., 2013). The pre-orogenic sedimentation is characterized by basin carbonates and marly lithostratigraphic units (Late Triassic to Paleogene in age; Pierantoni et al., 2013; Deiana and Piali, 1994 and references therein, Figure 3.1). Both syn- and post-orogenic sedimentation is characterized by prevalent

terrigenous deposits from Neogene to Quaternary in age and hosted in a wide foredeep basin (Periadriatic Foredeep; Carruba et al., 2006). This basin was generated by the flexure of the Adria plate under the Apennine Chain (Lucchi, 1986), migrating eastward. The foredeep filling includes siliciclastic turbidites (e.g., the Messinian Laga Basin), Plio–Pleistocene marine deposits (Lucchi, 1986; Cantalamessa et al., 2021; Marini et al., 2015), and wedge-top basin sediments (Bigi et al., 2011). The foredeep itself was gradually involved into the fold-and-thrust belt during the Late Miocene to present.

In the present study, we investigate an area lying in the outer portion of the Southern Marche Apennines between the Conero promontory and S. Benedetto del Tronto (Figure 3.1). In particular, the double effect of the Sibillini thrust to the west and the Gran Sasso thrust to the south (the Abruzzo area in Figure 3.1) influences the Messinian foredeep geometry and depth. The foredeep hosts thick, internally deformed, turbiditic fan complexes (the Laga Formation; Bigi et al., 2009; Artoni, 2003) and some positive structures (Acquasanta, Montagna dei Fiori and Coastal Structure) described in the literature (see Centamore et al., 1991; Ghielmi et al., 2010; Odlum et al., 2019; Bigi et al., 2009). The outcropping succession consists of Messinian turbiditic deposits (Figure 3.2), including a thick, arenaceous basal member whose source is partially provided by the Eocene–Oligocene westernmost chain (Centamore et al., 1991; Artoni, 2003) and shallow water facies (S. Donato and Argille a Colombacci Formations). The Argille a Colombacci Formation is always above S. Donato Formation, while the latter may rest discordantly above different members of the Laga Formation (see Conti et al., 2020 and references therein). Messinian deposits are followed by the Pliocene succession, whose base marks the marine transgression that occurred after the “lago-mare” phase (sedimentation breck-off; De Alteriis, 1986) and the subsequent filling of the Central Adriatic foredeep (Cantalamessa et al., 2021).

The Plio–Pleistocene foredeep basin is associated with deep marine to alluvial sedimentation that shows progressive infill of the basin and a final vertical regressive trend (Tavarnelli et al., 2004). The infill mainly consists of hemipelagic mudstones deeply incised by coarse-grained canyon-fill deposits (Di Celma, 2011; Di Celma et al., 2013) indicating slope degradation and sediment supply from the uplifted Apennines (Ghielmi et al., 2019). Many authors associate these deposits with the outermost part of the orogenic wedge (Artoni, 2013; Ghielmi et al., 2019) with the formation of thrust fronts and folded structures in the Early Pliocene (Cantalamessa et al., 2021; Ori et al., 1991), followed by intense deep water clayey sedimentation in the deepest areas until the Pleistocene, and a new compressive phase right after, likely linked to the reactivation of Late Pliocene thrusts (Cantalamessa et al., 1987).

Deformation of the foredeep via thrusting likely yielded open piggy-back basins, and structural highs filled up by shallow-water deposits, likely due to the tightness and blockage of the system against a stable platform, as hypothesized in Ori et al., 1991. The sedimentation within the basin was also partially controlled by the Pliocene–Pleistocene obliquity/precession cycles of the Earth’s orbit driving climatic changes, as suggested in Artoni, 2013.

In its outermost portion, the belt shows compressive to transpressive flower structures, which are NW–SE oriented and generally covered by Plio–Pleistocene deposits or partial outcropping on the seafloor. These structures were identified and described in Chicco et al., 2019, further north of the study area as well as some NE-SW trending faults which affects the continuity of the previous structures.

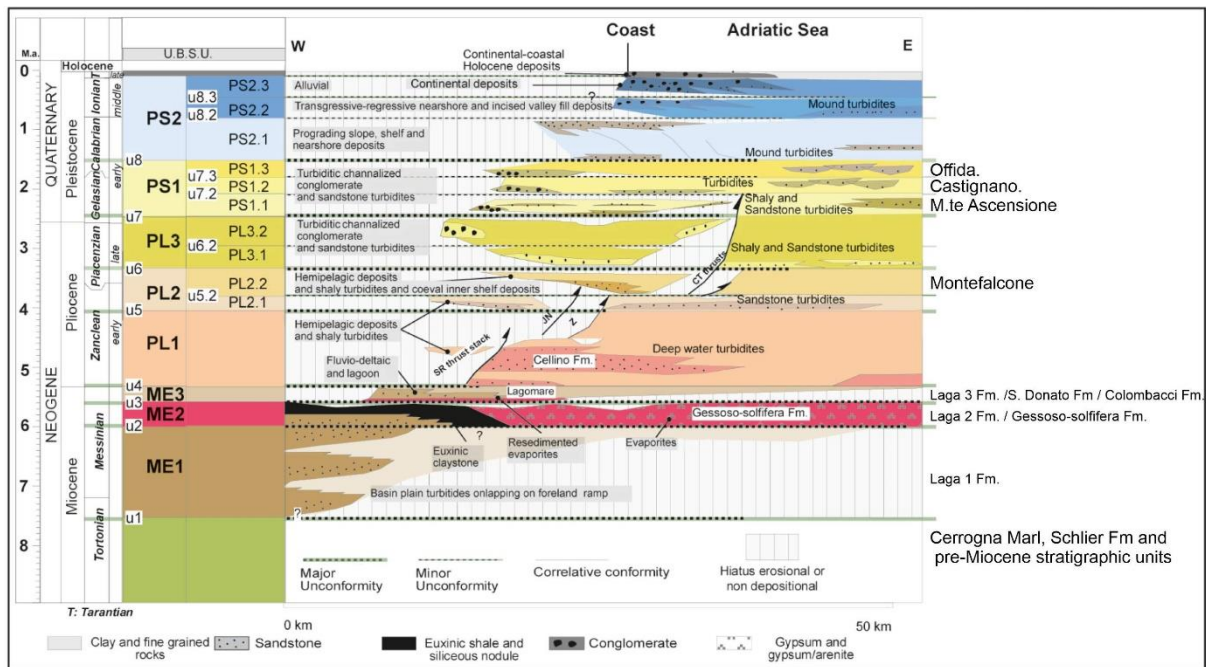


Fig. 3.2 - Synthetic stratigraphic scheme of the Messinian–Pleistocene of the Central Periadriatic Basin (CPB; slightly modified from (Ghielmi et al., 2019). This scheme includes the stratigraphic schemes of previous studies (Ori et al., 1991; Ghielmi et al., 2013; Bigi et al., 1999; Carruba et al., 2006; Roveri et al., 2003), but in the right column, we list only the units and members of our study area.

In the considered area, the main structural element is the NNW–SSE trending Coastal Structure (“Struttura Costiera” in Ori et al., 1991) which is located near the coastline. This structure continues southwards in the Abruzzo area with similar characteristics (Carruba et al., 2006).

Two main deformation events in the area were recognized by previous authors: an extensional Messinian–Early Pliocene event due to the Adria plate flexure (Carruba et al., 2006) followed by a compressive phase ascribable to the late Early Pliocene (De Alteriis, 1986) or to the Middle Pliocene (Carruba et al., 2006).

### 3.3. Dataset and working methods

In the onshore and offshore areas between the Conero promontory and San Benedetto del Tronto locality, numerous seismic profiles have been interpreted in addition to those available from VIDEPI (Geothermica, 2010). The ENI seismic profiles were migrated, while the VIDEPI ones were stacked and already interpreted. Some ENI profiles were of a MERGE type and good quality, resulting from advanced reprocessing. All the wells available in the area corresponding to the interpreted seismic profiles were used for the interpretation. However, the materials supplied by ENI S.p.A. are confidential, and we are thus not able to represent them on the seismic profiles. Only a general well location was reported. For the seismic velocities of the sedimentary sequences, we referred to Mancinelli and Scisciani, 2020; Bigi et al., 2013; Porreca et al., 2018; Centamore et al., 1991. We then compared the seismic stratigraphy of the seismic profile VIDEPI B-441 001 (Figure 3.1) with the log data of the Elisa 1 well placed on it (Figure 3.3). This comparison indicates that velocity,  $V_p$ , for the Plio–Pleistocene sequence is 2000 m/sec in agreement with the literature in the same area (Carruba et al., 2006; Pace et al., 2015).

Seismic profiles were then homogenized and scaled to 1:100.000 horizontally and 1 sec TWT = 2 cm vertically. In this way, the horizontal and vertical scales were harmonized for the Plio–Pleistocene sequence of the seismic profile. In this way, the geometries of the tectonic and seismic–stratigraphic elements were preserved. As velocity increased at depths below the lower Pliocene deposits, the dip angles of these structures became higher.

To determine the Plio–Quaternary’s tectono–stratigraphic evolution, specific seismo–stratigraphic horizons were taken into account, as follows:

- Top of the Messinian/Pre-Pliocene;
- Near the top of the Early Pliocene;
- Near the base of the Quaternary;
- Unconformities.

Within the interpreted profiles, the seismo–stratigraphic horizons are highlighted with different colors (see Figures 3.3 and 3.4 and Plate 1 in Supplementary materials). Unconformities are shown in green dots (see Figures 3.4, 3.5, and 3.8). Some additional reflectors are also highlighted (light blue) because these reflectors allow the main structures to be better marked and identified. The boundary between the Pliocene and Quaternary deposits has been always defined based on the available well stratigraphy, where Calabrian is considered to be the base of the Quaternary, while the new bio–stratigraphic scale from <https://stratigraphy.org/> includes

the Gelasian (2.58 - 1.8 Ma) to Quaternary. This scale could introduce some differences compared to recent cartography (Conti et al., 2020) but is consistent with Centamore et al., 1991a; Centamore et al., 1991b).

Some of the best seismic profiles were selected and organized in 5 almost-parallel Transects with a SW–NE direction within the above-mentioned area. Each Transect is composed of several seismic profiles that are aligned or partially overlapping and aim at realizing a single element.

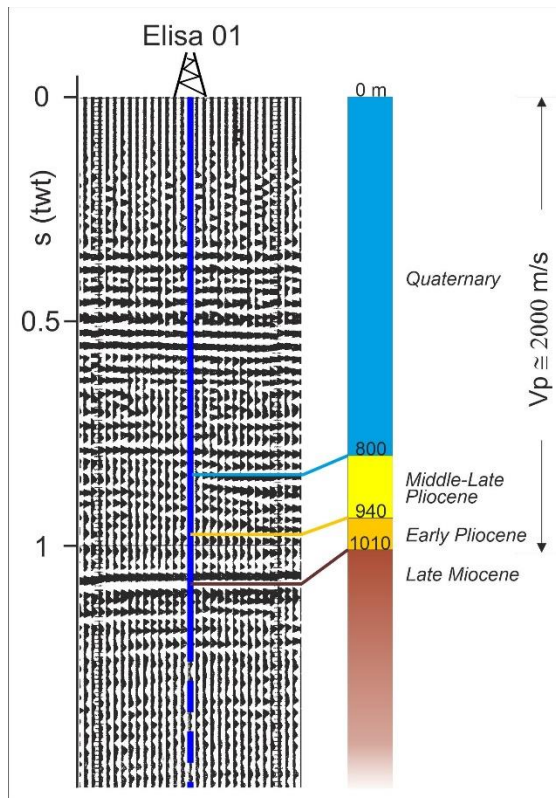


Fig. 3.3 - Stratigraphic correlation between the ELISA 1 well and a segment of the ViDEPI B-441 seismic profile where the well is placed (Figure 3.1).

Figure 3.1 presents traces of the Transects and each seismic profile within them. These traces complete our previous analyses of the outer Apennine Marche sector north of the Conero promontory, where seven Transects have already been observed (Chicco et al., 2019; Pierantoni et al., 2019). For this reason, the new Transects are numbered from 8 to 12.

These Transects are represented individually in Figures 3.4 to 3.8 and are reported using a high-resolution plate in the supplementary material (Plate 1).

### 3.4. Results by wells and seismic profiles interpretation

#### 3.4.1. *Transects*

The northernmost Transect (number 8 in this work; Figure 3.1) developed in the onshore and offshore areas just south of the Conero promontory and includes the seismic reflection profiles *a*, *b*, and *c* (Figure 3.4). Overall, the quality of these seismic reflection profiles is good; among these profiles, profile *b*, which was already interpreted in the VIDEPI catalogue, was further interpreted here using different colors.

In the onshore area, a WSW–ENE seismic profile (*a*) extends from the east of the Appignano locality to the coastline (ENE). Along this profile, some wells (Figure 3.1) allow good calibration of the top of the Messinian/Pre-Pliocene and near the top of the Early Pliocene seismo–stratigraphic horizons. An unconformity is also present within the Middle–Upper Pliocene deposits. In the offshore area, two seismic reflection profiles are present (*b*, *c*) and are aligned along a WSW–ENE direction. In particular, the *b* profile partly overlaps the *a* profile, and two hydrocarbon wells occur nearby.

Transect 8 is characterized by three structurally well-defined areas. On the western area a wide syncline is present, affecting a large thickness of about 3000 m Pliocene deposits. Lower Pliocene deposits cover the Messinian deposits in transgression. These deposits have an almost constant thickness, while those above the Middle–Upper Pliocene feature variable thickness (ranging between 1800 m in the syncline core and about 1000 m along the limbs). Quaternary deposits have a thickness of a few hundred meters.

The western limb of the syncline is affected by a high-angle, W-dipping reverse fault system. This system deforms the whole Lower to Middle Pliocene sequence without involving that of the Upper Pliocene. However, in the westernmost part, some faults deform the overlying unconformity placed within the uppermost part of the Middle–Upper Pliocene sequence.

In the central area a very complex compressive and uplifted structure (“Coastal Structure”) is present. This structure is characterized by shallow East-verging thrusts affecting the Lower–Middle Pliocene sequence and, marginally, the Upper Miocene sequence. Below this structure, an E-dipping reverse fault and a slightly W-dipping sub-vertical fault reaching the relevant depths (> 4 sec TWT) are present. Quaternary deposits were likely involved in the deformation of the upper and frontal sectors of this Coastal Structure. As highlighted in the *a* seismic profile, Quaternary deposits outcropping on the western side of the Coastal Structure show reduced thickness compared to those on the eastern side. The Lower Pliocene deposits are indeed less

than 100 m in thickness in front of the Coastal Structure and about 1000 m within the syncline behind.

On the eastern area (seismic profiles *b* and *c*), numerous reverse high angle W- and E-dipping faults are present. Overall, the vertical displacement of these faults is moderate, rarely exceeding 500 m. Lower Pliocene deposits have an average thickness of about 100 m or can be absent in the proximity of some structural highs (see *c* in Figure 3.4 and the wells presented here). The Middle–Upper Pliocene deposits show more variable thickness, from about one hundred meters on the structural highs to more than 1000 m in the proximity of faults and in structurally deeper areas. This extreme variability together with the characteristics of unevenness and chaos of the seismic horizons suggest a syn–tectonic origin of these deposits. The middle lower part of this sequence is certainly affected by reverse faults, while the upper part does not appear to be involved in deformation (seismic profiles *b* and *c* in Figure 3.4). Indeed, in this area the Quaternary deposits show a regular trend—increasing their thickness toward the east—and are not involved in deformation.

Transect 9 (Figure 3.5), which includes several wells, shows similar structural and stratigraphic characteristics to those of Transect 8. These differences relate to the greater thickness of the Lower Pliocene and Quaternary deposits facing the Coastal Structure and the high angle faults that are more evident below this structure. A Middle-Upper Pliocene unconformity is also clear in this area and was displaced by frontal thrusts. In this Transect, seismic reflection profile *a* overlaps profile *b* moving eastward toward the coastline. This profile exhibits a shallow compressive structure characterized by east- and west-verging thrusts.

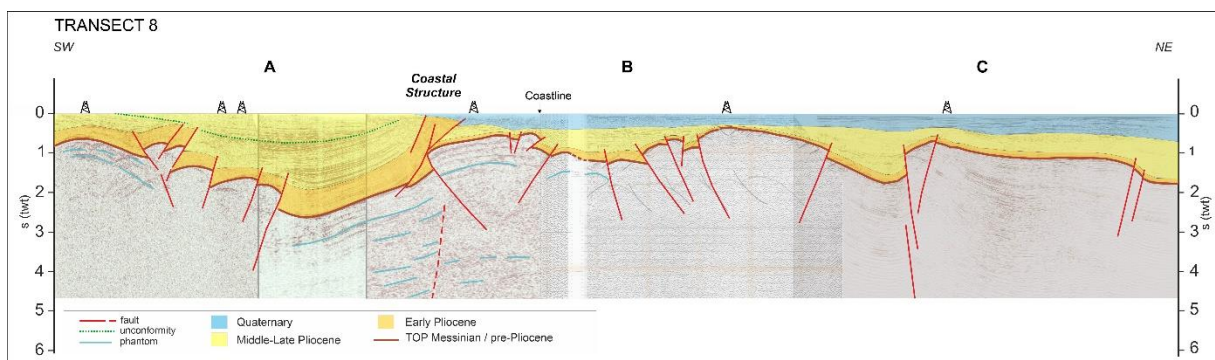


Fig. 3.4 - Transect 8. The Transect is composed of several seismic profiles labelled with letters (a, b, c, see Figure 3.1). Quaternary deposits are highlighted in blue, Middle–Upper Pliocene deposits are in yellow, Lower Pliocene deposits are in orange, and top Messinian/Pre-Pliocene deposits are in brown. No color is used for the pre-Pliocene sequence. Unconformities are shown in green dots. Light blue: undefined seismic reflectors. This legend is valid for all Transects (Figures 3.5 to 3.8).

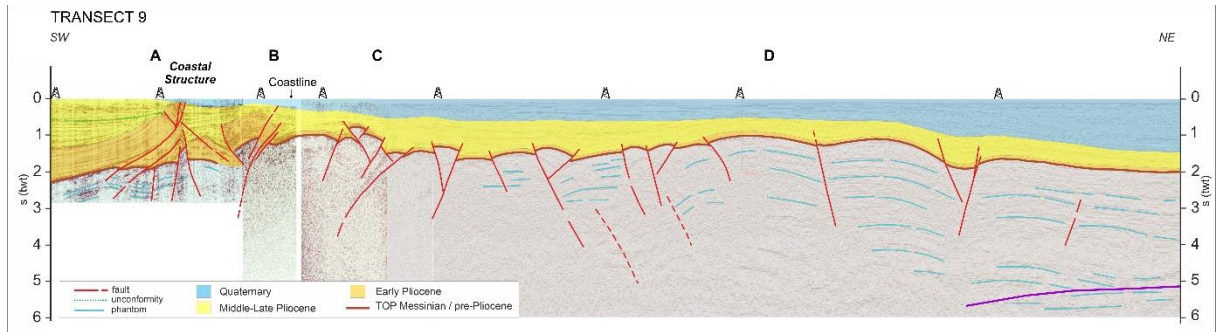


Fig. 3.5 -Transect 9. The purple line shows the hypothetical basement.

In this structure, the Lower Pliocene deposits are concordant with the Messinian ones, featuring a thickness of about 800 m and more than 1000 m. Eastward, the thickness is notably reduced (about 150 m). Moreover, an unconformity present in the Middle-Upper Pliocene deposits separates the upper portion of the sequence, which is characterized by onlap geometry, from the lower one featuring pinch-out geometry. Furthermore, below the surface thrusts of the Coastal Structure, seismic profiles *a* and *b* from Figures 3.4 and 3.5 show very evident high angle W- and E-dipping faults. Offshore, seismic reflection profiles *c* and *d* show pre-Pliocene bedrock widely deformed by high angle west- and east-dipping compressive faults forming gentle pop-up structures with reduced vertical displacement. The thickness of the Lower Pliocene deposits is always very low (<100 m, as also reported in well stratigraphy), while the Middle–Upper Pliocene deposits are syn–tectonic with high variable thickness (from a few to several hundreds of meters) close to compressive structures. Quaternary deposits have a relatively constant thickness (about 600–800 m) and are not affected by deformation. All the other Transects (10-12, see Figures 3.6, 3.7, 3.8) show similar characteristics to those described above. As already mentioned, due to the different resolutions of seismic profiles and/or local factors, certain features are clearer than others.

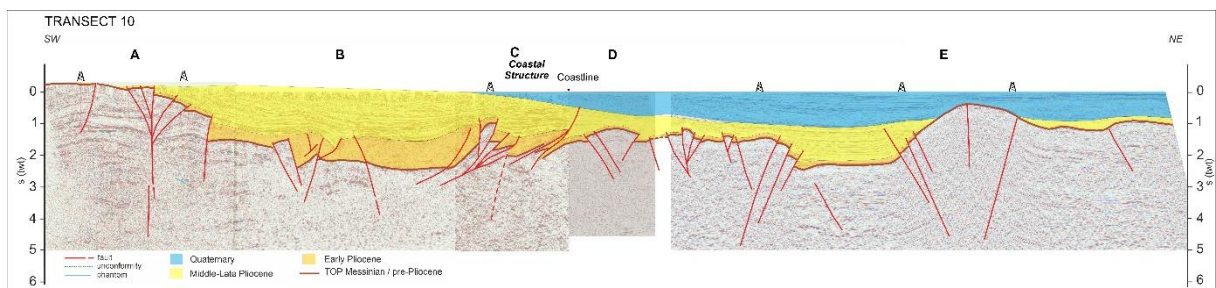


Fig. 3.6 - Transect 10.



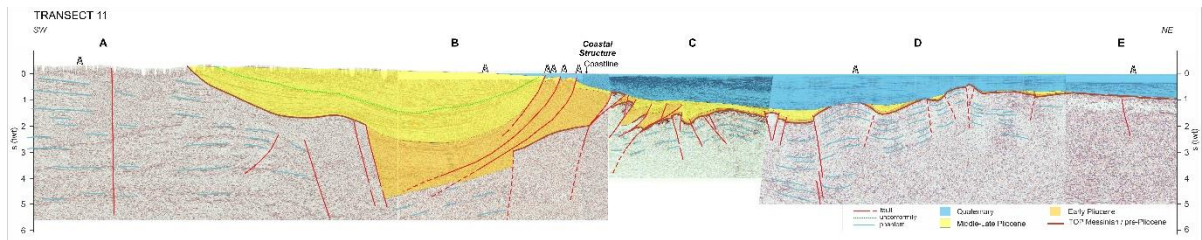


Fig. 3.7 - Transect 11.

In the westernmost sector of Transects 10 and 11, a deeply-rooted sub-vertical structure is highlighted. Transect 10 (Figure 3.6) shows a branched flower structure that separates the Laga Formation units by the Colombacci Formation at the surface (Figure 1; Chicco et al., 2019). This is a branched structure with a possible strike-slip component. In these two Transects, the compressive, W-dipping structures observed in Transect 8 are absent. Furthermore, along Transect 11 (profile a in Figure 3.7), an important normal E-dipping fault (more than 3000 m of vertical displacement) defines the Lower Pliocene basin to the west and is covered by transgressive deposits of the Middle–Upper Pliocene. In the same Transect, the above-mentioned unconformity within the Middle–Upper Pliocene sequence is clearly visible within the syncline. Transect 11 shows that during the Middle/Upper Pliocene, there was simultaneous subsidence (with transgression) in the current onshore to the west together with compression and uplift to the east (Coastal Structure, profiles a-b in Figure 3.7). In both Transect 11 and 12 (Figure 8), compressive E-dipping faults under the Coastal Structure thrusts are clearly present, as in Transects 8 and 9.

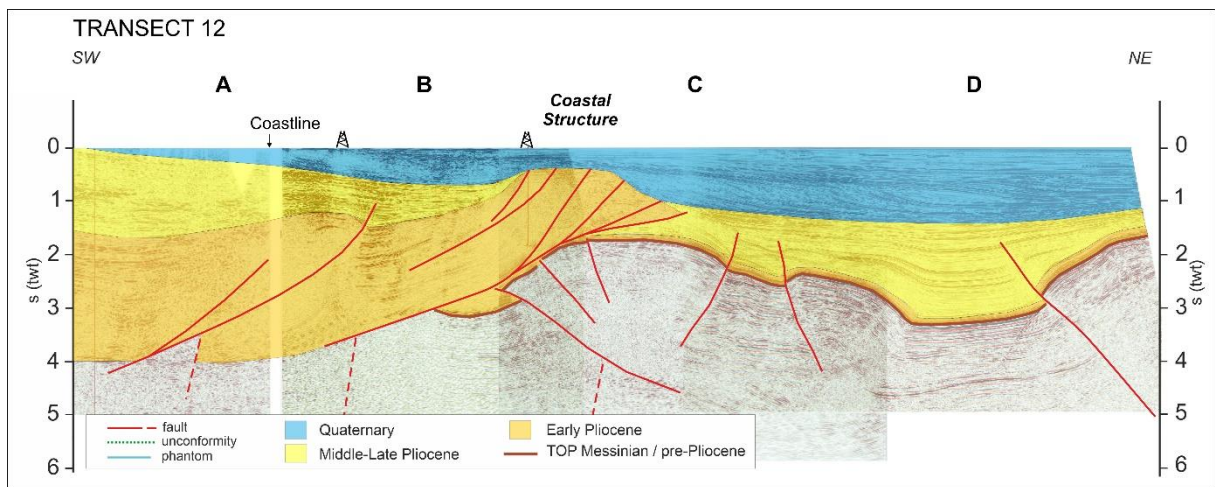


Fig. 3.8 - Transect 12.

Some thrusts of the Coastal Structure, as shown in Transect 11, affect the Quaternary deposits, such as in Transect 8. In Transect 12, only the shallowest Quaternary deposits are transgressive and are not involved in the deformation. Instead, in Transect 10, the thrusts affect only the Middle–Upper Pliocene sequence. In all Transects, the Quaternary succession covering the offshore flower structure is undeformed. Furthermore, evidence of fore-set Quaternary sedimentation is present in Transects 10 and 12 (Figures 3.6 and 3.8).

### 3.4.2. Characteristics and distribution of the Plio-Quaternary deformation

#### Early Pliocene

Based on well data logs and interpretations of both VIDEPI and ENI seismic profiles, we achieved a reconstruction of the thicknesses and distribution of the Lower Pliocene stratigraphic sequence (Figure 3.9).

This sequence has significant and sudden variations in thickness, and we were able to distinguish between the true sedimentary thicknesses and local tectonic repetitions or highly inclined bedding in proximity of compressive structures. This do not allow to reconstruct a reliable isopaches map. Afterward, for an immediate view of the Lower Pliocene deposits distribution, we identified two distinct thickness classes (less than 200 m and greater than 500 m). This simple representation makes it possible to easily locate the position, geometry and kinematics of the faults affecting this sequence. Finally, in Figure 3.9 the whole outer Marche Apennine sector has been reproduced to show the distribution of this succession.

The thickness distribution of the Lower Pliocene deposits shows evidence of a wide semi-submerged Marche Adriatic Structural High (MASH) area mainly located on the current Adriatic offshore (light green in Figure 3.9), as well as evidence of a wide basin area located in the northern portion of the same offshore area and in the south onshore area (dark green in Figure 3.9). This area also includes the northern part of the Marche territory, which is only marginally examined in this work.

Within the MASH area, the thickness of these deposits is very modest (a few tens of meters and, locally, not more than 200 m). In the basin area, the thickness rapidly increases, ranging from more than 500 to 3330 m. The limit between the plateau and basin areas features a NNW–SSE trend south of the Conero promontory lies slightly eastward of the current coastline, which shows instead a NE–SW trend in proximity to the Fano offshore area.

This spatial distribution is likely due to a normal or transtensive fault system that separates the wide and stable MASH area. This area appears to be slightly subsident and located in the central–southern Adriatic offshore from a basin area that is strongly subsident towards its western and northern portions.

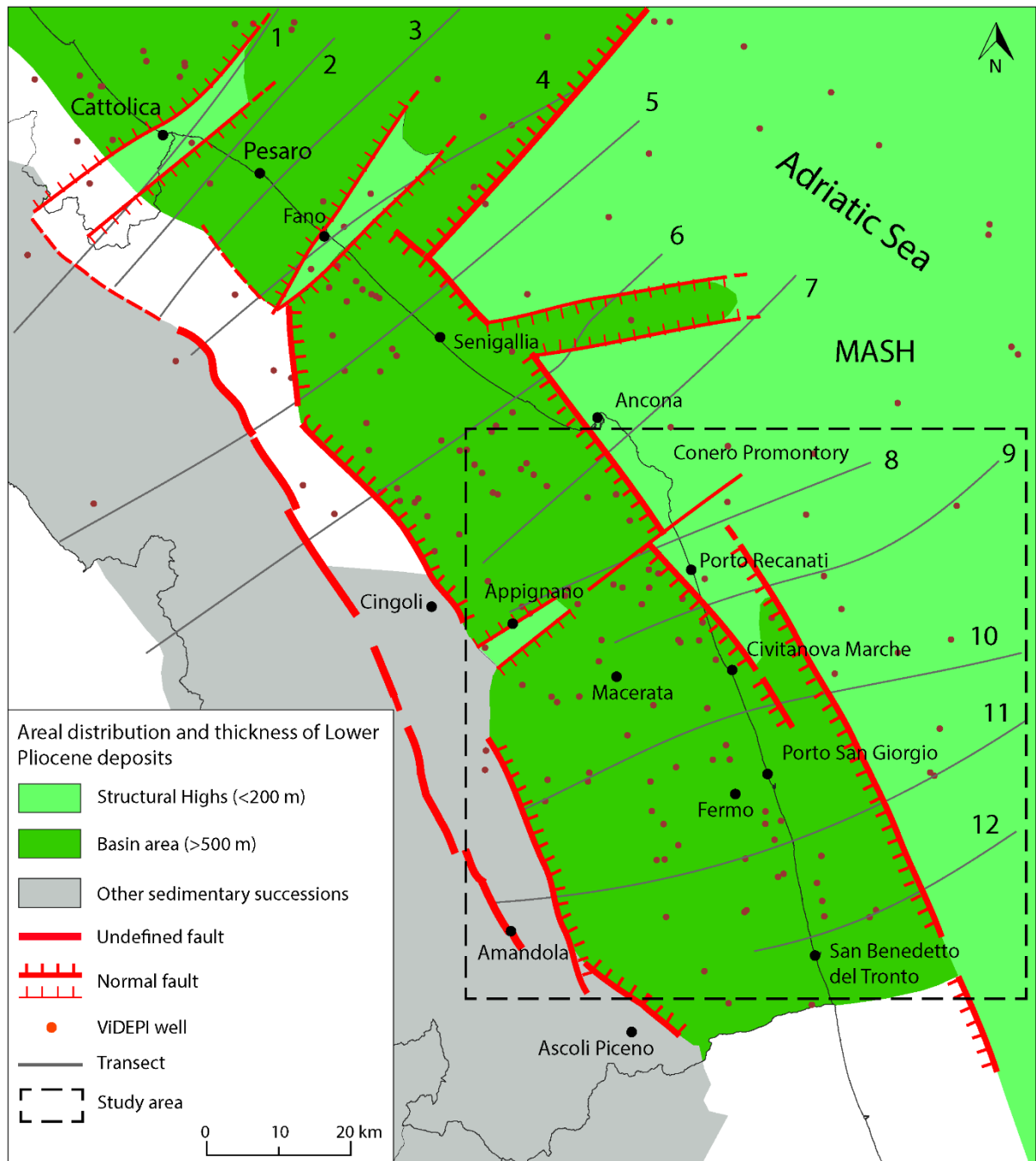


Fig. 3.9 - Schematic map of the distribution and thickness of Lower Pliocene deposits within the Marche region and the adjacent Adriatic Sea. Marche Adriatic Structural High (MASH) and smaller structural highs and basins are highlighted with the same color. The study area is located in the dashed square.

Furthermore, the western side of the basin is marked by a normal fault system (Transects 10a, 11a; Figures 3.6-3.7). This transtensive fault system was active soon before the onset of the compressive phase highlighted within the Transect.

As underlined in the previous section, this normal fault system consists of syn-sedimentary high angle W- and E-dipping faults characterized by remarkable vertical displacement reaching thousands of meters, which is clearly detectable in the interpreted seismic profiles.

The main faults were likely placed in proximity of the NNW-SSE and NE-SW boundaries of uplifted and subsident areas. Other minor faults further disarticulated both the basin and the MASH areas, defining local thickness variations in the sequence.

#### *Middle-Late Pliocene -Quaternary*

Based on our investigation, three structurally well-defined areas along a W-E direction are identified (Figure 3.10).

The western area is characterized by a wide syncline. In the northern part of this area, the syncline is locally intersected by W-dipping high-angle reverse faults (Figure 3.4); in the southern portion, Lower Pliocene deposits end against a high-angle E-dipping normal fault to the West, covered by transgressive Middle-Upper Pliocene deposits. The syncline axis is about N-S oriented. W of the syncline, a sub-vertical fault system deeply rooted with a N-S trend can be observed.

The central area is marked by a compressive structure (Coastal Structure). This structure consists of a series of E-verging thrusts within the shallower sequence, mainly affecting the Lower-Middle Pliocene deposits and only marginally affecting the Messinian ones. Thrust displacements are rapidly reduced within the Messinian and Lower Pliocene deposits. Just below this horizon, E-dipping reverse faults and deeper high-angle W-dipping faults are present. The Coastal Structure shows a NNW-SSE, almost continuous, trend, and sometimes crops out close to the coastline. This structure was formed starting during the Middle Pliocene, and its deformation continued until the Upper Pliocene, in some parts up to the Quaternary.

The eastern area is characterized by W- and E-verging high-angle reverse faults, giving rise to gentle flower structures with a NW-SE trend. These structures were formed from the Middle Pliocene and developed structural highs, some of which were still emerging during the Upper Pliocene/Pleistocene (Transects 10, 11; Figures 3.6-3.7). Compressive deformation stopped during the Upper Pliocene, and Quaternary deposits were not affected.

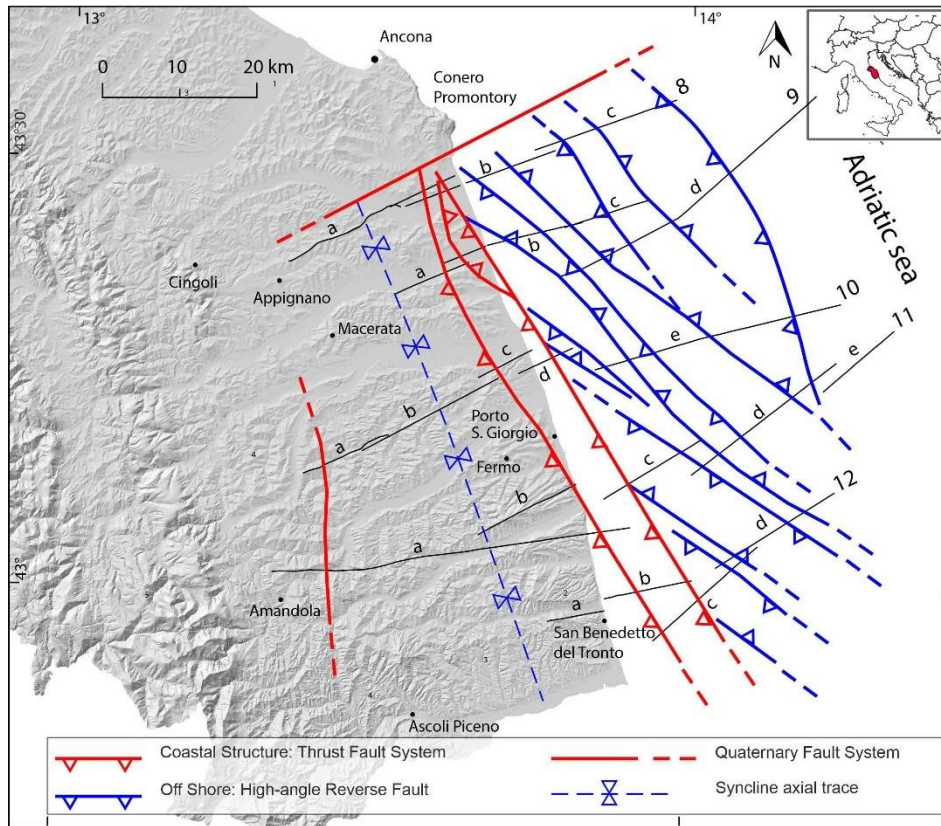


Fig. 3.10 - Structural sketch map of the outer Marche area south of Conero Promontory. The main Plio–Quaternary structures are highlighted.

### 3.5. Discussion

During the Messinian, this part of the Marche Apennines outer sector emerged or was close to emersion (the “lago-mare” succession in Figure 3.2), with sedimentary break-off (De Alteriis, 1986). The top Messinian/pre-Pliocene seismic horizon was always clearly evident in the examined seismic lines, with frequent characteristics of an erosive surface (Figures 3.6-3.7). The Lower Pliocene deposits, however, are often transgressive or discordant over the underlying Messinian or pre-Pliocene ones. Furthermore, no important evidence of Messinian active tectonics was found in this area. This part of the sector started to deform during the Early Pliocene when normal or transtensive faults with a NNW–SSE trend were enucleated. These faults separated heavily subsident basin areas from almost-stable structural highs (Figure 3.9). The basin area was mainly located along the current onshore, while the Marche Adriatic Structural High (MASH) was located in the current offshore. This feature continued southward in the Abruzzo region with quite similar characteristics, as described in Artoni, 2013. According to the author, in Abruzzo, the basin formed due to horst and graben structures starting in the Messinian–Pliocene transition due to flexural extension of the under-thrusting Adria Plate. In

our study area, this extensional phase started in the Early Pliocene, as indicated by the erosive top Messinian and the transgressive and discordant Pliocene deposits above it.

North of the Conero Promontory, the area's slightly more complex setting was also due to an important NE–SW trending fault that segmented the MASH, yielding a basin area to the NW (Figure 3.9). This structure, already identified in Pierantoni et al., 2019, continues from the Fano offshore to the SW along the river valley (Figure 3.1). Other local features with a NE–SW trend segmented both the basin and the MASH, forming lower-ranking depressions and structural highs (Figure 3.9). The northernmost transverse structures correspond to the Cattolica seismogenic system (Pierantoni et al., 2019).

Starting from the Middle Pliocene, a compressive regime was established in the sector south of the Conero Promontory, growing the structures underlined in the Transects and in Figure 3.10.

In more detail, in the study area we highlighted a wide syncline with an almost N–S trend to the west, the Coastal Structure with a NNW–SSE trend in the central portion, and the NW–SE-trending gentle-flower structure system to the east. The syncline was thus formed in correspondence with the Lower Pliocene basin, and the Coastal Structure formed in correspondence with the normal faults bordering the same basin to the east (Figures 3.9-3.10). The Middle Pliocene deposits are continuous with those of the Lower Pliocene at the syncline core while resting on the same deposits with a pinch-out feature and reduced thickness in proximity to the growing Coastal Structure western flank (Transects 9, 11, 12; Figs. 3.5-3.7-3.8). Variable thickness, with greater thickness close to the faults, attests to the syn-tectonic origins of these deposits in the offshore area.

Further to the west of the syncline, the N–S Amandola-positive flower structure (Figure 3.6) separates different Messinian units (Centamore et al., 1991). This structure is high-angle and deeply rooted (Transects 10 and 11; Figures 3.6-3.7), likely extending farther than the representation in Figure 3.10. The push-up in the western part of 8a (Figure 3.4) is likely a continuation of the Amandola structure or one of its branches. All these structural elements are slightly divergent from each other and are interrupted along a complex transverse structure approximately ENE–WSW oriented and located immediately south of the Conero Promontory (Figure 3.10).

The compressive deformation phase ended in the western and eastern areas during the Late Pliocene-Early Pleistocene. The unconformity within the Middle–Upper Pliocene deposits (Transects 9, 11; Figures 3.5 and 3.7) indicates that the syncline has not deepened since the Late Pliocene. Upper Pliocene deposits rest in an on-lap over the underlying ones above the

unconformity and reduce their thickness in proximity of the western flank of the Coastal Structure. These features indicate that, within the syncline, the lower parts of the Middle–Upper Pliocene deposits are syn–tectonic, while those of the upper part are post-tectonic.

The flower structures of the Adriatic offshore are sealed by the Quaternary deposits. In the central area, the Coastal Structure continued its activity even during the Quaternary, as shown in several areas (Transects 8-9-11 in Figures 3.4-3.5-3.7). Therefore, all these structures were formed during the Middle Pliocene. Most of these were deactivated at the end of the Late Pliocene, while a few others were probably still active during the Early Pleistocene (Transects 10-11-12 in Figures 3.6-3.7-3.8).

The Coastal Structure is characterized by low-angle faults close to the surface and high angle faults at depth. Low-angle faults are mainly involved in the Lower Pliocene deposits, making their repetition clearly visible in all Transects. The underlying Messinian deposits were, instead, not significantly involved, likely due to detachment between the two sequences. In Ori et al., 1991, however, Messinian deposits were considered to be strongly involved in deformation. At the western edge of the syncline, and underneath the highly deformed close-to-the-surface succession (Transect 11), parts of the original faults bordering the Lower Pliocene basin are still recognizable. Looking at the Lower Pliocene deposits distribution map (Figure 3.9), it can be seen that the Coastal Structure is nucleated in the same position as the faults bordering the previous Lower Pliocene basin to the east and perfectly follows the trend of the latter. Therefore, this structure was formed by partially inverting or deforming (Figure 3.11) the previous high-angle normal/transpressive faults (see also Figures 3.5 to 3.8). These faults may have acted initially as a barrier, forcing the involved sequences to climb upwards; in some cases (Fig. 3.5, 3.7, 3.8), the innermost thrusts show a higher angle than the external ones. Subsequently, as the shortening increased, the upper parts of the Early Pliocene faults were decapitated (see Tavarnelli et al., 2004) and included within the superficial low-angle, E-verging thrust sheets, which mainly affect the Lower Pliocene succession that is partially detached from the underlying one (Figure 3.11).

Thus, in the later stage (Late Pliocene–Quaternary), some of the thrust sheets partially covered the westernmost flower structures of the eastern Adriatic area (Transects 8-10-12 in Figures 3.4-3.6-3.8). The compressive Coastal Structure formed due to the inversion of previous extensional features following the “interaction of extensional and contractional deformation” model proposed by Williams et al., 1989; Scisciani, 2009; Scisciani et al., 2002 and Bolis et al., 2003 for the nearby Montagna dei Fiori and Cingoli structures (Figure 3.11).

The Coastal Structure continues southward, in the Abruzzo region, with quite similar litho-structural characteristics and ages of deformation (Bolis et al., 2003; Carruba et al., 2006). Also in that area, E-vergent thrusts are mainly found in the Lower Pliocene deposits, which, in this case, are completely detached from the underlying Messinian ones. However, unlike the process proposed for our study area, these authors suggest that the previous Early Pliocene normal faults bordering the basin were already enucleated during the Messinian. Furthermore, these normal faults were not involved in compressive deformation but were simply covered by the thrust sheets. According to these authors, compressive deformation began in the Early Pliocene.

As a result of the compression that determined the Coastal Structure's development, tilting of the block between this structure and the Amandola structure to the W likely also have occurred. During the Middle Pliocene, there was simultaneous uplift of the eastern front (enucleation and uplift of the Coastal Structure) and subsidence of the western side (transgression of the Middle Pliocene deposits on those previously raised during the pre-Pliocene time; Transect 11). The horizontal rotational axis may correspond to the syncline axis. This mechanism is similar to that described in Costa, 2003 for the Po Valley. During the Late Pliocene–Quaternary, this rotation ceased, and the deposits of the same age became horizontal.

The Amandola structure, the syncline, and the Coastal Structure show a straight and regular trend. As previously mentioned, the trend of these main onshore structures is somewhat divergent from the offshore one, even though they all formed during the same time interval. This can be attributed to the influence of pre-existing features inherited by previous deformation phases such as the faults shown in Figure 3.9. These structures are compatible with the main local shortening oriented in a NNE–SSW direction during the Middle–Late Pliocene (compression with the P axis about NNE–SSW; Figure 3.12), which emerged in the northern sector of the Marche region (Pierantoni et al., 2019; Mazzoli et al., 2015; Mazzoli et al., 2014) and, more generally, in the overall Central Adriatic area (Mantovani et al., 2017; Mantovani et al., 2020).



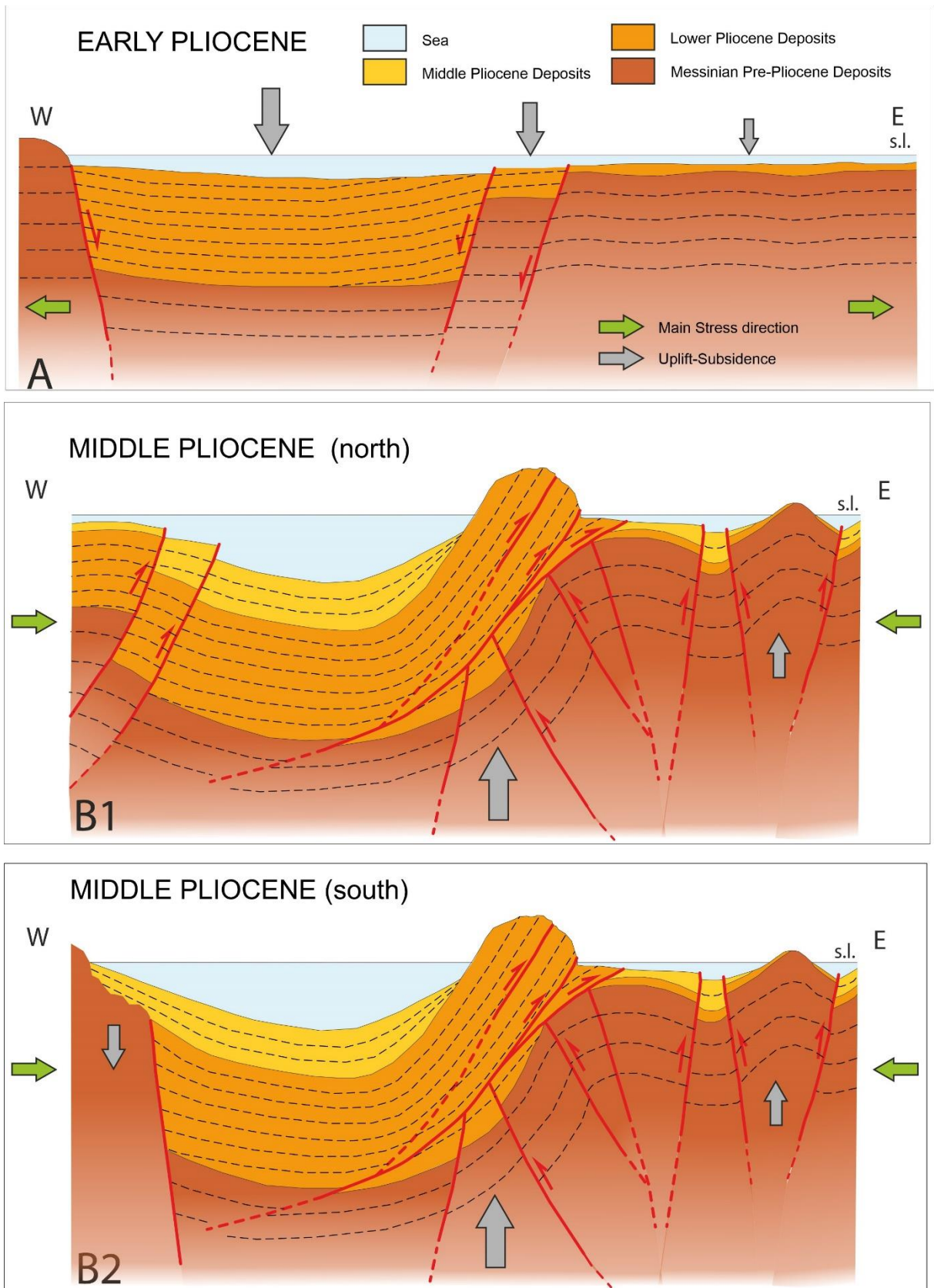


Fig. 3.11 - Sketch diagram showing the evolution of the Coastal Structure from the Early to Middle Pliocene across two representative cross-sections (not to scale). The size of the gray arrows is proportional to the intensity of vertical movement.

In this context, right-lateral transpression developed along the Coastal Structure and likely enhanced the gentle flower systems of the Adriatic offshore (Figure 3.12)

The Coastal Structure schematically represented as continuous and regular in Figure 3.10 is most likely composed of several structures, some of which were still active during the Quaternary, as shown by fairly significant earthquake sequences ( $M_w = 5$ , Porto San Giorgio sequence; Riguzzi et al., 1989; Battimelli et al., 2018) that occurred recently (Figure 3.12).

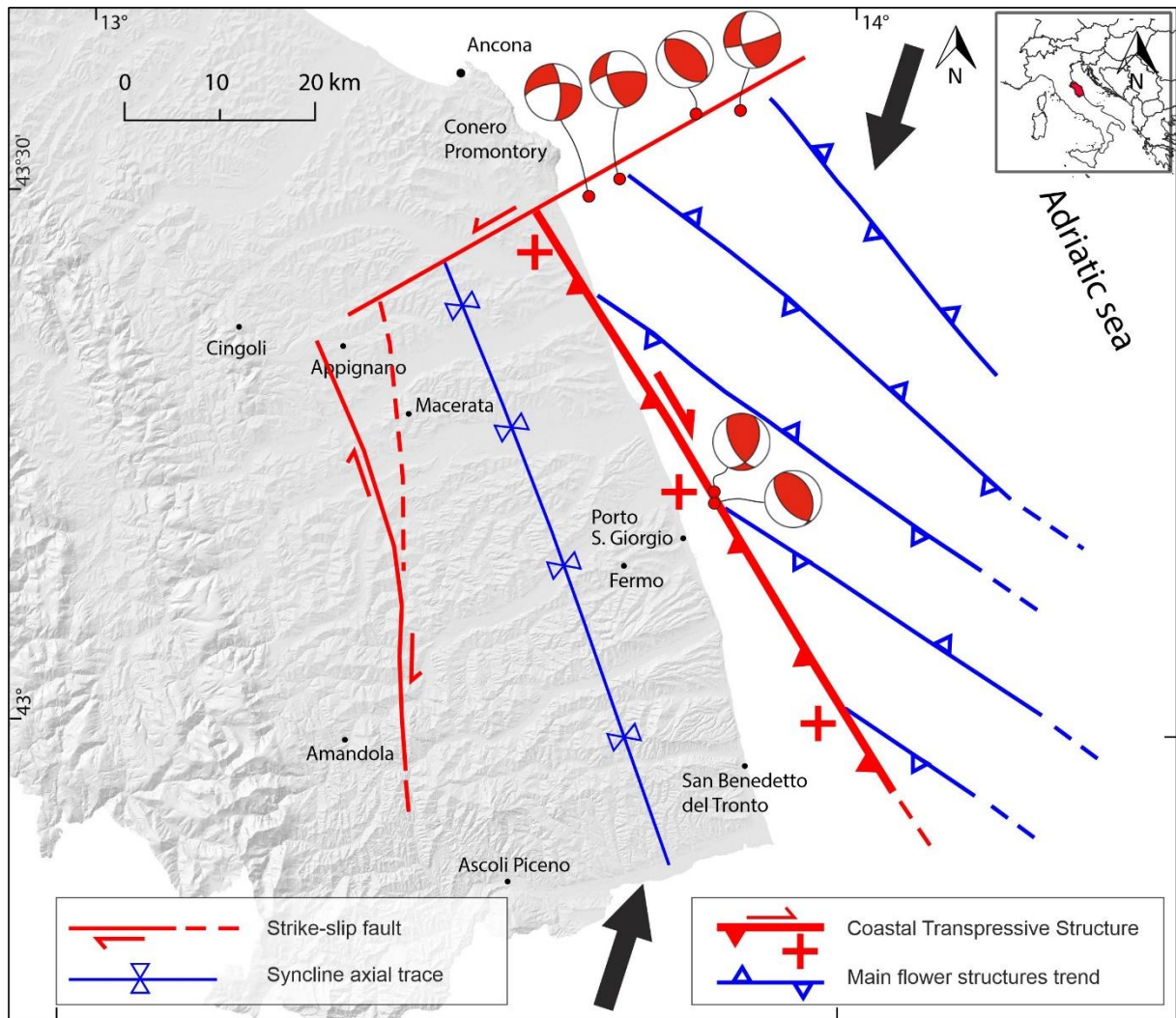


Fig. 3.12 - Kinematic sketch map. Red lines indicate fault systems still active during the Quaternary. The black arrow represents the main shortening direction, red arrows describe the right lateral strike-slip component, and the plus symbol (+) is the narrow strongly uplifted area. Focal mechanisms (beach balls) of the main earthquakes of 1987 Porto S. Giorgio and 2013 south of Conero seismic sequences are shown.

As previously mentioned, the described structures were somehow interrupted to the north along a transverse ENE-WSW-oriented structure. The existence of transverse faults has been highlighted in literature by various authors, particularly in the Marche - Abruzzo onshore (see

Centamore et al., 1991; Pierantoni et al., 2019; Pierantoni et al., 2017 and reference therein). In our study area, several structures underwent sudden changes in characteristics (age of deformation, geometry and direction) that are observable when compared to those mapped in Pierantoni et al., 2019 in the areas west, east, and north of the Conero Promontory. Furthermore, the structures present immediately northward of this transverse element and of our study area, e.g., the Early Pliocene transpressive structure of Strada-Moie-S and Andrea di Suasa (see Figure 7 in Pierantoni et al., 2013) are no longer present in the south. Indeed, in this southern area, extension was still occurring during the Early Pliocene.

The transverse structure south of the Conero Promontory, already partially present in Centamore et al., 1991, interrupts structures with Quaternary activity, i.e., the Coastal Structure to the south and the Conero compressional structure (Chicco et al., 2019) to the north. Therefore, this tectonic element must be Quaternary itself, as also attested by recent earthquakes and seismic sequences in the offshore along the element (Figure 3.12). These focal mechanisms are predominantly strike-slip, with P-axes oriented around the ENE–WSW and sub-vertical planes (Mazzoli et al., 2015; Mazzoli et al., 2014). Furthermore, the epicenters of the seismic sequences described by these authors are aligned ENE–WSW.

### **3.6. Conclusions**

Seismic profile interpretations and well stratigraphic data allowed us to describe the Plio–Quaternary evolution of the outer Marche Apennines south of the Conero promontory. The main results can be summarized as follows:

- During the Early Pliocene, the area was affected by extensional or transtensive tectonics, resulting in the formation of a strongly subsident basin and a more stable structural high. More than 2000 meters of sediment accumulated in the basin zone, while the structural high (MASH) hosts less than 200 m of Lower Pliocene deposits.
- The basins and structural highs are separated by an approximately NNW–SSE normal and transtensive fault system located close to the current coastline. Other normal faults with a NNW–SSE trend developed in the current onshore area border the basin to the W. The structural high is instead located in the current offshore area.
- Starting from the Middle Pliocene, the entire area underwent compression, with the P axis oriented about NNE–SSW leading the formation, from W to E, of the NNW-SSE dextral strike-slip Amandola structure, the NNW–SSE dextral transpressive Coastal Structure and a NW–SE-striking system of gentle flower structures (offshore).

- The Coastal Structure is the most complex and important structure in the study area. It consists of an E-vergent thrust system at surface and high-angle E and W-vergent faults at depth. Shallow thrusts mainly affected the Pliocene deposits and, locally, the Quaternary ones. The mainly-Messinian underlying deposits were marginally involved in deformation. Deeper faults affect Mio-Pliocene and older deposits. As a result, in the shallower part of the Coastal Structure, pre-existing normal faults were inverted or cross-cut and incorporated into the ongoing thrusts, while at depth, they were not deformed.
- The trends of the Coastal Structure and the flower structures within the offshore are slightly divergent despite being contemporaneous because the former was strongly influenced by inherited structures.
- The compressive phase was finished during the Late Pliocene in the syncline, as well as along the flower structures. The Coastal Structure was still active during the Quaternary. This is also testified by recently recorded seismic activity.
- A complex transverse structure with a general ENE–WSW trend (at least partially active and seismogenic) traces the boundary between the outer areas north and south of the Conero promontory, where the styles, geometry and times of deformation of the Plio-Quaternary structures are significantly different.

Based on our results, we conclude that during the Plio-Quaternary times, this portion of the outer Apennine sector is mainly affected by a right-lateral transpressive deformation, and by widespread kinematic inversion of pre-existing structures. Former studies proposed a simple E-vergent compressive deformation for the same area.

### 3.7. References

- Amadori, C., Toscani, G., Di Giulio, A., Maesano, F. E., D’Ambrogi, C., Ghielmi, M., & Fantoni, R. (2019). From cylindrical to non-cylindrical foreland basin: Pliocene–Pleistocene evolution of the Po Plain–Northern Adriatic basin (Italy). *Basin Research*, *31*(5), 991-1015.
- Artoni, A. (2003). Messinian events within the tectono-stratigraphic evolution of the Southern Laga Basin (Central Apennines, Italy). *BOLLETTINO-SOCIETA GEOLOGICA ITALIANA*, *122*(3), 447-466.
- Artoni, A. (2013). The Pliocene-Pleistocene stratigraphic and tectonic evolution of the central sector of the Western Periadriatic Basin of Italy. *Marine and Petroleum Geology*, *42*, 82-106.

- Bally, A. W. (1986). Balanced sections and seismic reflection profiles across the Central Apennines. *Mem. Soc. Geol. It.*, 35, 257-310.
- Barchi, M. R., Alvarez, W., & Shimabukuro, D. H. (2012). The Umbria-Marche Apennines as a double orogen: observations and hypotheses. *Italian Journal of Geosciences*, 131(2), 258-271.
- Battimelli, E., Adinolfi, G. M., Amoroso, O., & Capuano, P. (2018, November). Un Nuovo Studio Della Sequenza Sismica del 1987 di Porto San Giorgio. In *Proceedings of the 37th National Conference GNGTS, Bologna, Italy* (pp. 19-21).
- Bigi, S., Calamita, F., Cello, G., Centamore, E., Deiana, G., Paltrinieri, W., ... & Ridolfi, M. (1999). Tectonics and sedimentation within a Messinian foredeep in the Central Apennines, Italy. *Journal of Petroleum Geology*, 22(1), 5-18.
- Bigi, S., Casero, P., & Ciotoli, G. (2011). Seismic interpretation of the Laga basin; constraints on the structural setting and kinematics of the Central Apennines. *Journal of the Geological Society*, 168(1), 179-190.
- Bigi, S., Conti, A., Casero, P., Ruggiero, L., Recanati, R., & Lipparini, L. (2013). Geological model of the central Periadriatic basin (Apennines, Italy). *Marine and Petroleum Geology*, 42, 107-121.
- Bigi, S., Milli, S., Corrado, S., Casero, P., Aldega, L., Botti, F., & Cannata, D. (2009). Stratigraphy, structural setting and burial history of the Messinian Laga basin in the context of Apennine foreland basin system. *Journal of Mediterranean Earth Sciences*, 1, 61-84.
- Boccaletti, M., Calamita, F., Deiana, G., Gelati, R., Massari, F., Moratti, G., & Lucchi, F. R. (1990). Migrating foredeep-thrust belt systems in the northern Apennines and southern Alps. *Palaeogeography, Palaeoclimatology, Palaeoecology*, 77(1), 3-14.
- Bolis, G., Carruba, S., Casnedi, R., Perotti, C. R., Ravaglia, A., Tornaghi, M., & Paltrinieri, W. (2003). Compressional tectonics overprinting extensional structures in the Abruzzo Periadriatic Foredeep (Central Italy) during Pliocene times. *Bollettino della Società Geologica Italiana*, 122(2), 251-266.
- Bonini, L., Basili, R., Burrato, P., Cannelli, V., Fracassi, U., Maesano, F. E., ... & Valensise, G. (2019). Testing different tectonic models for the source of the Mw 6.5, 30 October 2016, Norcia earthquake (central Italy): a youthful normal fault, or negative inversion of an old thrust?. *Tectonics*, 38(3), 990-1017.

- Calamita, F., & Deiana, G. (1986). Evoluzione strutturale neogenico-quadernaria dell'Appennino Umbro-Marchigiano.
- Calamita, F., Coltorti, M., Piccinini, D., Pierantoni, P. P., Pizzi, A., Ripepe, M., & Turco, E. (2000). Quaternary faults and seismicity in the Umbro-Marchean Apennines (Central Italy): evidence from the 1997 Colfiorito earthquake. *Journal of Geodynamics*, 29(3-5), 245-264.
- Calamita, F., Scisciani, V., Montefalcone, R., Paltrinieri, W., & Pizzi, A. (2002). L'ereditarietà del paleomargine dell'Adria nella geometria del sistema orogenico centro-appenninico: l'area abruzzese esterna. *Memorie della Società Geologica Italiana*, 57, 355-368.
- Cantalamesa, G., Cantemore, E., Chiocchini, U., Colalongo, M.L., Micarelli, A., Nanni, T., Pasini, G., Potetti M., Ricci Lucchi F, Cristallini, C. and Di Lorito L., "Il Plio-Pleistocene marchigiano-abruzzese," 73° Congr. della Soc. Geol. Ital. Guid. all'escursione, 7-10 Ottobre 1986, pp. 1-45, 1986.ackwell Scientific Oxford.
- Cantalamesa, G., Centamore, E., Chiocchini, U., Micarelli, A., Potetti, M., & Di Lorito, L. (1986). Il miocene delle Marche.
- Cantalamesa, G., Centamore, E., Cristallini, C., Invernizzi, C., Matteucci, R., Micarelli, A., & Potetti, M. (1987). Nuovi dati sulla geologia dell'area di Porto San Giorgio (Ascoli Piceno, Marche). *Geologica Romana*, 26, 359-369.
- Carminati, E., & Doglioni, C. (2012). Alps vs. Apennines: The paradigm of a tectonically asymmetric Earth. *Earth-Science Reviews*, 112(1-2), 67-96.
- Carruba, S., Casnedi, R., Perotti, C. R., Tornaghi, M., & Bolis, G. (2006). Tectonic and sedimentary evolution of the Lower Pliocene Periadriatic foredeep in Central Italy. *International Journal of Earth Sciences*, 95(4), 665-683.
- Cello, G., Deiana, G., Ferelli, L., Marchegiani, L., Maschio, L., Mazzoli, S., & Vittori, T. (2000). Geological constraints for earthquake faulting studies in the Colfiorito area (central Italy). *Journal of Seismology*, 4(4), 357-364.
- Centamore, E., & Rossi, D. (2009). Neogene-Quaternary tectonics and sedimentation in the Central Apennines. *Italian Journal of Geosciences*, 128(1), 73-88.
- Centamore, E., Cantalamesa, G., Micarelli, A., Potetti, M., Berti, D., Bigi, S., & Ridolfi, M. (1991). Stratigrafia e analisi di facies dei depositi del Miocene e del Pliocene inferiore dell'avanfossa marchigiano-abruzzese e delle zone limitrofe.

- Centamore, E., Pambianchi, G., Minetti, A., (1991). Ambiente fisico delle Marche: geologia-geomorfologia-idrogeologia/Regione Marche. Giunta regionale. Firenze S.E:L.C.A..
- Chicco, J. M., Pierantoni, P. P., Costa, M., & Invernizzi, C. (2019). Plio-Quaternary tectonics and possible implications for geothermal fluids in the Marche Region (Italy). *Tectonophysics*, 755, 21-34.
- Conti, P., Cornamusini, G., & Carmignani, L. (2020). An outline of the geology of the Northern Apennines (Italy), with geological map at 1: 250,000 scale. *Italian Journal of Geosciences*, 139(2), 149-194.
- Costa, M. (2003). The buried, Apenninic arcs of the Po Plain and northern Adriatic Sea (Italy); a new model. *Bollettino della Società geologica italiana*, 122(1), 3-23.
- Cuffaro, M., Riguzzi, F., Scrocca, D., Antonioli, F., Carminati, E., Livani, M., & Doglioni, C. (2010). On the geodynamics of the northern Adriatic plate. *Rendiconti Lincei*, 21(1), 253-279.
- de Alteriis, G. (1995). Different foreland basins in Italy: examples from the central and southern Adriatic Sea. *Tectonophysics*, 252(1-4), 349-373.
- De Donatis, M., Invernizzi, C., Landuzzi, A., Mazzoli, S., & Potetti, M. (1998). CROP 03: Structure of the Montecalvo in Foglia-Adriatic Sea segment.
- Deiana, G., & Pialli, G. (1994). The structural provinces of the Umbro-Marchean Apennines. *Memorie della Società Geologica Italiana*, 48, 473-484.
- Dewey, J. F., Helman, M. L., Knott, S. D., Turco, E., & Hutton, D. H. W. (1989). Kinematics of the western Mediterranean. *Geological Society, London, Special Publications*, 45(1), 265-283.
- Di Celma, C. (2011). Sedimentology, architecture, and depositional evolution of a coarse-grained submarine canyon fill from the Gelasian (early Pleistocene) of the Peri-Adriatic basin, Offida, central Italy. *Sedimentary Geology*, 238(3-4), 233-253.
- Di Celma, C., Cantalamessa, G., & Didaskalou, P. (2013). Stratigraphic organization and predictability of mixed coarse-grained and fine-grained successions in an upper slope Pleistocene turbidite system of the Peri-Adriatic basin. *Sedimentology*, 60(3), 763-799.
- Ghielmi, M., Minervini, M., Nini, C., Rogledi, S., & Rossi, M. (2013). Late Miocene–Middle Pleistocene sequences in the Po Plain–Northern Adriatic Sea (Italy): the stratigraphic record of modification phases affecting a complex foreland basin. *Marine and Petroleum Geology*, 42, 50-81.

- Ghielmi, M., Minervini, M., Nini, C., Rogledi, S., Rossi, M., & Vignolo, A. (2010). Sedimentary and tectonic evolution in the eastern Po-Plain and northern Adriatic Sea area from Messinian to Middle Pleistocene (Italy). *Rendiconti Lincei*, 21(1), 131-166.
- Ghielmi, M., Serafini, G., Artoni, A., Di Celma, C., & Pitts, A. (2019, September). From Messinian to Pleistocene: tectonic evolution and stratigraphic architecture of the central Adriatic foredeep (Abruzzo and Marche, Central Italy). In *34th IAS Meeting of Sedimentology, Rome-Italy, September 10th-13th 2019, Field Trip A4-Guide Book* (p. 44).
- Invernizzi C. (1992). Relazioni tra costruzione della catena e migrazione dell'avanfossa nell'area marchigiana esterna: alcune osservazioni, *Studi Geol. Camerti*, vol XII, pp. 71-78.
- Lucchi, F. R. (1986). The Oligocene to Recent foreland basins of the northern Apennines. In *Foreland basins* (Vol. 8, pp. 105-139). B1
- Mancinelli, P., & Scisciani, V. (2020). Seismic velocity-depth relation in a siliciclastic turbiditic foreland basin: a case study from the Central Adriatic Sea. *Marine and Petroleum Geology*, 120, 104554.
- Mantovani, E., Viti, M., Babbucci, D., Tamburelli, C., & Cenni, N. (2017). Possible location of the next major earthquakes in the Northern Apennines: present key role of the Romagna-Marche-Umbria wedge. *International Journal of Geosciences*, 8(11), 1301.
- Mantovani, E., Viti, M., Babbucci, D., Tamburelli, C., & Cenni, N. (2020). Geodynamics of the central-western Mediterranean region: plausible and non-plausible driving forces. *Marine and Petroleum Geology*, 113, 104121.
- Marini, M., Milli, S., Ravnås, R., & Moscatelli, M. (2015). A comparative study of confined vs. semi-confined turbidite lobes from the Lower Messinian Laga Basin (Central Apennines, Italy): implications for assessment of reservoir architecture. *Marine and Petroleum Geology*, 63, 142-165.
- Mazzoli, S., Deiana, G., Galdenzi, S., & Cello, G. (2002). Miocene fault-controlled sedimentation and thrust propagation in the previously faulted external zones of the Umbria-Marche Apennines, Italy. *EGU Stephan Mueller Special Publication Series*, 1, 195-209.
- Mazzoli, S., Macchiavelli, C., & Ascione, A. (2014). The 2013 Marche offshore earthquakes: new insights into the active tectonic setting of the outer northern Apennines. *Journal of the Geological Society*, 171(4), 457-460.



- Mazzoli, S., Pierantoni, P. P., Borraccini, F., Paltrinieri, W., & Deiana, G. (2005). Geometry, segmentation pattern and displacement variations along a major Apennine thrust zone, central Italy. *Journal of Structural Geology*, 27(11), 1940-1953.
- Mazzoli, S., Santini, S., Macchiavelli, C., & Ascione, A. (2015). Active tectonics of the outer northern Apennines: Adriatic vs. Po Plain seismicity and stress fields. *Journal of Geodynamics*, 84, 62-76.
- Milli, S., Moscatelli, M., Stanzione, O., & Falcini, F. (2007). Sedimentology and physical stratigraphy of the Messinian turbidite deposits of the Laga basin (central Apennines, Italy). *BOLLETTINO-SOCIETA GEOLOGICA ITALIANA*, 126(2), 255.
- Odlum, M. L., Stockli, D. F., Capaldi, T. N., Thomson, K. D., Clark, J., Puigdefàbregas, C., & Fildani, A. (2019). Tectonic and sediment provenance evolution of the South Eastern Pyrenean foreland basins during rift margin inversion and orogenic uplift. *Tectonophysics*, 765, 226-248.
- Ori, G. G., Serafini, G., Visentin, C., Ricci Lucchi, F., Casnedi, R., Colalongo, M. L., & Mosna, S. (1991, May). The Pliocene-Pleistocene Adriatic Foredeep (Marche and Abruzzo, Italy): an integrated approach to surface and subsurface geology. In *3rd EAPG Conference, Adriatic foredeep field trip guide book* (pp. 26-30). Florence, Italy: EAPG and AGIP.
- Pace, P., Scisciani, V., Calamita, F., Butler, R. W., Iacopini, D., Esetime, P., & Hodgson, N. (2015). Inversion structures in a foreland domain: seismic examples from the Italian Adriatic Sea. *Interpretation*, 3(4), SAA161-SAA176.
- Pierantoni, P. P., Centamore, E. R. N. E. S. T. O., & Costa, M. (2017). Geological and seismologic data review of the 2009 L'Aquila seismic sequence (Central Apennines, Italy): deep-seated seismogenic structures and seismic hazard. *Italian Journal of Engineering Geology and Environment*, 17(2), 5-40.
- Pierantoni, P. P., Chicco, J., Costa, M., & Invernizzi, C. (2019). Plio-Quaternary transpressive tectonics: a key factor in the structural evolution of the outer Apennine-Adriatic system, Italy. *Journal of the Geological Society*, 176(6), 1273-1283.
- Pierantoni, P. P., Penza, G., Macchiavelli, C., Schettino, A., & Turco, E. (2020). Kinematics of the Tyrrhenian-Apennine system and implications for the origin of the Campanian magmatism. In *Vesuvius, Campi Flegrei, and Campanian Volcanism* (pp. 33-56). Elsevier.
- Pierantoni, P., Deiana, G., & Galdenzi, S. (2013). Stratigraphic and structural features of the Sibillini mountains (Umbria-Marche Apennines, Italy). *Italian Journal of Geosciences*, 132(3), 497-520.

- Pierantoni, P.P., Deiana, A., Romano A., Paltrinieri, W., Borracini, F., Mazzoli, S. (2005). Carte geologiche e sezioni attraverso la thrust zone del fronte montuoso umbro-marchigiano-sabino (parte meridionale). Vol. 124, p 3000.
- Porreca, M., Minelli, G., Ercoli, M., Brobia, A., Mancinelli, P., Cruciani, F., ... & Barchi, M. R. (2018). Seismic reflection profiles and subsurface geology of the area interested by the 2016–2017 earthquake sequence (Central Italy). *Tectonics*, 37(4), 1116-1137.
- Riguzzi, F., Tertulliani, A., & Gasparini, C. (1989). Study of the seismic sequence of Porto San Giorgio (Marche)–3 July 1987. *Il Nuovo Cimento C*, 12(4), 453-466.
- Roveri, M., Manzi, V., Lucchi, F. R., & Rogledi, S. (2003). Sedimentary and tectonic evolution of the Vena del Gesso basin (Northern Apennines, Italy): Implications for the onset of the Messinian salinity crisis. *Geological Society of America Bulletin*, 115(4), 387-405.
- Schettino, A., & Turco, E. (2006). Plate kinematics of the Western Mediterranean region during the Oligocene and Early Miocene. *Geophysical Journal International*, 166(3), 1398-1423.
- Scisciani, V. (2009). Styles of positive inversion tectonics in the Central Apennines and in the Adriatic foreland: Implications for the evolution of the Apennine chain (Italy). *Journal of Structural Geology*, 31(11), 1276-1294.
- Scisciani, V., Agostini, S., Calamita, F., Pace, P., Cilli, A., Giori, I., & Paltrinieri, W. (2014). Positive inversion tectonics in foreland fold-and-thrust belts: a reappraisal of the Umbria–Marche Northern Apennines (Central Italy) by integrating geological and geophysical data. *Tectonophysics*, 637, 218-237.
- Scisciani, V., Calamita, F., Tavarnelli, E., Rusciadelli, G., Ori, G. G., & Paltrinieri, W. (2001). Foreland-dipping normal faults in the inner edges of syn-orogenic basins: a case from the Central Apennines, Italy. *Tectonophysics*, 330(3-4), 211-224.
- Scisciani, V., Montefalcone, R., Mazzoli, S., & Butler, R. W. H. (2006). Coexistence of thin-and thick-skinned tectonics: an example from the Central Apennines, Italy. *SPECIAL PAPERS-GEOLOGICAL SOCIETY OF AMERICA*, 414, 33.
- Scisciani, V., Patruno, S., Tavarnelli, E., Calamita, F., Pace, P., & Iacopini, D. (2019). Multi-phase reactivations and inversions of Paleozoic–Mesozoic extensional basins during the Wilson cycle: case studies from the North Sea (UK) and the Northern Apennines (Italy). *Geological Society, London, Special Publications*, 470(1), 205-243.

- Scisciani, V., Tavarnelli, E., & Calamita, F. (2002). The interaction of extensional and contractional deformations in the outer zones of the Central Apennines, Italy. *Journal of Structural Geology*, 24(10), 1647-1658.
- Tavarnelli, E., Butler, R. W. H., Decandia, F. A., Calamita, F., Grasso, M., Alvarez, W., ... & D'offizi, S. (2004). Implications of fault reactivation and structural inheritance in the Cenozoic tectonic evolution of Italy. *The Geology of Italy, Special, 1*, 209-222.
- Tavarnelli, E., Scisciani, V., Patruno, S., Calamita, F., Pace, P., & Iacopini, D. (2019). The role of structural inheritance in the evolution of fold-and-thrust belts: insights from the Umbria-Marche Apennines, Italy. In *250 million years of Earth history in Central Italy: Celebrating 25 years of the Geological Observatory of Coldigioco* (Vol. 542, pp. 191-211). Boulder, CO: Geological Society of America.
- Tondi, E., Jablonská, D., Volatili, T., Michele, M., Mazzoli, S., & Pierantoni, P. P. (2021). The Campotosto linkage fault zone between the 2009 and 2016 seismic sequences of central Italy: Implications for seismic hazard analysis. *GSA Bulletin*, 133(7-8), 1679-1694.
- Turco, E., Macchiavelli, C., Mazzoli, S., Schettino, A., & Pierantoni, P. P. (2012). Kinematic evolution of Alpine Corsica in the framework of Mediterranean mountain belts. *Tectonophysics*, 579, 193-206.
- Turrini, C., Toscani, G., Lacombe, O., & Roure, F. (2016). Influence of structural inheritance on foreland-foredeep system evolution: An example from the Po valley region (northern Italy). *Marine and Petroleum Geology*, 77, 376-398.
- Williams, G. D., Powell, C. M., & Cooper, M. A. (1989). Geometry and kinematics of inversion tectonics. *Geological Society, London, Special Publications*, 44(1), 3-15.

## 4. THE SEISMOTECTONIC ROLE OF TRANSVERSAL STRUCTURES IN THE PLIO-QUATERNARY EVOLUTION OF THE OUTER MARCHE APENNINES

M. Costa<sup>1</sup>, P.P. Pierantoni<sup>2</sup>, S. Telsoni<sup>2</sup> and C. Invernizzi<sup>2</sup>

<sup>1</sup> *Via Selvelli, 6, 61032 Fano (PU), Italy;*

<sup>2</sup> *School of Science and Technology – Geology Division, University of Camerino, Via Gentile III da Varano, 62032 Camerino, MC, Italy*

### **Abstract:**

We integrate geomorphological, structural, and seismological data on the outer Marche Apennines (Central Italy) to define the seismotectonic setting of this region. The investigated area is the locus of strong historical earthquakes and the geometry and kinematics of the seismogenic sources are not always well defined. Plio-Quaternary NW-SE structures, both extensional and compressional, are segmented by NE-SW oriented transversal faults, the origin and role of which are still debated. We characterize the geometry, kinematics, and activity of these main transversal faults to better define their seismogenic potential. Four main WSW–ENE to WNW–ESE transversal fault systems have been mapped. These are high-angle and deeply rooted fault systems that separate the outer Apennine sector into blocks and sub-blocks with different structural and evolutionary features. The combination of morphologic, stratigraphic and structural features together with seismological data and seismic reflection profiles reveals that some inherited fault segments have recently been reactivated because they have displaced Quaternary deposits. An analysis of the spatial distribution of seismicity indicates that some clusters of hypocenters are located within the crystalline basement. Stress field analysis using available focal mechanism solutions confirms the prevalence of left-lateral kinematics on roughly SW–NE oriented structures. The transversal structures thus contribute to the longitudinal segmentation of the Apennine structures. In addition, the high number of seismic events evidenced by the instrumental seismicity, as well as the history of earthquakes in this area, support the hypothesis that these faults are still potentially active, and this can be of prime importance in assessing seismic hazard and planning to mitigate risk in populated areas close to the Adriatic coast.

**Keywords:** Transversal faults; strike-slip; active tectonic; outer Apennine.

## 4.1. Introduction

During the last few decades, several structural and geomorphological studies have been conducted in the Apennine chain and foothill aiming to understand the tectonic evolution of the fold and thrust belt (Bally et al. 1986; Calamita et al., 1994; Boccaletti et al. 1990; Barchi et al. 1998b; Coward et al., 1999; Ghisetti and Vezzani, 1998; Tavernelli et al., 2004; Costa et al., 2021 between others).

Both the Apennine sector and the Adriatic offshore are characterized by NW-SE trending fault systems segmented by NE-SW transversal structures, which apparently were active simultaneously to the main one. Although in the past there was a growing research interest on these latter structures (Signorini, 1953; Ghelardoni, 1965; Locardi, 1988; Dramis et al., 1991; Coltorti et al., 1996; Pascucci et al., 2007; Vannoli et al., 2015), their origin, role and the seismotectonic implication are partially still debated and not completely understood.

The NE-SW structures are generally pre-existing normal faults, deeply rooted within the crystalline basement, inherited from the earlier extensional phase and reactivated during the shortening stage as strike slip faults. Their presence has been largely recognized and mapped in the whole Apennine (Nanni and Vivalda, 1987; Centamore et al. 1991a,b; Tavarnelli et al., 2001; Butler et al., 2006; Argnani et al., 2009; Di Bucci et al., 2010; Zampieri et al., 2021), in the southern Pyrenees foreland (Carrillo et al., 2020), in the Himalayan foreland (Duvall et al., 2020) and in many other foreland areas worldwide.

The seismic activity of these long-lived structures in the Apennine is also well constrained using different approaches such as the study of Travertine deposits in geothermal areas (Brogi and Capezzuoli, 2014; Brogi et al. 2017, 2020), analysis of historical earthquakes (Vannoli et al. 2016; Materazzi et al. 2022) and instrumental seismicity (Brogi and Fabbrini, 2009; Brogi et al., 2014; Mirabella et al., 2022).

In this regard, several studies and analysis were performed in the Umbria-Marche Apennines and its piedmont sector, considered one of the most seismically active area, locus of important historical and recent earthquakes in terms of victims and damages (e.g. Mw 6.17, 1741 Fabriano; Mw 6.51, 1781 Cagli; Mw 5.83, 1930 Senigallia; Mw 4.68, Ancona 1972; Mw 6, Colfiorito 1997; and Mw 6.5, Amatrice-Visso-Norcia, 2016 earthquakes).

Although both the Apennines inner sector and the coastal zone are characterized by high to moderate peak ground acceleration (PGA) in the seismic hazard map MPS04 (Meletti et al., 2006; Stucchi et al., 2011) and high concentration of individual seismogenic sources (DISS

Working Group, 2021), robust and validate correlation between historical strong events and seismogenic sources are still lacking.

The seismicity in this area is essentially attributed to NW-SE oriented Apennine extensional/transpressive and compressive faults, and focal mechanisms for the major earthquakes are generally consistent with these assumptions. However, some earthquakes with strike slip focal mechanism and nodal planes in both Apennine (NW-SE) and anti-Apennine (NE-SW) directions have been identified.

The strike slip focal mechanisms distribution suggests the presence of localized strike-slip seismogenic structures. In the offshore area facing the Conero promontory, Mazzoli et al. (2014) correlated some strike-slip focal mechanisms to a possible NE-SW trending wrench fault in the Apennine compressive context (Mazzoli et al., 2015). Recent reconstructions of the Plio-Quaternary structures in the outer Apennine sector highlighted a system of subparallel positive flower structures with a NW-SE trend and some important transversal fault systems with a NE-SW trend. Most of the latter structures show a Quaternary activity (Chicco et al., 2019; Pierantoni et al., 2019; Costa et al., 2021).

This study presents a seismotectonic characterization of the previously identified main transversal structures of the outer sector of the Marche Apennines playing a crucial role to define the seismic hazard of the investigated area.

## **4.2. Tectonic setting, main structural and evolutionary characteristics**

Over the years, numerous geological studies and detailed mappings concerned the Marche Region (Centamore et al., 1991a; Carta Geologica d'Italia 1:50.000, 2009), and unearthed its stratigraphic (Argnani et al., 1991; Centamore et al., 1991c; Centamore and Rossi, 2009; Invernizzi et al., 1995; Ghielmi et al., 2010, 2013; Artoni, 2013), structural (Bally et al., 1986; Ori et al., 1986; 1991; De Donatis et al., 1998; Carruba et al., 2006; Scisciani and Calamita, 2009; Fantoni e Franciosi, 2010; Bigi et al., 2013; Scisciani et al., 2014) and evolutionary (Boccaletti et al., 1990; Invernizzi, 1992; Bigi et al., 1995) characteristics.

The Neogene-Quaternary stratigraphic and structural evolution of this territory caused a morpho-structural division into two distinct sectors affected by the Apennine orogenic phase: i) the inner sector to the west, highly deformed and uplifted, where the deepest Mesozoic carbonate units of the stratigraphic sequence crop out; and ii) the outer sector to the east, apparently less deformed at surface, where the most recent Neogene-Quaternary terrigenous

units prevail. In both sectors, Apennine deformation migrating from W to E since Miocene times created a series of E-vergent NW-SE to NNW-SSE compressive structures.

During the upper Miocene/lower Pliocene, while the internal sector was marked by orogenic compression and uplifting, the outer one was characterized by the subsiding foredeep with the accumulation of thick terrigenous deposits resulting both from the dismantling of the growing chain and from the Po plain (Centamore et al., 1991c; Bigi et al., 1999; 2009; 2011; Artoni, 2003; Milli et al., 2007; Ghielmi et al., 2010, Marini et al., 2015). During the Quaternary, an extensional regime with NW-SE trending normal/transpressive faults was established in the inner sector of the Apennine chain. On the other hand, the compressive deformation affected all the outer sector during the Plio-Quaternary time, and some local extensional faults are thought to be accommodation faults related to compressive structures (Centamore and Rossi, 2009; Pierantoni et al., 2021). The internal and higher Apennine sector is separated from the outer foothills by the Urbino-S. San Quirico alignment (Fig. 4.1), an important Plio-Quaternary NW-SE trending, high angle and east deeping transpressive system.

In the outer Apennine sector of the Marche Region, compressive structures are delimited by on-shore and off-shore E-vergent thrusts on the eastern side, often buried below younger Plio-Quaternary terrigenous deposits that are slightly or not involved in the deformation. Bally et al. (1986), Ori et al. (1986) envisaged thin-skinned tectonics involving the sedimentary cover, while Coward et al. (1999) suggested that thrusting involves the crystalline basement in the onshore of the northern Marche Apennines, and data from the CROP project in the northernmost Marche area (Barchi et al., 1998) highlighted limited crystalline basement involvement with the presence of some high-angle reverse faults.

Recent structural studies based on the interpretation of several seismic ENI and Videpi profiles (Videpi Project, [www.videpi.com](http://www.videpi.com)), well data and surface geology (Chicco et al., 2019; Pierantoni et al., 2019; Costa et al., 2021) improved the structural and stratigraphic configuration of this sector. In particular, these authors posited that the deformation of the outer Apennine sector is thick-skinned since the main Apennine compressive structures are deeply rooted positive flower structures.

Frequently, both the on-shore and off-shore compressive structures are truncated and dislocated by NE-SW trending transversal fault systems (Mazzoli et al., 2014; Pierantoni et al., 2019; Costa et al., 2021). The influence of NE-SW long-lived structures represents a key factor in the evolution of the fold and thrust belt, creating structural highs in the early extensional phase, along-strike segmentation and differential displacement on the Umbria-Marche-Sabina Thrust

Zone (Mazzoli et al., 2005), and controlling the foredeep basins evolution and consequently the Mio-Pliocene foredeep infilling with marked lateral variation in thickness (Cantalamesa et al. 1986; Bigi et al. 1997; Milli et al., 2013).

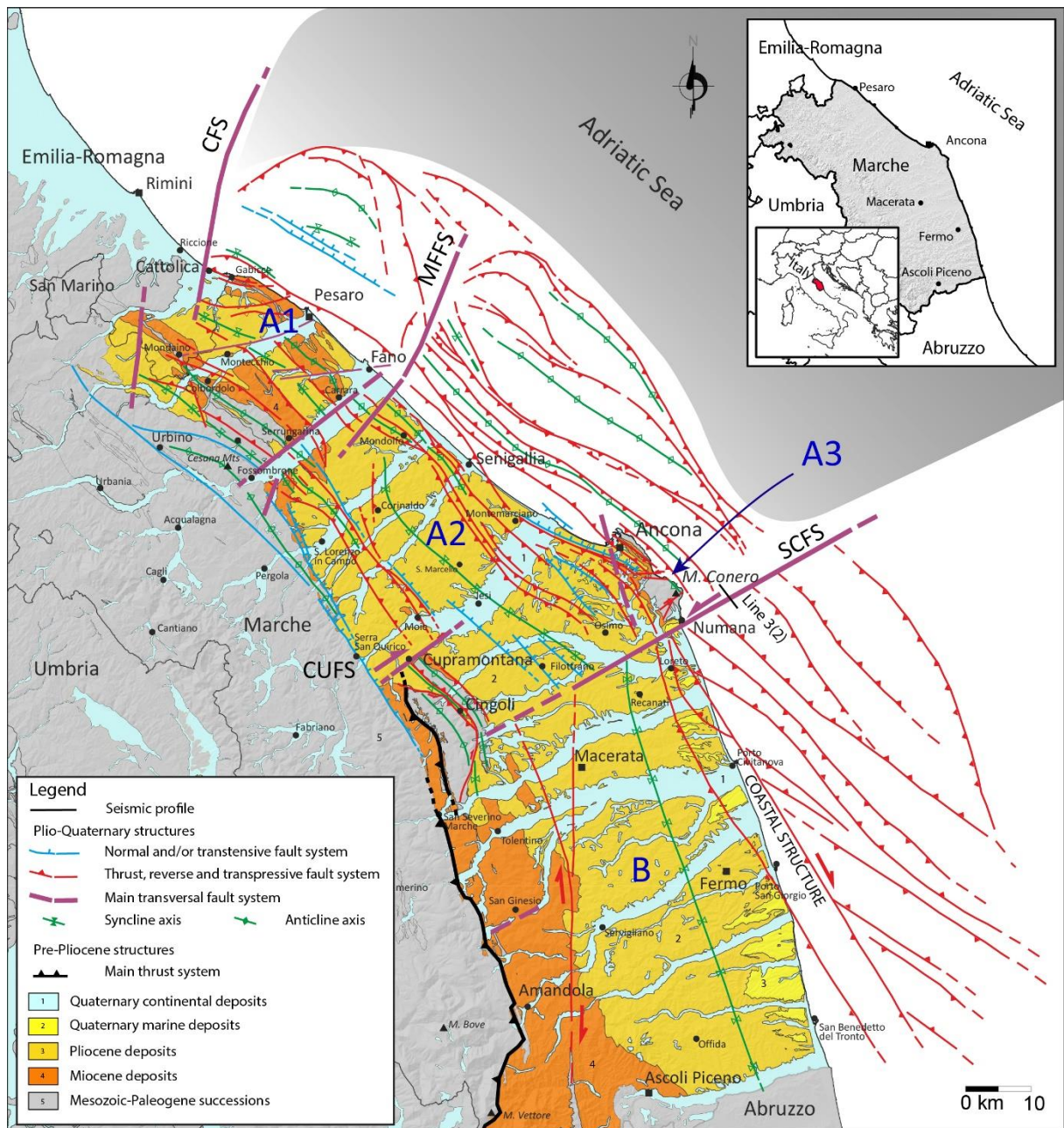


Fig. 4.1 - Geo-Structural sketch (modified after Pierantoni et al., 2013; Pierantoni et al., 2019; Costa et al., 2021 and Contiet al., 2020). Shaded gray: area not affected by the compressive Plio-Quaternary Apennine deformation. A, B: Main structural blocks.

The complex syn-sedimentary tectonics starting since the Upper Tortonian to Lower Pliocene strongly conditioned the depocenter morphology and the depositional environments (Centamore and Rossi, 2009). The Fiastrone-Fiastrella streamline, located to the south to San



Ginesio (Fig. 4.1), represents one of the most important example of transversal structure marking a sharp change of sedimentary thickness of the Laga deposits and delimiting the boundary from the Northern Laga Basin to the north, and the deeper subsiding Southern Laga Basin to the south (Cantalamesa et al., 1980, 1983).

Although the displacement measured at surface ranges from 50 to 200 m (Coltorti et al. 1996), several authors suggest the importance of transversal faults in controlling geomorphological evolution of landscape actually developing a NE-SW sub-parallel drainage and perpendicular to the carbonate anticlines (Di Bucci and Mazzoli, 2003; Wegmann and Pazzaglia, 2009; Nesci et al., 2012)., The NE-SW transversal structures play a double role in the seismotectonic context acting as structural boundaries and preventing the propagation of the earthquake ruptures, (Valensise and Pantosti, 2001; Pace et al. 2002; Boncio et al. 2004; Chiaraluce et al. 2005; Pizzi et al., 2017), or as a source of large to small seismic events (Brogi et al. 2014, 2017; Materazzi et al. 2022; Mirabella et al., 2022).

The historical and recent seismicity of the studied area has been described (ISIDe working group 2007, Rovida et al. 2022) and studied by various authors (DISS Working group 2021; Riguzzi et al., 1989; Valensise and Pantosti 2001; Console et al., 1973; Santini, 2003; Santini and Martellini, 2004; Elter et al., 2011; Santini et al., 2011; Kastelic et al., 2013; Vannoli et al., 2015; Mantovani et al., 2017; Battimelli et alii, 2019). In most cases, the seismicity is attributed to the activity of the Apennine trending compressive structures. Nevertheless, Mazzoli et al. (2014), Brogi and Capezzuoli (2014), Brogi et al. (2014; 2017), Pierantoni et al. (2019) and Mirabella et al. (2022) highlighted recent and historical seismicity linked to some active transversal structures in the Central and Northern Apennines. The transversal structures (excluding the Cattolica Fault System CFS, with no data available) and some of the Apennine structures re-activate previous normal or transtensive lower Pliocene structures (Costa et al., 2021). Pierantoni et al. (2019) and Costa et al. (2021) also identified different characteristics within the outer sector, hitherto considered structurally homogeneous. This sector can be divided into two parts, each one with its own structural and evolutionary characteristics (Fig. 4.1). The northern part extends from Gabicce to the Conero Promontory, while the southern part goes from the Conero Promontory to the Tronto River valley (hereafter respectively blocks A and B in Fig. 4.1). The blocks are separated by the South Conero Fault System (SCFS), an ENE-WSW trending complex transversal structure located immediately south of the Conero promontory (Centamore et al., 1991a; Mazzoli et al., 2014, 2015; Costa et al., 2021). This feature cuts Quaternary deposits (Fig. 4.2) and structures, showing a Quaternary activity. The Fig. 4.2, an excerpt of the Videpi 3 (2) seismic profile located shows a strongly deformed area

in the offshore part of the SCFS, where some faults disturb even the uppermost seismic horizons with visible vertical shift.

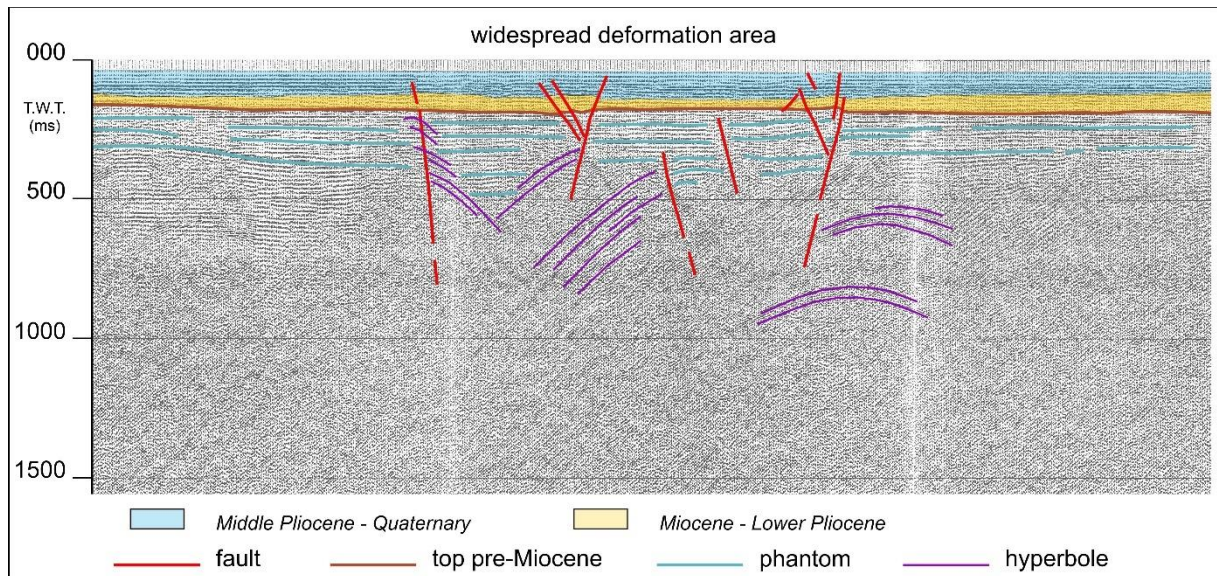


Fig. 4.2 - VIDEPI seismic profile: 3(2) (see Fig. 4.1 for location). Middle Pliocene–Quaternary deposits are highlighted in blue, Lower Pliocene deposits are in orange. No color is used for the pre-Pliocene sequence. ([https://www.videpi.com Linea 3\(2\)](https://www.videpi.com Linea 3(2))).

Further to the north, block A is separated from the Romagna Apennines by a NNE-SSW Quaternary transversal structure, the Cattolica Fault System (CFS). To the south of the Tronto River, block B continues in the Abruzzo Region apparently without litho-structural variations, according to the findings of Carruba et al., 2006.

Within block A (Fig. 4.1), a series of NW-SE trending subparallel flower or push-up structures enucleated starting from the Lower Pliocene to the W, and from the Middle-Upper Pliocene to the E. These structures involve the underlying basement and show sub-vertical faults at the core cutting all the succession up to the surface (Chicco et al., 2019; Pierantoni et al., 2019). The Apennine structures are sometimes dislocated by transversal NE-SW faults or fault systems, with structural and age characteristics like those of the faults delimiting block A to the north (CFS) and to the south (SCFS). Most of the transversal structures are located along the Metauro River valley, in the Fano offshore (the Metauro Valley-offshore Fano Fault System MFFS) and close to Cupramontana (the Cupramontana Fault System CUFS). These structures further divided block A into three sub-blocks (A1, A2, A3; Fig. 4.1) with differences in the morphotectonic and stratigraphic characteristics, The MFFS separates sub-block A1 from sub-block A2, while the W-Ancona Fault system separates sub-block A3. The CUFS is located at the southwestern end of sub-block A2.

The Apennine flower structures in the onshore and coastal area within sub-block A2 are the continuation of those in block A1 (Chicco et al., 2019; Pierantoni et al., 2021). The MFFS transversal structure cuts the Apennine structures, with a southward lowering of sub-block A2, which diminish the morphological evidence of Apennine structures involving Plio-Quaternary deposits within the sub-block itself. In the offshore of sub-block A1, the outermost Apennine structures are interrupted against CFS, forming a large, NW-verging, asymmetrical arc. In the offshore of sub-block A2, the outermost Apennine structures have a NW-SE trend and are interrupted against MFFS to the north and SCFS to the south. Local segments of minor NW-verging low angle thrusts within sub-blocks A1 and A2 are related to MFFS kinematics (Fig.4.1; Pierantoni et al., 2019). Sub-block A3 is mainly developed onshore where the deep units of the Umbria-Marche succession crop out. The transversal faults delimiting the three sub-blocks are all Quaternary in age.

Block B has structural and evolutionary characteristics remarkably different from those of block A. The western part of block B is marked by an approximately NNE-SSW structure characterized by sub-vertical fault planes at depth and less inclined in the more superficial horizons (Amandola structure; Costa et al., 2021). Immediately to E, a large and deep N-S oriented syncline is present. Further to the E, there is a complex compressive structure (Coastal Structure of Ori et al., 1991) characterized by E-verging thrusts in the more superficial horizons and by high angle faults at depth. Some of these faults cut Quaternary deposits and are seismically active (Costa et al., 2021), while others are sealed by Quaternary deposits. Compressive flower or push-up structures with a NW-SE trend mark the offshore E of the Coastal structure and are sealed by Quaternary deposits. The Apennine flower structures identified in the onshore of block A are not present in the onshore of block B, and they stop abruptly at the SCFS transversal structure. Within block B, no important transversal structures have been identified and the structural and stratigraphic characteristics of the block are homogeneous.

Finally, from the evolutionary point of view, it can be observed that in block A the Apennine compressive deformation began during the lower Pliocene, while in block B it began during the middle-upper Pliocene.

### 4.3. Materials and methods

This study exploited surface geological data from the literature and Plio-Quaternary structural reconstructions proposed by Pierantoni et al., 2019 and Costa et al., 2021, as well as the new interpretation of a ViDEPI seismic profile ([https://www.videpi.com/Linea\\_3\\_\(2\)](https://www.videpi.com/Linea_3_(2))) close to the transversal structure south of the Conero promontory (SCFS).

The seismicity distribution was analyzed to infer the geometry of the above mentioned four transversal fault systems by comparing the instrumental and historical seismic data from the study area in ArcGIS environment.





















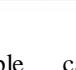
The instrumental seismicity for events with magnitude  $M \geq 1$  parametrized since 1985 were drawn from catalogues from the Italian Seismic Instrumental and Parametric Database – ISIDE (ISIDE Working Group, 2007, available at <http://iside.rm.ingv.it/>, last accessed 22 February 2022). This catalogue provides various types of magnitude depending on the size of the event, with  $M_L$  in over 90 % of the events and  $M_W$  in less than 10 %. In this regard, different magnitude scales for each seismic event were used. When instrumental seismicity data were lacking (for example, to define CFS geometry), we used information on the historical earthquake epicentres, based on macroseismic intensity provided by the Parametric Catalogue of Italian Earthquakes (Rovida et al. 2022 – <http://emidius.mi.ingv.it/CPTI15-DBMI15>, last accessed 22 February 2022).

Focal mechanism solutions along the fault systems analyzed in the present work are derived from available catalogue (INGV – Ancona <http://www.an.ingv.it/BB/home.html>, by Monachesi et al. 2021, last accessed 15 January 2022) and the literature (Santini et al., 2011; Mazzoli et al., 2014). The stress field analysis of each fault system was carried out using WinTensor software (Delvaux and Sperner, 2003) and available data.

The focal mechanisms (shown in Tab. 4.1) and relative kinematics were used to calculate the active stress field by applying the PBT kinematic axes method (Turner, 1953). Based on the Mohr–Coulomb fracture criterion, widely used in structural geology, this method calculates the stresses from the orientation of single fault planes, where P is the compression axis, B is the neutral axis (contained in the fault plane) and T is the extension axis (Sippel et al., 2009).

This method can be applied assuming that all the faults were formed and moved by the same stress field. The quality of the stress tensor estimation (QRfm) for the focal mechanism solutions is expressed on a scale ranging from A (best result) to E (worst result) according to

the World Stress Map quality ranking scheme (Heidbach et al., 2016; <http://www.world-stress-map.org/>).

		DATE	TIME (UTC)	M	STRIKE	DIP	RAKE	
MFFS	1	27/08/1990	23:24	3.9	25	50	0	
	2	05/05/2000	20:42	4.1	105	25	30	
	3	25/06/2000	20:24	3.5	40	90	- 50	
	4	27/06/2000	02:15	3.4	25	85	40	
CUFS	5	18/08/2012	14:43	2	25	25	- 40	
	6	19/08/2012	1:21	1.5	125	65	-110	
	7	19/08/2012	1:57	1.3	15	30	- 10	
	8	01/07/2013	0:16	2	45	90	0	
	9	02/07/2013	0:36	2.2	55	65	- 30	
	10	02/07/2013	5:36	2.3	55	85	40	
	11	03/07/2013	20:22	2.3	55	85	- 80	
	12	04/07/2013	21:9	2.5	65	75	-20	
	13	03/07/2013	17:59	3	60	45	- 30	
	14	08/07/2013	19:33	2.7	75	65	-20	
	15	09/07/2013	17:11	2.3	55	90	0	
	16	10/07/2013	17:11	2.3	335	85	-120	
	17	08/08/2013	2:57	2.4	20	90	0	
	18	09/08/2013	17:59	2.7	100	75	-160	
SCFS	19	21/07/2013	01:32	4.9	170	70	160	
	20	21/07/2013	03:07	4	170	65	150	
	21	23/07/2013	19:30	4.4	130	50	70	

Tab. 4.1 - Earthquake focal mechanism dataset derived from available catalogue (<http://www.an.ingv.it/BB/home.html>, last accessed 15 January 2022) and the literature (Santini et al., 2011, Mazzoli et al., 2015) and used to perform the stress field analysis.

## 4.4. Results: seismicity close to transversal structures

### 4.4.1. *The Cattolica Fault System*

In May-August 1916, there was an important seismic sequence characterized by two main shocks of  $M_w = 5.82$  (CPTI15, Rovida et al. 2022), which caused deaths and significant destruction in the Rimini and northern Marche territory. While no instrumental seismic data for this sequence are available, the intensity distribution was reconstructed based on the macroseismic data in the area affected by earthquakes. The epicenters of the two main shocks were positioned in the offshore of the Marche-Romagna coast (INGV, 2015) in correspondence with CFS (Fig.4.3).

Between March and April 2013, a seismic sequence consisting of about 30 earthquakes with  $M_l$  ranging between 1.3 and 2.5 occurred in the Cattolica offshore. The epicenters were arranged over a N-S oriented area, about 7 km long. Some of the epicenters belonging to this sequence fell onshore near Cattolica, Mondaino and Rimini. The depth of hypocenters ranged between 17 and 24 km, and follows the CFS alignment (Fig. 4.3).

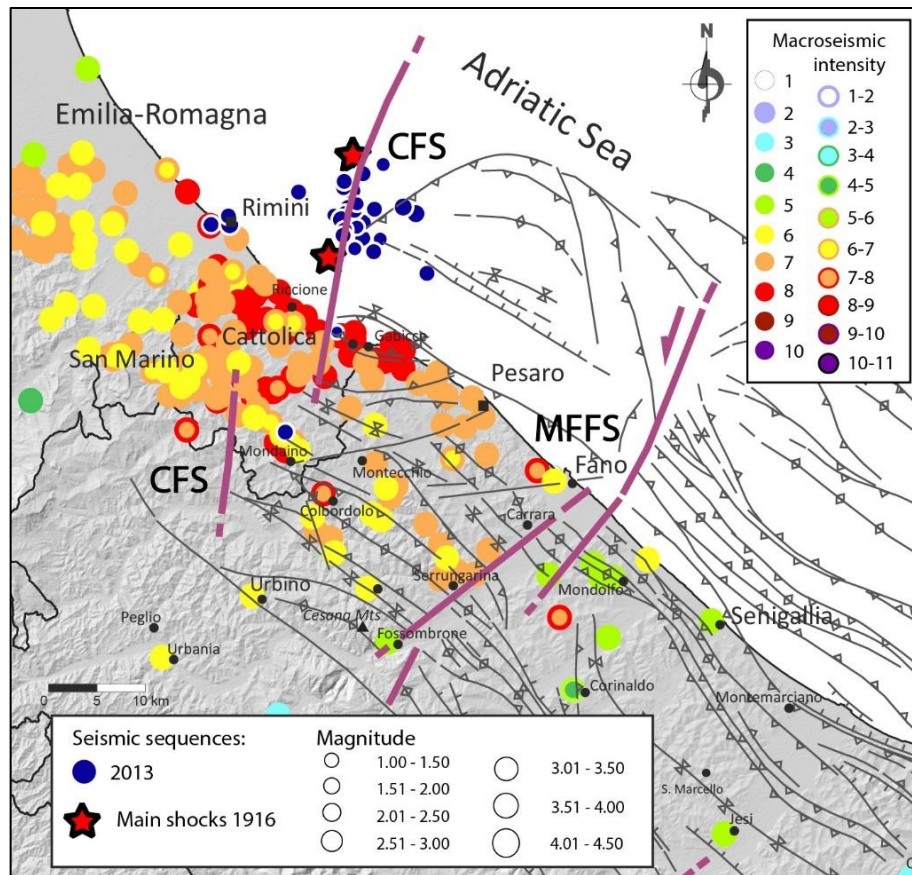


Fig. 4.3 - Cattolica Fault System (1916 and 2013 seismic sequences data). The macro-seismic data refer to the 1916 sequence. The transversalfaults are indicated in purple, while all the other structures are in black.

#### 4.4.2. The Metauro valley offshore Fano Fault System

Two main seismic sequences fall along this fault system, both offshore of Fano (Fig. 4.4).

A seismic sequence consisting of 10 events of  $M_d$  between 2.4 and 4.1 occurred from March to November 2000. It included nine hypocenters between 3 and 5 km depth and one at 10 km. The epicenters were distributed over a narrow ellipsoidal area 20 km long and trending NE-SW. Three focal mechanisms are available (Santini, 2003; Tab. 4.1), namely, a transpressive one with nodal planes roughly WNW to N-S oriented (2 in Fig. 4.4 by Santini, 2003), and two strike slip ones (indicated as 3, 4 in Fig. 4.4) with NNE-SSW oriented sub-vertical nodal planes. In 1990, a minor sequence with an earthquake of  $M=3.9$  and a strike slip focal mechanism occurred with a NNE-SSW highly inclined nodal plane (Santini, 2003). The MFFS seismological stress tensor (shown in Fig. 4.4) obtained from focal mechanism inversion shows a strike-slip regime with  $\sigma_1$  ( $22^\circ/004^\circ$ ),  $\sigma_2$  ( $55^\circ/130^\circ$ ),  $\sigma_3$  ( $25^\circ/263^\circ$ ), and rank quality of QRfm = A.

In July-August 2021, a seismic sequence composed of 45 events occurred ( $M_l$  between 1.3 and 2.3). Thirty hypocenters were located between 6 and 10 km depth, nine between 10 and 20 km and six deeper than 20 km (maximum 26 km). The hypocenters of the deepest earthquakes were temporally interspersed with those of the most superficial ones. Epicenters were distributed over a narrow elliptical area with a 15 km long major axis NE-SW oriented (Fig.4.4). The epicenters of the deepest events were all located in the western sector of the ellipse. No focal mechanism data are available for this sequence.

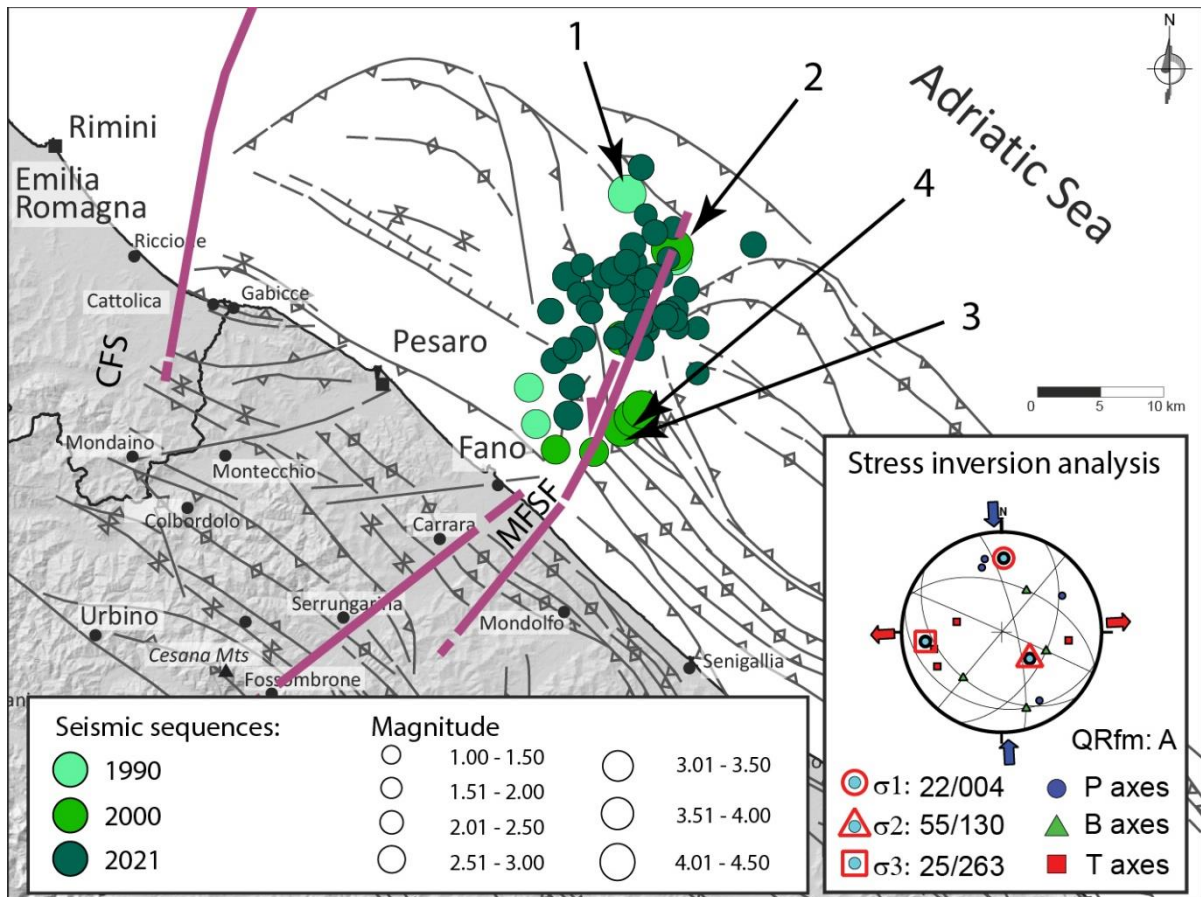


Fig. 4.4 - Metauro-Fano Fault System and seismic sequences data. Results of the stress inversion analysis are shown in the rectangle in the lower right. The transversal faults are indicated in purple, all the other structures in black. Black arrows indicate the seismic events with a available focal mechanism solutions (see Tab. 4.1).

#### 4.4.3. The Cupramontana Fault System

Two seismic sequences have been reconstructed falling along this structure (August 2012 and June-September 2013, Fig. 4.5).

A low-energy seismic sequence in August 2012 was composed of 32 events of  $M_I$  equal to or greater than 1, and only one greater than 2 ( $M_I = 2.2$ ). These events occurred within a radius of 5 km from the city center of Cupramontana, with hypocenters ranging from 6 to 10 km of depth. Epicenters were distributed within a narrow elliptical NE-SW oriented area 2.5 km long, located immediately SE of Cupramontana. Three focal mechanisms are available (Tab. 4.1), two of which suggest two alternative solutions.

From late June to late September 2013, the SE of Cupramontana area was affected by a seismic sequence of approximately 270 events ranging from  $M_1$  to slightly over  $M_3$ , (only three cases). This sequence reached its highest frequency in July, with 208 events. The hypocenters were located between 6 and 12 km of depth, with the greatest frequency between 8 and 10 km. The



epicenters were distributed mainly over a 5 km long NE-SW highly elliptical area immediately SE of Cupramontana, while the minor axis was about 2 km wide (Fig. 4.5). Most of the focal mechanisms (Tab. 4.1) were characterized by a nodal plane oriented from NE-SW to ENE-WSW and inclination from vertical to about 65°. These nodal planes almost coincided with the major axis of the distribution ellipse. The stress inversion result (shown in fig. 4.5) of the CUFS focal mechanism solutions highlights a tensor coherent with left-lateral kinematics with  $\sigma_1$  (19°/008°),  $\sigma_2$  (71°/186°)  $\sigma_3$  (01°/278°) and a quality factor A (QRfm = A).

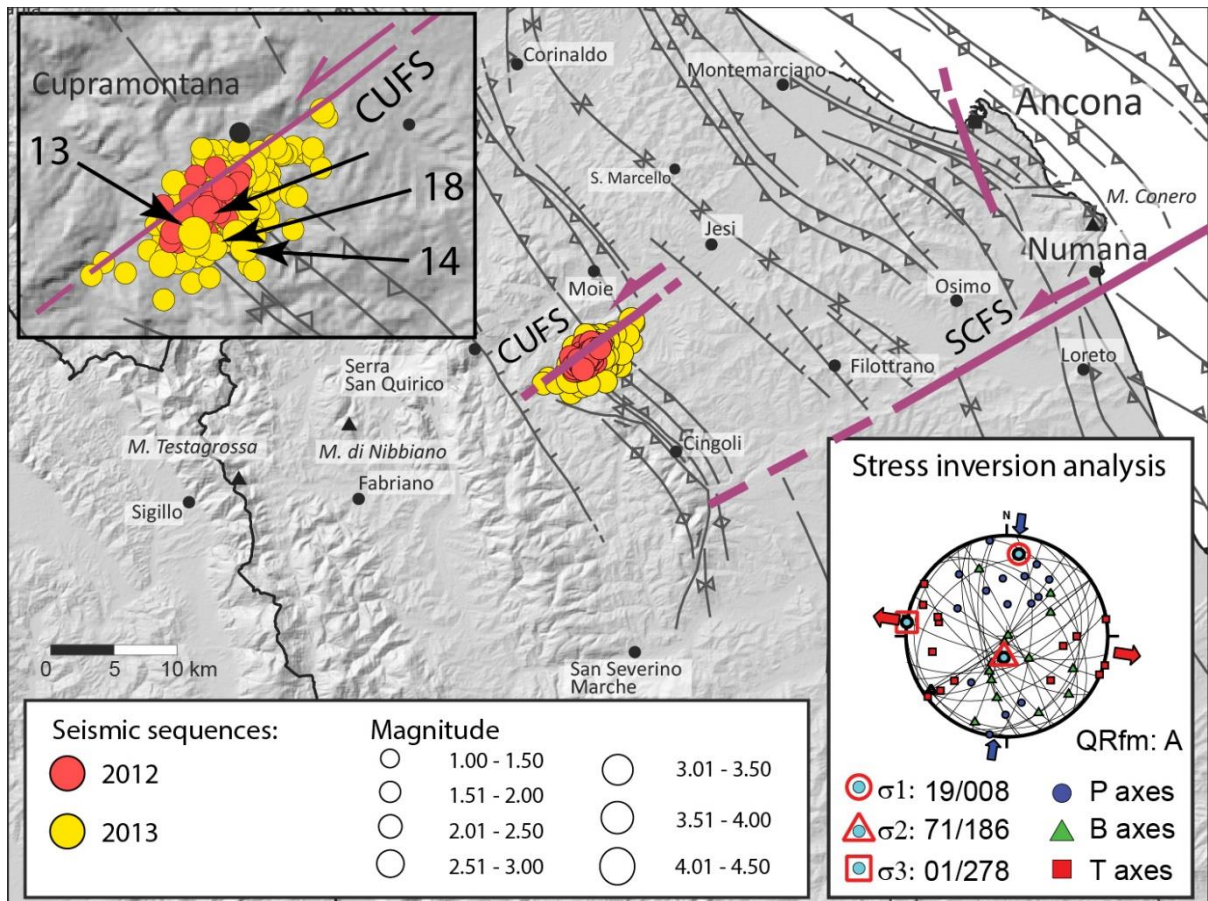


Fig. 4.5 - The Cupramontana Fault System and the 2012 and 2013 seismic sequence. Results of the stress inversion analysis are shown in the rectangle in the lower right. The transverse faults are indicated in purple, all the other structures in black. Black arrows indicate the seismic events with available focal mechanism solutions (see Tab. 4.1).

#### 4.4.4. The South Conero Fault System

Two seismic sequences have been identified within this fault system.

Between June and October 2013, a seismic sequence of about 160 earthquakes of M equal to or greater than 1 occurred in the offshore of the Conero promontory. The highest recorded magnitude was  $M_w = 4.9$ . Two other earthquakes of  $M_w = 4.2$  and  $M_w = 4.0$ , and three of M

= 3.1, 3.3 and 3.8 were recorded. The other events had  $M$  between 1 and 2.9. Most of the hypocenters fell within the range of 8-10 km in depth. Two were around 20 km deep and five less than 6 km. A significant majority of the epicenters was distributed within a 20 km long elliptical surface immediately east of Numara, and ENE-WSW oriented: the minor axis was about 8 km wide (Fig. 4.6). According to INGV data, the main shock  $M_w = 4.9$  was transpressive with NW-SE oriented nodal planes. The  $M_w = 3.8$  event was strike slip with ENE sub-vertical nodal planes ( $83^\circ$  of dip), and NNW-SSE  $57^\circ$  dipping. According to the elaborations of Mazzoli et al., (2015), the  $M_w = 4.9$  focal mechanism is instead strike slip with nodal planes about E-W sub-vertical and N-S oriented (Tab. 4.1).

Between January and November 2014, a seismic sequence of about 50 earthquakes of  $M$  equal to or greater than 1 occurred again in the offshore of the Conero promontory. The greatest frequency of events was in August, and included the strongest of the earthquakes, at 3.4 and 3.3  $M_w$ . The recorded magnitudes  $M$  of the other events ranged between 1 and 2.9. Hypocenters were within the range of 5-11 km depth, while the epicenters were located within a highly eccentric 10 km long elliptical ENE-WSW oriented area in the offshore east of Numana town. The minor axis was about 4 km wide (Fig. 4.6). According to INGV data, both the  $M > 3$  earthquakes were strike slip. That of  $M_w = 3.4$  had nodal planes oriented  $235^\circ/86^\circ$  and  $144^\circ/79^\circ$  respectively. The  $M_w = 3.3$  earthquake had nodal planes oriented  $237^\circ/81^\circ$  and  $146^\circ/84^\circ$  (Tab. 4.1). The stress inversion obtained from focal mechanisms of the 2013-2014 Numana seismic sequences (SCFS) yielded only slightly different results in comparison with the previously analyzed seismic sequences:  $\sigma_1$  ( $01^\circ/225^\circ$ ),  $\sigma_2$  ( $33^\circ/315^\circ$ )  $\sigma_3$  ( $57^\circ/133^\circ$ ) and a QRfm: A.

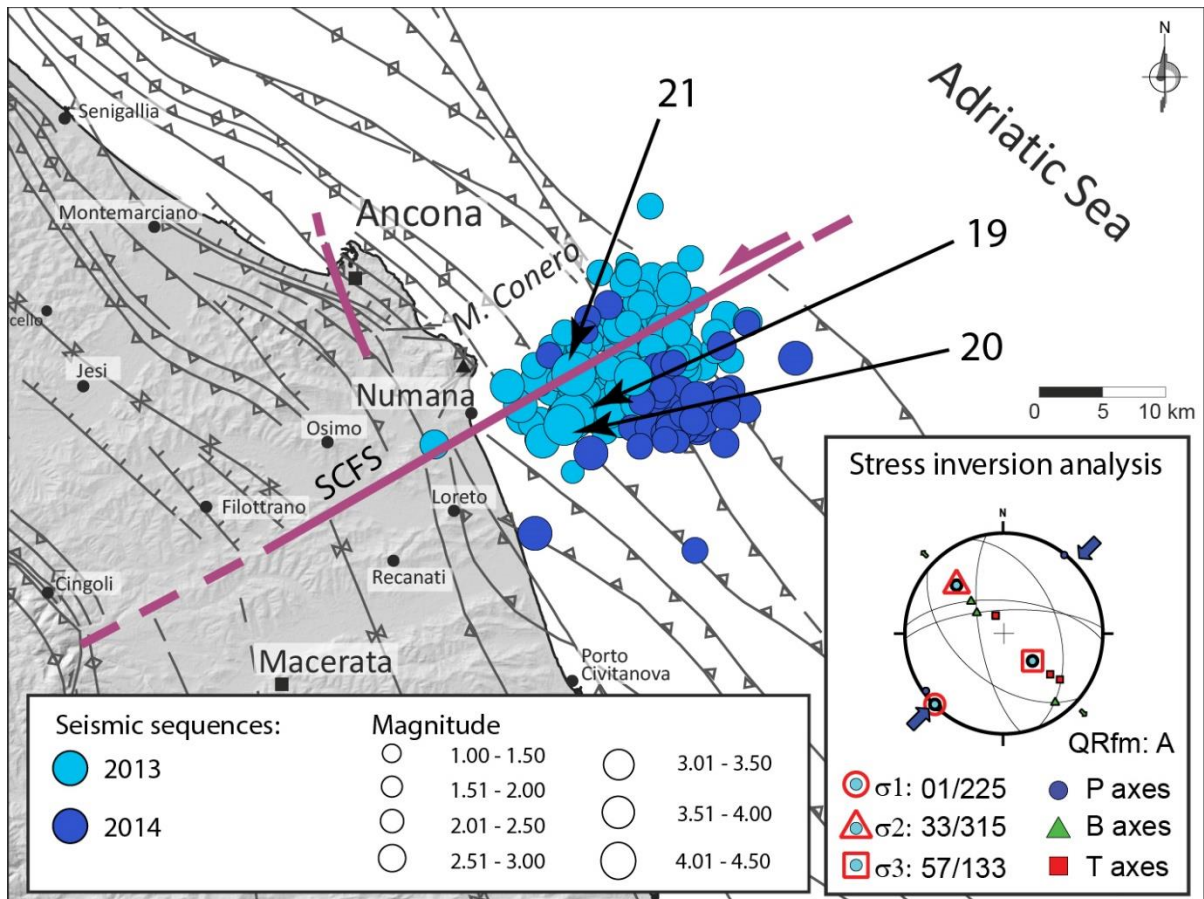


Fig. 4.6 - The South Conero Fault System and seismic sequence. Results of the stress inversion analysis are shown in the rectangle in the lower right. The transverse faults are indicated in purple, all the other structures in black. Black arrows indicate the seismic events with a available focal mechanism solutions (see Tab.4.1).

## 4.5. Discussions

### 4.5.1. *Seismotectonic considerations*

The acquired structural and seismological data allow the following seismotectonic considerations.

**The Cattolica system (CFS).** The offshore section of the CFS shows a high-angle NNE-SSW trend and is active and seismogenic (Pierantoni et al., 2019), based on the macroseismic data of the 1916 seismic sequences (INGV, 2015) and on the characteristics of the 2013 seismic sequence (Fig. 4.3). The highest macroseismic intensities were near Cattolica and the main shocks were offshore near CFS (Fig. 4.3). Moreover, the 2013 sequence is consistent with the proposed seismotectonic correlation because it was located near the offshore segment (and part of the onshore segment) of this structure, following its trend. The 17-24 km depth of the hypocenters, and more than a thousand meters of undeformed Upper Pliocene-Quaternary

deposits allow to exclude any correlation with Apennine thrust structures. The activation of a deeply rooted, sub-vertical to high angle structure is instead more compatible with the abovementioned features. The onshore segment of the CFS shows sporadic and widespread seismicity (ISIDe Working Group, 2007). The kinematics of this system is not well known due to the lack of focal mechanism data.

**The Metauro valley offshore Fano Fault System (MFFS).** This structure is NE-SW oriented in the onshore segment, and NNE-SSW trending in the offshore segment. The offshore segment is high angle, deeply rooted (hypocenters deeper than 20 km) and Quaternary in age (Pierantoni et al., 2019). The reconstructed seismic sequences (2000 and 2021) concern mainly the offshore part. The event distribution is consistent, and focal mechanisms show NNE-SSW oriented nodal planes, also confirming a high angle, NW-dipping left lateral fault plane. Sporadic and widespread seismicity is reported along the onshore segment of this system (ISIDe Working Group, 2007).

**The Cupramontana Fault System (CUFS).** Based on geological and structural data, this structure is right lateral and NE-SW trending (Fig. 1; Pierantoni et al., 2019). The epicenters and hypocenters distribution between the first (2012) and the second sequence (2013) are quite consistent with this structure, with a slight difference in the position (Fig. 4.5). If this does not depend on the seismological data acquisition, it could indicate that two subparallel and neighboring faults of the same system have been activated in succession. Most of the focal mechanisms show left lateral/transpressive kinematics along high angle, NE-SW oriented nodal planes. Some other focal mechanisms indicate different kinematics and direction (Tab. 4.1) probably because during the sequences, different but nearby structures were activated by accommodation. The different CUFS kinematics deriving from structural and seismological data will be discussed below.

**The South Conero Fault System (SCFS).** This structure, immediately south of the Conero promontory, has an overall ENE-WSW trend (SCFS; Figs. 4.1, 4.7). It separates the outer Apennine sector into two blocks, A and B (Fig. 4.1). The epicenter distribution of both the 2013 and 2014 offshore seismic sequences is entirely consistent with this orientation. Again, the epicenter distribution ellipse slightly different between the first and second sequence (Fig. 4.6), probably indicating that two subparallel faults were activated. Focal mechanisms indicate left lateral kinematics, also confirmed by stress inversion analysis (Fig. 4.6), and high-angle fault plane. The E-W oriented nodal planes coincide with the major axis of the sequence distribution ellipse. Among the focal mechanisms of the 2013 sequence, there was an earthquake with

compressive kinematics and Apennine direction (Mazzoli et al., 2014). This could indicate that a segment of the neighboring Apennine structure was activated by accommodation following the strike slip movement of the transversal structure.

In correspondence with the western onshore end of SCFS, WSW of the Conero promontory (at the intersection area with the Cingoli structure; Fig. 4.1), further recent seismic sequences have been recorded with a NE-SW to ENE-WSW distribution. These sequences are not analyzed in this work (see ISIDe catalogue of the INGV).

Length, continuity, geo-structural and kinematic characteristics give to CFS, MFFS and SCFS an important role: they interrupt or displace all the Apennine compressional structures of the outer sector. The CUFS and the hypothesized W-Ancona system are more localized systems and apparently displace only a few Apennine structures. These transversal systems seem to be interrupted or less visible westward where the inner and outer Apennine sectors are separated (Fig. 4.1; 4.7) The continuation of CFS, MFFS and SCFS towards the NE in the Adriatic Sea cannot be excluded.

#### 4.5.2. *General discussion*

Structural reconstructions for the outer Apennine sector of the Marche Region highlighted the presence of four sub-parallel structures running from NNE-SSW to ENE-WSW, transversal to the trend of the main compressive and extensional structures and cutting Quaternary deposits and features (Fig. 4.7).

Part of the SCFS was already known in the literature (Mazzoli et al., 2014), while the others have been recognized only recently (Pierantoni et al., 2019; Costa et al., 2021). A fifth transversal fault system has been hypothesized west of the city of Ancona (Figs. 4.1, 4.7). All these structures are seismogenic systems with historical, recent, and current earthquakes, characterized by weak but frequent seismicity. However, in correspondence with CFS, MFFS and SCFS some stronger seismic events occurred, from about  $M = 5$  to  $M = 5.8$  (CPTI15, Rovida et al. 2022).

Regarding the South Conero Fault System (SCFS), our analysis supports the seismotectonic correlation proposed in Mazzoli et al., (2014; 2015), also consistent with the stress inversion analysis (Fig. 4.6). CUFS, SCFS and MFFS show left-lateral kinematics. The CUFS was identified and represented by Pierantoni et al. (2019) with right kinematics, based on geo-structural data (Fig. 4.1). However, seismological data highlight a left lateral kinematics,

indicating that the current stress field differs from previous phases (Lower Pliocene if the right kinematics was syn-tectonic; Middle Pliocene-Pleistocene if it was post-tectonic).

The MFFS and SCFS are placed where previous lower Pliocene extensional/transpressive structures developed (see Fig. 9 in Costa et alii, 2021), and thus they likely represent reactivated structures in a different geodynamic context during the Quaternary.

The outer Apennine sector shows an overall oroclinal trend where the identified transversal structures determine the progressive curvature of the central-northern outer Apennine belt separating blocks characterized by changing in the direction of the structural trends. The CFS and SCFS are in correspondence with the hinge areas of the orocline and represent the main kinematic junctions (transfer faults). The SCFS arises where the Apennine structure trends pass from about NNW-SSE (to the south) to about NW-SE (to the north), as also indicated by the coastal line. The CFS is located where the Apennine structure trends pass from about NW-SE (to the south) to about WNW-ESE in the western Emilia-Romagna block (Bigi et al., Edits 1983. Structural Model of Italy, C.N.R. / Selca 1990; Costa, 2003).

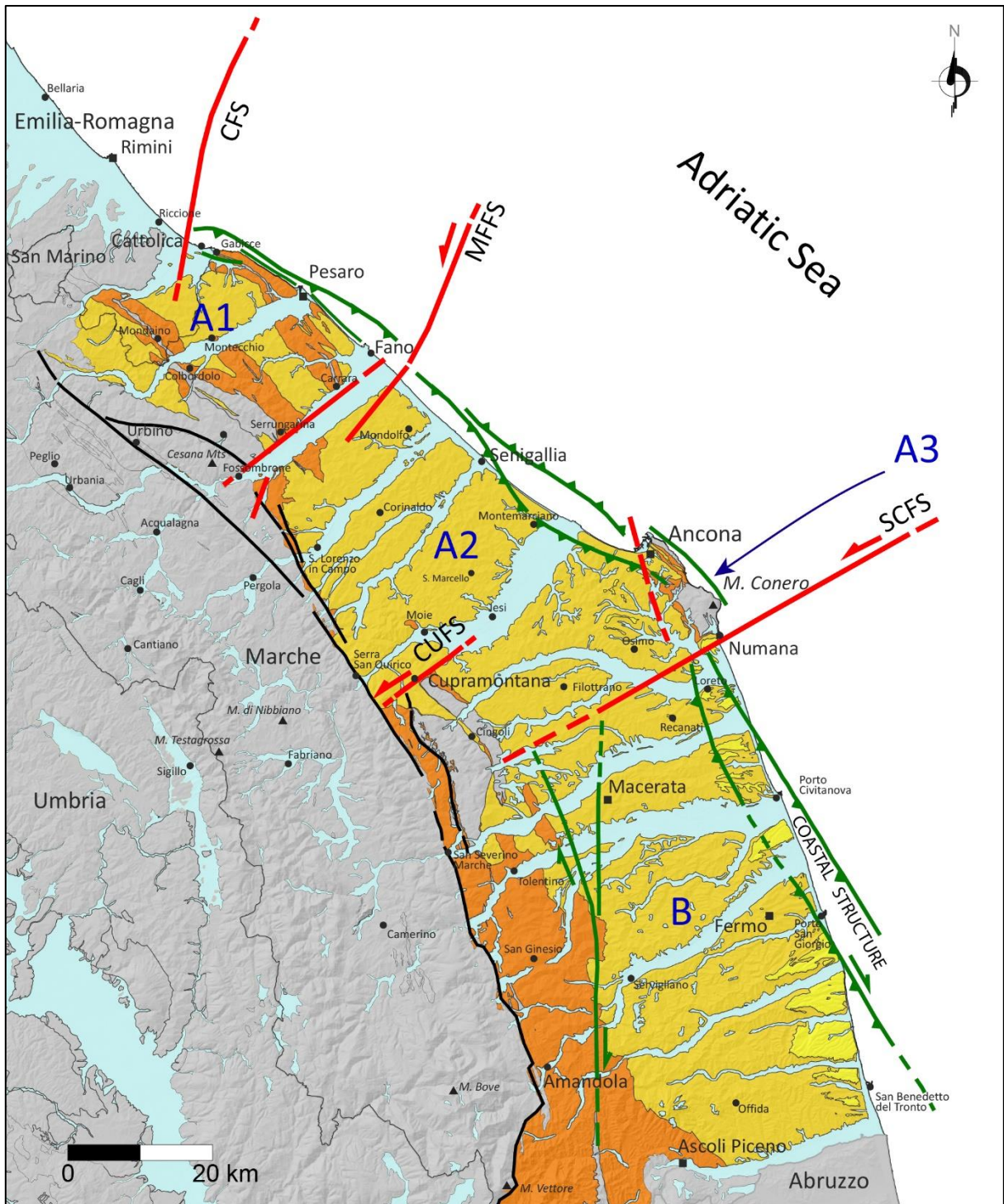


Fig. 4.7 - Geological sketch map representing the main active and seismogenic structures belonging to the outer sector (in red: SW-NE transversal fault system; in green: NW-SE/N-S Apennine structures) analyzed in this work. Black are the structures separating the internal and the outer Apennine sectors not discussed in this work.

Stress analysis suggests a horizontal N-S oriented  $\sigma_1$  for the MFFS and CUFS, and horizontal NE-SW oriented  $\sigma_1$  in correspondence to the SCFS. These structures are inherited, and therefore their orientation does not depend on the direction of the current stress field. It is

probable that there are variations in the current stress field between the two blocks, given the available data, a mismatch of  $45^\circ$  in  $\sigma_1$  orientation, and the different trending of structures between block A and B in the outer sector.

The importance of CFS, MFFS and SCFS structures is related to their geodynamic role and their high-angle planes, deeply rooted in the crust, as also indicated by the hypocenters of the associated earthquake sequences. The CUFS and the hypothesized structure W of Ancona seem to be secondary junctions with local character (CUFS) or connected with the adjacent transversal structure (SCFS for W Ancona). The Conero promontory, surrounded by Plio-Quaternary deposits, consists mainly of Mesozoic-Paleogenic carbonate units of the Umbria-Marche succession, which are strongly raised and emerge to about 570 m of altitude. It is the only structure with these characteristics and position within the outer Marche-Abruzzo Apennine sector. It constitutes a push-up wedge at the contact area between blocks A and B, formed at the hinge of the central-northern Apennine orocline. Furthermore, this push-up structure, being largely bounded by Quaternary faults to the W, SE, and NE (Fig. 4.7), is still active.

For the CFS, only the en-echelon arrangement suggests that it is marked by transcurrent kinematics.

Fig. 4.7 indicates the active Quaternary or seismogenic compressive and transversal structures recognized with confidence. Most of the Apennine onshore structures have not been indicated as active because the Quaternary deposits are absent or very thin and discontinuous, and the instrumental seismicity is sporadic or not significant. However, seismogenic activity cannot be excluded. This is the case of the Amandola structure (Fig. 4.1) associated with deep earthquakes (from 15 to 29 km) with compressive/transpressive focal mechanisms along high-angle N-S oriented nodal planes (e.g. the 2010 seismic sequence: ISIDe Working Group, 2007). Other active Apennine structures are probably present between the Amandola and the Sibillini thrust front, as suggested by the seismicity of the area.

Most of the offshore Apennine flower structures are also considered not active because they are covered by undeformed Quaternary deposits. Only parts of the Coastal Structure and of the Ancona and Osimo-Montemarciano-Mondolfo-Carrara-Gabicce flower structures (CFS2 in Pierantoni et al., 2019) are active, because they involve Quaternary deposits. Following Vannoli et al. (2015), the 1930 Senigallia earthquake main shock epicenter lay within these structures. Between Fano and Gabicce, the continuous and morphologically fresh cliff up to about a hundred meters high along the coast-line is very likely an expression of the recent or active sub-



vertical faults present at the core of the CFS2 flower structure. The cliff is present only in the Fano-Gabicce segment because sub-block A1 is higher than sub-block A2 (Figs. 4.1 and 4.7). Looking at the epicenters and focal mechanisms included in the CPTI (Rovida et al. 2022) catalog, Santini (2003) and Vannoli et al. (2015), the Ancona 1972 seismic sequence could be associated with the transversal W of Ancona fault system.

Within block B, the most important active Apennine structures are some parts of the Coastal Structure and the Amandola structure (Figs. 4.1 and 4.7). The Porto San Giorgio 1987 seismic sequence is associated with the Coastal structure (Costa et al., 2021; Battimelli et al., 2019).

Mazzoli et al., (2014; 2015) considered the ENE-WSW south of Conero promontory (SCFS in the present work) transversal fault to be a wrench fault linked to the Apennine compressive structures of the area. In our interpretation, it assumes the role of separating blocks of the outer Apennine sector with very different Plio-Quaternary evolution and kinematics.

Finally, also in the internal Marche-Umbria-Abruzzo Apennine sector, the transversal structures segmented the main active Apennine structures (Pizzi and Galadini, 2009; Pierantoni et al., 2017a) and border clusters of earthquakes during the development of recent and historical seismic sequences (L'Aquila 2009: Pierantoni et al., 2017a; Amatrice-Accumoli, 2016: Pierantoni et al., 2017b; Marche-Abruzzo 1703: Pierantoni et al., 2015). However, except for the transversal structures of the outer sector, most of these structures seem to have played a predominantly passive role during the recent and historical seismic sequences. The internal sector is separated from the external one by an active transtensive fault system (Pierantoni et al., 2019) or by a predominantly left lateral strike slip system (according to Elter et al., 2011), suggesting that the two Apennine sectors are evolving in a different way within the same Adriatic microplate.

## **4.6. Conclusions**

Some active transversal structures that are approximately NE-SW oriented, together with active Plio-Quaternary NW-SE structures, have been identified in the outer Apennine sector of the Marche Region, based on the literature and results of this and previous studies by the same authors. The dataset includes structural, morphotectonic, stratigraphic and seismological data.

The main results can be summarized as follows.

Four main transversal structures (CFS, MFFS, CUFS, SCFS) have been identified. These high angle and deeply rooted fault systems separate blocks (A and B) or sub-blocks (A1, A2 and A3)

of the outer Apennine sector, characterized by different recent structural and evolutionary characteristics. A fifth transversal structure was hypothesized immediately W of the Conero promontory. Recent and historical seismic sequences of low to medium energy occurred ( $M = 5.8$ ) along these structures, and they are characterized by hypocenters sometimes more than 20 km deep and are predominantly strike slip movement.

The most important of these transversal structure runs approximately ENE-WSW just south of the Conero promontory and separates the orocline outer Apennine sector in two blocks (A and B) with different structural characteristics and trends. The Conero promontory is an active push up wedge structure located at the hinge zone. The other transverse structures, instead, are located inside or at the edges of block A, allowing its fragmentation into lower rank blocks (A1, A2 and A3). All these structures have predominantly left-lateral kinematics.

Some of the Apennine structures (NW-SE trending) or portions of them are still active and seismogenic. The instrumental seismicity recorded along these structures is generally more superficial (maximum 10 km) except that near the important Amandola structure (16-30 km depth).

It can be concluded that the Apennine structures and parts of the transversal structures are activated independently. In fact, it can be posited that during the Pliocene-Quaternary age, the outer Apennine sector evolved in a different way than the internal one, considering that the four transversal structures of the outer sector seem to be interrupted toward the transtensive NW-SE trending faults delimiting the internal Apennine sector by the external one.

## **4.7. References**

- Argnani, A., Artoni, A., Ori, G., Roveri, M., (1991). L'avanfossa centro-adriatica: stili strutturali e sedimentazione. *Studi Geol Camerti* 1, 371-381.
- Argnani, A., Rovere, M., & Bonazzi, C. (2009). Tectonics of the Mattinata fault, offshore south Gargano (southern Adriatic Sea, Italy): Implications for active deformation and seismotectonics in the foreland of the Southern Apennines. *Geological Society of America Bulletin*, 121(9-10), 1421-1440.
- Artoni, A. (2003). Messinian events within the tectono-stratigraphic evolution of the Southern Laga Basin (Central Apennines, Italy). *BOLLETTINO-SOCIETA GEOLOGICA ITALIANA*, 122(3), 447-466.

- Artoni, A. (2013). The Pliocene-Pleistocene stratigraphic and tectonic evolution of the central sector of the Western Periadriatic Basin of Italy. *Marine and Petroleum Geology*, 42, 82-106.
- Bally, A. W. (1986). Balanced sections and seismic reflection profiles across the Central Apennines. *Mem. Soc. Geol. It.*, 35, 257-310.
- Barchi, M. (1998)a. The CROP 03 profile: a synthesis of results on deep structures of the Northern Apennines. *Mem. Soc. Geol. It.*, 52, 383-400.
- Barchi, M. R., De Feyter, A., Magnani, M. B., Minelli, G., Piali, G., & Sotera, B. M. (1998)b. The structural style of the Umbria-Marche fold and thrust belt. *Mem. Soc. Geol. It.*, 52(527), 38.
- Battimelli, E., Adinolfi, G. M., Amoroso, O., & Capuano, P. (2019). Seismic activity in the central adriatic offshore of Italy: a review of the 1987 ML 5 Porto San Giorgio earthquake. *Seismological Research Letters*, 90(5), 1889-1901.
- Bigi, G., Cosentino, D., Parotto, M., Sartori, R., & Scandone, P. (1992). Structural model of Italy. Scala 1: 500,000. CNR, Progetto Finalizzato Geodinamica, Sottoprogetto: Modello strutturale tridimensionale. *Quaderni della Ricerca Scientifica*, 114(3).
- Bigi, S., Calamita, F., Cello, G., Centamore, E., Deiana, G., Paltrinieri, W., & Ridolfi, M. (1995). Evoluzione messiniano-pliocenica del sistema catena-avanfossa nell'area marchigiano-abruzzese esterna. *Geodinamica e Tettonica Attiva del Sistema Tirreno-Appennino, Special Volume 1995/1*, 29-35.
- Bigi, S., Centamore, E., & Nisio, S. (1997). Elementi di tettonica quaternaria nell'area pedeappenninica marchigiano-abruzzese. *Il Quaternario*, 10(2), 359-362.
- Bigi, S., Calamita, F., Cello, G., Centamore, E., Deiana, G., Paltrinieri, W., & Ridolfi, M. (1999). Tectonics and sedimentation within a Messinian foredeep in the Central Apennines, Italy. *Journal of Petroleum Geology*, 22(1), 5-18.
- Bigi, S., Milli, S., Corrado, S., Casero, P., Aldega, L., Botti, F., ... & Cannata, D. (2009). Stratigraphy, structural setting and burial history of the Messinian Laga basin in the context of Apennine foreland basin system. *Journal of Mediterranean Earth Sciences*, 1, 61-84.
- Bigi, S., Casero, P., & Ciotoli, G. (2011). Seismic interpretation of the Laga basin; constraints on the structural setting and kinematics of the Central Apennines. *Journal of the Geological Society*, 168(1), 179-190.

- Bigi, S., Conti, A., Casero, P., Ruggiero, L., Recanati, R., & Lipparini, L. (2013). Geological model of the central Periadriatic basin (Apennines, Italy). *Marine and Petroleum Geology*, 42, 107-121.
- Boccaletti, M., Calamita, F., Deiana, G., Gelati, R., Massari, F., Moratti, G., & Lucchi, F. R. (1990). Migrating foredeep-thrust belt systems in the northern Apennines and southern Alps. *Palaeogeography, Palaeoclimatology, Palaeoecology*, 77(1), 3-14.
- Boncio, P., Lavecchia, G., & Pace, B. (2004). Defining a model of 3D seismogenic sources for Seismic Hazard Assessment applications: the case of central Apennines (Italy). *Journal of Seismology*, 8(3), 407-425.
- Brogi, A., & Fabbrini, L. (2009). Extensional and strike-slip tectonics across the Monte Amiata–Monte Cetona transect (Northern Apennines, Italy) and seismotectonic implications. *Tectonophysics*, 476(1-2), 195-209.
- Brogi, A., & Capezzuoli, E. (2014). Earthquake impact on fissure-ridge type travertine deposition. *Geological Magazine*, 151(6), 1135-1143.
- Brogi, A., Capezzuoli, E., Martini, I., Picozzi, M., & Sandrelli, F. (2014). Late Quaternary tectonics in the inner Northern Apennines (Siena Basin, southern Tuscany, Italy) and their seismotectonic implication. *Journal of Geodynamics*, 76, 25-45.
- Brogi, A., Capezzuoli, E., Kele, S., Baykara, M. O., & Shen, C. C. (2017). Key travertine tectofacies for neotectonics and palaeoseismicity reconstruction: effects of hydrothermal overpressured fluid injection. *Journal of the Geological Society*, 174(4), 679-699.
- Brogi, A., Liotta, D., Capezzuoli, E., Matera, P. F., Kele, S., Soligo, M., ... & Huntington, K. W. (2020). Travertine deposits constraining transfer zone neotectonics in geothermal areas: An example from the inner Northern Apennines (Bagno Vignoni-Val d'Orcia area, Italy). *Geothermics*, 85, 101763.
- Butler, R. W. H., Tavarnelli, E., and Grasso, M.: Structural inheritance in mountain belts: an Alpine-Apennine perspective, *J. Struct. Geol.*, 28, 1891–1892, <https://doi.org/10.1016/j.jsg.2006.09.006>, 2006.
- Calamita, F., Cello, G., Deiana, G., & Paltrinieri, W. (1994). Structural styles, chronology rates of deformation, and time-space relationships in the Umbria-Marche thrust system (central Apennines, Italy). *Tectonics*, 13(4), 873-881.

- Cantalamessa, G., Centamore, E., Chiocchini, U., Di Lorito, L., Leonelli, M., Micarelli, A., ... & Venanzini, D. (1980). Analisi dell'evoluzione tettonico-sedimentaria dei "bacini minori" torbiditici del Miocene-Medio-Superiore nell'Appennino Umbro-Marchigiano e Laziale-Abruzzese: 8) Il Bacino della tra il F.Fiastrone-T. Fiastrella ed il T. Fluvione. *Studi Geologici Camerti*, 6, 1980. <http://dx.doi.org/10.15165/studgeocam-1247>
- Cantalamessa, G., Centamore, E., Chiocchini, U., Di Lorito, L., Micarelli, A., & Potetti, M. (1983). I depositi terrigeni Neogenico-Quaternari affioranti tra il F.Potenza ed il F. Tronto. *Studi geologici camerti*, n. speciale, 1983. <http://dx.doi.org/10.15165/studgeocam-818>
- Cantalamessa G., Centamore E., Chiocchini U., Micarelli A., Potetti M., con la coll. di Di Lorito L. (1986). Il Miocene delle Marche. *Studi Geologici Camerti*: vol. spec. "La Geologia delle Marche", 35-55.
- Carrillo, E., Guinea, A., Casas, A., Rivero, L., Cox, N., and Vázquez-Taset, Y. M.: Tectono-sedimentary evolution of transverse extensional faults in a foreland basin: Response to changes in tectonic plate processes, *Basin Res.*, 32, 1388–1412, <https://doi.org/10.1111/bre.12434>, 2020.
- Carta Geologica d'Italia Scala 1:50:000, sheets no. 268, 269, 279, 280, 281, 282, 290, 291, 292, 293, 301, 302, 303, 304. Servizio Geologico d'Italia, 2009. Regione Marche.
- Carruba, S., Casnedi, R., Perotti, C. R., Tornaghi, M., & Bolis, G. (2006). Tectonic and sedimentary evolution of the Lower Pliocene Periadriatic foredeep in Central Italy. *International Journal of Earth Sciences*, 95(4), 665-683.
- Centamore, E., Adamoli, L., Berti, D., Bigi, G., Bigi, S., Casnedi, R., ... & Salvucci, R. (1991). Carta geologica dei bacini della Laga e del Cellino e dei rilievi carbonatici circostanti (Marche meridionali, Lazio nord-orientale, Abruzzo settentrionale).
- Centamore, E., Pambianchi, G. et al. (1991). Ambiente fisico delle Marche: geologia – geomorfologia – idrogeologia, Regione Marche, Giunta Regionale. *Studi Geologici Camerti*, 1991/2, 125–131.
- Centamore, E., Cantalamessa, G., Micarelli, A., Potetti, M., Berti, D., Bigi, S., & Ridolfi, M. (1991). Stratigrafia e analisi di facies dei depositi del Miocene e del Pliocene inferiore dell'avanfossa marchigiano-abruzzese e delle zone limitrofe. *Stud. Geol. Camerti* 1991, 11, 125–131.
- Centamore, E., & Rossi, D. (2009). Neogene-Quaternary tectonics and sedimentation in the Central Apennines. *Italian Journal of Geosciences*, 128(1), 73-88.

- Chiaraluce, L., Barchi, M., Collettini, C., Mirabella, F., & Pucci, S. (2005). Connecting seismically active normal faults with Quaternary geological structures in a complex extensional environment: The Colfiorito 1997 case history (northern Apennines, Italy). *Tectonics*, 24(1).
- Chicco, J. M., Pierantoni, P. P., Costa, M., & Invernizzi, C. (2019). Plio-Quaternary tectonics and possible implications for geothermal fluids in the Marche Region (Italy). *Tectonophysics*, 755, 21-34, <https://doi.org/10.1016/j.tecto.2019.02.005>.
- Coltorti, M., Farabollini, P., Gentili, B., & Pambianchi, G. (1996). Geomorphological evidence for anti-Apennine faults in the Umbro-Marchean Apennines and in the peri-Adriatic basin, Italy. *Geomorphology*, 15(1), 33-45
- Console, R., Peronaci, F., & Sonaglia, A. (1973). Relazione sui fenomeni sismici dell'Anconetano (1972). *Annali di Geofisica*, 26(4), 3-148.
- Conti, P., Cornamusini, G., & Carmignani, L. (2020). An outline of the geology of the Northern Apennines (Italy), with geological map at 1: 250,000 scale. *Italian Journal of Geosciences*, 139(2), 149-194.
- Costa, M. (2003). The buried, Apenninic arcs of the Po Plain and northern Adriatic Sea (Italy): a new model. *Bollettino Della Società Geologica Italiana*, 122, 3–23.
- Costa, M., Chicco, J. M., Invernizzi, C., Teloni, S., and Pierantoni, P.P. (2021). Plio–Quaternary Structural Evolution of the Outer Sector of the Marche Apennines South of the Conero Promontory, Italy. *Geosciences*, 11, 184, <https://doi.org/10.3390/geosciences11050184>
- Coward, M. P., De Donatis, M., Mazzoli, S., Paltrinieri, W., & Wezel, F. C. (1999). Frontal part of the northern Apennines fold and thrust belt in the Romagna-Marche area (Italy): Shallow and deep structural styles. *Tectonics*, 18(3), 559-574, <https://doi.org/10.1029/1999TC900003>.
- De Donatis, M., Invernizzi, C., Landuzzi, A., Mazzoli, S. & Potetti, M. 1998. CROP 03: structure of the Monte Calvo in Foglia–Adriatic Sea Segment. *Memorie della Società Geologica Italiana*, 52, 617–630.
- Delvaux, D. and Sperner, B. 2003. New aspects of tectonic stress inversion with reference to the TENSOR program. Geological Society, London, Special Publications, 212,75–100, <https://doi.org/10.1144/GSL.SP.2003.212.01.06>
- Di Bucci, D., & Mazzoli, S. (2002). Active tectonics of the Northern Apennines and Adriatic geodynamics: new data and a discussion. *Journal of Geodynamics*, 34(5), 687-707

- Di Bucci, D., Burrato, P., Vannoli, P., & Valensise, G. (2010). Tectonic evidence for the ongoing Africa-Eurasia convergence in central Mediterranean foreland areas: A journey among long-lived shear zones, large earthquakes, and elusive fault motions. *Journal of Geophysical Research: Solid Earth*, 115(B12)
- DISS Working Group, 2021. Database of Individual Seismogenic Sources (DISS). Version 3.3.0: A compilation of potential sources for earthquakes larger than M 5.5 in Italy and surrounding areas. Istituto Nazionale di Geofisica e Vulcanologia. <http://diss.rm.ingv.it/diss/>.
- Dramis, F., Pambianchi, G., Nesci, O., & Consoli, M. 1991. Il ruolo di elementi strutturali trasversali nell'evoluzione tettonico-sedimentaria e geomorfologica della regione marchigiana.
- Duvall, M. J., Waldron, J. W., Godin, L., & Najman, Y. (2020). Active strike-slip faults and an outer frontal thrust in the Himalayan foreland basin. *Proceedings of the National Academy of Sciences*, 117(30), 17615-17621.
- Elter, F. M., Piero, E., Claudio, E., Elena, E., Katharina, K. R., Matteo, P., & Stefano, S. (2011). Strike-slip geometry inferred from the seismicity of the Northern-Central Apennines (Italy). *Journal of Geodynamics*, 52(5), 379-388.
- Fantoni, R., & Franciosi, R. (2010). Tectono-sedimentary setting of the Po Plain and Adriatic foreland. *Rendiconti Lincei*, 21(1), 197-209. <https://doi.org/10.1007/s12210-010-0102-4>
- Frepoli, A., & Amato, A. (1997). Contemporaneous extension and compression in the Northern Apennines from earthquake fault-plane solutions. *Geophysical Journal International*, 129(2), 368-388.
- Ghelardoni, R. (1965). Osservazioni sulla tettonica trasversale dell'Appennino settentrionale. *Arti grafiche Pacini Mariotti*.
- Ghielmi, M., Minervini, M., Nini, C., Rogledi, S., Rossi, M., & Vignolo, A. (2010). Sedimentary and tectonic evolution in the eastern Po-Plain and northern Adriatic Sea area from Messinian to Middle Pleistocene (Italy). *Rendiconti Lincei*, 21(1), 131-166.
- Ghielmi, M., Minervini, M., Nini, C., Rogledi, S., & Rossi, M. (2013). Late Miocene–Middle Pleistocene sequences in the Po Plain–Northern Adriatic Sea (Italy): the stratigraphic record of modification phases affecting a complex foreland basin. *Marine and Petroleum Geology*, 42, 50-81.
- Ghisetti, F., & Vezzani, L. (1998). Segmentation and tectonic evolution of the Abruzzi-Molise thrust belt (central Apennines, Italy). In *Annales Tectonicae* (Vol. 12, No. 1/2, pp. 97-112).

- Heidbach, O., Custodio, C., Kingdon, A., Mariucci, M. T., Montone, P., Müller, B., ... & Ziegler, M. (2016). Stress map of the Mediterranean and Central Europe 2016.
- INGV (2015). Catalogo Parametrico dei Terremoti Italiani. I terremoti del '900: I terremoti riminesi del 1916. INGV, Rome.
- Invernizzi, C. (1992). Relazioni tra Costruzione Della Catena e Migrazione Dell'avanfossa Nell'area Marchigiana Esterna: Alcune Osservazioni. *Stud. Geol. Camerti* 1992, 12, 71–78.
- Invernizzi, C., Landuzzi, A., Negri, A. & Potetti, M. (1995). Stratigrafie ed evoluzione tettonico-sedimentaria mio-pliocenica dell'area pesarese tra il F. Foglia e il F. Metauro. *Studi Geologici Camerti*, 1995/1, 451–463.
- ISIDE Working Group. (2007). Italian Seismological Instrumental and Parametric Database (ISIDE). Istituto Nazionale di Geofisica e Vulcanologia (INGV). <https://doi.org/10.13127/ISIDE>.
- Locardi, E. (1988). The origin of the Apenninic arcs. *Tectonophysics*, 146(1-4), 105-123.
- Mantovani, E., Viti, M., Babbucci, D., Tamburelli, C., & Cenni, N. (2017). Possible location of the next major earthquakes in the Northern Apennines: present key role of the Romagna-Marche-Umbria wedge. *International Journal of Geosciences*, 8(11), 1301.
- Marini, M., Milli, S., Ravnås, R., & Moscatelli, M. (2015). A comparative study of confined vs. semi-confined turbidite lobes from the Lower Messinian Laga Basin (Central Apennines, Italy): implications for assessment of reservoir architecture. *Marine and Petroleum Geology*, 63, 142-165.
- Materazzi, M., Bufalini, M., Dramis, F., Pambianchi, G., Gentili, B., & Di Leo, M. (2022). Active tectonics and paleoseismicity of a transverse lineament in the Fabriano valley, Umbria-Marche Apennine (central Italy). *International Journal of Earth Sciences*, 1-11.
- Mazzoli, S., Macchiavelli, C., & Ascione, A. (2014). The 2013 Marche offshore earthquakes: new insights into the active tectonic setting of the outer northern Apennines. *Journal of the Geological Society*, 171(4), 457-460.
- Mazzoli, S., Santini, S., Macchiavelli, C., & Ascione, A. (2015). Active tectonics of the outer northern Apennines: Adriatic vs. Po Plain seismicity and stress fields. *Journal of Geodynamics*, 84, 62-76.



- Meletti, C., Montaldo, V., Stucchi, M., Martinelli, F. (2006). Database della pericolosità sismica MPS04. Istituto Nazionale di Geofisica e Vulcanologia (INGV). DOI: 10.13127/SH/MPS04/DB.
- Milli, S., Moscatelli, M., Stanzione, O., & Falcini, F. (2007). Sedimentology and physical stratigraphy of the Messinian turbidite deposits of the Laga basin (central Apennines, Italy). *BOLLETTINO-SOCIETA GEOLOGICA ITALIANA*, 126(2), 255.
- Milli, S., Cannata, D., Marini, M., & Moscatelli, M. (2013). Facies and geometries of lower Messinian Laga Basin turbidite deposits (central Apennines, Italy). *Journal of Mediterranean Earth Sciences Special Issue*, 179, 225.
- Mirabella, F., Braun, T., Brogi, A., & Capezzuoli, E. (2022). Pliocene–Quaternary seismogenic faults in the inner Northern Apennines (Valdelsa Basin, southern Tuscany) and their role in controlling the local seismicity. *Geological Magazine*, 159(6), 853-872
- Nanni, T., & Vivalda, P. (1987). Influenza della tettonica trasversale sulla morfogenesi delle pianure alluvionali marchigiane. *Geogr. Fis. Din. Quat*, 10, 180-192
- Ori, G. G., Roveri, M., Vannoni, F., Allen, P. A., & Homewood, P. (1986). Plio-Pleistocene sedimentation in the Apenninic-Adriatic foredeep (Central Adriatic Sea, Italy). In *Foreland basins* (Vol. 8, pp. 183-198). IAS Special Publication.
- Ori, G. G., Serafini, G., Visentin, C., Ricci Lucchi, F., Casnedi, R., Colalongo, M. L., & Mosna, S. (1991, May). The Plio-Pleistocene Adriatic foredeep (Marche and Abruzzo, Italy)—an integrated approach to surface and subsurface geology. In *Third Conference of European Association of Petroleum Geology, Adriatic Foredeep Field Trip Guidebook*, Florence, Italy. Milano, Agip SpA (pp. 1-85).
- Pace, B., Boncio, P., & Lavecchia, G. (2002). The 1984 Abruzzo earthquake (Italy): an example of seismogenic process controlled by interaction between differently oriented synkinematic faults. *Tectonophysics*, 350(3), 237-254.
- Pascucci, V., Martini, I. P., Sagri, M., Sandrelli, F., & Nichols, G. (2007). Effects of transverse structural lineaments on the Neogene-Quaternary basins of Tuscany (inner Northern Apennines, Italy). *Sedimentary processes, environments and basins: a tribute to Peter Friend*, 38, 155-182.
- Pierantoni, P., Deiana, G., & Galdenzi, S. (2013). Stratigraphic and structural features of the Sibillini mountains (Umbria-Marche Apennines, Italy). *Italian Journal of Geosciences*, 132(3), 497-520.

- Pierantoni, P.P., Centamore, E., Costa, M. (2015). Comparison among some seismotectonic characteristics of the main historical earthquakes in the Central Apennines (Italy). *Miscellanea INGV*, Vol. 27, 384-385.
- Pierantoni, P.P.; Centamore, E.; Costa, M. (2017a). Geological and Seismological data Review of the 2009 L'Aquila Seismic Sequence (Central Apennines, Italy): Deep Seated Seismogenic Structures and Seismic Hazard. *Ital. J. Eng. Geol. Environ.* 17, 5–40
- Pierantoni, P.P.; Centamore, E.; Chicco, J., Costa, M. (2017b). Early seismogenic faults of the 2016 Accumoli-Amatrice seismic sequence (Central Apennines, Italy). *EGU 2017*
- Pierantoni, P.P.; Chicco, J.; Costa, M.; Invernizzi, C. (2019). Plio-Quaternary Transpressive Tectonics: A Key Factor in the Structural Evolution of the Outer Apennine–Adriatic System, Italy. *J. Geol. Soc. Lond.* 2019, 176, 1273–1283.
- Pizzi, A., & Galadini, F. (2009). Pre-existing cross-structures and active fault segmentation in the northern-central Apennines (Italy). *Tectonophysics*, 476(1-2), 304-319.
- Pizzi, A., Di Domenica, A., Gallovič, F., Luzi, L., & Puglia, R. (2017). Fault segmentation as constraint to the occurrence of the main shocks of the 2016 Central Italy seismic sequence. *Tectonics*, 36(11), 2370-2387.
- Riguzzi, F., Tertulliani, A., & Gasparini, C. (1989). Study of the seismic sequence of Porto San Giorgio (Marche)–3 July 1987. *Il Nuovo Cimento C*, 12(4), 453-466.
- Rovida A., Locati M., Camassi R., Lolli B., Gasperini P., Antonucci A. (2022). Italian Parametric Earthquake Catalogue (CPTI15), version 4.0. Istituto Nazionale di Geofisica e Vulcanologia (INGV).
- Santini, S. (2003). A note on Northern Marche seismicity: new focal mechanisms and seismological evidence. *Annals of Geophysics*, 46(4), 725731-725731.
- Santini, S., & Martellini, A. (2006). Focal mechanisms and tectonic seismological evidence in the Pesaro and Urbino province. In *ADRIA 2006-International Congress on the Adriatic Area Adria*. Adria 2006 Abstract-Arti Grafiche Editoriali, Urbino (Italy). Santini S., Saggese F., Megna A., Mazzoli S. A note on central-northern Marche seismicity: new focal mechanisms for events recorded in years 2003-2009. *Boll. Geof. Teor, e Appl.* 2011. 52 (4), 639-649.
- Santini, S., Saggese, F., Megna, A., & Mazzoli, S. (2011). A note on central-northern Marche seismicity: new focal mechanisms for events recorded in years 2003-2009. *Bollettino di Geofisica Teorica ed Applicata*, 52(4).

- Scisciani, V., & Calamita, F. (2009). Active intraplate deformation within Adria: Examples from the Adriatic region. *Tectonophysics*, 476(1-2), 57-72. <http://dx.doi.org/10.1016/j.tecto.2008.10.030>.
- Scisciani, V., Agostini, S., Calamita, F., Pace, P., Cilli, A., Giori, I., & Paltrinieri, W. (2014). Positive inversion tectonics in foreland fold-and-thrust belts: a reappraisal of the Umbria–Marche Northern Apennines (Central Italy) by integrating geological and geophysical data. *Tectonophysics*, 637, 218-237. <https://doi.org/10.1016/j.tecto.2014.10.010>.
- Signorini, R. (1935). Linee tettoniche trasversali nell'Appennino settentrionale. Giovanni Bardi.
- Sippel, J., Scheck-Wenderoth, M., Reicherter, K. and Mazur, S. (2009). Paleostress states at the south-western margin of the Central European Basin System—application of fault-slip analysis to unravel a polyphase deformation pattern. *Tectonophysics*, 470, 129–146, <https://doi.org/10.1016/j.tecto.2008.04.010>.
- Stucchi, M., Meletti, C., Montaldo, V., Crowley, H., Calvi, G. M., & Boschi, E. (2011). Seismic hazard assessment (2003–2009) for the Italian building code. *Bulletin of the Seismological Society of America*, 101(4), 1885-1911.
- Tavarnelli, E., Decandia, F. A., Renda, P., Tramutoli, M., Gueguen, E., & Alberti, M. (2001). Repeated reactivation in the Apennine-Maghrebide system, Italy: a possible example of fault-zone weakening?. *Geological Society, London, Special Publications*, 186(1), 273-286.
- Tavarnelli, E., Butler, R. W. H., Decandia, F. A., Calamita, F., Grasso, M., Alvarez, W., ... & D'offizi, S. (2004). Implications of fault reactivation and structural inheritance in the Cenozoic tectonic evolution of Italy. *The Geology of Italy, Special*, 1, 209-222.
- Turner, F. J. (1953). Nature and dynamic interpretation of deformation lamellae in calcite of three marbles. *American Journal of Science*, 251(4), 276-298. <https://doi.org/10.2475/ajs.251.4.276>
- Valensise, G., & Pantatosti, D. (2001). Database of potential sources for earthquakes larger than M 5.5 in Italy. Version 2.0-2001. *Annali di Geofisica*, 44.
- Vannoli, P., Burrato, P., & Valensise, G. (2015). The seismotectonics of the Po Plain (northern Italy): Tectonic diversity in a blind faulting domain. *Pure and Applied Geophysics*, 172(5), 1105-1142.
- Vannoli, P., Vannucci, G., Bernardi, F., Palombo, B., & Ferrari, G. (2015). The source of the 30 October 1930 M w 5.8 Senigallia (Central Italy) earthquake: A convergent solution from

instrumental, macroseismic, and geological data. *Bulletin of the Seismological Society of America*, 105(3), 1548-1561.

Vannoli, P., Bernardi, F., Palombo, B., Vannucci, G., Console, R., & Ferrari, G. (2016). New constraints shed light on strike-slip faulting beneath the southern Apennines (Italy): The 21 August 1962 Irpinia multiple earthquake. *Tectonophysics*, 691, 375-384.

Kastelic, V., Vannoli, P., Burrato, P., Fracassi, U., Tiberti, M. M., & Valensise, G. (2013). Seismogenic sources in the Adriatic Domain. *Marine and Petroleum Geology*, 42, 191-213.

ViDEPI Project. (2012). Visibility of petroleum exploration data in Italy. Ministry for Economic Development DGRME—Italian Geological Society—Assomineraria. (Accessed November 2021).

Zampieri, D., Vannoli, P., & Burrato, P. (2021). Geodynamic and seismotectonic model of a long-lived transverse structure: The Schio-Vicenza Fault System (NE Italy). *Solid Earth*, 12(8), 1967-1986.

## 5. MORPHOSTRUCTURAL EVIDENCE OF ACTIVE ALONG-STRIKE SEGMENTATION OF THE UMBRIA-MARCHE APENNINES, ITALY

Teloni S.<sup>1</sup>, Valente E.<sup>2</sup>, Ascione, A.<sup>2</sup>, Mazzoli S.<sup>1</sup>, Pierantoni P. P.<sup>1</sup>, Invernizzi C.<sup>1</sup>

<sup>1</sup> *School of Science and Technology – Geology Division, University of Camerino, Via Gentile III da Varano, 62032 Camerino, MC, Italy*

<sup>2</sup> *Department of Earth, Environment and Resources Sciences - DiSTAR, University of Naples Federico II, Complesso Universitario Monte Sant'Angelo, via Vicinale Cupa Cintia 21, 80126, Naples, Italy*

### Abstract

During the last millennium, several moderate to strong earthquakes occurred in the Umbria-Marche Apennines and Marche foredeep making this region one of the most seismically active areas of Italy. In addition, the lack of reliable instrumental data for strong seismic events and the poor exposures of fault planes affecting Quaternary sediments make the characterization of active seismogenic structures problematic. Seismic activity is mainly clustered to the south and such a difference in spatial distribution of seismic activity should be reflected in topography and river network features. To tackle this issue, a morphometry study of the Umbria-Marche Apennines was carried out. Topography analysis includes the creation of seven swath profiles (20 km in width) and the analysis of the elevation map and maps derived from it (i.e., maximum, minimum, mean and relief maps). River network analysis includes river long profile and transformed ( $\chi$ ) long profile coupled with slope/area analysis. The former allowed the location of knickpoints/knickzones, whereas the latter allowed the spatial distribution of the Ksn (normalized steepness) index to be deciphered. Combined data from topography and river network suggest a difference between the northern and the southern sector of the Umbria-Marche Apennines. In fact, the southward increase in mean and minimum elevations as well as in local relief, the abundance of non-lithology controlled knickpoints and high to very high Ksn values, suggest the presence of a locus of enhanced vertical motion (i.e., surface uplift) in the south. Here, the largest historical earthquakes and the strongest instrumental seismicity also occur, thus suggesting active tectonics is more intense in this area of stronger uplift. The results of our tectonic geomorphology analysis are consistent with published evidence of along-strike segmentation of the fold and thrust belt. Furthermore, overall data suggest that transversal faults mapped by seismic interpretation in the foredeep area are likely to also compartmentalize the axial zone of the chain.

**Keywords:** Active fault; Tectonic geomorphology, river long profile, knickpoint, swath profile

## 5.1. Introduction

The Umbria-Marche Apennines and foothills (hereinafter UMAF) is the locus of moderate to high tectonic activity, as shown by the occurrence of several historical strong earthquakes (e.g. Mw 6.92, 1703 Valnerina earthquake; Mw 6.17, 1741 Fabriano earthquake; Mw 6.51, 1781 Cagli earthquake and the Mw 6.18, 1799 Camerino earthquake - Castelli & Monachesi, 2001; Monachesi et al., 1991; Rovida et al., 2022; Stucchi et al., 1991), together with recent seismic sequences in central Italy (e.g. the 2016-2017 Amatrice-Visso-Norcia seismic sequence with maximum magnitude of 6.5 - Civico et al., 2018; EMERGEO working group, 2016). Earthquakes are mainly clustered to the south of the UMAF but the lack of reliable instrumental data of strong historical seismic events and the obliterated field evidence of faulting at surface, make the characterization of active seismogenic structures problematic. Despite such difficulties, a morphotectonic approach would highlight differences between the northern and southern sectors of the UMAF that could be correlated with the uneven spatial distribution of tectonic activity. Some analysis has been already carried out by combining geomorphological field data with analysis of alluvial terraces and other morphotectonic indicators (Ciccacci et al. 1985; Della Seta et al. 2008; Dramis, 1992; Gentili et al., 2017; Mayer et al., 2003), but a regional scale morphotectonic analysis has never been performed. In this context, topography and river network features may provide fundamental data to the identification and characterization of areas affected by recent and active tectonic deformation (Bishop, 2007; Bull, 2008; Bull & McFadden, 1977; Burbank & Anderson, 2011; Keller & Pinter, 2002). Regarding the UMAF, topography is characterized by the occurrence of two ridges carved in carbonate units, the Marche ridge to the east and the Umbria-Marche ridge to the west, which are separated by a low relief area where “soft” arenaceous units crop out and that tend to join towards the south. The river network includes SW-NE and NW-SE river segments, the former cutting across the Apennine chain and foothills, while the latter are parallel to the main tectonic depressions. Previous studies on river network features at the drainage basin scale have highlighted the role of local tectonic structure (SW-NE and NW-SE trending) in river organization, controlling the stream flow directions (Di Bucci et al., 2003; Mayer et al., 2003; Molin & Fubelli 2005; Nesci et al., 2012; Wegmann & Pazzaglia, 2009).

In recent years, GIS and MATLAB based analysis on digital elevation models have been largely diffused in morphotectonic analysis (Schwanghart & Kuhn, 2010; Schwanghart & Scherler, 2014; Whipple et al., 2007; Lanari et al. 2020). More in detail, swath profiles, ksn index, river long profile and chi plots have been used to perform morphotectonic analysis, distinguishing active tectonic perturbations from other processes (Basilici et al., 2020; Eizenhöfer et al., 2019:

Forte et al., 2014; Gallen & Wegmann, 2017; Kirby & Whipple, 2001; Pazzaglia & Fisher, 2022).

In this paper, a GIS-aided large scale morphotectonic analysis of the topography and river network features has been applied to verify landscape response to uneven distribution of seismic activity. Results have been compared with available geological, seismological and structural data and may provide new constraints for earthquake hazard assessment in this sector of the northern Apennines.

## **5.2. Geological and morphostructural setting**

The study area is located in the central–eastern sector of the Italian peninsula, within the UMAF, which forms part of the peri-Mediterranean Alpine orogenic belt (inset in Figure 5.1).

The Apennines are an arcuate, mostly NW-SE striking fold and thrust belt (Calamita et al., 1994). It evolved during the Neogene, in the frame of Africa-Eurasia plate convergence since the Late Cretaceous (Dewey et al., 1989; Coward et al., 1999; Mazzoli & Helman, 1994; Turco et al., 2021).

The evolution of the studied area can be summarized in three main stages:

- Pre-orogenic stage (Trias-Paleogene): the extension related to the Tethyan rifting gradually affected the Adria paleo-continental margin. During the Early Jurassic, the dissection of the former carbonate-platform involved the development of a series of horsts and grabens/half grabens, accompanied by transversal oblique-slip faults segmenting the extensional system (Centamore et al., 2002; Centamore & Rossi, 2009; Lavecchia et al., 1988; Mazzoli et al., 2005; Pierantoni et al., 2013; Scisciani et al., 2014). The extensional phase and related subsidence allowed the deposition of the well-bedded carbonate-marly Umbria-Marche sedimentary succession.
- Syn-orogenic stage (Miocene-Pliocene): the various sectors of the area were progressively involved in the fold and thrust belt from west to east, as shown by foredeep siliciclastic deposits. The basement is locally involved in the thrust system and the oblique faults are reactivated as transfer faults across the Apennines. During the shortening stages, transversal faults bounded crustal blocks characterized by different tectonic movements (Calamita et al., 1994; Calamita & Pizzi, 1994).
- Post-orogenic stage: a general eastward migration of the thrust front toward the foreland characterized the Pliocene to present time (Barchi et al., 2012; Patacca et al., 1990), while

extensional processes involved the hinterland of the Umbria-Marche Apennines generating NW-SE-striking crustal extensional faults (Barchi & Mirabella, 2009; Dewey, 1988; Doglioni, 1995; Keller et al., 1994). Extensional basins host mainly continental deposits (e.g. Gubbio, Norcia and Colfiorito basins. Bartole, 1995; Brogi et al., 2014; Cipollari et al., 1999; Cosentino et al., 2017; Doglioni et al., 1998; Galadini & Messina, 2001; Mancini et al., 2005; Martini & Sagri, 1993; Patacca et al., 1990).

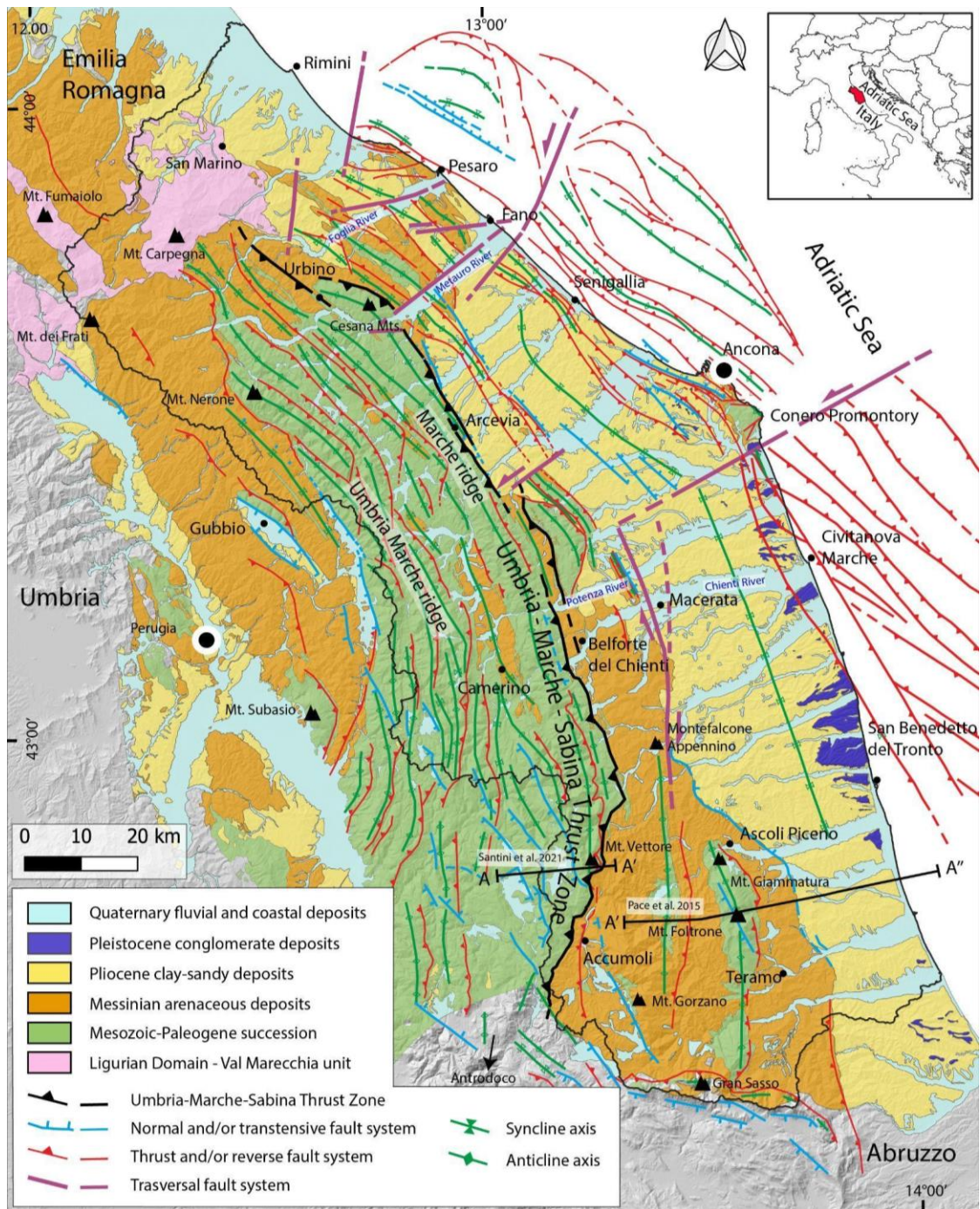


Fig. 5.1 - Structural map of Umbria-Marche Apennines and foothill (modified from Pierantoni et al., 2019 and Costa et al. 2021). The black lines A-A' and A'-A'' represent the geological cross-section traces of figure 5.2.



The Neogene-Quaternary stratigraphic and structural evolution influenced the study area developing two main morpho-structural sectors. The western-inner sector is characterized by two NW-SE carbonate mountain ridges: the Umbria-Marche ridge and the Marche ridge separated by a syncline filled by Upper Miocene terrigenous deposits (Fig. 5.1). This sector is highly deformed and largely uplifted and involves the Mesozoic-Paleogene Umbria-Marche succession (a calcareous and marly succession with thickness ranging between 1000 and 2000 m). The eastern-outer sector is less deformed and shows minor structures at surface mainly involving the Messinian siliciclastic succession (ranging from a few hundred meters to the north to 3000 m to the south) and marine to continental Plio-Pleistocene terrigenous deposits extensively outcropping in the Marche foothills (Fig. 5.1).

The main fault systems affecting both sectors are NW-SE to NNW-SSE striking and include the NNE-SSW inherited transversal systems (Calamita et al., 1994). The axial zone of the chain includes 15-20 km long en-echelon normal fault segments.

The Mesozoic-Paleogene Umbria-Marche and Marche carbonate ridges, characterized by the typical arcuate shape, extends from the Foglia river valley to the north and the Sibillini-Sabina Mts. to the south. The Apennine Mountain front is bounded eastward by the Umbria-Marche-Sabina Thrust Zone (UMSTZ), a major thrust fault consisting of several WNW-ESE to NE-SW right-stepping en-échelon segments. Generally, the UMSTZ is composed of two main thrust portions with an overlap zone 10 to 20 km wide between the Potenza and Chienti River Valleys. The northern one has a general NW-SE trend, changing to WNW-ESE north of the Metauro river valley (Fig. 5.1). The “Belforte-Urbino” segment represents the northern portion of the thrust zone. It is largely buried and extends from the Chienti river valley, to the south, to the Foglia river valley to the north. The “Belforte-Urbino” Thrust has mainly a NW-SE trend. In the northern part, from the Cesana Mts. to Arcevia, it is imaged in two seismic profiles (including the CROP03 deep seismic reflection profile; Barchi et al., 1998; Calamita, 1991). It shows offsets ranging from 2 km to to 4.5 km (Mazzoli et al. 2005). The thrust activity in this section is attributable to the late Messinian (Deiana et al., 2003). The southern portion extends from the Potenza river valley to the north to Olevano Romano to the south. The maximum displacements along the UMSTZ occur along the Monte Vettore - Accumoli segment with values of about 10 km (Mazzoli et al. 2005; Fig. 5.2). Thrust activity can be referred to the late Messinian (post-evaporite) time, locally continuing during the Pliocene.

The fold-and-thrust system involves the Jurassic–Neogene pre-orogenic calcareous-marly succession overlaid by Neogene-Quaternary syn-orogenic foredeep siliciclastic deposits. Also,

the Triassic evaporites (Burano Anidrites Fm.), which represent the main detachment, and the crystalline basement of the succession are involved in the contractional deformation, and the thick-skinned tectonic style is also highlighted by the interpretation of the CROP 03 seismic reflection profile provided by Barchi et al. (1998).

The carbonate mountain front overthrust the Neogene-Quaternary foredeep succession by gently W-SW dipping (10–20°) thrust system (Lavecchia, 1985; Pierantoni et al., 2013). As mentioned above, the innermost sector of the Apennine fold and thrust belt is characterized by the presence of NW-SE post-orogenic and still active Quaternary normal faults cross-cutting the compressional structures of the area. The normal fault system is responsible for the formation of large intermontane basins and hence for the recent central Italy seismic sequences recorded in the last decades. On the contrary, within the foredeep, the thrust system is generally buried, forming a detachment at the base of the Laga Fm.

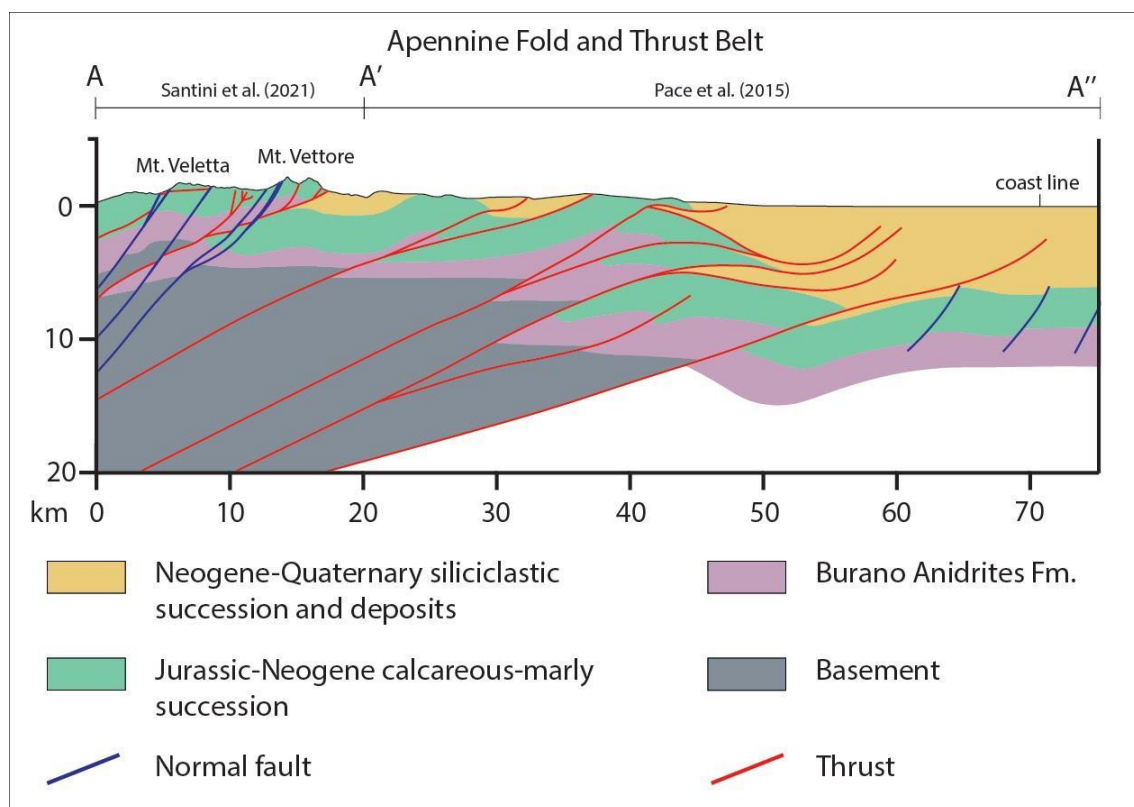


Fig. 5.2 - WSW-ENE regional geological section across the Umbria-Marche Apennines based on the Mt. Vettore section by Mazzoli et al., 2005, modified, merged with the section by Pace et al., 2015 for the outer zone (section traces in fig. 1).

The simplified geological map in figure 5.3 was modified after the 1:250.000 geologic map of the northern Apennines (Conti et al., 2020). In the map of Fig. 5.3, some of the outcropping lithostratigraphic units have been grouped according to their similar lithological characteristics ending with eleven rock categories.

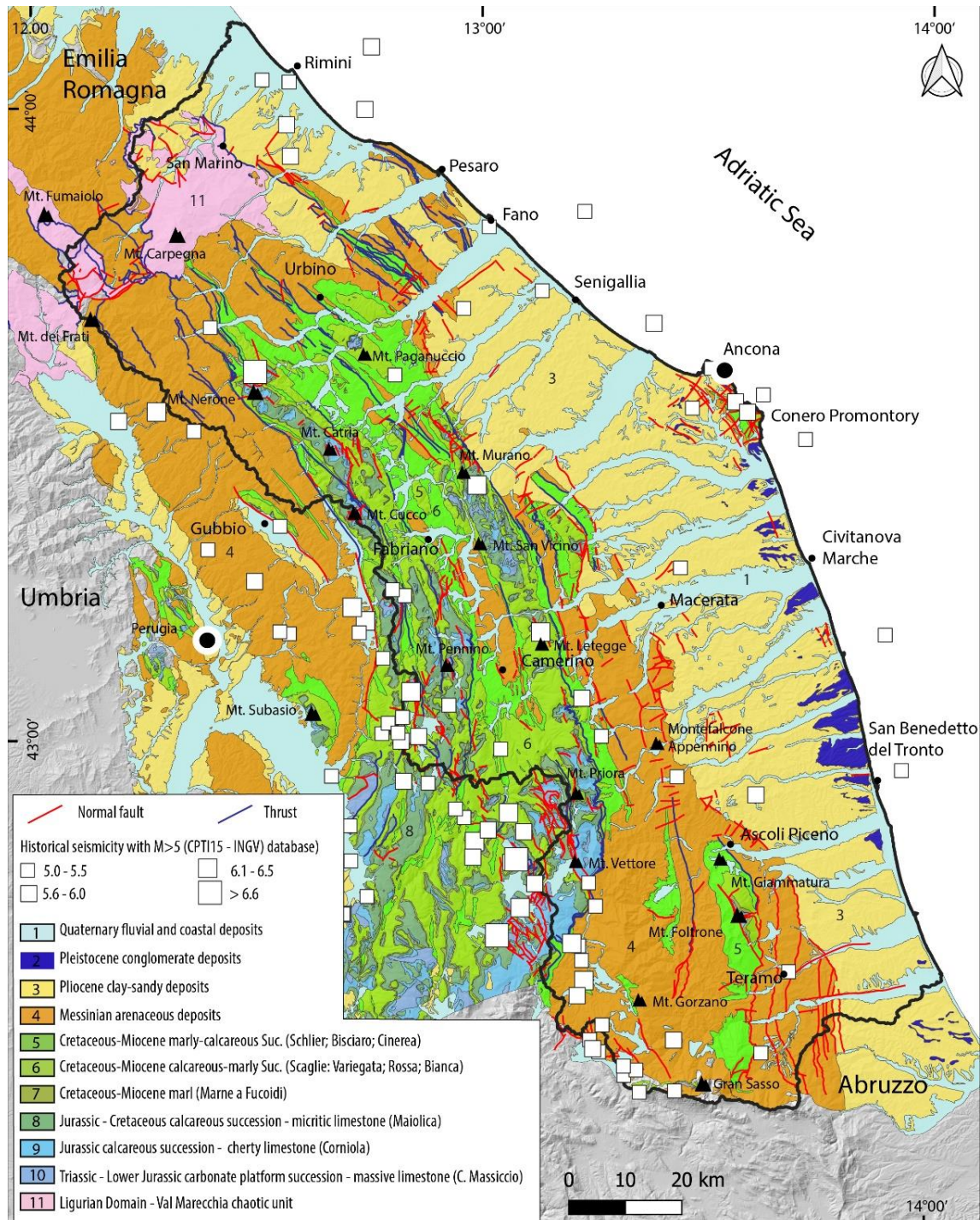


Fig. 5.3 - Geological sketch of Umbria-Marche Apennines and foothill (modified from Conti et al., 2020). The geologic units were grouped into 11 rock categories according to their qualitative resistance to erosion. White squares represent the historical seismic events with  $M > 5$  (Rovida et al., 2022).

The Calcare Massiccio Fm. (carbonatic platform limestone , Trias-Lower Jurassic in age) is present at the base of the stratigraphic succession and represents the oldest outcropping formation within the study area. The Jurassic-Cretaceous series is mainly composed of pelagic micritic limestones (Corniola Fm. and Maiolica Fm.), whereas moving upward, the deposition of the Marne a Fucoidi Fm. establishes the end of the calcareous sedimentation and the inception of marly sedimentation throughout. Marly sedimentation continues during the Cretaceous to Eocene, with the deposition of Scaglia Bianca, Scaglia Rossa and Scaglia Variegata Fms. The pelagic calcareous sedimentation ends with the deposition of the Scaglia Cinerea Fm. (Late Eocene- Early Miocene), consisting of alternating marly limestones and marls. Since the Miocene, hemipelagic deposits consisting of alternating marly limestones, marls and clays are represented by the Bisciario Fm. (Aquitainian p.p.-Burdigalian p.p.) and Schlier Fm (alternating marls and clays, with locally marly limestones and calcarenites). The eastward migration of thrust fronts toward the foreland influenced the Umbria-Marche domain developing the Messinian turbiditic foredeep in the Marche foothills (Ori et al., 1991; Ricci Lucchi, 1986). On the eastern side, the contact between calcareous-marly succession and Plio-Quaternary sequences displays a straight geometry, locally bordered by high angle faults (Deiana et al., 2002). Eastward and along the coastline south to the Conero Promontory, the Pleistocene deposits composed of littoral sands and conglomerates crop out extensively (Bigi et al., 1997; Cantalamessa & di Celma, 2004; Cantalamessa et al. 1986). Allochthonous tectonic units belonging to the Ligurian domain are present just north to the study area (northern Marche – south-eastern Romagna) with the Val Marecchia “chaotic” unit (Cornamusini et al., 2017; Veneri, 1986).

A dense river network, which consists of NE-SW oriented, NE flowing main trunks and related tributaries, dissects the orogenic belt through a couple of kilometers to tens kilometers spaced transverse valleys. Most of the NE-SW trending rivers cut the anticline carbonate ridges forming very deeply incised gorges, and locally follow the syncline structures (e.g., the upper Esino Valley) for several kilometers. The long-term evolution of the river network mainly consisted in superimposition and stream-piracy phenomena even if local antecedence cannot be ruled out (Mayer et al., 2003). Valleys evolution in the foothills proceeded through different morphodynamic processes described in detail by Nesci & Savelli (2003). In this area, evidence of recent tectonic activity has been proved by Della Seta et al. (2008) by combination of morphotectonic analysis of topography and river network with field survey in the area between the Tronto, Vibrata and the Salinello river valleys (respectively numbers 14, 15 and 16 in Figs. 5.5, 5.8, 5.9 and 5.10).

### 5.3. Seismicity

The Umbria-Marche study area (Fig. 5.1) is the locus of moderate to strong earthquakes underlined by instrumental baseline seismicity and highlighted by historical seismic events that occurred in the last centuries.

In order to analyze the Umbria-Marche seismicity distribution, the instrumental seismic data recorded since 1985 from the Italian Seismological Instrumental and Parametric Data-Base (<http://terremoti.ingv.it/iside> ISIDe -INGV, last access on 21 February 2022) and the re-localized earthquakes by INGV Ancona (Cattaneo et al., 2017) of the study area have been downloaded and merged together in a new database. In this regard, a dataset of 3931 earthquakes data have been selected among more than 70.000 events upon the horizontal error ( $erh < 2.5$  km), vertical error ( $erz < 2.5$  km) and number of phases of the seismogram ( $> 8$ ), which are considered reliable to avoid uncertainties due to epicenters position. Furthermore, historical earthquakes with  $M > 5.0$  by the Parametric Catalog of Italian Earthquakes – CPTI15-DBMI15 (Rovida et al., 2022) have been considered for this study to compare major seismic events since 1000 a.d. with the instrumental seismicity and morphotectonic anomalies (Fig. 5.3). In this dataset the 2016-17 Amatrice-Visso-Norcia seismic events and the 1997 Colfiorito seismic sequence are also present and differentiated from the baseline seismicity (Fig. 5.4) through the ZMAP decluster algorithm (Wiemer, 2001).

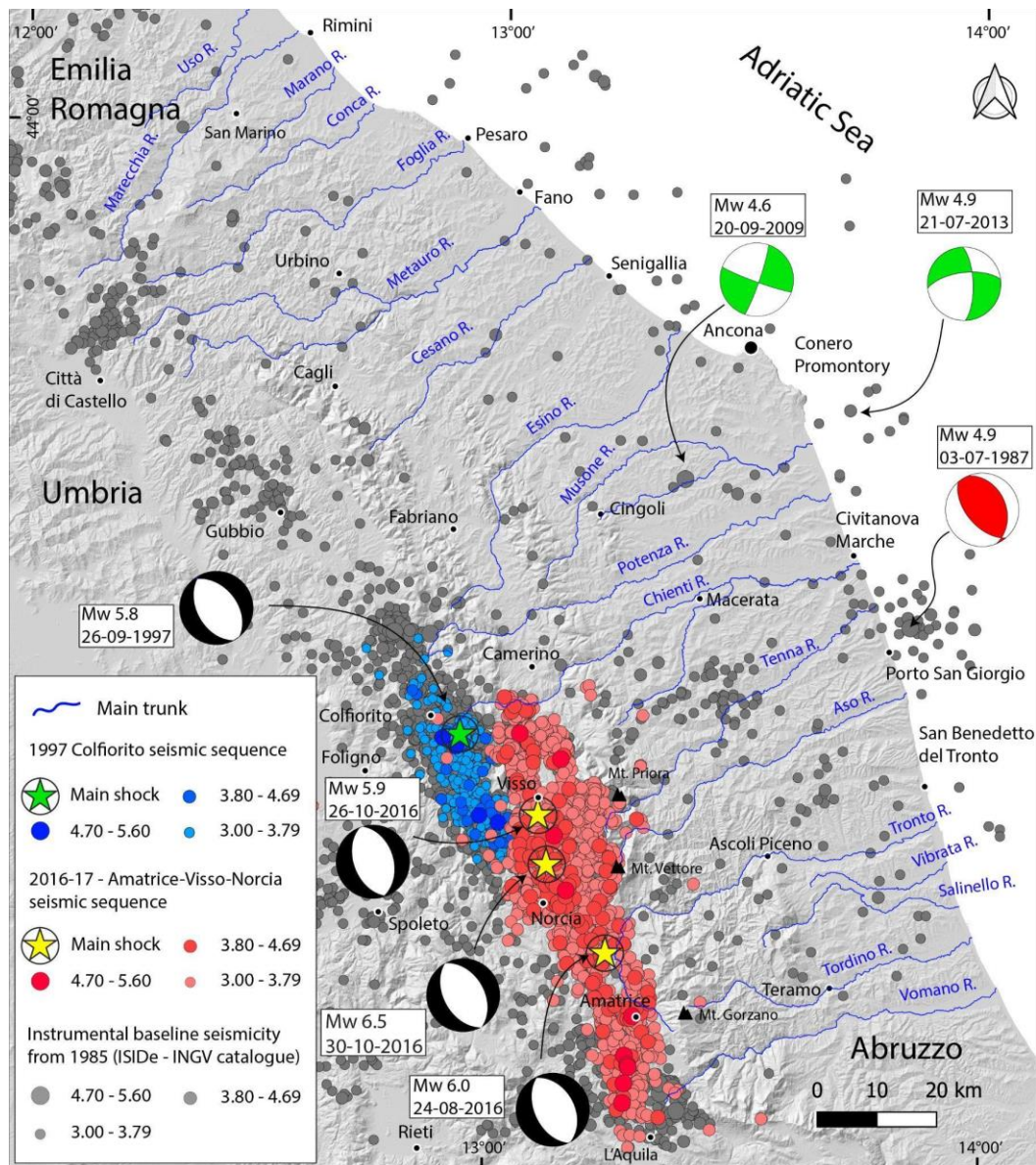


Fig. 5.4 - Instrumental seismicity with magnitude higher than 3 for the eastern central Italy and surrounding area from 1985 to present. Red circles show the 2016-2017 Amatrice-Visso-Norcia seismic sequence whereas yellow stars highlight the main shocks. Gray circles show previous seismic events; blue circles and green stars represent the 1997 Colfiorito seismic sequence and main shock (Mw 5.8) respectively. Focal mechanism solutions are from ISIDe database (ISIDe Working Group, 2007) and the literature (Mazzoli et al. 2014; Santini et al. 2011).

Both the major historical earthquakes occurred in the study area and the spatial distribution of instrumental seismicity confirm the high tectonic activity along the Apennine ridge within the eastern central Italy, with the highest magnitude concentrated in the southern sector, as highlighted by the 2016-2017 seismic sequence. Furthermore, seismic events with magnitude ranging between 3 and 6.5 are generally located along the chain axis and associated with NW-SE striking normal faults, including the Monte Vettore and Monte Gorzano faults. The 2016-2017 aftershocks are confined between the Chienti river valley to the north and the Vomano

river valley to the south. Earthquake focal mechanism solutions available from the ISIDE catalog (ISIDE Working Group, 2007) indicate a predominant normal faulting along the Apennine chain (black focal mechanisms in fig. 5.4) with NE-SW oriented T-axis in agreement with the Quaternary tectonics of this sector (Frepoli & Amato, 1997).

On the contrary, the seismicity of the Marche foothill and Adriatic offshore is not well defined, partly due to poor seismic network distribution and lack of historical macroseismic information (Monachesi et al., 1991). The southern outer sector is instead characterized by moderate historical events and by low to moderate instrumental seismicity (e.g., Ancona 1972, Porto San Giorgio 1987, Costa Marchigiana-Picena 2022 earthquakes), influenced by the presence of NW-SE oriented compressive structures (red focal mechanism in fig. 5.4). Furthermore, studies related to the 2013 Conero seismic sequence (Costa et al. 2021; Mazzoli et al. 2014) reported the presence of deep-seated WSW-ENE strike-slip faults dissecting the thrust belt as testified by the available focal mechanisms (green beach balls in fig. 5.4).

## **5.4. Materials and methods**

To unravel vertical motion distribution within the Umbria-Marche Apennines and its relationship with historical and instrumental seismicity, a GIS-aided analysis of both the topography and the river network has been carried out. The 30 m NASA ASTER GDEM V2 (<https://asterweb.jpl.nasa.gov/gdem.asp>, last access on 8 December 2021) provided the dataset for morphotectonic analysis through ArcGis 10.8 © and Matlab © softwares.

The map of Fig. 5.3, which synthesizes the spatial distribution of the main rock groups outcropping in the study area, has been used as a reference frame for the topography and river network analyses.

### *5.4.1. Topography analysis*

The features of topography have been derived by the elevation map and its derivative maps (maximum, minimum, mean and relief maps), which have been coupled with the analysis of seven swath profiles. The spatial distribution of elevation depends on both the resistance to erosion of the outcropping rocks and tectonics (e.g., surface uplift). The maximum elevation mainly reflects the spatial distribution of rock-types, while mean elevation is considered to be representative of surface uplift distribution (England & Molnar, 1990) and minimum elevation reflects valley floor distribution (Valente et al., 2019). In addition, spatial variations in rock

uplift may be revealed by local relief distribution, especially in areas where rock types with homogeneous resistance to erosion outcrop (DiBiase et al., 2010). Maximum, mean and minimum elevation maps have been derived by applying a 5x5 km large moving window to the 30 m DTM, whereas relief map has been derived as the difference between maximum and minimum elevation.

Swath profiles analysis has been carried out using the SwathProfiler ArcGIS add-in tool (Pérez-Peña et al., 2017). Seven swath profiles, 20 km in width and with different orientations were constructed: five profiles, with SW-NE orientations, are roughly perpendicular to the trend of the main morphostructures i.e. from the Umbria-Marche chain to the foreland basin; one profile follows the bending of the Umbria-Marche Apennine arc, thus including both chain and foreland units; one profile, NW-SE trending, moves within the foreland units.

#### 5.4.2. *Quantitative analysis of the river network*

River network analysis included the construction of river longitudinal profiles and transformed river long profiles (chi-plot), which have been coupled with the slope/area analysis to derive the spatial distribution of the normalized channel steepness index ( $K_{sn}$ ). Analyzed rivers are 18 main trunks that drain from the SW to the NE across the Umbria-Marche chain and its foredeep (Fig. 5.8).

River long profile may reflect either lithological, climatic, or tectonic control (Duvall et al., 2004; Pazzaglia et al., 1998; Stock & Montgomery, 1999; Zaprowsky et al., 2005). Changes from the theoretical graded, concave-upward profile (Hack, 1957), such as rectilinear or convex upward profiles, may be correlated either to an uneven distribution of surface uplift or to variable erodibility of the rock-types (e.g., Attal et al., 2011; Kirby & Whipple, 2001; Whittaker et al., 2008).

Large scale features of the river network may be revealed by the slope/area analysis. Such analysis provides quantitative data useful to distinguish between areas with different behavior in terms of vertical motions, besides rock-type distribution (Flint, 1974; Hack, 1957; Kirby & Whipple, 2001; Snyder et al., 2000; Whipple & Tucker, 1999). We applied this method by means of the Topotoolbox scripts of Matlab (Schwanghart & Kuhn, 2010; Schwanghart & Scherler, 2014) and the Run-Chi profiler script (Gallen & Wegmann, 2017). Slope/area analysis relates channel slope with the drainage area following the hyperbolic equation:

$$S = k_s A^{-\theta} \quad (1)$$



where  $S$  is the channel slope,  $k_s$  is the steepness index,  $A$  is the drainage area and  $\theta$  is the channel concavity index. The analysis is synthesized in a log-log slope vs area diagram with  $\theta$  being the angle of the regression line and the  $K_s$  being the y-intercept. Because small variation in  $\theta$  may provide significant variation in the Y intercept, to compare basins with different drainage areas a reference concavity must be defined. We determined a reference concavity ( $\theta_{ref}$ ) of 0.59 that derives from averaging reference concavity between each of the 18 analyzed drainage basins. Furthermore, a smoothing window of 500 m and a reference drainage area  $A_0 = 1\text{km}^2$  have been adopted

The  $k_{sn}$  index condenses information about (i) active uplift, (ii) enhanced incision associated with knickpoints, and (iii) bedrock erodibility (e.g., DiBiase et al., 2010).

Transformed river long profiles are a powerful tool to discern between steady-state or transient-state profiles. The assumption of this analysis is that topographic data are often subject to errors that may extend to values of slope and areas and, consequently, to the identification of the  $K_s$  and the  $\theta$  indexes (Perron & Royden, 2013). To avoid a propagation of the error, transformed river long profiles use the elevation as the dependent variable and the spatial integral of the drainage area as the independent variable. This analysis removes the downstream increased concavity due to the downstream increased drainage area and allows a meaningful comparison of river profiles despite variable spatial scales, erodibility and uplift rates, also enhancing the presence of knickpoints and transient signals (Perron & Royden, 2013; Royden & Perron, 2013). Transformed river long profiles dissecting a uniform rock-type and equilibrated with uplift have a linear shape, with the uplift rate being reflected by the slope of the transformed profiles. Knickpoints or transient signals that deviate the shape of the chi plot from the linear may be due to either variable erodibility or variable uplift (Perron & Royden, 2013). To obtain transformed river long profiles (chi plots), Equation 1 can be rewritten as follows:

$$S = \left(\frac{U}{K}\right)^{\frac{1}{n}} A^{-\frac{m}{n}} \quad (2)$$

where  $U$  is the rock uplift rate,  $K$  is an erodibility coefficient,  $A$  is the drainage area, and  $m$  and  $n$  are constants. Under constant  $U$  and  $K$ , separating variables in Equation 2 and integrating them, produces

$$z(x) = z(x_b) + \left(\frac{U}{KA_0^m}\right)^{\frac{1}{n}} \chi \quad (3)$$

with

$$\chi = \int_{x_b}^x \left( \frac{A_0}{A(x)} \right)^{\frac{m}{n}} dx \quad (4)$$

where  $z(x)$  is the elevation of an observation point along the river long profile,  $z(x_b)$  is the elevation of the local base level,  $A(x)$  is the drainage area at the observation point  $z(x)$ , and  $A_0$  is a reference drainage area.

Reference drainage area ( $A_0$ ) is 1 km<sup>2</sup> whereas the smoothing window is 500 m.

In the chi-plot analysis it is crucial the recognition of the best-fit  $m/n$  ratio ( $\theta$ , concavity index) at the drainage basin scale, whereas to compare rivers with different drainage areas a reference concavity must be defined, which derives from averaging the  $m/n$  values of all the analyzed rivers (Perron and Royden, 2013). The best fit  $m/n$  ratio at the basin scale has been derived by the Bayesian optimization script of Topotoolbox (Schwanghart & Kuhn, 2010; Schwanghart & Scherler, 2014), and the derived average reference concavity value is 0.59.

## 5.5. Results

### 5.5.1. *Features of topography*

The Umbria-M arche Apennines is characterized by an increasing elevation towards the SW, with the poorly elevated and low-gradient foothills that pass to the hilly and mountainous landscape of the chain (Fig. 5.5). The foothill exhibits a smooth landscape in the north (i.e., from the Uso R. basin to the Esino R. basin) and a relatively rugged topography in the south (i.e., from the Musone R. basin to the Vomano R. basin) where valleys are narrower and conglomerate deposits, testifying the closure of the foredeep infill, are preserved in some remnants of paleosurfaces (unit 2 in Fig. 5.3). Parallel to the foothills, the chain exhibits lower elevations and a smooth topography in the north, where the highest peaks correspond with narrow NNW-SSE trending ridges formed in the Scaglia carbonate units (unit 6 in Fig. 5.3; e.g., Mt. Paganuccio 976 m a.s.l.; Mt. Catria 1702 m a.s.l.; Mt. Cucco 1566 m a.s.l.; Mt. Murano 882 m a.s.l.). The ridges are aligned along two distinct NNW-SSE trends that are separated by a large area where softer rock-types outcrop (e.g., Messinian sandstones and the Schlier, Bisciaro and Cinerea calcareous marly succession, which correspond to units 4 and 5, respectively, in Fig. 5.3). Towards the south, the chain is more elevated and looks rugged. The above-mentioned two NNW-SSE trending ridges are clearly recognisable in the area spanning from the Esino R. to the Chienti R. valleys and are separated by the Camerino Basin where

Messinian arenaceous deposits crop out. The ridge to the NE (hereinafter the Marche ridge) is carved in the Scaglia units (unit 6 in Fig. 5.3) and reaches a maximum elevation of 1021 m a.s.l. at Mt. Letegge. In the SW, the Umbria-Marche ridge is carved both in the Scaglia and the Calcare Massiccio units (units 6 and 10 in Fig. 5.3, respectively) and its highest peak is Mt. Pennino (1571 m a.s.l.). Moving to the south (from the Chienti R. to the Aso R. valleys) the two ridges converge, and the chain exhibits its highest elevation with the peaks of Mt. Vettore (2467 m a.s.l.) and Mt. Priora (2333 m a.s.l.), which are carved in the Calcare Massiccio (unit 10 in Fig. 5.3) and the Scaglia deposits (unit 6 in Fig. 5.3), respectively. The southern portion of the investigated area (e.g., from the Tronto R. to the Vomano R. valleys), where Messinian arenaceous deposits crop out (unit 4 in Fig. 5.3), exhibits high to very high elevations that culminate in the peak of Mt. Gorzano (2458 m.a.s.l.).

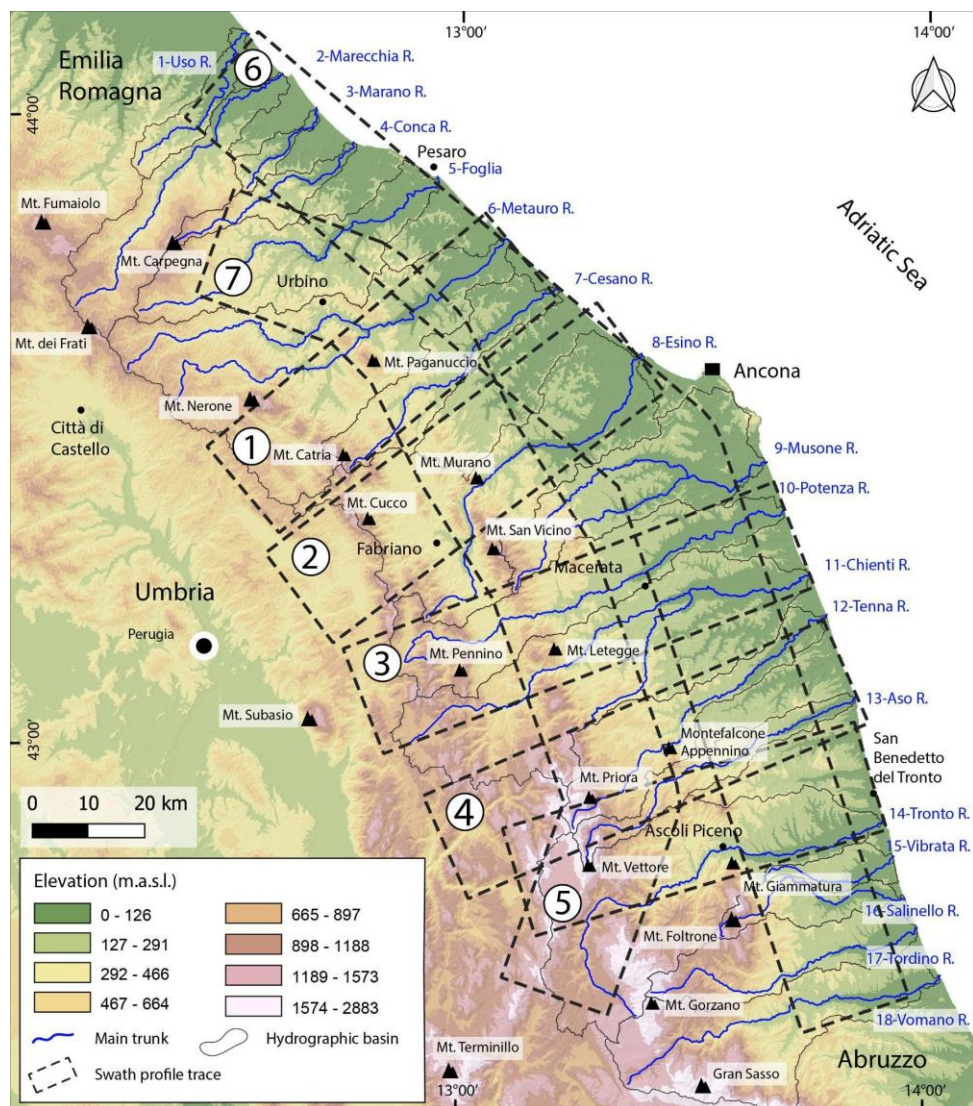


Fig. 5.5 - Elevation map of the Umbria-Marche Apennines with location of the investigated main trunks, and correlative hydrographic basin, and the swath profiles.

The above-described topography setting is also highlighted by the maximum (Fig. 5.6a), the minimum (Fig. 5.6b) and the mean (Fig. 5.6c) elevation maps. All these maps point to the presence of a locus of high elevations to the south of the investigated area (e.g., in the area between Mt. Vettore and Mt. Gorzano). In this area rock-types with different lithology outcrop, such as the hard carbonate of the Calcare Massiccio and the soft Messinian siliciclastic deposits.

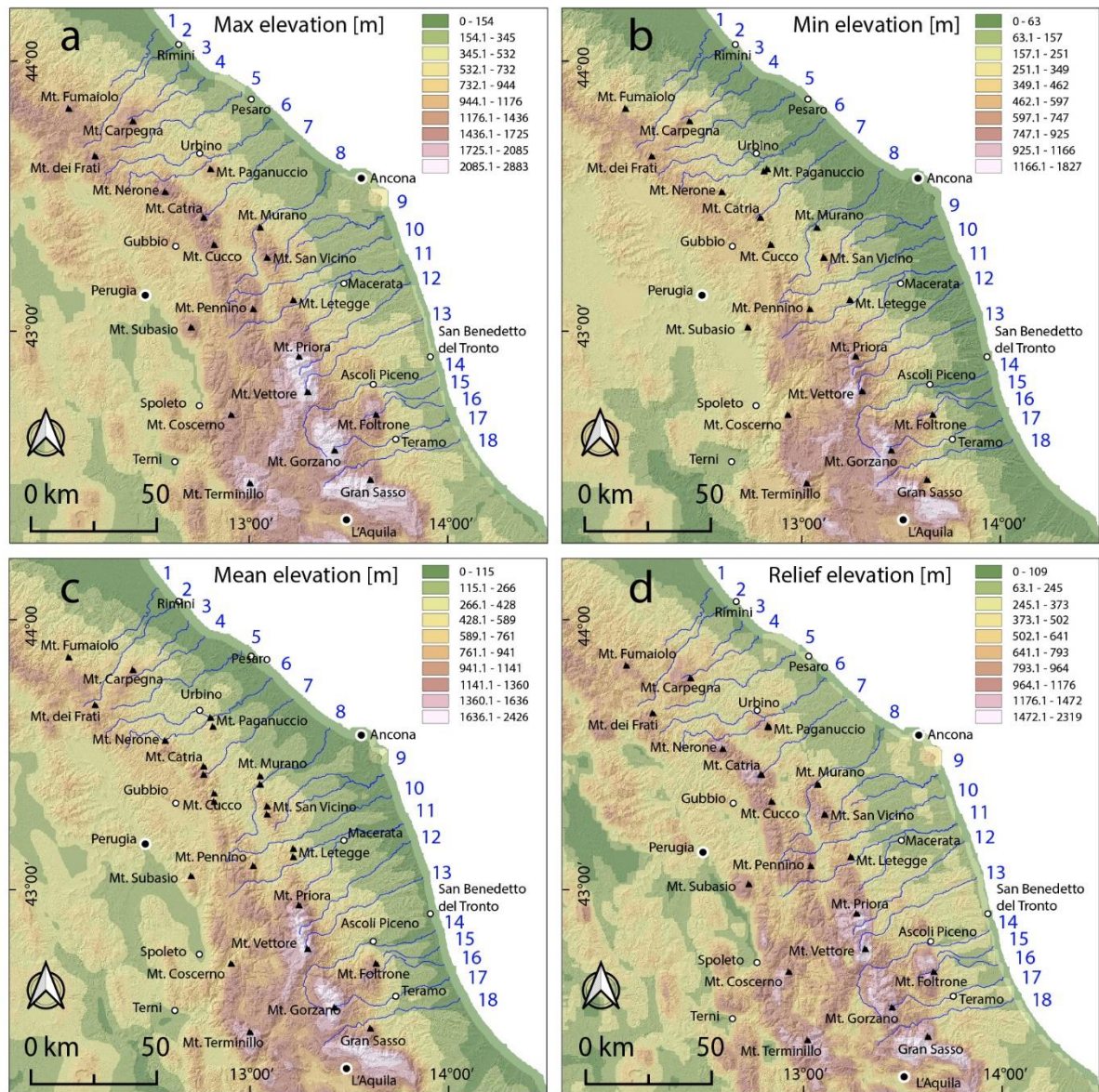
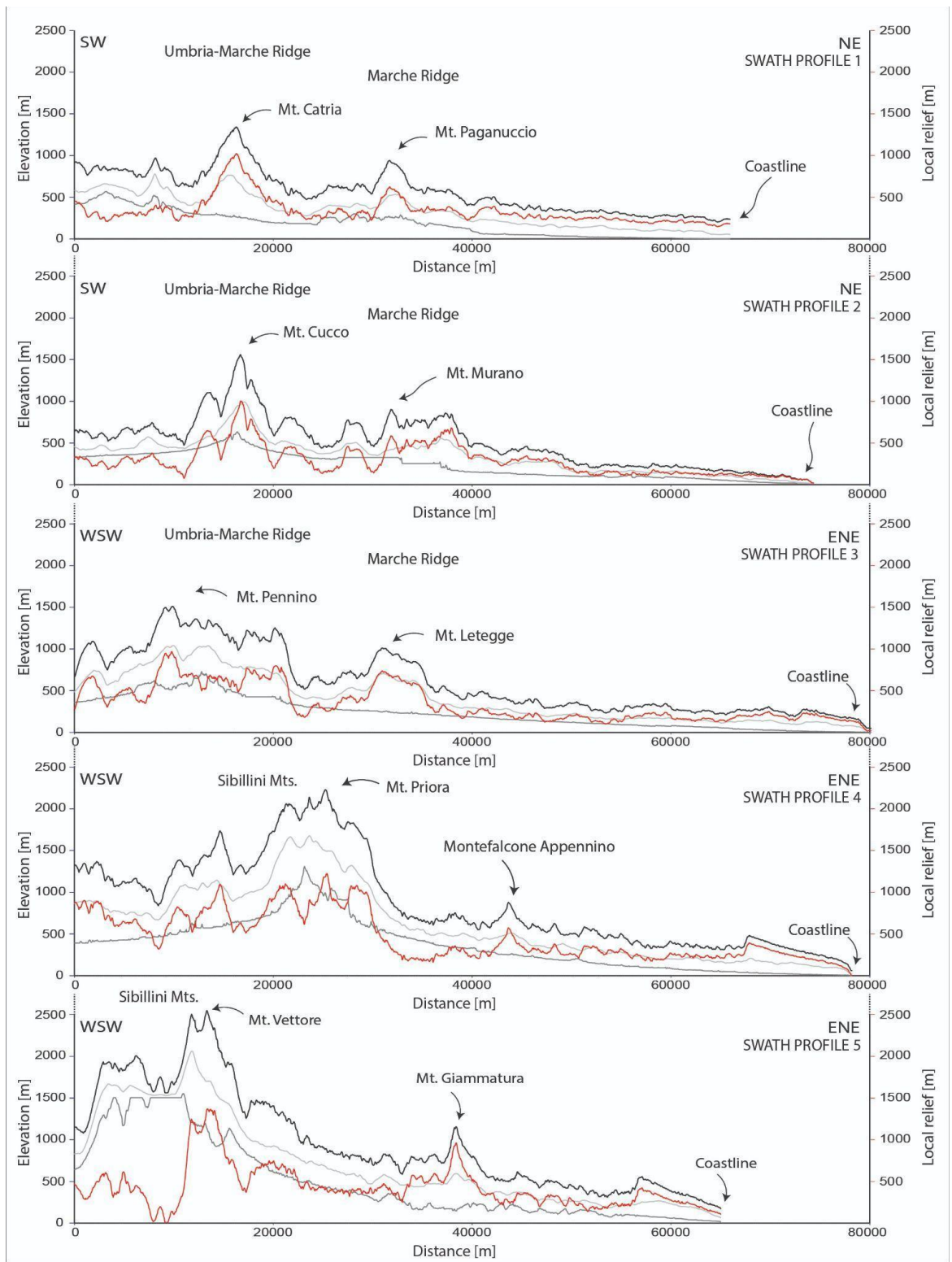


Fig. 5.6 - Elevation maps from neighborhood statistical analysis in ArcGIS environment applied to the 30 m NASA ASTERDEM of the study area; a) maximum elevation map, b) minimum elevation map, c) mean elevation map, and d) local relief map.

### 5.5.2. *Swath profiles*

Swath profile analysis provides further detail about the topography setting of the investigated area. Overall, swaths perpendicular to the belt (swaths n. 1 to 5 in Fig. 5.7) point to features of topography that are consistent with the main structural units of the Umbria-Marche Apennine. The sudden drop in the maximum, mean and the minimum elevation curves at around 40 km in swaths 1, 2 and 3, at around 30 km in swath 4 and at around 20 km in swath 5, mark the location of the Umbria-Marche-Sabina Thrust Zone (hereinafter UMSTZ). To the west of UMSTZ, the elevation curves are more elevated and depict the occurrence of the two NNW-SSE trending regionally extended anticlines, i.e. the Umbria-Marche Ridge (culminating with Mt. Catria, Mt. Cucco, Mt. Pennino, Mt. Priora and Mt. Vettore) and the Marche Ridge (culminating with Mt. Paganuccio, Mt. Murano, Mt. Letegge and Mt. Giammatura). The ridges are separated by a broad syncline depression filled by Miocene siliciclastic sediments (e.g., Camerino Basin in swath profile 3). The anticline ridges, characterized by maximum elevation between 750 and 1500 m a.s.l., are composed of stiff Jurassic and Cretaceous carbonate rocks and clearly identified in swaths from number 1 to 3. In the area of swaths 4 and 5, the chain exhibits its highest elevations that exceed 2000 m a.s.l. with the peaks of Mt. Priora and Mt. Vettore. To the east of the UMSTZ, topography looks smooth in the north (i.e., swaths n. 1, 2 and 3) and rugged in the south (i.e., swaths n. 4 and 5). Such a difference may be related to the different rock types outcropping in these areas, which correspond with the Pliocene mainly pelitic deposits filling of the foothills to the north and the Miocene arenaceous deposits to the south. Comparison of the profiles of Fig. 5.7 points to an overall increase of the elevation values towards the south (i.e., from swath n. 1 to swath n. 5). Such a trend is also evident by swaths n. 6 and 7 (Fig. 5.7), which run parallel to the foothills and to the outer sector of the orogenic belt, respectively. Moreover, highest peaks in the maximum elevation curves correspond with “hard” carbonate units, and this trend is mirrored by the mean elevation curves. Regarding the minimum elevation curve, it is smooth in the north (swaths n. 1, 2 and 3) with values not exceeding 500 m a.s.l., whereas in the south (swaths n. 4 and 5) it exhibits two relevant peaks exceeding 1000 m a.s.l., which correspond with Mt. Priora (swath 4) and with the area to the west of Mt. Vettore (swath 5).

The relief curve mirrors the elevation curves, with the relief peaks that correspond with the highest elevation peaks, and with increasing local relief towards the south (i.e., from swath n. 1 to swath n. 5). The only case in which the relief curve is opposite to the elevation curves is in the first 10 km of swath n. 5, where high values in the maximum, mean and minimum elevation curves are coupled by low values in the relief curve.



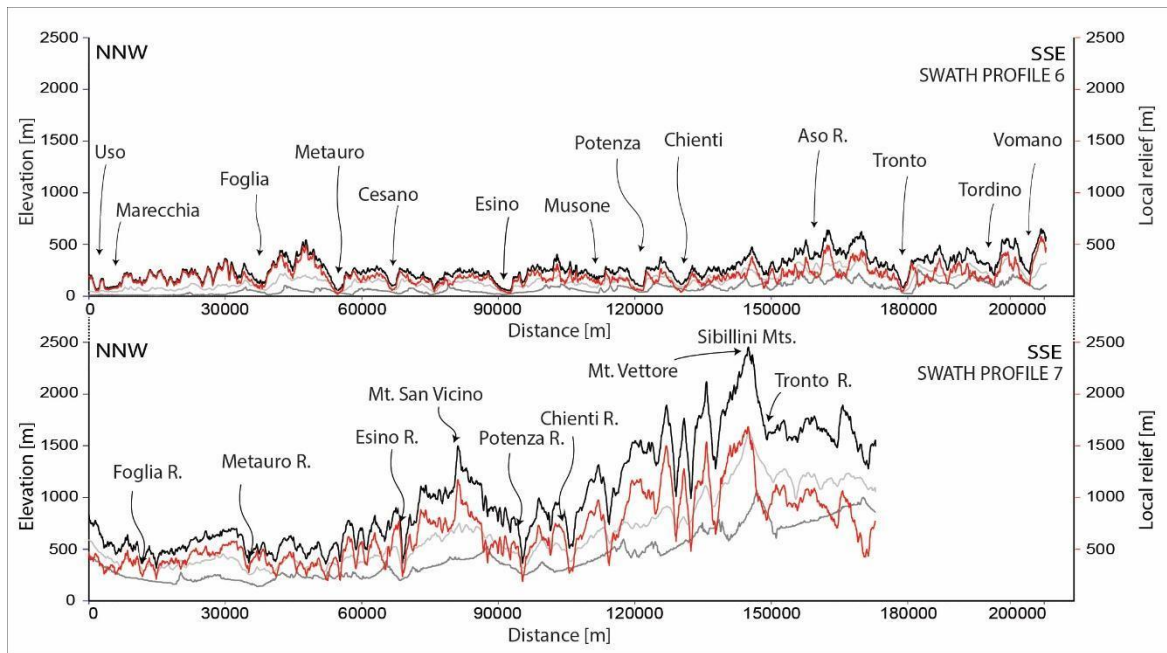


Fig. 5.7 - Swath profiles within the Umbria-Marche Apennines and foothills (see Fig. 5.5 for the location). Swath profiles 1 to 5 are SW-NE trending and run perpendicular to the chain. Swath profiles 6 and 7 are parallel to the mountain front and perpendicular to river valleys. Black line indicates maximum elevation curve, grey line indicates mean elevation curve, light grey line indicates minimum elevation curve and red line indicates relief curve.

### 5.5.3. Longitudinal river profiles analysis

The first step in the analysis of river long profiles and chi-plots is the definition of the best fit  $m/n$  value at the drainage basin scale, whose value is reported in Fig. 5.8 for each investigated river. This analysis allows identifying either the steady-state conditions or the presence of transient signals at the drainage basin scale. Furthermore, it also allows knickpoints to be located, which have been distinguished according to their proximity to lithological contact between rock types of different erodibility (Fig. 5.9): knickpoints that are less than 200 m far from lithological contact have been classified as “lithology-controlled knickpoints”, whereas knickpoints that are more than 200 m far from lithological contact have been classified as “non-lithology-controlled knickpoints” (Buscher et al., 2017).

River long profiles and chi-plots exhibit variable features along the strike of the Umbria-Marche Apennine. In the northern sector, e.g., in the area between the Uso River and the Foglia River (rivers 1 to 5 in Fig. 5.8), chi-plots look rectilinear to slightly convex upward with the only exception of the Foglia River that exhibits a concave upward chi plot. Several knickpoints are identified, some of which have been classified as lithology-controlled knickpoints because of their proximity to contacts between the “Valmarecchia chaotic units”, the Messinian arenaceous

deposits and the sandy-silty Plio-Pleistocene deposits. However, the Conca and Foglia Rivers exhibit only knickpoints related to non-lithological control (Fig. 5.8 and 5.9).

In the central sector of the investigated area, between the Metauro River and the Potenza River (rivers 6 to 10 in Fig. 5.8), the chi profiles are characterized by convex shapes with knickpoints associated with non-lithological control (Fig. 5.8); some of these are located within deep gorges incised into carbonate anticlines (e.g., Esino and Potenza River – Fig. 5.9).

Rivers in the southern sector of the study area (rivers 11 to 18 in Fig. 5.8) show different chi-plots, which vary from rectilinear and steep (11 - Fiastra River which is a tributary of the Chienti River), to convex or slightly convex (15 - Vibrata River; 11 - Chienti River; 14 - Tronto River) and to rectilinear in the lower reach to convex upward in the upper reach (river 12, 13, 16, 17 and 18 in Fig. 5.8). Associated with variable chi-plots is the diffuse presence of knickpoints, most of which have been classified as non-lithology controlled knickpoints. The lithological control on the genesis of knickpoints has been recognised for the Chienti, Tenna and Aso rivers and is associated with contacts between the carbonate units and the Messinian arenaceous deposits and between these deposits and the Plio-Pleistocene deposits of the Periadriatic foredeep.



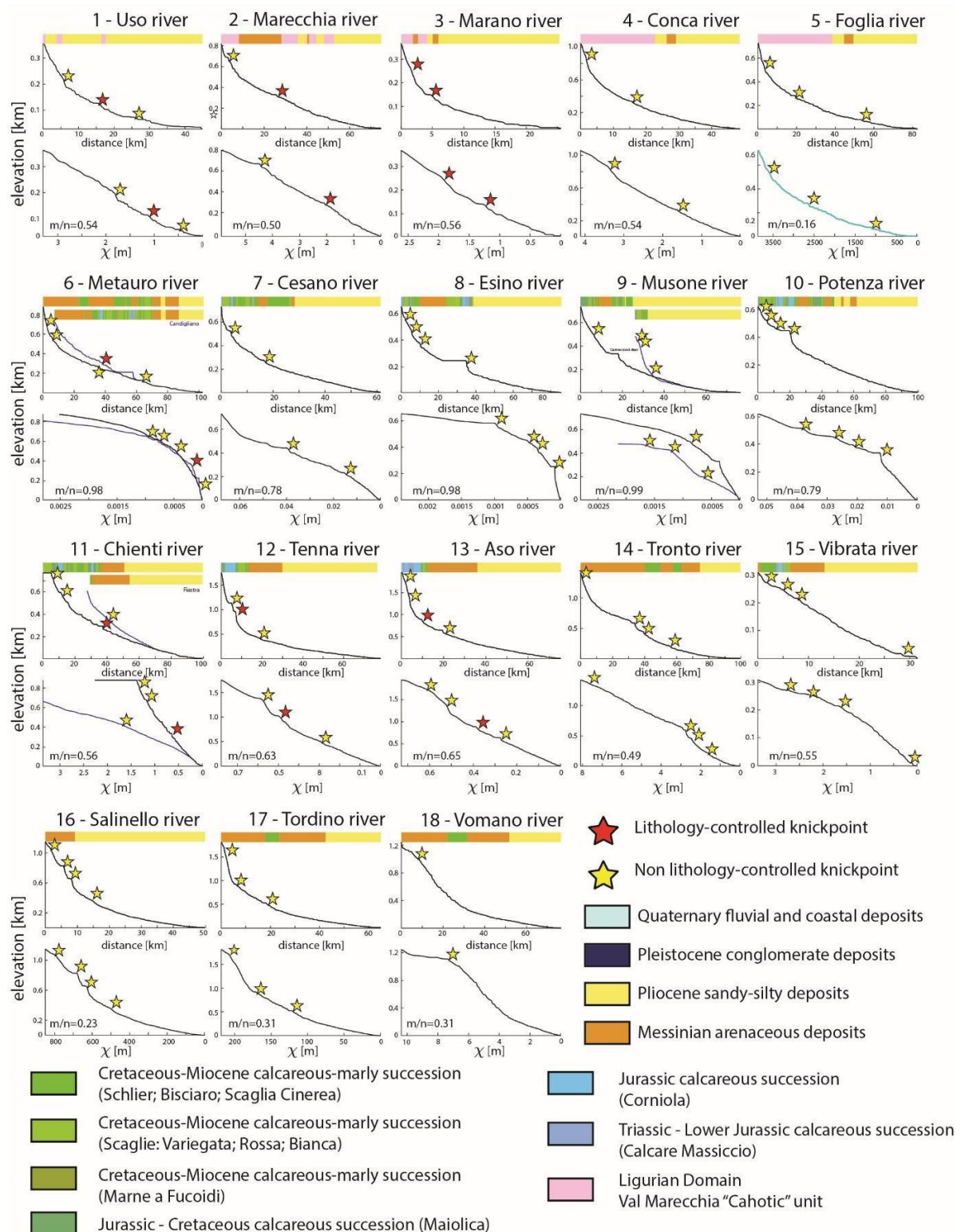


Fig. 5.8 - Longitudinal profiles and chi plot (performed by Topotoolbox MATLAB-based software) of the 18 rivers analyzed in the present work. The chi plots were processed using a smoothing window of 250 m, a reference drainage area  $A_0 = 1 \text{ km}^2$ . The  $m/n$  ratio has been calculated for each plot using the Bayesian optimization script in MATLAB. The colored bars above long river profiles represent the lithology of the bedrock reported in Fig. 5.2.

The spatial distribution of knickpoints is shown in Fig. 5.9. All investigated rivers are characterized by the presence of knickpoints, which have been mainly classified as non-lithology controlled knickpoints. Most of the knickpoints are clustered in the southern sector of the Umbria-Marche region, e.g. in the area spanning from the Tenna River (number 12 in Figs. 5.8 and 5.9) and the Vomano River (number 18 in Figs. 5.8 and 5.9).

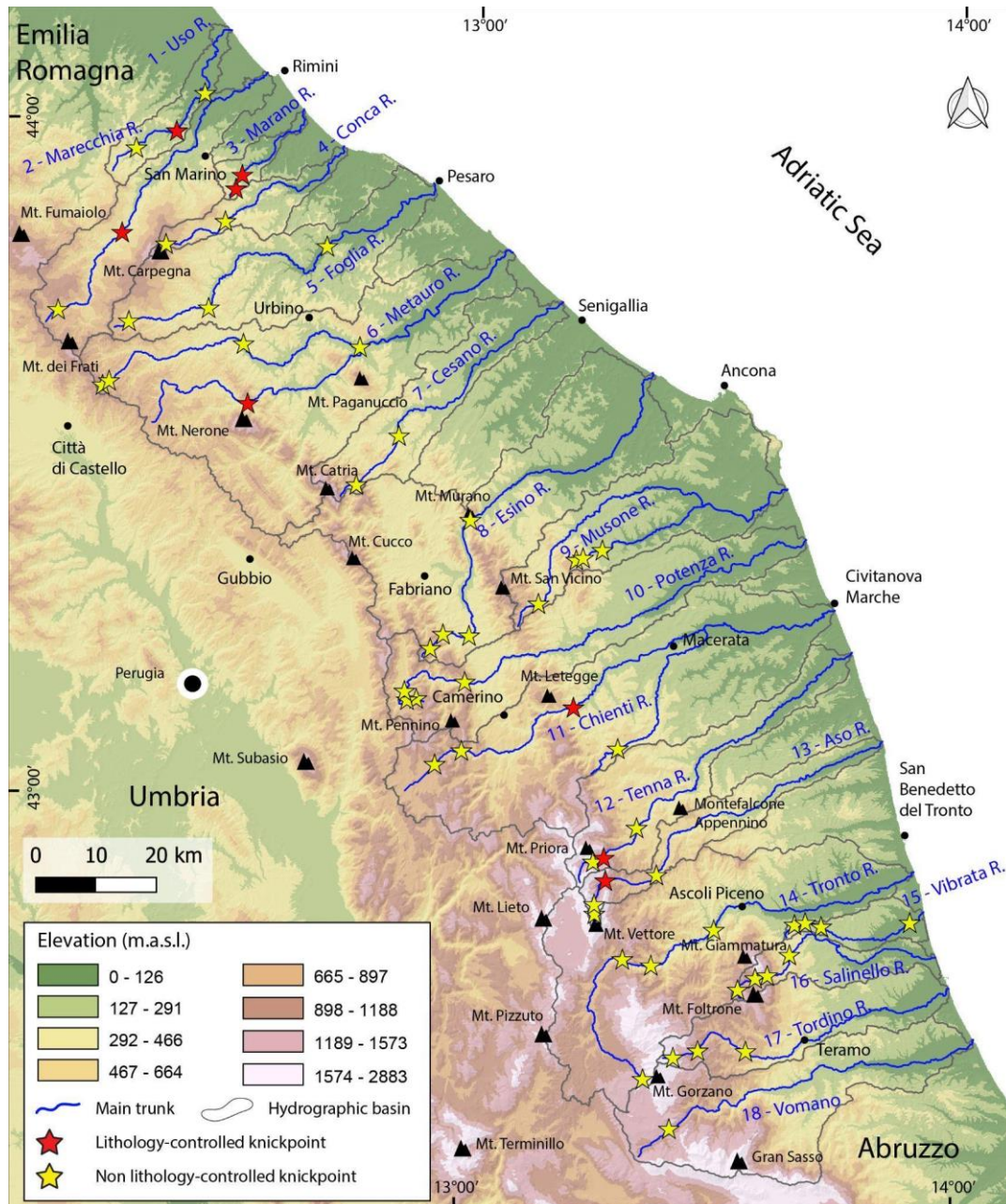


Fig. 5.9 - Topographic map showing the knickpoints/knickzones spatial distribution along the 18 river channels analyzed in the study area. The identified knickpoints are distinguished in lithology-controlled knickpoints and non lithology-controlled ones, using the geological map of Fig. 5.3. In this regard, red stars represent sharp change in channel slope due to lithological contrast while yellow ones are the knickpoints related to possible tectonic perturbation.

To explore the nature of the signals that govern the nonlinearity of the chi plots, and to compare all the chi-plots, we extracted the transformed river long-profiles using a  $m/n$  ratio of 0.56, a value obtained averaging the  $m/n$  ratios of all the investigated rivers.

The new chi-plots are shown in Fig. 5.10. Chi-plots of rivers in the northern Marche region have mainly rectilinear shapes (rivers 1 to 6) with some slight convex upward segment in the upper reaches of rivers 2 and 4. For the central Marche region (rivers 7 to 10), chi-plots have rectilinear to slightly convex upward shapes, whereas (rivers 11 to 18) rivers located in the southern Marche region are characterized by overall steeper chi-plots, which show enhanced convex upward segments that locally pass to steep rectilinear segments in the lower reaches (rivers 11, 12, 13, 16 and 17).

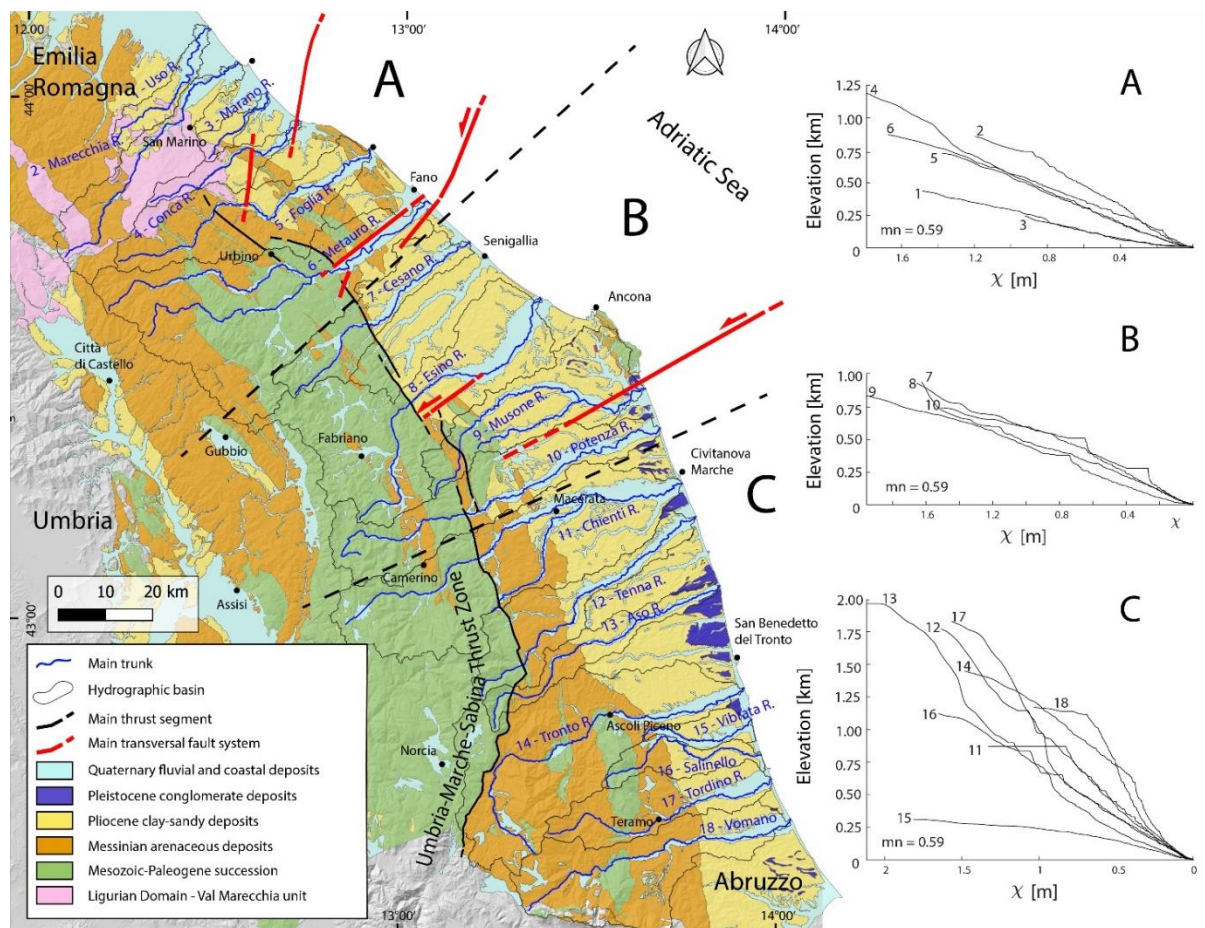


Fig. 5.10 - Chi plots of the main rivers of hydrographic basins (locations and numbering in Fig. 5.5), constructed using a best fit  $m/n$  value of 0.59.

#### 5.5.4. *K<sub>sn</sub> index*

The spatial distribution of the  $K_{sn}$  index has been obtained by applying the slope/area analysis and considering the average  $m/n$  value of 0.56. Results are shown in Fig. 5.11.

In the northern and central sectors of the Marche region (i.e., in the area between the Uso River and the Musone River), high K<sub>sn</sub> values are clustered near the Marche ridge and the Umbria-Marche ridge. In these areas hard carbonate units crop out, thus suggesting that lithology plays a primary role in controlling the spatial distribution of this index. On the contrary, a large area with high K<sub>sn</sub> values occurs to the south (i.e., in the area between the Potenza River and the Vomano River).

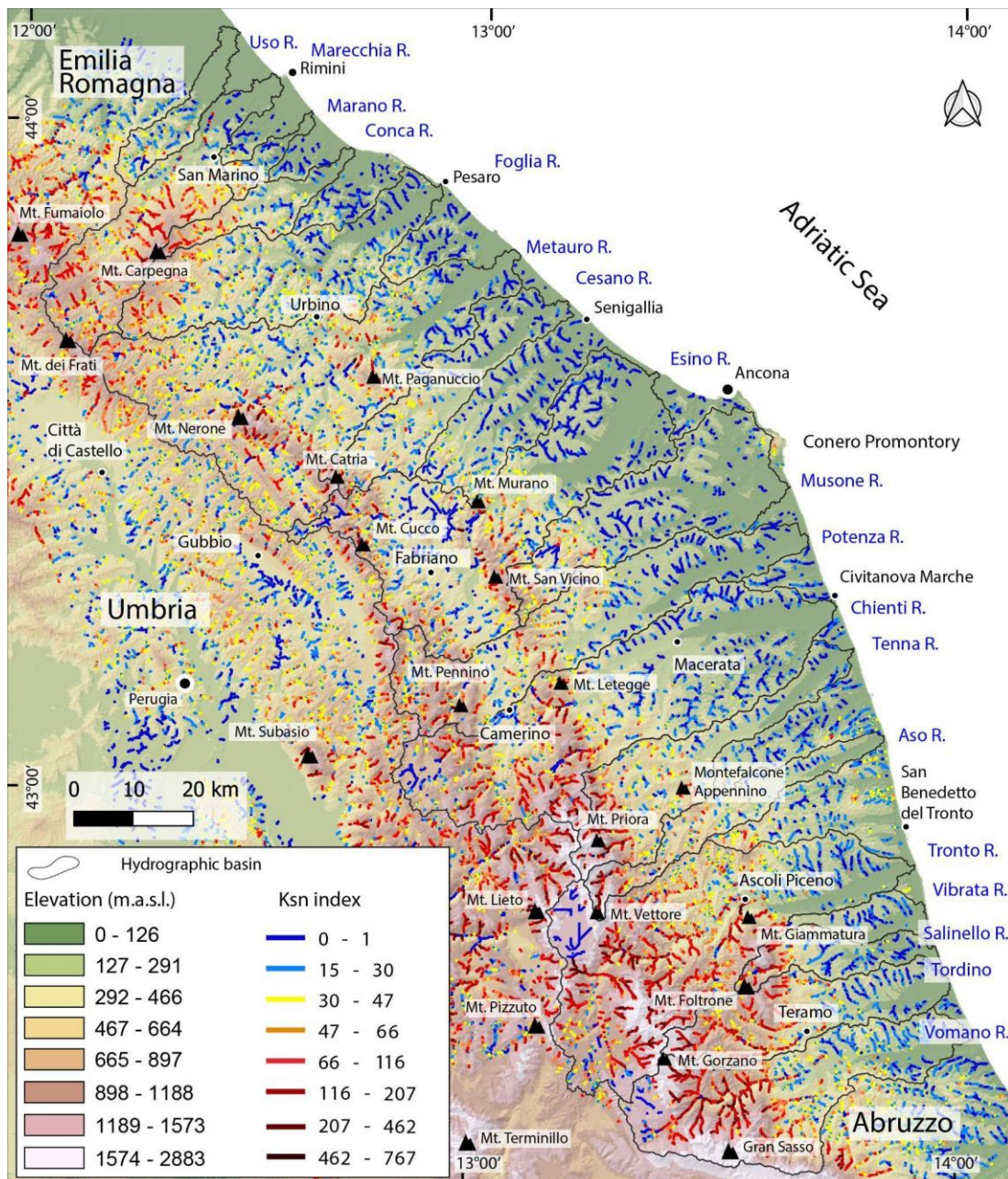


Fig. 5.11 - K<sub>sn</sub> index map of the eastern central Apennines identifying the alluvial basins (black outlines) and the spatial distribution of ksn; high ksn values are indicated with red darker color whereas low ksn values are in blue color. Areas with high ksn are in relationship with zones of high local reliefs of the statistical elevation map and swath profiles.

## 5.6. Discussion

### 5.6.1. *Along-strike variation of uplift*

The shape of mountain ranges, such as the Apennine chain in the Umbria-Marche area, depends on the combination of several factors that include lithology, climate and tectonics (Ellis & Densmore, 2006; Forte et al., 2014; Whipple & Tucker, 1999; Willett et al., 2001), which makes the reconstruction of vertical motions distribution a challenging task. Information about the spatial distribution of vertical motions (i.e., surface uplift) may be obtained by combining morphotectonic analysis of the topography and river network (Eizenhöfer et al., 2019; Ellis & Densmore, 2006). This approach has been already tested in different morphotectonic and morphoclimatic settings, such as Iberia (Scotti et al., 2014), the Zagros chain in Iran (Basilici et al., 2020), and Turkey (Schildgen et al., 2012) and the Caucasus (Forte et al., 2014).

In our case study, we focused our morphometric investigation on the north-eastern slope of the Umbria-Marche Apennines, therefore minimizing the role of variations in the amount of precipitation, which may significantly affect parameters (e.g. river long profiles and Ksn index) that describe the drainage network on the opposite sides of mountain belts (Molin and Fubelli, 2005). Conversely, the features of topography and drainage network in our study area are strongly controlled by the variable bedrock lithology, as it is inferred from the spatial coincidence of high vs. low values of parameters such as elevation and Ksn index with outcrops of carbonate rocks (Umbria-Marche and Marche ridges) and clayey and/or arenaceous rocks (foothill), respectively. However, the variability of bedrock lithology is much greater across than along the strike of the investigated region of the mountain belt and, therefore, the along-strike variation in topography and river network features may be considered as less affected by the lithology parameter. Our analysis has shown that elevation data and its derivative (maximum, mean and minimum elevation and local relief) increase towards the south (Figs. 5.5 and 6), with maximum values in the area between the Tenna River and the Vomano River valleys (number 12 and 18, respectively, in Fig. 5.8). The southeastward increasing elevation is also clearly imaged by the swath profiles, which point to the occurrence of a locus of high elevation and high relief located in the southern part of the study region (Fig. 5.7). Noteworthy, the locus of high elevation and relief involves both hard carbonate units, which culminate with the Mt. Vettore (2467 m a.s.l.) peak, and softer arenaceous units that peak with Mt. Gorzano (2458 m.a.s.l.).

The coupling of soft rock-types with high elevation suggests that lithology does not play a primary role in the landscape features of the southern sector of the Umbria-Marche Apennines

and supports the idea that the study region was affected by differential long-term uplift and, in particular, the southern part of the study area recorded the greatest cumulative, long-term surface uplift.

The spatial and chronological distribution of differential uplift in the study area may be better deciphered if evidence from topography is integrated by evidence from the drainage features/parameters, which are more sensitive to recent/active tectonic perturbations. Among the parameters we used to analyze the river network, the Ksn index is indicative of uneven along-strike recent uplift of the study region. In particular, by the Ksn map (Fig. 5.11) is evident that the southern sector of the Umbria-Marche region corresponds a locus of high Ksn values that span over an area underlain by both carbonates and softer arenaceous deposits, which are widespread in Mt. Gorzano area. This evidence suggests that the lithological control on the Ksn values is overprinted by other input and is consistent with differential uplift continuing until recent times and related greater rise of the southern part of the study area. Literature data support our findings on a south-eastward increasing recent uplift. Centamore and Nisio (2003) recognised an increased trend in uplift rate moving from the Musone River to the Tronto River (rivers numbers 9 and 14 in Figs. 5.5, 5.8, 5.9 and 5.10). By dating alluvial terraces, Wegmann and Pazzaglia (2009) estimated in the Musone River basin (number 9 in Figs. 5.5, 5.8, 5.9 and 5.10) a mean incision rate of 0.2 mm/yr in the last 0.45 Ma that accelerated up to 0.6 mm/yr in the last 0.04 Ma downstream the Cingoli dam. Pazzaglia and Fischer (2022), by applying the celerity model to several rivers of our study area, estimated uplift increasing southwards in the last 0.5 Ma, with rates of 0.1 - 0.25 mm/yr for the Metauro River (our river 6) basin, of 0.25 - 0.18 for the Esino River (river 9) basin, of 0.35 - 0.2 mm/yr for the Chienti River (river 11) basin, and 0.4 - 0.3 mm/yr for the Tronto River (river 14) basin, with the latter value close to the 0.5 mm/yr value estimated by Sembroni et al. (2020; based on river terrace dating) for the same basin and time span.

The uplift rate estimated by Pazzaglia and Fischer (2022) for the Esino River basin is in the same range, to slightly in excess, of the incision rate of  $0.2 \pm 0.1$  mm/yr estimated for the Esino river by Cyr and Granger (2008). Such a consistency, which implies conditions close to balancing between incision and uplift for the Esino River, supports evidence from the compared chi-plots of Fig. 5.10. In fact, the chi-plots of the Esino and nearby rivers (7 to 10; Fig. 5.8 and Fig. 5.9), which are slightly convex upward and with low slope angle (Fig. 5.10), are suggestive of rivers that register only some minor perturbation and are not far from keeping pace with moderate uplift. In comparison, the smooth long-profiles and rectilinear chi plots of rivers located in the northern part of the study area, suggest that those rivers (1 to 6; Fig. 5.8 and Fig.

5.9) are substantially keeping pace with subdued uplift. On the other hand, comparison between chi-plots of rivers 7 to 10 vs. rivers 11 to 18 is indicative of a sharp change in the river dynamics and, particularly, of a south-eastward transition towards marked disequilibrium conditions for rivers 10 to 14. The longitudinal profiles of the latter rivers are the more perturbed, being affected by a high concentration of non-lithology-controlled knickpoints (Fig. 5.8 and Fig. 5.9) and compared with rivers in the north, are either overall convex upward or with convex upper reaches that pass to steep rectilinear lower reaches (Fig. 5.10). Considering the large sizes of the convex upward reaches, the variable nature of the bedrock (that includes both carbonate and arenaceous deposits) that is incised, and the abundance of non-lithology controlled knickpoints, the nature of the transient signals observed in the rivers that dissect the southern part of the study area is reasonably correlated to migrating tectonic signals. In addition, the transformed profiles of the southern rivers, relative to those located in the central-northern part of the study area, are overall steeper even in their straight lower reaches. Such a feature that would suggest (e.g., Perron Royden Mendocino) a tendency of rivers 10 to 18 to the attainment of equilibrium with uplift faster than uplift that affects the area in the north of the study region, consistent with estimates for the Chienti and Tronto rivers basins by Sembroni et al. (2020) and Pazzaglia & Fischer (2022). Worthy to note, the river long-profile analyses we performed allows putting net boundaries between sectors (A, B, C) that feature different behaviors across the strike of the mountain belt.

#### 5.6.2. *The role of transversal structures*

The boundaries among sectors (A, B, C), characterized by different behavior in tectonic activity, roughly coincide with major transversal faults segmenting the outer portion of the fold and thrust belt in the Marche foothills and adjacent offshore area (Fig. 5.1). This feature suggests that such transversal ‘lineaments’ mark the loci of long-lived, deep-seated fault zones that exert a major control on the active tectonic behavior of large crustal blocks. The recent reactivation of inherited crustal faults in the foreland plate has been unraveled in the southern Apennines by Bitonte et al. (2021). The latter authors also documented fault propagation into the foreland basin deposits as a result of basement fault reactivation. A similar process is envisaged to have occurred also in the present study area, where pre-existing deep-seated faults of the foreland plate appear to have controlled fold and thrust belt propagation and related segmentation of the deformed Plio-Pleistocene foredeep (Costa et al. 2021; Pierantoni et al. 2019). The fact that the crustal sectors (A, B, C) characterized by different active tectonic behavior extend SW-ward into the axial zone of the mountain chain (i.e., also in the hanging wall of the major UMSTZ defining the mountain front) further suggests that the transversal

‘lineaments’ mapped in the frontal part of the fold and thrust belt actually mark major crustal structures extending beneath the high mountain chain. As the latter area is presently dominated by ongoing extension, it may be envisaged that the deep-seated transversal faults interact with the active normal faults, actually segmenting the Quaternary extensional system in the axial zone of the chain. This is consistent with seismicity distribution, and in particular with the abrupt northward truncation of the events associated with the 2016-2017 Amatrice-Visso-Norcia and the 1997 Colfiorito seismic sequences (Fig. 5.4) along the boundary between block C and block B in Fig. 5.10. Moreover, recent studies based on instrumental seismicity (Mazzoli et al., 2014, 2015), seismic interpretation (Costa et al., 2021) and paleoseismological evidence (Materazzi et al., 2022) highlight the fact that major transversal structures can also host moderate to significant seismic events (e.g., the Mw 6.17, 1741 Fabriano earthquake; the Mw 4.68, 1972 Ancona and Mw 4.9, 2013 Conero offshore earthquakes).

A general continuity of transversal major structures from the Adriatic Sea, through the Marche foothills, to the axial zone of the chain is consistent with such structures representing long-lived faults in the basement of the foreland plate. This model implies a recent upward propagation of these structures into the hanging wall of the UMSTZ. However, this is not at all surprising, taking into account the clear linkage between deep and shallow seismogenic fault segments cutting across the UMSTZ (which is offset by the Quaternary normal faults, e.g., Mazzoli et al., 2005; Porreca et al., 2018).

## **5.7. Conclusions**

The multidisciplinary approach that combines morphotectonic and seismotectonic analysis presented in this work allowed better investigation of the neotectonic processes in a high tectonically active area such as the Umbria-Marche Apennines (central Italy). Topography and river network features exhibit along strike variations that are consistent with uneven distribution of vertical motion (e.g., surface uplift) that increase towards the south-east.

Furthermore, the combination between morphotectonic data with the instrumental seismicity analysis was used to improve the knowledge about the relation between landscape evolution and tectonic deformation processes induced by the ongoing activity of inherited-deep-seated tectonic structures.

The main results are summarized as follow:



- The morphotectonic analysis suggests a southeastward increasing trend in surface uplift, which is maximum in correspondence of the Sibillini Mts. – Laga Mts.
- In the Marche foothills and Adriatic offshore, the boundaries among crustal blocks characterized by different active tectonic behavior roughly coincide with major transversal faults recently mapped by seismic interpretation.
- The crustal blocks characterized by different active tectonic behavior extend SW-ward into the axial zone of the mountain chain, which is characterized by active extension.
- The tectonic geomorphology analysis carried out in this study provides the first evidence of crustal-scale, along-strike segmentation of the axial zone of the mountain chain and of the extensional system active there.
- The segmentation, proposed in this study, of the active extensional system affecting the axial zone of the mountain chain is consistent with seismicity distribution, and in particular with the pattern of the 2016-2017 seismicity.
- The segmentation, proposed in this study, of the extensional system in the axial zone of the mountain chain has major implications for the seismotectonic behavior of the most active area of the Umbria-Marche Apennines. This, in turn, may have a fundamental impact on the assessment of seismic hazard in central Italy.

## 5.8. References

- Attal, M., Cowie, P. A., Whittaker, A. C., Hobley, D., Tucker, G. E., & Roberts, G. P. (2011). Testing fluvial erosion models using the transient response of bedrock rivers to tectonic forcing in the Apennines, Italy. *Journal of Geophysical Research: Earth Surface*, 116(F2). <https://doi.org/10.1029/2010JF001875>
- Barchi, M. (1998). The CROP 03 profile: a synthesis of results on deep structures of the Northern Apennines. *Mem. Soc. Geol. It.*, 52, 383-400
- Barchi, M. R., Alvarez, W., & Shimabukuro, D. H. (2012). The Umbria-Marche Apennines as a double orogen: observations and hypotheses. *Italian Journal of Geosciences*, 131(2), 258-271. <https://doi.org/10.3301/IJG.2012.17>
- Barchi, M. R., & Mirabella, F. (2009). The 1997–98 Umbria–Marche earthquake sequence: “Geological” vs. “seismological” faults. *Tectonophysics*, 476(1-2), 170-179. <https://doi.org/10.1016/j.tecto.2008.09.013>

- Basilici, M., Ascione, A., Megna, A., Santini, S., Tavani, S., Valente, E., & Mazzoli, S. (2020). Active deformation and relief evolution in the western Lurestan region of the Zagros mountain belt: new insights from tectonic geomorphology analysis and finite element modeling. *Tectonics*, 39(12), e2020TC006402. <https://doi.org/10.1029/2020TC006402>
- Bigi, S., Cantalamessa, G., Centamore, E., Didaskalou, P., Micarelli, A., Nisio, S., et al. (1997). The periadriatic basin (Marche-Abruzzi sector, central Italy) during the Plio-Pleistocene. *Giornale di Geologia*, 59(1-2), 245-259.
- Bishop, P. (2007). Long-term landscape evolution: linking tectonics and surface processes. *Earth Surface Processes and Landforms: the Journal of the British Geomorphological Research Group*, 32(3), 329-365. <https://doi.org/10.1002/esp.1493>
- Bitonte, R., Livio, F. A., Mazzoli, S., Bellentani, G., Di Cesare, L., Dall'Igna, M., et al. (2021). Frontal accretion vs. foreland plate deformation: Discriminating the style of post-collisional shortening in the Apennines. *Journal of Structural Geology*, 145, 104290. <https://doi.org/10.1016/j.jsg.2021.104290>
- Brogi, A., Capezzuoli, E., Martini, I., Picozzi, M., & Sandrelli, F. (2014). Late Quaternary tectonics in the inner Northern Apennines (Siena Basin, southern Tuscany, Italy) and their seismotectonic implication. *Journal of Geodynamics*, 76, 25-45. <https://doi.org/10.1016/j.jog.2014.03.001>
- Bull, W. B. (2008). *Tectonic geomorphology of mountains: a new approach to paleoseismology*. John Wiley & Sons. <https://doi.org/10.1002/9780470692318>
- Bull, W.B. & McFadden, L.D. (1977) Tectonic Geomorphology North and South of the Garlock Fault, California. In: Doehring, D.O., Ed., *Geomorphology in Arid Regions: A Proceedings Volume of the 8th Annual Geomorphology Symposium*, State University of New York, Binghamton, 23-24 September 1977, 115-138. <https://doi.org/10.4324/9780429299230-5>
- Burbank, D. W & Anderson, R. S. (2011). *Tectonic Geomorphology*. John Wiley & Sons, Chichester. <https://doi.org/10.1002/9781444345063.refs>
- Buscher, J. T., Ascione, A., & Valente, E. (2017). Decoding the role of tectonics, incision and lithology on drainage divide migration in the Mt. Alpi region, southern Apennines, Italy. *Geomorphology*, 276, 37-50. <https://doi.org/10.1016/j.geomorph.2016.10.003>
- Calamita, F., Cello, G., Deiana, G., & Paltrinieri, W. (1994). Structural styles, chronology rates of deformation, and time-space relationships in the Umbria-Marche thrust system (central Apennines, Italy). *Tectonics*, 13(4), 873-881. <https://doi.org/10.1029/94TC00276>

- Calamita, F., Deiana, G., Invernizzi, C., & Pizzi, A. (1991). Tettonica. *L'ambiente fisico delle Marche. Regione Marche Assessorato Urbanistica Ed. Selca Firenze*, 69-80.
- Calamita, F., & Pizzi, A. (1994). Recent and active extensional tectonics in the southern Umbro-Marchean Apennines (central Italy). *Memorie della Società Geologica Italiana*, 48, 541-548.
- Cantalamesa, G., Centamore, E., Chiocchini, U., Colalongo, M. L., Micarelli, A., Nanni, T., et al. (1986). Il Plio-Pleistocene delle Marche. *Studi geologici camerti*, 61-81.
- Cantalamesa, G., & Di Celma, C. (2004). Sequence response to syndepositional regional uplift: insights from high-resolution sequence stratigraphy of late Early Pleistocene strata, Periadriatic Basin, central Italy. *Sedimentary Geology*, 164(3-4), 283-309. <https://doi.org/10.1016/j.sedgeo.2003.11.003>
- Castelli, V., & Monachesi, G. (2001). Seismic history and historical earthquake scenario for the town of Fabriano (Central Italy). *Italian Geotechnical Journal*, 35(2), 36-46.
- Cattaneo, M., Frapiccini, M., Ladina, C., Marzorati, S., & Monachesi, G. (2017). A mixed automatic-manual seismic catalog for central-eastern Italy: Analysis of homogeneity. *Annals of Geophysics*, 60(6). <https://doi.org/10.4401/AG-7333>
- Centamore, E., Fumanti, F., & Nisio, S. (2002). The central-northern Apennines geological evolution from Triassic to Neogene time. *Boll. Soc. Geol. It., Vol. Spec., 1*, 181-197.
- Centamore, E., & Nisio, S. (2003). Effects of uplift and tilting in the Central-Northern Apennines (Italy). *Quaternary international*, 101, 93-101. [https://doi.org/10.1016/S1040-6182\(02\)00092-7](https://doi.org/10.1016/S1040-6182(02)00092-7)
- Centamore, E., & Rossi, D. (2009). Neogene-Quaternary tectonics and sedimentation in the Central Apennines. *Italian Journal of Geosciences*, 128(1), 73-88. <https://doi.org/10.3301/ijg.2009.128.1.73>
- Ciccacci, S., D'Alessandro, L., Dramis, F., Fredi, P., & Pambianchi, G. (1985). Geomorphological and neotectonic evolution of the Umbria-Marche ridge northern sector. *Studi geologici camerti*, 10, 1985, pp. 7-16.
- Cipollari, P., Cosentino, D., & Gliozzi, E. (1999). Extension and compression related basins in central Italy during the Messinian Lago-Mare event. *Tectonophysics*, 315(1-4), 163-185. [https://doi.org/10.1016/S0040-1951\(99\)00287-5](https://doi.org/10.1016/S0040-1951(99)00287-5)

- Civico, R., Pucci, S., Villani, F., Pizzimenti, L., de Martini, P. M., Nappi, R., et al. (2018). Surface ruptures following the 30 October 2016 Mw 6.5 Norcia earthquake, central Italy. *Journal of Maps*, *14*(2). <https://doi.org/10.1080/17445647.2018.1441756>
- Conti, P., Cornamusini, G., & Carmignani, L. (2020). An outline of the geology of the Northern Apennines (Italy), with geological map at 1: 250,000 scale. *Italian Journal of Geosciences*, *139*(2), 149-194. <https://doi.org/10.3301/IJG.2019.25>
- Cornamusini, G., Conti, P., Bonciani, F., Callegari, I., & Martelli, L. (2017). Geology of the 'Coltre della Val Marecchia' (Romagna-Marche Northern Apennines, Italy). *Journal of Maps*, *13*(2), 207-218. <https://doi.org/10.1080/17445647.2017.1290555>
- Cosentino, D., Asti, R., Nocentini, M., Gliozzi, E., Kotsakis, T., Mattei, M., et al. (2017). New insights into the onset and evolution of the central Apennine extensional intermontane basins based on the tectonically active L'Aquila Basin (central Italy). *GSA Bulletin*, *129*(9-10), 1314-1336. <https://doi.org/10.1130/B31679.1>
- Costa, M., Chicco, J., Invernizzi, C., Teloni, S., & Pierantoni, P. P. (2021). Plio-Quaternary Structural Evolution of the Outer Sector of the Marche Apennines South of the Conero Promontory, Italy. *Geosciences*, *11*(5), 184. <https://doi.org/10.3390/geosciences11050184>
- Coward, M. P., De Donatis, M., Mazzoli, S., Paltrinieri, W., & Wezel, F. C. (1999). Frontal part of the northern Apennines fold and thrust belt in the Romagna-Marche area (Italy): Shallow and deep structural styles. *Tectonics*, *18*(3), 559-574. <https://doi.org/10.1029/1999TC900003>
- Cyr, A. J., & Granger, D. E. (2008). Dynamic equilibrium among erosion, river incision, and coastal uplift in the northern and central Apennines, Italy. *Geology*, *36*(2), 103-106. <https://doi.org/10.1130/G24003A.1>
- Deiana, G., Cello, G., Chiocchini, M., Galdenzi, S., Mazzoli, S., Pistolesi, E., et al. (2002). Tectonic evolution of the external zones of the Umbria-Marche Apennines in the Monte San Vicino-Cingoli area. *Bollettino Della Società Geologica Italiana*, *121*(1), 229-238.
- Deiana, G., Mazzoli, S., Paltrinieri, W., Pierantoni, P. P., & Romano, A. (2003). Struttura del fronte montuoso umbro-marchigiano-sabino. *Studi geologici camerti*, n. speciale, 2003, pp. 15-36.
- Della Seta, M., Del Monte, M., Fredi, P., Miccadei, E., Nesci, O., Pambianchi, G., et al. (2008). Morphotectonic evolution of the Adriatic piedmont of the Apennines: an advancement in the knowledge of the Marche-Abruzzo border area. *Geomorphology*, *102*(1), 119-129. <https://doi.org/10.1016/j.geomorph.2007.06.018>

- Dewey, J. F. (1988). Extensional collapse of orogens. *Tectonics*, 7(6), 1123-1139. <https://doi.org/10.1029/TC007i006p01123>
- Dewey, J. F., Helman, M. L., Knott, S. D., Turco, E., & Hutton, D. H. W. (1989). Kinematics of the western Mediterranean. *Geological Society, London, Special Publications*, 45(1), 265-283. <https://doi.org/10.1144/GSL.SP.1989.045.01.15>
- Di Bucci, D., Mazzoli, S., Nesci, O., Savelli, D., Tramontana, M., de Donatis, M., & Borraccini, F. (2003). Active deformation in the frontal part of the Northern Apennines: Insights from the lower Metauro River basin area (northern Marche, Italy) and adjacent Adriatic off-shore. *Journal of Geodynamics*, 36(1-2), 213-238. [https://doi.org/10.1016/S0264-3707\(03\)00048-6](https://doi.org/10.1016/S0264-3707(03)00048-6)
- Di Biase, R. A., Whipple, K. X., Heimsath, A. M., & Ouimet, W. B. (2010). Landscape form and millennial erosion rates in the San Gabriel Mountains, CA. *Earth and Planetary Science Letters*, 289(1-2), 134-144. <https://doi.org/10.1016/j.epsl.2009.10.036>
- Doglioni, C. (1995). Geological remarks on the relationships between extension and convergent geodynamic settings. *Tectonophysics*, 252(1-4), 253-267. [https://doi.org/10.1016/0040-1951\(95\)00087-9](https://doi.org/10.1016/0040-1951(95)00087-9)
- Doglioni, C., Dagostino, N., & Mariotti, G. (1998). Normal faulting vs regional subsidence and sedimentation rate. *Marine and Petroleum Geology*, 15(8), 737-750. [https://doi.org/10.1016/S0264-8172\(98\)00052-X](https://doi.org/10.1016/S0264-8172(98)00052-X)
- Dramis, F. (1992). Il ruolo dei sollevamenti tettonici a largo raggio nella genesi del rilievo appenninico. *Studi Geologici Camerti, Studi geologici camerti, n. speciale, 1992*, pp. 9-15.
- Duvall, A., Kirby, E., & Burbank, D. (2004). Tectonic and lithologic controls on bedrock channel profiles and processes in coastal California. *Journal of Geophysical Research: Earth Surface*, 109(F3). <https://doi.org/10.1029/2003jf000086>
- Eizenhöfer, P. R., McQuarrie, N., Shelef, E., & Ehlers, T. A. (2019). Landscape response to lateral advection in convergent orogens over geologic time scales. *Journal of Geophysical Research: Earth Surface*, 124, 2056-2078. <https://doi.org/10.1029/2019JF005100>
- Ellis, M. A., & Densmore, A. L. (2006). First-order topography over blind thrusts. In S. D. Willett, N. Hovius, M. T. Brandon, & D. Fisher (Eds.), *Tectonics, climate, and landscape evolution: Geological Society of America Special Paper 398*, Penrose Conference Series (pp. 251-266). Boulder, CO: The Geological Society of America, Inc. [https://doi.org/10.1130/2006.2398\(15\)](https://doi.org/10.1130/2006.2398(15))

- EMERGEO Working Group (2016). Coseismic effects of the 2016 Amatrice seismic sequence: First geological results, *Annals of Geophysics Italy*, 59 (5). doi:10.4401/ag-7195.
- England, P., & Molnar, P. (1990). Surface uplift, uplift of rocks, and exhumation of rocks. *Geology*, 18(12), 1173-1177. [https://doi.org/10.1130/0091-7613\(1990\)018<1173:SUUORA>2.3.CO;2](https://doi.org/10.1130/0091-7613(1990)018<1173:SUUORA>2.3.CO;2)
- Flint, J. J. (1974). Stream gradient as a function of order, magnitude, and discharge. *Water Resources Research*, 10(5), 969-973. <https://doi.org/10.1029/WR010i005p00969>
- Forte, A. M., Cowgill, E., & Whipple, K. X. (2014). Transition from a singly vergent to doubly vergent wedge in a young orogen: The Greater Caucasus. *Tectonics*, 33(11), 2077-2101. <https://doi.org/10.1002/2014TC003651>
- Frepoli, A., & Amato, A. (1997). Contemporaneous extension and compression in the Northern Apennines from earthquake fault-plane solutions. *Geophysical Journal International*, 129(2), 368-388. <https://doi.org/10.1111/j.1365-246X.1997.tb01589.x>
- Galadini, F., & Messina, P. (2001). Plio-Quaternary changes of the normal fault architecture in the central Apennines (Italy). *Geodinamica Acta*, 14(6), 321-344. <https://doi.org/10.1080/09853111.2001.10510727>
- Gallen, S. F., & Wegmann, K. W. (2017). River profile response to normal fault growth and linkage: An example from the Hellenic forearc of south-central Crete, Greece. *Earth Surface Dynamics*, 5(1), 161-186. <https://doi.org/10.5194/esurf-5-161-2017>
- Gentili, B., Pambianchi, G., Aringoli, D., Materazzi, M., & Giacometti, M. (2017). Pliocene-Pleistocene geomorphological evolution of the Adriatic side of central Italy. *Geologica Carpathica*, 68(1), 6. <https://doi.org/10.1515/geoca-2017-0001>
- Hack, J. T. (1957). *Studies of longitudinal stream profiles in Virginia and Maryland* (Vol. 294). US Government Printing Office. <https://doi.org/10.3133/pp294B>
- ISIDE Working Group. (2007). Italian Seismological Instrumental and Parametric Database (ISIDE). Istituto Nazionale di Geofisica e Vulcanologia (INGV). <https://doi.org/10.13127/ISIDE>
- Keller, J. V. A., Minelli, G., & Pialli, G. (1994). Anatomy of late orogenic extension: the Northern Apennines case. *Tectonophysics*, 238(1-4), 275-294. [https://doi.org/10.1016/0040-1951\(94\)90060-4](https://doi.org/10.1016/0040-1951(94)90060-4)

- Keller, A. E., & Pinter, N. (2002). *Active Tectonics and Earthquakes, Uplift, and Landscape*, second ed. Prentice Hall, London.: Vol. Prentice Hall (second ed.).
- Kirby, E., & Whipple, K. (2001). Quantifying differential rock-uplift rates via stream profile analysis. *Geology*, 29(5), 415-418. [https://doi.org/10.1130/0091-7613\(2001\)029<0415:QDRURV>2.0.CO;2](https://doi.org/10.1130/0091-7613(2001)029<0415:QDRURV>2.0.CO;2)
- Lanari, R., Fellin, M. G., Faccenna, C., Balestrieri, M. L., Pazzaglia, F. J., Youbi, N., & Maden, C. (2020). Exhumation and surface evolution of the western high atlas and surrounding regions as constrained by low-temperature thermochronology. *Tectonics*, 39(3), e2019TC005562.
- Lavecchia G., (1985). Il sovrascorrimento dei Monti Sibillini: analisi strutturale e cinematica. *Bollettino della Società Geologica Italiana*, 104(1), 161-194.
- Lavecchia, G., Minelli, G., & Piali, G. (1988). The Umbria-Marche arcuate fold belt (Italy). *Tectonophysics*, 146(1-4), 125-137. [https://doi.org/10.1016/0040-1951\(88\)90086-8](https://doi.org/10.1016/0040-1951(88)90086-8).
- Mancini, M., Cavinato, G. P., Blum, M., Marriot, S., & Leclair, S. (2005). The Middle Valley of the Tiber River, central Italy: Plio-Pleistocene fluvial and coastal sedimentation, extensional tectonics and volcanism. *Fluvial Sedimentology VII. IAS Spec. Publ*, 35, 373-396. <https://doi.org/10.1002/9781444304350.ch20>
- Martini, I. P., & Sagri, M. (1993). Tectono-sedimentary characteristics of Late Miocene-Quaternary extensional basins of the Northern Apennines, Italy. *Earth-Science Reviews*, 34(3), 197-233. [https://doi.org/10.1016/0012-8252\(93\)90034-5](https://doi.org/10.1016/0012-8252(93)90034-5)
- Materazzi, M., Bufalini, M., Dramis, F., Pambianchi, G., Gentili, B., & Di Leo, M. (2022). Active tectonics and paleoseismicity of a transverse lineament in the Fabriano valley, Umbria-Marche Apennine (central Italy). *International Journal of Earth Sciences*, 1-11. <https://doi.org/10.1007/s00531-022-02198-x>
- Mayer, L., Menichetti, M., Nesci, O., & Savelli, D. (2003). Morphotectonic approach to the drainage analysis in the North Marche region, central Italy. *Quaternary International*, 101, 157-167. [https://doi.org/10.1016/S1040-6182\(02\)00098-8](https://doi.org/10.1016/S1040-6182(02)00098-8)
- Mazzoli, S., & Helman, M. (1994). Neogene patterns of relative plate motion for Africa-Europe: some implications for recent central Mediterranean tectonics. In *Active continental margins- Present and past* (pp. 464-468). Springer, Berlin, Heidelberg. <https://doi.org/10.1007/BF00210558>

- Mazzoli, S., Macchiavelli, C., & Ascione, A. (2014). The 2013 Marche offshore earthquakes: new insights into the active tectonic setting of the outer northern Apennines. *Journal of the Geological Society*, *171*(4), 457-460. <https://doi.org/10.1144/jgs2013-091>
- Mazzoli, S., Santini, S., Macchiavelli, C., & Ascione, A. (2015). Active tectonics of the outer northern Apennines: Adriatic vs. Po Plain seismicity and stress fields. *Journal of Geodynamics*, *84*, 62-76, <https://doi.org/10.1016/j.jog.2014.10.002>.
- Mazzoli, S., Pierantoni, P. P., Borraccini, F., Paltrinieri, W., & Deiana, G. (2005). Geometry, segmentation pattern and displacement variations along a major Apennine thrust zone, central Italy. *Journal of Structural Geology*, *27*(11), 1940-1953. <https://doi.org/10.1016/j.jsg.2005.06.002>
- Molin P. & Fubelli G. (2005) - Morphometric evidence of the topographic growth of the Central Apennines. *Geografia Fisica e Dinamica Quaternaria*, *28*(3), 47-61.
- Monachesi, G., Castelli, V., & Vasapollo, N. (1991). Historical earthquakes in Central Italy: case histories in the Marche area. *Tectonophysics*, *193*(1-3), 95-107. [https://doi.org/10.1016/0040-1951\(91\)90191-T](https://doi.org/10.1016/0040-1951(91)90191-T)
- Nesci, O., & Savelli, D. (2003). Diverging drainage in the Marche Apennines (central Italy). *Quaternary International*, *101*, 203-209. [https://doi.org/10.1016/S1040-6182\(02\)00102-7](https://doi.org/10.1016/S1040-6182(02)00102-7)
- Nesci, O., Savelli, D., & Troiani, F. (2012). Types and development of stream terraces in the Marche Apennines (central Italy): a review and remarks on recent appraisals. *Géomorphologie: relief, processus, environnement*, *18*(2), 215-238. <https://doi.org/10.4000/geomorphologie.9838>
- Pace, P., Scisciani, V., Calamita, F., Butler, R. W., Iacopini, D., Esestime, P., & Hodgson, N. (2015). Inversion structures in a foreland domain: seismic examples from the Italian Adriatic Sea. *Interpretation*, *3*(4), SAA161-SAA176. <https://doi.org/10.1190/INT-2015-0013.1>
- Patacca, E., Sartori, R., & Scandone, P. (1990). Tyrrhenian basin and Apenninic arcs: kinematic relations since late Tortonian times. *Memorie della Società Geologica Italiana*, *45*, 425-451.
- Pazzaglia, F. J., & Fisher, J. A. (2022). A reconstruction of Apennine uplift history and the development of transverse drainages from longitudinal profile inversion. In *From the Guajira Desert to the Apennines, and from Mediterranean Microplates to the Mexican Killer Asteroid: Honoring the Career of Walter Alvarez*. Geological Society of America. [https://doi.org/10.1130/2022.2557\(09\)](https://doi.org/10.1130/2022.2557(09))



- Pazzaglia, F. J., Gardner, T. W., & Merritts, D. J. (1998). Bedrock fluvial incision and longitudinal profile development over geologic time scales determined by fluvial terraces. *Geophysical Monograph-American Geophysical Union*, *107*, 207-236. <https://doi.org/10.1029/GM107p0207>
- Pérez-Peña, J. V., Al-Awabdeh, M., Azañón, J. M., Galve, J. P., Booth-Rea, G., & Notti, D. (2017). SwathProfiler and NProfiler: Two new ArcGIS Add-ins for the automatic extraction of swath and normalized river profiles. *Computers & Geosciences*, *104*, 135-150. <https://doi.org/10.1016/j.cageo.2016.08.008>
- Perron, J. T., & Royden, L. (2013). An integral approach to bedrock river profile analysis. *Earth surface processes and landforms*, *38*(6), 570-576. <https://doi.org/10.1002/esp.3302>
- Pierantoni, P. P., Chicco, J., Costa, M., & Invernizzi, C. (2019). Plio-Quaternary transpressive tectonics: a key factor in the structural evolution of the outer Apennine–Adriatic system, Italy. *Journal of the Geological Society*, *176*(6), 1273-1283. <https://doi.org/10.1144/jgs2018-199>
- Pierantoni, P., Deiana, G., & Galdenzi, S. (2013). Stratigraphic and structural features of the Sibillini mountains (Umbria-Marche Apennines, Italy). *Italian Journal of Geosciences*, *132*(3), 497-520. <https://doi.org/10.3301/IJG.2013.08>
- Porreca, M., Minelli, G., Ercoli, M., Brobia, A., Mancinelli, P., Cruciani, F., et al. (2018). Seismic reflection profiles and subsurface geology of the area interested by the 2016–2017 earthquake sequence (Central Italy). *Tectonics*, *37*(4), 1116-1137. <https://doi.org/10.1002/2017TC004915>
- Ricci Lucchi, F. (1986). The Oligocene to Recent foreland basins of the northern Apennines. In *Foreland basins* (Vol. 8, pp. 105-139). Blackwell Scientific Oxford.
- Rovida, A., Locati, M., Camassi, R., Lolli, B., Gasperini, P., & Antonucci, A. (2022). Catalogo Parametrico dei Terremoti Italiani CPTI15, versione 4.0. <https://doi.org/10.13127/cpti/cpti15.4>
- Royden, L., & Taylor Perron, J. (2013). Solutions of the stream power equation and application to the evolution of river longitudinal profiles. *Journal of Geophysical Research: Earth Surface*, *118*(2), 497-518. <https://doi.org/10.1002/jgrf.20031>
- Santini, S., Saggese, F., Megna, A., & Mazzoli, S. (2011). A note on central-northern Marche seismicity: new focal mechanisms for events recorded in years 2003-2009. *Bollettino di Geofisica Teorica ed Applicata*, *52*(4). <https://doi.org/10.4430/bgta0025>
- Schildgen, T. F., Cosentino, D., Caruso, A., Buchwaldt, R., Yıldırım, C., Bowring, S. A., et al. (2012). Surface expression of eastern Mediterranean slab dynamics: Neogene topographic and

- structural evolution of the southwest margin of the Central Anatolian Plateau, Turkey. *Tectonics*, 31(2). <https://doi.org/10.1029/2011TC003021>
- Schwanghart, W., & Kuhn, N. J. (2010). TopoToolbox: A set of Matlab functions for topographic analysis. *Environmental Modelling & Software*, 25(6), 770-781. <https://doi.org/10.1016/j.envsoft.2009.12.002>
- Schwanghart, W., & Scherler, D. (2014). TopoToolbox 2—MATLAB-based software for topographic analysis and modeling in Earth surface sciences. *Earth Surface Dynamics*, 2(1), 1-7. <https://doi.org/10.5194/esurf-2-1-2014>
- Scisciani, V., Agostini, S., Calamita, F., Pace, P., Cilli, A., Giori, I., & Paltrinieri, W. (2014). Positive inversion tectonics in foreland fold-and-thrust belts: a reappraisal of the Umbria–Marche Northern Apennines (Central Italy) by integrating geological and geophysical data. *Tectonophysics*, 637, 218-237. <https://doi.org/10.1016/j.tecto.2014.10.010>
- Scotti, V. N., Molin, P., Faccenna, C., Soligo, M., & Casas-Sainz, A. (2014). The influence of surface and tectonic processes on landscape evolution of the Iberian Chain (Spain): Quantitative geomorphological analysis and geochronology. *Geomorphology*, 206, 37-57. <https://doi.org/10.1016/j.geomorph.2013.09.017>
- Sembroni, A., Molin, P., Soligo, M., Tuccimei, P., Anzalone, E., Billi, A., et al. (2020). The uplift of the Adriatic flank of the Apennines since the Middle Pleistocene: New insights from the Tronto River basin and the Acquasanta Terme Travertine (central Italy). *Geomorphology*, 352, 106990. <https://doi.org/10.1016/j.geomorph.2019.106990>
- Snyder, N. P., Whipple, K. X., Tucker, G. E., & Merritts, D. J. (2000). Landscape response to tectonic forcing: Digital elevation model analysis of stream profiles in the Mendocino triple junction region, northern California. *Geological Society of America Bulletin*, 112(8), 1250-1263. [https://doi.org/10.1130/0016-7606\(2000\)112<1250:LRTTFD>2.0.CO;2](https://doi.org/10.1130/0016-7606(2000)112<1250:LRTTFD>2.0.CO;2)
- Stock, J. D., & Montgomery, D. R. (1999). Geologic constraints on bedrock river incision using the stream power law. *Journal of Geophysical Research: Solid Earth*, 104(B3), 4983-4993. <https://doi.org/10.1029/98JB02139>
- Stucchi, M., Monachesi, G., & Mandrelli, F. M. (1991). Investigation of 18th century seismicity in central Italy in the light of the 1741 Fabriano earthquake. *Tectonophysics*, 193(1-3), 65-82. [https://doi.org/10.1016/0040-1951\(91\)90189-Y](https://doi.org/10.1016/0040-1951(91)90189-Y)

- Turco, E., Macchiavelli, C., Penza, G., Schettino, A., & Pierantoni, P. P. (2021). Kinematics of deformable blocks: application to the opening of the tyrrhenian basin and the formation of the apennine Chain. *Geosciences*, *11*(4), 177. <https://doi.org/10.3390/geosciences11040177>
- Valente, E., Buscher, J. T., Jourdan, F., Petrosino, P., Reddy, S. M., Tavani, S., et al. (2019). Constraining mountain front tectonic activity in extensional setting from geomorphology and Quaternary stratigraphy: A case study from the Matese ridge, southern Apennines. *Quaternary Science Reviews*, *219*, 47-67. <https://doi.org/10.1016/j.quascirev.2019.07.001>
- Veneri F. (1986). La colata gravitativa della Val Marecchia. Studi geologici camerti, n. speciale, 1986, pp. 83-87.
- Wegmann, K. W., & Pazzaglia, F. J. (2009). Late Quaternary fluvial terraces of the Romagna and Marche Apennines, Italy: Climatic, lithologic, and tectonic controls on terrace genesis in an active orogen. *Quaternary Science Reviews*, *28*(1–2), 137–165. <https://doi.org/10.1016/j.quascirev.2008.10.006>
- Whipple, K. X., & Tucker, G. E. (1999). Dynamics of the stream-power river incision model: Implications for height limits of mountain ranges, landscape response timescales, and research needs. *Journal of Geophysical Research: Solid Earth*, *104*(B8), 17661-17674. <https://doi.org/10.1029/1999JB900120>
- Whipple, K. X., Wobus, C., Crosby, B., Kirby, E., & Sheehan, D. (2007). New tools for quantitative geomorphology: Extraction and interpretation of stream profiles from digital topographic data. *GSA short course*, *506*, [Http://Geomorphools.Org/Tools/StPro/Tutorials/StPro\\_UserGuidees\\_Final.Pdf](Http://Geomorphools.Org/Tools/StPro/Tutorials/StPro_UserGuidees_Final.Pdf)
- Whittaker, A. C., Attal, M., Cowie, P. A., Tucker, G. E., & Roberts, G. (2008). Decoding temporal and spatial patterns of fault uplift using transient river long profiles. *Geomorphology*, *100*(3-4), 506-526. <https://doi.org/10.1016/j.geomorph.2008.01.018>
- Wiemer, S. (2001). A software package to analyze seismicity: ZMAP. *Seismological Research Letters*, *72*(3), 373-382. <https://doi.org/10.1785/gssrl.72.3.373>
- Willett, S. D., Slingerland, R., & Hovius, N. (2001). Uplift, shortening and steady state topography in active mountain belts. *American Journal of Science*, *301*, 455–485. <https://doi.org/10.2475/ajs.301.4-5.455>
- Zaprowski, B. J., Pazzaglia, F. J., & Evenson, E. B. (2005). Climatic influences on profile concavity and river incision. *Journal of Geophysical Research: Earth Surface*, *110*(F3). <https://doi.org/10.1029/2004JF000138>

## 6. DISCUSSION AND CONCLUSIONS

One of the key elements of modern probabilistic seismic hazard assessment is represented by the identification and characterization of the earthquake source, necessary to define the seismic source model based on earthquake catalogues, active faults, and present-day tectonic regime.

Blind faults, namely hidden subsurface faults that do not rupture the surface often covered by unconsolidated sediments, can be responsible of unexpected, damaging, and fatal earthquakes, representing a major seismic hazard criticality for urban areas and for the building heritage in general. For this reason, the detection and geographical representation of active blind faults are essential to a reliable seismic hazard assessment of a region; however, this work remains highly challenging, especially in seismically silent areas where no significant earthquakes were recorded recently and a significant lack of instrumentally recorded seismicity (i.e.  $M_L > 2.5$  earthquakes) is experienced, with the few small-size available instrumental seismic events that are not enough accurate to depict fault geometries.

In this regard, recent large seismic sequences may provide new useful data such as in situ coseismic deformation (Pucci et al., 2017; Civico et al., 2018; Tondi et al., 2021) which, together with large number of accurate hypocenters locations (Ercoli et al., 2020; Porreca et al., 2020; Spallarossa et al., 2021), and remote sensing techniques (Bignami et al., 2016; Valente et al., 2019), provide important details on fault architecture, geometrical and kinematic features of seismogenic sources, through a multidisciplinary approach (Amato et al., 2017), contributing to the identification and detection of hidden structures for assessing and improving the current seismic maps.

The south-eastern Europe, including Italy, Albania, Greece and Turkey, represents a crucial area because of the highest seismic hazard in Europe (<http://www.efehr.org>) and, at the same time, the large amount of seismic data recorded in the last decades by the respective accelerometric networks. The present PhD project fits into this framework, focusing on multiple studies conducted in central Italy (e.g. the 2016-17 seismic sequence), but also analyzing the southern Balkans (e.g. 2019-2020 Albania seismic sequences) to test an integrated methodological approach based on available geological data together with the analysis of high resolution seismological data and performing the stress inversion analysis to confirm the kinematic of the seismogenic sources identified by the interpretation of oil and gas seismic reflection profiles. Furthermore, the GIS based morphotectonic analysis is also used to study

the correlation between the previously identified structures and the neotectonic processes acting at surface.

The Albania case study (Chapter 2) has been chosen as a pilot area to work on high-resolution seismological data and stress inversion techniques.

The seismological data are related to the 2019-2020 seismic sequence and were used to identify the fault source of the M 6.4 mainshock and to improve the knowledge about the Albanian fold and thrust belt evolution. The comprehensive picture of the structural architecture of the northern sector of the outer Albanides shows analogies and similarities with the central Apennines (study area), such as lack of geological information, strong earthquakes in the past and thick Periadriatic deposits that cover the faults.

The critical analysis of literature on the seismicity of Albania shows that the strongest earthquakes are located in 3 well-defined seismic belts:

- 1) The Ionian-Adriatic NW-SE trending coastal earthquake belt at the eastern margin of the Adria microplate, characterized by compressive structures.
- 2) The Peshkopi-Korça earthquake belt, in the internal Albanides, where N-S normal faults prevail.
- 3) The Vlora-Elbasan transfer zone, which represents the most relevant NE-SW transversal lineaments, crosscutting perpendicularly both the internal and External Albanides. The earthquake epicenters are concentrated mostly along active faults or fault zones. These topographically and structurally well-defined faults, played and still play an essential role during all the tectonic development of Albania.

a critical reassessment of published geological sections and subsurface data, integrated with the new seismological datasets made available by the 2019–20 seismic sequence, allowed to unravel the basement-involved thrusting style characterizing the frontal portion of the fold–thrust belt at the latitude of Durrës. The hypocentral distribution analysis suggested that the 2019–20 seismic events are located from 10 to 36 km depth and tend to deepen moving to east. The shallower seismic events could have involved rupturing along the seismogenic sources proposed in the DISS catalogue. However, most of the earthquakes, including the Mw 6.4 main shock (22 km), ruptured a basement fault that we identified as the Northern Albanide Frontal Thrust (NAFT), nucleated within the crystalline basement, much deeper than the seismogenic source reported in the DISS database.

Moving to the Italian territory, in the outer Marche region, a GIS-based dataset was developed in the initial phase of the Ph.D. research. It consisted in the integration of both historical and relocated instrumental seismicity with the interpretation of hundreds of kilometers of seismic reflection profiles and surface geological information and is used to perform a multi-methodological approach through the combination of seismotectonic and morphotectonic studies.

Seismic reflection profiles of the central Apennines have been acquired from the oil & gas industry and their interpretation calibrated with well logs (Chapter 3). They allowed the identification of the faults architectures in the South Marche offshore (south to Conero promontory), and the definition of the Plio-Quaternary structural evolution of the outer sector of the Marche Apennines through the reconstruction of the thicknesses and distribution of the Lower Pliocene stratigraphic sequence

Five seismic transects were built merging several seismic reflection profiles, which highlighted, from west to east: (i) the N–S Amandola-positive flower structure, (ii) a wide syncline with an almost N–S trend to the west, (iii) the Coastal Structure with an NNW–SSE trend in the central portion, and (iv) the offshore NW–SE-trending gentle-flower structure system.

The Coastal Structure (Fig. 6.1) represents the most important structural element of the area, characterized by shallow east-verging thrusts involving the Lower–Middle Pliocene sequence and, marginally, the Upper-Miocene sequence. Under this structure, an east-dipping reverse fault and a slightly west-dipping sub-vertical fault reaching the relevant depths ( $>4$  s TWT), are present. Quaternary deposits were likely involved in the deformation of the upper and frontal sectors of the Coastal Structure. This structure was formed starting during the Middle Pliocene, and its deformation continued until the Upper Pliocene, being still active in some parts during the Quaternary, as shown by fairly significant earthquake sequences ( $M_w = 5$ , 1987 Porto San Giorgio sequence - Riguzzi et al. 1989; Battimelli et al. 2019 and  $M_w = 4$ , 2022 Costa Marchigiana-Picena, [ISIDe Working Group, 2007](#)) that occurred recently. However, no seismic activity was detected for the flower structures of the Adriatic offshore, where the Quaternary deposits seem to be not involved in the deformation processes.

The Coastal Structure continues southward, in the Abruzzo region, with quite similar litho–structural characteristics and ages of deformation, meanwhile in the northern portion of the study area, the described structural elements are interrupted along a transversal ENE–WSW-oriented structure approximately located immediately south of the Conero Promontory. This latter, is identified by NW-SE seismic reflection profiles and represents one of the main

transversal elements in the Marche outer sector, interrupting both the onshore and offshore NW-SE identified structures and separating the area in two principal blocks with very different structural setting (age of deformation, geometries, and directions) and evolutionary characteristics as shown by different thickness of Plio-Pleistocene deposits in the two adjacent areas.

The existence of NE-SE transverse faults has been highlighted in literature by various authors, particularly in the Marche-Abruzzo onshore (see Centamore et al. 1991; Pierantoni et al. 2017; Pierantoni et al. 2019 and reference therein) and in Northern Apennines (Pascucci et al., 2007; Brogi and Fabbrini, 2009; Brogi and Capezzuoli, 2014; Brogi et al. 2014; Mirabella et al. 2022). The transversal lineaments in the Apennines have been interpreted in the literature as transfer zones, transfer faults, lateral thrust ramps, strike, and oblique slip faults. These latter may have acted in all of the different ways mentioned during different times of the orogenic and post-orogenic phases.

Based on what emerged from the study of seismic transects, the baseline instrumental seismicity ( $M > 1$ ) and the stress inversion analysis of available focal mechanisms were particularly useful to characterize the activity and role of the transversal structures of the central Apennines (see Chapter 4).

The low magnitude seismic sequences (ISIDe Working Group, 2007) affecting the Apennine outer sector in the last three decades allowed the identification and characterization of four sub-parallel ENE-WSW transversal fault systems (Fig. 6.1):

- The Cattolica Fault System (CFS)
- The Metauro-Fano Fault System (MFFS)
- The Cupramontana Fault System (CUFS)
- The South Conero Fault System (SCFS)

The integrated analysis of epicenter spatial distribution, hypocenter depth and fault plane solutions indicate that coseismic slip occurred dominantly along steep ENE-WSW striking faults, involving the crystalline basement. For the Cattolica fault system, responsible of the Mw 5.8, Riminese 1916 earthquakes, there are no elements to establish its kinematics with certainty. Nevertheless, the *en-echelon* arrangement suggests that it is marked by a transcurrent kinematics.

Furthermore, the results of the stress inversion analysis, performed using the WinTensor software, applying the PBT kinematic axes method on available nodal planes correlated with

the CUFS, SCFS and MFFS, show left-lateral kinematics with a maximum horizontal compression trending N-S.

This study also highlighted the separation of the external Apennine sector into blocks with different structural characteristics and trends.

A large-scale morphotectonic approach combined with geological and seismological data was used (Chapter 5) to highlight the role of active tectonics at surface, to describe differences in the Quaternary evolution of central Apennines foothills, and to highlight further features of the blocks of the external area. In this approach, a geomorphological characterization at the drainage basin-scale was carried out using the topographic analysis as elevation maps and swath profiles performed in MATLAB and GIS environment. Therefore, integrating the analysis of 18 main river basins and using morphometric parameters to perform the slope *vs* area analysis, such as the normalized steepness channel (K<sub>sn</sub> index), allowed to discriminate anomalies and perturbation (knickpoints or knickzones) acting on river long profiles due to erosional or tectonic processes.

About 50 knickpoints were identified that are not controlled by lithology. Two segments separated by one main knickpoint and some minor knickpoints characterize the majority of the longitudinal profiles. The profile segments separated by knickpoints have different *k<sub>sn</sub>* values upstream and downstream of the knickpoints.

The results of the morphotectonic approach show how the boundaries between sectors (A, B, C in figure 6.1) characterized by different active tectonic behavior and thickness of Plio-Pleistocene deposits roughly coincide with major transversal fault systems, segmenting the outer portion of the fold and thrust belt in the Marche foothills. This feature suggests that such transversal systems mark the loci of long-lived, deep-seated fault zones that exert a major control on the active tectonic behavior of large crustal blocks.

These pre-existing deep-seated faults of the foreland plate appear to have controlled fold and thrust belt propagation and related segmentation of the deformed Plio-Pleistocene foredeep. (Pierantoni et al. 2019, Costa et al. 2021).

The fact that the crustal sectors (A, B, C), characterized by different active tectonic behavior, extend SW-ward into the axial zone of the mountain chain (i.e., also in the hanging wall of the major Olevano-Antrdoco-M.ti Sibillini – OAMS - thrust defining the mountain front), suggest that the transversal ‘lineaments’ mapped in the frontal part of the fold and thrust belt mark major crustal structures extending beneath the high mountain chain.



Along the Apennine chain, where the ongoing extension prevail, the deep-seated transversal faults interact with the active normal faults, segmenting the Quaternary extensional system in the axial zone of the chain and bounding the intramountain basins.

This concept is consistent with seismicity distribution, and, with the abrupt northward truncation of the seismic events associated with the 2016-2017 Amatrice-Visso-Norcia and the 1997 Colfiorito seismic sequences along the boundary between block C and block B.

A general continuity of transversal major structures from the Adriatic Sea, through the Marche foothills, to the axial zone of the chain is also consistent with such structures representing long-lived faults in the basement of the foreland plate. This model implies a recent upward propagation of such structures into the hanging wall of the OAMS Thrust. However, this is not at all surprising, considering the clear linkage between deep and shallow seismogenic fault segments cutting across the OAMS Thrust, which is offset by the Quaternary normal faults. WSW-ENE transversal faults also influence many aspects of the present-day landscape (e.g., capturing many river courses, flowing in ENE direction to the coastline) constituting one of the main structural features in the Central Apennines sector.

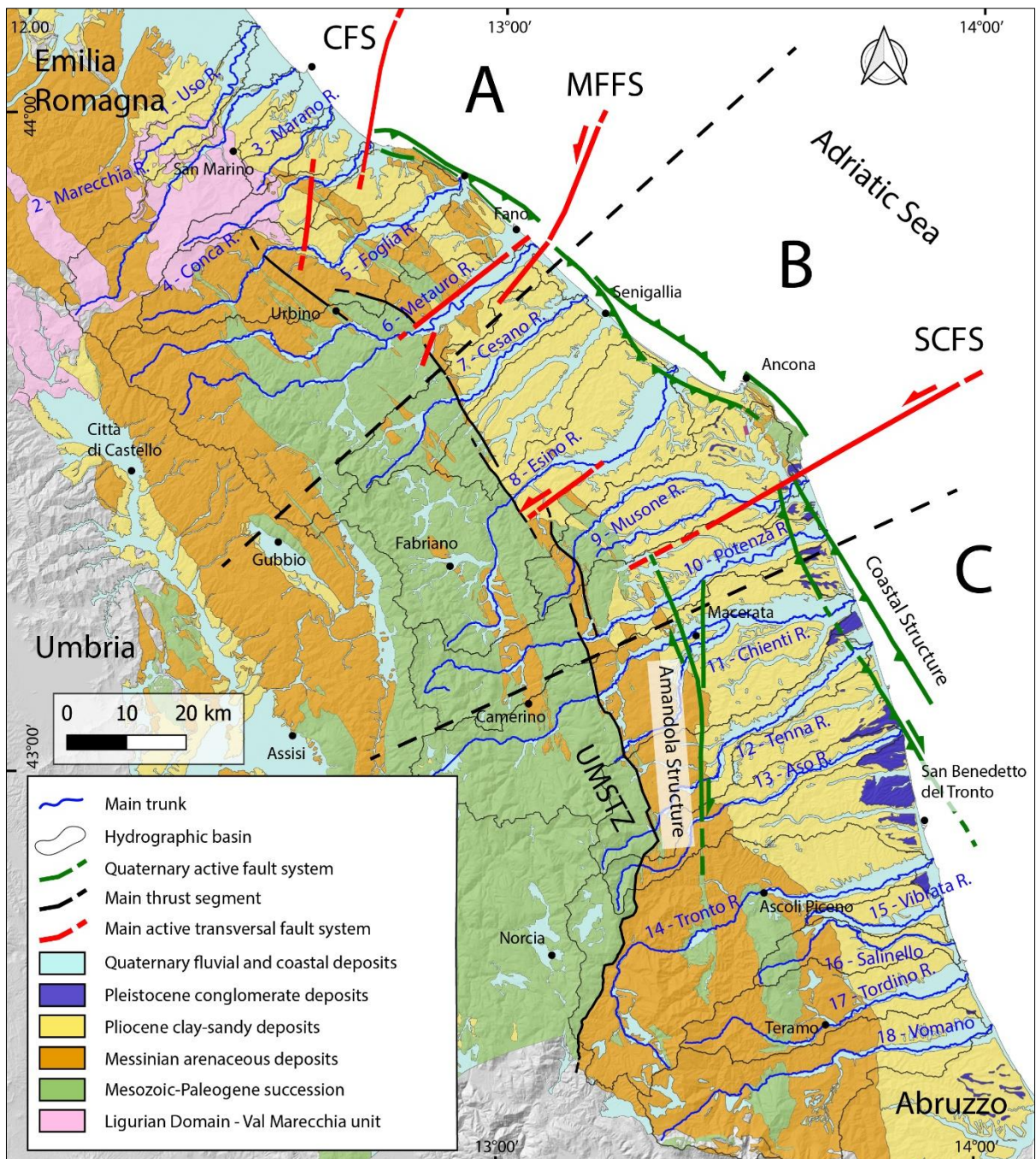


Fig. 6.1 - Geological sketch map showing the major active and seismogenic fault systems identified and discussed in the present work.

## 6.1. Implication for seismic hazard improvement

Small blind faults capable of infrequent moderate-size earthquakes clearly produce only subtle displacement of the ground surface. Therefore, it does not surprise those classical geological investigations fall short in detecting such displacement, even after it accumulated over several seismic cycles.

The multi-methodological approach proposed in this research, combining geological, seismological, geophysical and morphotectonic analysis, allowed to map hidden signals of potential seismogenic faults. Some of these faults were previously unknown. Part of the detected structures show a relationship with instrumental seismicity but other, which according to geological or geophysical data have been active in Plio-Quaternary times, are not seismogenic or their slip-rates are too low to produce seismicity in the time span covered by the seismic catalogue.

Following the model proposed by DISS for the Adriatic sector of central Apennines, NW–SE-trending Quaternary normal faults in the inner sector and active thrusts in the outer sector have been considered as the only active seismogenic sources (Mazzoli et al. 2014; Costa et al. 2021). However, the seismological evidence provided by this study also highlight the presence of ENE-WSW transversal structures acting as seismic sequences barrier within the Apennine chain (passive role) and as active seismogenic structures in the external sector of the Marche Region.

An enhanced seismotectonic model for the Adriatic sector of the outer central Apennines should take into account the key role played by such deep-seated and long-lived inherited crustal faults characterized by dominant strike-slip kinematics, similarly, to faults kinematic present in the Gargano sector.

The results emerging from this thesis work contribute to the improvement of knowledge about the seismotectonic settings of the area, with the identification of some seismogenic sources, and a better definition of the style and fault architecture which are essential input to raise the reliability of probabilistic seismic hazard models and maps. In fact, the source characteristic as fault geometry and magnitude are important parameters used to perform the Ground-Motion Prediction Equations (GMPE) estimating the peak ground acceleration related to earthquakes and to draw a new fault system based probabilistic seismic hazard map.

In this regard new models and methodologies of seismic hazard assessment will be taken into consideration to update the Italian building code [NTC, 2018], currently based on MPS04 (Stucchi et al. 2004), defining the best anti-seismic construction techniques for building civil houses or public infrastructures; this will in turn reduce the seismic vulnerability of the building heritage and therefore the mitigation of seismic risks in densely populated areas of the central Apennines and worldwide.

## 6.2. Further works

Determining the fault parameters of an earthquake is fundamental to better understanding the seismotectonic character of a region, and in turn the potential future seismicity in surrounding areas.

Crustal deformation may precede and/or succeed earthquake occurrences. Continuous monitoring of the crustal deformation has become an essential task for geo-observatories and fast response systems in term of seismic hazard mitigation. Due to non-linear behaviour of the crustal deformation fields in time and space, measuring these movements is often difficult using only conventional geodetic methods, and hence innovative techniques of monitoring and analysis are required. In the recent years, the growing diffusion of the InSAR technique combined with GPS data provided an innovated approach for the estimation of the fault area and slip.

With the advancement of Synthetic Aperture Radar (SAR) satellite missions, Interferometric SAR (InSAR) has become an established method to measure the deformation of Earth's surface caused by major seismic events ( $M > 6$ ), greatly improving our ability to observe active tectonic processes. In fact, InSAR offers an alternative approach, other than seismology, to provide independent measures of fault location, depth, and orientation.

The accuracy of the millimeter-scale measurements made so far by the SAR technique, as well as the multi-temporal analysis methodologies, have provided impressive images of surface displacements in areas affected by strong earthquakes, and contributed to constrain the geometric and kinematic features of earthquake generating faults. The multi-temporal analysis of InSAR data is also being acknowledged as promising for the search of earthquake precursors. In fact, recent studies have clearly demonstrated the potential of InSAR to measure slow tectonic signals such as interseismic strain accumulation in places with good interferometric conditions. This, is the case of the 2009 L'Aquila earthquakes where Permanent Scatterers Synthetic Aperture Radar Interferometry (PS-InSAR) processing technique (Ferretti 2000, 2001), allowed detecting a pre-seismic vertical displacement (Nardò et al.2020). In turn, in the long term, InSAR may have the potential to produce continental scale fault maps, which identify all active structures and measure the rate of strain accumulation across them.

All these new data on location, geometry, and behavior of active faults in the Apennines, together with the constraints obtained from regional scale studies, could be transferred into modern seismic hazard analysis, and may contribute to the development of new deterministic approaches to the seismic risk prevention.

### 6.3. References

- Amato, V., Aucelli, P. P., Sessa, E. B., Cesarano, M., Incontri, P., Pappone, G., ... & Vilardo, G. (2017). Multidisciplinary approach for fault detection: Integration of PS-InSAR, geomorphological, stratigraphic and structural data in the Venafro intermontane basin (Central-Southern Apennines, Italy). *Geomorphology*, 283, 80-101.
- Battimelli, E., Adinolfi, G. M., Amoroso, O., & Capuano, P. (2019). Seismic activity in the central adriatic offshore of Italy: a review of the 1987 ML 5 Porto San Giorgio earthquake. *Seismological Research Letters*, 90(5), 1889-1901.
- Bignami, C., Valerio, E., Carminati, E., Doglioni, C., Tizzani, P., & Lanari, R. (2019). Volume unbalance on the 2016 Amatrice-Norcia (Central Italy) seismic sequence and insights on normal fault earthquake mechanism. *Scientific reports*, 9(1), 1-13.
- Brogi, A., & Fabbrini, L. (2009). Extensional and strike-slip tectonics across the Monte Amiata–Monte Cetona transect (Northern Apennines, Italy) and seismotectonic implications. *Tectonophysics*, 476(1-2), 195-209.
- Brogi, A., & Capezzuoli, E. (2014). Earthquake impact on fissure-ridge type travertine deposition. *Geological Magazine*, 151(6), 1135-1143.
- Brogi, A., Capezzuoli, E., Martini, I., Picozzi, M., & Sandrelli, F. (2014). Late Quaternary tectonics in the inner Northern Apennines (Siena Basin, southern Tuscany, Italy) and their seismotectonic implication. *Journal of Geodynamics*, 76, 25-45.
- Centamore, E.; Pambianchi, G.; Minetti, A. *Ambiente Fisico Delle Marche: Geologia Geomorfologia Idrogeologia Regione Marche*, Giunta Regionale; Firenze: S.E.L.C.A.: Florence, Italy, 1991.
- Civico, R., Pucci, S., Villani, F., Pizzimenti, L., de Martini, P. M., Nappi, R., Agosta, F., Alessio, G., Alfonsi, L., Amanti, M., Amoroso, S., Aringoli, D., Auciello, E., Azzaro, R., Baize, S., Bello, S., Benedetti, L., Bertagnini, A., Binda, G., ... Zambrano, M. (2018). Surface ruptures following the 30 October 2016 Mw 6.5 Norcia earthquake, central Italy. *Journal of Maps*, 14(2). <https://doi.org/10.1080/17445647.2018.1441756>.
- Costa, M., Chicco, J. M., Invernizzi, C., Teloni, S., and Pierantoni, P.P.. (2021). Plio–Quaternary Structural Evolution of the Outer Sector of the Marche Apennines South of the Conero Promontory, Italy. *Geosciences*, 11, 184. <https://doi.org/10.3390/geosciences11050184>.

- Ercoli, M., Forte, E., Porreca, M., Carbonell, R., Pauselli, C., Minelli, G., & Barchi, M. R. (2020). Using seismic attributes in seismotectonic research: an application to the Norcia M<sub>w</sub> = 6.5 earthquake (30 October 2016) in central Italy. *Solid Earth*, 11(2), 329-348.
- Ferretti, A., Prati, C., & Rocca, F. (2000). Nonlinear subsidence rate estimation using permanent scatterers in differential SAR interferometry. *IEEE Transactions on geoscience and remote sensing*, 38(5), 2202-2212.
- Ferretti, A., Prati, C., & Rocca, F. (2001). Permanent scatterers in SAR interferometry. *IEEE Transactions on geoscience and remote sensing*, 39(1), 8-20.
- ISIDE Working Group. (2007). Italian Seismological Instrumental and parametric Database (ISIDE). In *Istituto Nazionale di Geofisica e Vulcanologia*.
- Mazzoli, S., Macchiavelli, C., & Ascione, A. (2014). The 2013 Marche offshore earthquakes: new insights into the active tectonic setting of the outer northern Apennines. *Journal of the Geological Society*, 171(4), 457-460.
- Mirabella, F., Braun, T., Brogi, A., & Capezzuoli, E. (2022). Pliocene–Quaternary seismogenic faults in the inner Northern Apennines (Valdelsa Basin, southern Tuscany) and their role in controlling the local seismicity. *Geological Magazine*, 159(6), 853-872
- Nardò, S., Ascione, A., Mazzuoli, S., Terranova, C., & Vilardo, G. (2020). PS-InSAR data analysis: pre-seismic ground deformation in the 2009 L'Aquila earthquake region. *Bollettino di Geofisica Teorica ed Applicata*.
- Pascucci, V., Martini, I. P., Sagri, M., Sandrelli, F., & Nichols, G. (2007). Effects of transverse structural lineaments on the Neogene-Quaternary basins of Tuscany (inner Northern Apennines, Italy). *Sedimentary processes, environments and basins: a tribute to Peter Friend*, 38, 155-182.
- Pierantoni, P.P.; Centamore, E.; Costa, M. (2017). Geological and Seismological data Review of the 2009 L'Aquila Seismic Sequence (Central Apennines, Italy): Deep Seated Seismogenic Structures and Seismic Hazard. *Ital. J. Eng. Geol. Environ.* 17, 5–40.
- Pierantoni, P.P.; Chicco, J.; Costa, M.; Invernizzi, C. (2019). Plio-Quaternary Transpressive Tectonics: A Key Factor in the Structural Evolution of the Outer Apennine–Adriatic System, Italy. *J. Geol. Soc. Lond.* 2019, 176, 1273–1283.

- Porreca, M., Minelli, G., Ercoli, M., Brobia, A., Mancinelli, P., Cruciani, F., ... & Barchi, M. R. (2018). Seismic reflection profiles and subsurface geology of the area interested by the 2016–2017 earthquake sequence (Central Italy). *Tectonics*, 37(4), 1116-1137.
- Pucci, S., De Martini, P. M., Civico, R., Villani, F., Nappi, R., Ricci, T., ... & Pantosti, D. (2017). Coseismic ruptures of the 24 August 2016, Mw 6.0 Amatrice earthquake (central Italy). *Geophysical Research Letters*, 44(5), 2138-2147.
- Riguzzi, F., Tertulliani, A., & Gasparini, C. (1989). Study of the seismic sequence of Porto San Giorgio (Marche)–3 July 1987. *Il Nuovo Cimento C*, 12(4), 453-466.
- Spallarossa, D., Cattaneo, M., Scafidi, D., Michele, M., Chiaraluce, L., Segou, M., & Main, I. G. (2021). An automatically generated high-resolution earthquake catalogue for the 2016-2017 Central Italy seismic sequence, including P and S phase arrival times. *Geophysical Journal International*, 225(1). <https://doi.org/10.1093/gji/ggaa604>.
- Stucchi M., Meletti C., Montaldo V., Akinci A., Faccioli E., Gasperini P., Malagnini L., Valensise G. (2004). Pericolosità sismica di riferimento per il territorio nazionale MPS04 [Data set]. Istituto Nazionale di Geofisica e Vulcanologia (INGV). <https://doi.org/10.13127/sh/mps04/ag>.
- Tondi, E., Blumetti, A. M., Čičak, M., Di Manna, P., Galli, P., Invernizzi, C., ... & Volatili, T. (2021). ‘Conjugate’ coseismic surface faulting related with the 29 December 2020, Mw 6.4, Petrinja earthquake (Sisak-Moslavina, Croatia). *Scientific reports*, 11(1), 1-15.
- Valente, E., Buscher, J. T., Jourdan, F., Petrosino, P., Reddy, S. M., Tavani, S., ... & Ascione, A. (2019). Constraining mountain front tectonic activity in extensional setting from geomorphology and Quaternary stratigraphy: A case study from the Matese ridge, southern Apennines. *Quaternary Science Reviews*, 219, 47-67.